
Lobula Plate Tangential Cells in *Drosophila melanogaster*; Response Properties, Synaptic Organization & Input Channels



Maximilian Albert Jösch Krotki

München 2009



Lobula Plate Tangential Cells in *Drosophila melanogaster*; Response Properties, Synaptic Organization & Input Channels

Dissertation

Zur Erlangung des Doktorgrades

der Naturwissenschaften (Dr.rer.nat.)

der Fakultät für Biologie

der Ludwig-Maximilians-Universität München

Angefertigt am Max-Planck-Institut für Neurobiologie,

Abteilung 'Neuronale Informationsverarbeitung'

Vorgelegt von

Maximilian Albert Jösch Krotki

München 2009



Hiermit erkläre ich, daß ich die vorliegende Dissertation selbständig und ohne unerlaubte Hilfe angefertigt habe. Sämtliche Experimente wurden von mir selbst durchgeführt, außer wenn explizit auf Dritte verwiesen wird. Ich habe weder anderweitig versucht, eine Dissertation oder Teile einer Dissertation einzureichen bzw. einer Prüfungskommission vorzulegen, noch eine Doktorprüfung durchzuführen.

München, den 01.10.2009

1. Gutachter: Prof. Dr. Alexander Borst

2. Gutachter: Prof. Dr. Rainer Uhl

Tag der mündlichen Prüfung: 26. November 2009

Table of Contents

Table of Contents	5
List of Figures	8
1 Abstract	11
2 Introduction	13
2.1 General remarks.....	13
2.2 Visual course control in insects.....	14
2.3 The fly visual system	16
2.3.1 The retina	16
2.3.2 Phototransduction	17
2.3.3 The optic lobes	19
2.3.4 Motion sensitive interneurons in the lobula plate of large fly species.....	22
2.4 The Reichardt detector.....	25
2.4.1 Experimental evidence	26
2.4.2 Biological correlates of the motion computation pathway.....	28
2.4.2.1 Motion detection in the retina	28
2.4.2.2 Motion detection in the lamina	29
2.4.2.3 Motion detection in the in the medulla and lobula	30
2.4.2.4 Motion detection in the in the lobula plate.....	31
2.4.3 Motion computation in other organisms.....	32
2.5 The genetic armory of <i>Drosophila melanogaster</i>	32
2.6 Project goals and achievements	35
3 Manuscript Nr. 1	39
Synaptic Organization of Lobula Plate Tangential Cells in <i>Drosophila</i>: GABA-receptors and chemical release sites	39
<i>Abstract</i>	40
<i>Introduction</i>	41
<i>Materials and methods</i>	45
<i>Results</i>	48
The Gal4-3A expression pattern	48
Protocerebral projections of VS- and HS-cells express markers for output synapses	50
MARCM analysis identifies protocerebral projections as sole expression sites of presynaptic markers in VS-cells.....	50
Dendritic tips and central projections of all VS-cells show evidence for inhibitory input synapses ..	52
Dendritic tips and central projections of the HSE-cell show evidence for inhibitory input synapses	55
Indications for GABAergic input onto LPTCs.....	56
<i>Discussion</i>	58
Connectivity of VS- and HS-cells in the fly visual system	58
Genetic methods for the analysis of synaptic connectivity	59
Evidence for exclusively postsynaptic VS- and HS-cell dendrites in the lobula plate.....	60
Evidence for inhibitory input to VS- and HS-cell axon terminals in the protocerebrum	62
<i>Supplementary Material</i>	64
<i>Acknowledgements</i>	65

<i>References</i>	65
4 Manuscript Nr.2	71
Response Properties of Motion-Sensitive Visual Interneurons in the Lobula Plate of <i>Drosophila melanogaster</i>	71
<i>Summary</i>	72
<i>Results and Discussion</i>	73
Whole Cell Patch Recordings Reveal Six Motion Sensitive <i>Drosophila</i> VS-cells (VS1-VS6).....	75
Receptive Field Organization and Evidence for a <i>Drosophila</i> VS-cell network.	76
Computational Structure of the Presynaptic Motion Detection Circuitry	78
<i>Experimental procedures</i>	84
<i>Supplementary Material</i>	87
Supplementary Reference.....	89
<i>Acknowledgements</i>	89
<i>References</i>	90
5 Manuscript Nr. 3	93
Synaptic Organization of Lobula Plate Tangential Cells in <i>Drosophila</i>: Dα7 Cholinergic Receptors. ..	93
<i>Abstract</i>	94
<i>Introduction</i>	95
<i>Materials and Methods</i>	98
<i>Results</i>	101
Immunolabeling provides evidence for excitatory cholinergic input to the dendritic tips of VS and HS cells.	101
D α 7-GFP is located to the fine dendritic tips of VS and HS cells.	103
Direction selectivity of VS cells is retained in the absence of D α 7.....	106
<i>Discussion</i>	109
<i>Acknowledgments</i>	110
<i>Abbreviations</i>	111
<i>References</i>	111
6 Manuscript Nr.4	115
Processing of horizontal optic flow in three visual interneurons of the <i>Drosophila</i> brain	115
<i>Abstract</i>	116
<i>Introduction</i>	117
<i>Materials and Methods</i>	118
<i>Results</i>	122
HSN- and HSE are tuned to horizontal motion in a direction-selective way.....	124
HS-cell responses suggest input from correlation-type motion detectors.....	124
HS-cells of one hemisphere have strongly overlapping, binocular receptive fields	126
Dye-coupling suggests that HS-cells are central to a complex network of electrically coupled neurons.....	130
<i>Discussion</i>	132
Basic response properties of <i>Drosophila</i> HS-cells.....	132
Anatomical layout of HS-cell dendrites and receptive fields.	133
(1) Ipsilateral columnar input.	134
(2) Coupling to neighboring HS-cells.....	134

(3) Input from neurons with contralateral receptive fields.....	135
Behavioral relevance	136
Concluding remarks	137
<i>Acknowledgements</i>	137
<i>Reference List</i>	137
7 Manuscript Nr.5	141
Contribution of different lamina cells to the fly motion detection circuitry.....	141
<i>Abstract</i>	142
<i>Manuscript</i>	143
<i>Materials</i>	150
<i>Supplementary Material</i>	152
Temperature sensitivity of TNT.....	152
TNT induced lethality	153
<i>Reference List</i>	155
8 Discussion.....	157
8.1 Introduction of <i>Drosophila</i> as a model organism for the analysis of the motion detection circuitry.....	157
8.2 Basic response properties of VS- and HS-cells.	158
8.3 Fingerprints of computations according to the Reichardt detector model of visual motion detection.	158
8.4 The VS-cell network in <i>Drosophila</i>	160
8.5 <i>Drosophila</i> 's HS cell network	161
8.6 Synaptic organization of LPTCs in the <i>Drosophila</i> brain.....	162
8.7 Chemical release sites of <i>Drosophila</i> VS- and HS-cells.....	163
8.8 Evidence of a cellular implementation of the Reichardt detector	164
8.9 Concluding remarks.....	167
9 Reference List.....	169
Acknowledgements	177
Curriculum vitae	179

List of Figures

Introduction

Fig.1.	The fly's retina.	16
Fig.2.	<i>Drosophila</i> phototransduction.	19
Fig.3.	Schematic overview of the visual system of the fly.	20
Fig. 4.	Columnar cell types in the optic lobes of <i>Drosophila</i> .	21
Fig. 5.	Intracellular recording of an equatorial horizontal cell (HSE) to moving stimuli.	22
Fig. 6.	Functional grouping of LPTCs.	23
Fig.7.	The Reichardt detector model.	26
Fig.8.	Key evidences for the Reichardt detector model.	27
Fig.9.	Different proposed pathways for motion vision.	31
Fig. 10.	Genetic toolbox available in <i>Drosophila</i> .	34

Manuscript Nr.1 **Synaptic Organization of Lobula Plate Tangential Cells in *Drosophila*: GABA-receptors and chemical release sites.**

Fig.1.	Expression pattern of the enhancer trap line Gal4-3A.	49
Fig.2.	Elimination of expression in the central brain and in columnar elements allows the unambiguous localization of fluorescently labeled Synaptobrevin and suggests chemical output synapses on VS- and HS-cell ramifications in the protocerebrum.	51
Fig.3.	Distribution of Rdl-type GABA receptors on VS-cells.	54
Fig.4.	Distribution of Rdl-type GABA receptors on an HSE-cell.	55
Fig.5.	Single VS3-cell filled with Alexa-Fluor 594 in an anti-GABA immunolabeled brain.	56
Fig.6.	Single HSE-cell filled with Alexa-Fluor 594 in an anti-GABA immunolabeled brain.	57
Fig.S1.	Specificity of immunolabeling with GFP-, HA- and GABA-antibodies.	64

Manuscript Nr. 2 **Response Properties of Motion-Sensitive Visual Interneurons in the Lobula Plate of *Drosophila melanogaster*.**

Fig.1.	Whole cell patch clamp recordings from genetically labeled visual interneurons in the lobula plate.	74
Fig.2.	Receptive fields of the six <i>Drosophila</i> VS-cells (VS1-VS6).	77
Fig.3.	Velocity tuning (A, B) and step-responses (C, D) of <i>Drosophila</i> VS-cells.	79
Fig.4.	Further response characteristics of VS-cells.	82
Fig.S1.	Recording traces of two VS-cells during presentation of a periodic sinusoidal grating.	87
Fig.S2	Active membrane properties in <i>Drosophila</i> VS-cells involve TTX-sensitive fast voltage-activated sodium currents.	88
Fig.S3	Analysis of receptive field width.	88

**Manuscript Nr.3 Synaptic Organization of Lobula Plate Tangential Cells in
Drosophila: D α 7 Cholinergic Receptors**

Fig.1.	Localization of D α 7 immunoreactivity in VS cells of the adult fly visual system.	102
Fig.2.	Localization of D α 7 immunoreactivity in HS cells of the adult fly visual system.	103
Fig.3.	GFP-tagged D α 7 nAChRs are exclusively localized on dendritic tips of all six VS cells.	104
Fig.4.	GFP-tagged D α 7 nAChRs are exclusively localized on dendritic tips of all three HS cells.	105
Fig.5.	D α 7 nAChRs are not expressed on the protocerebral branches of VS and HS cells.	106
Fig.6.	Directional selective responses are largely retained in D α 7 mutant flies.	107

**Manuscript Nr.4 Processing of horizontal optic flow in three visual
interneurons of the *Drosophila* brain**

Fig.1.	Basic response properties of HS-cells in <i>Drosophila</i> .	123
Fig.2.	HSN and HSE responses match the predictions of a correlation-type motion detector.	125
Fig.3.	Dendritic structure and receptive fields of HSN and HSE.	128
Fig.4.	Vector fields of HSN (A), HSE (B) and HSS (C).	130
Fig.5.	Spread of Neurobiotin within the HS-circuitry.	131

**Manuscript Nr.5 Segregation in On- and Off-Channels for motion detection in
the fly**

Fig. 1.	Combined electrophysiological and neurogenetic approach.	144
Fig. 2.	Contrast dependency	146
Fig. 3.	On- and Off-edge motion detection.	147
Fig. 4.	TNT expression under the Ln-Gal4 line disrupts photoreceptor output.	149
Fig. S1.	Receptive field properties of VS cells.	152
Fig. S2.	Quantitative analysis of TNT block.	153
Fig. S3.	Contrast dependence of 21D-Gal4 line	154
Fig. S4.	On- and Off-edge motion detection of 21D-Gal4 line	155
Supp. Table 1.	Viability of different driver lines with TNT.	154

1 Abstract

Half a century ago, Reichardt and Hassenstein proposed a model for the detection of visual motion. This 'Reichardt detector' describes, in mathematical terms of filtering and correlation, how the processing of luminance input to the retina results in a directionally selective output. The Reichardt detector was extremely successful in predicting visually guided behavior of insects as well as the basic response properties of large-field motion-sensitive neurons in their brain. These cellular response properties can be explained if we assume that the neurons receive input from large arrays of such Reichardt detectors. Interestingly, the animal's behavior can then be assumed to be guided by the output of the same neurons that supply to motor circuitries to control walk and acrobatic flight maneuvers. However, the cellular implementation of the Reichardt detector and the function of the 'course control center' are still not known to date. This is mainly due to the small size of the neurons and the complexity of the neural circuitry in the optic lobe. Furthermore, it was so far difficult to introduce specific functional manipulations to the network and impossible to directly monitor cellular responses. In my thesis, I set out to elucidate the cellular implementation of the Reichardt detector and the network of large-field motion-sensitive neurons combining electrophysiology with genetic intervention in *Drosophila*.

1. My first achievement was to establish *in vivo* whole-cell recordings from the large-field motion-sensitive neurons in the fly lobula plate ('lobula plate tangential cells', LPTCs). This allowed, for the first time, a functional characterization of these neurons in *Drosophila*. LPTCs in *Drosophila* turned out to have similar response characteristics as similar neurons in larger fly species: the group of vertically sensitive (VS) cells is excited by downward motion and is inhibited by upward motion. Horizontally sensitive (HS) cells are excited by front-to-back motion and are inhibited by motion in the opposite direction. Moreover, the dependence of the response on image velocity and contrast revealed all the signatures that are indicative for receiving input from Reichardt detectors.

2. I analyzed the complex receptive field properties of VS- and HS-cells by developing a new stimulus paradigm. This stimulus revealed that each morphologically

defined VS- and HS-cell possesses a distinct receptive field. Moreover, I could show that both lateral VS-cells and the dorsal HS-cell have different preferred directions in different parts of their visual field. Interestingly, all VS- and HS-cells showed much wider receptive fields than expected from the position and size of their dendrite in the retinotopically organized lobula plate. Perfusion of individual cells with Neurobiotin, a molecule small enough to pass gap junctions, revealed coupling of neighboring VS- and HS-cells, respectively. This finding provides indirect evidence for electric coupling as the basis of their large receptive fields.

3. Using cell-specific expression of transgenes encoding for postsynaptic receptors and presynaptic molecules tagged with GFP, I contributed to the analysis of the functional synaptic organization of LPTCs: *Drosophila* LPTCs turned out to be postsynaptic in the lobula plate and presynaptic in the protocerebrum. The specific localization of Acetylcholine- and GABA-receptors suggests that excitatory and inhibitory motion-sensitive elements with opposite preferred direction provide input onto the fine dendritic branches of LPTCs.

4. Finally, I combined whole-cell recording from LPTCs with genetic manipulation of neurons within the presynaptic circuitry. Starting at the first relay station of visual signals in the fly brain, the lamina, I blocked synaptic transmission from specific lamina cell-types. Curiously, blocking any of the cell-types did not severely impede the motion response to drifting gratings as measured in the LPTCs. However, specific response deficits became obvious when moving edges of single contrast polarity were used as visual stimuli instead of gratings. These findings suggest that the visual input stream to the motion detection circuitry is segregated into ON- and OFF-channels, carrying information about increasing or decreasing image contrast separately.

The combination of whole-cell patch recording from LPTCs with genetic manipulation of their presynaptic neurons proved to be an extremely useful paradigm which will be instrumental for the functional dissection of the motion detection circuitry and the network of motion sensitive interneurons in *Drosophila*.

2 Introduction

2.1 General remarks

The neural mechanisms underlying the control of behavior rely on (i) the transformation of environmental stimuli into a neural code, (ii) the transmission of this code to the brain where it converges with other sensory information and (iii) the decision making necessary to act on the incoming signal. (iv) In a final step, a motor program is generated to produce the properly timed and concrete muscle activity we recognize as behavior. A textbook example for the generation of such a behavior is the visually guided course control in flies. The underlying neural circuit computes incoming visual information and controls the acrobatic flight maneuvers. The formidable speed and precision of this computation enable the chasing of mates at turning velocities of up to $3000^\circ/\text{s}$ and the initiation of compensatory flight maneuvers with a time-lag of less than 30 ms (Land and Collett, 1974; Wagner, 1986). The proper functioning of this circuitry is fundamental for orientation and navigation through the environment and thus for the survival of the fly. Half a century ago, based on behavioral studies of visual motion responses in the beetle *Chlorophnus*, a model was proposed that precisely describes insect's optomotor behavior and the electrophysiological responses of large field motion sensitive cell in bigger fly species. This model became known as the 'corretlation-type' motion detector or simply as the Reichardt detector. The Reichardt detector is thought to be implemented in the insect's optic lobe. It computes visual motion based on the luminance changes seen by the insect's eye. In a subsequent processing step this motion information is used by the network composed of large field motion sensitive cells to control the course and acrobatic performance of flies. The robustness of these computations, its algorithmic interpretation and the supposed simplicity of the underlying neuronal network raised the hope that the cellular implementation of both the Reichardt detector and the course control network will be understood in the near future. Yet, the small size of the majority of the constituting neurons and their complex organization presented a formidable barrier for functional studies so far. A circumstance anticipated by Ramón y Cajal who recognized more than 100 years ago that the insect's visual system resembles a "cell labyrinth with an understated complexity" (Ramón y Cajal, 1923).

In my PhD work I set out to establish an experimental approach to overcome mentioned problems by taking advantage of the genetic toolbox available for the fruit fly *Drosophila melanogaster*. Using this approach I could start dissecting the network from a cardinal point: the motion selective large tangential cells in *Drosophila*. To guide the reader into the intriguing world of insect visually driven behavior, I will summarize the knowledge ranging from insect eye optics to the most novel findings of course control computations. I aim to give a comprehensive outline of this fascinating field and highlight the need of a novel approach to reach deeper insight into these outstanding brain functions.

2.2 Visual course control in insects

Flies, as most other insects, heavily rely on visual information to guide their acrobatic flight maneuvers in space. Flying insects use optic flow patterns induced by their self motion to generate motor programs and ultimately execute compensatory flight maneuvers that enable them, among other things, to maintain a straight course. For example if an insect is displaced from its course by a gust of wind, the image in its frontal field of view moves quickly inducing a characteristic optic flow pattern on the insect's eye. This information is then processed and used to command the flight motor system. A counteractive torque can be generated bringing the insect back on course (Reichardt, 1957; Srinivasan, 1977). As another example, bees tend to fly through the very center of a narrow hole, implying that they can regulate their distance from the borders. Intriguingly, the insect eyes are, compared to human ones, positioned much closer and possess an extremely low spatial acuity making binocular stereopsis too imprecise to account for this behavior (but see (Rossel, 1983)). Bees solve this problem by balancing the speed of image motions experienced by the left and right facet-eye (Kirchner and Srinivasan, 1989). But such optic course control only works well in a symmetrically structured environment. If the insect is facing irregular patches of contrast and texture, substantial differences in the computed motion occur between both eyes. This arises due to the dependency of the motion computation on the features of the visual stimulus itself. A possible way to solve this problem is to sense and balance image motion in only a small patch of the visual field. This has been shown for the hoverfly that, when flying straight ahead, minimizes image motion within a small visual field located in the forward direction (Collett, 1980).

Interestingly, visual motion information is not only needed for course stabilization. Bees, for example use the integration of optic flow to correctly estimate flight distance (Srinivasan et al., 2000). In contrast to this kind of processing, some walking insects do not rely on translational optic flow to estimate distance. The desert ant *Cataglyphis fortis* measures distance by counting steps (Wittlinger et al., 2006), but can only register the distance if they can see the sky (Sommer and Wehner, 2005). The reason for this is that they use polarized light from the sun, scattered by the atmosphere, as a compass to estimate the direction of movement. Combining those two sources of information, these ants can compute the shortest way back to the nest after having explored their environment for food for hundreds of meters in a random fashion.

Considering that the amount of neuronal hardware dedicated to vision in insects and especially in flies sum to approximately half of the brain's volume (Strausfeld, 1976), the dominance of visual input for the insect's course control can be assumed. Yet, visual information on its own, as exemplified for the desert ant, is not sufficient to account for all their astonishing behavior. In flies, an additional flight aid is provided by the halteres, small hind-wings that oscillate in antiphase with the main wings and act as miniature gyroscopes to provide information about the body's rotation (Dickinson, 1999). While visually driven compensatory responses deal with slower turning velocities, the haltere input can be used to compensate for very rapid rotations as shown for yaw rotations (Sherman and Dickinson, 2002). In addition, in dragonflies and locust, the visual stabilization of roll and pitch is thought to be accomplished by input from the ocelli, three single-lens eyes situated on the top of the head. The medial ocellus stabilizes pitch by monitoring the elevation of the horizon, whereas the two lateral ocelli monitor the position of the horizon on either side and can therefore stabilize roll (Stange, 1981; Stange et al., 2002). However, it has been shown in the blowfly that incident dorsal light has only little influence on the optomotor roll torque response (Schuppe and Hengstenberg, 1993).

The neuronal circuitry and the computational steps that underlie the robust and reproducible behavior are still elusive and have been treated as a 'black box'. Due to the small size of the constituting interneurons it has been difficult and in most cases impossible to dissect this neural circuitry. Exceptionally, in large flies, mostly *Calliphora vicina*, insights have been gained into the function of large motion sensitive cells in the

lobula plate. Likely, these neurons represent the course control center of the fly (reviewed in (Borst and Haag, 2002)). To tackle the many problems outlined above, new methods are required. A combined physiological and behavioral approach that takes advantage of the new genetic toolbox available in *Drosophila* (reviewed in (Luo et al., 2008)), is a timely approach to circumvent previous experimental limitations and forms the conceptual framework of this work (reviewed in (Borst, 2009)).

2.3 The fly visual system

2.3.1 The retina

The processing of visual information starts in the fly's compound eyes. Its mosaic like structure is composed of repetitive elements called facets or ommatidia (Fig.1A). Each ommatidium contains a cluster of 8 photoreceptor cells surrounded by support and pigment cells and an individual transparent lens (Fig.1B)

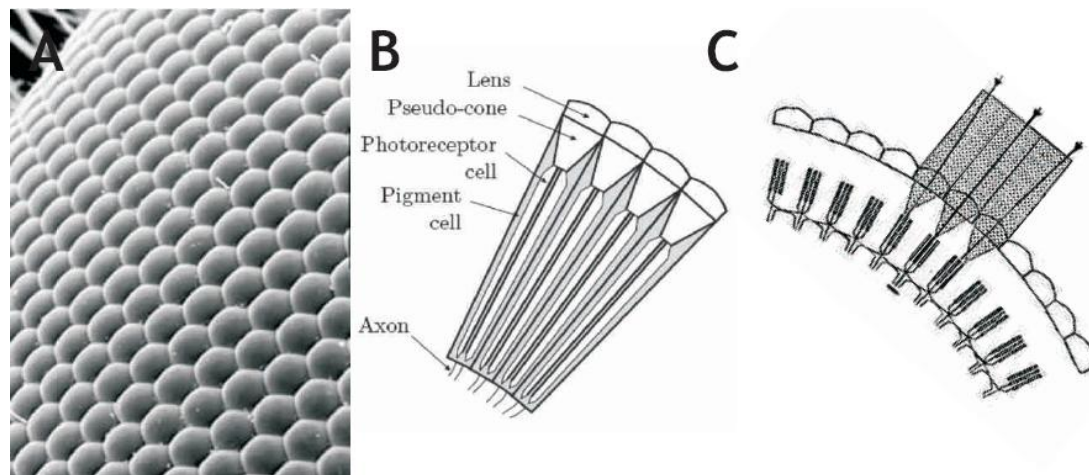


Fig.1. The fly's retina. (A) An electron micrograph of the facet-eye of a blowfly at a magnification of $\sim 375\times$. (from www.bath.ac.uk/ceos/Insects1; B) A schematic of the fly retina illustrates the basic structure of the light capturing device of a fly (adapted from (Hardie, 1984). (C) Schematic of the neuronal superposition eye, as encountered in dipteran flies (adapted from Land (1997)).

The basic structures of insect compound eyes can be separated in three groups: the apposition, the optical superposition and the neuronal superposition eye. In the apposition eye, the group of photoreceptors that reside within an individual ommatidium are optically isolated from other ommatidia. In the optical superposition eye, the optical apparatus of the facets bundles light from neighboring ommatidia acting together as a single optical device. Finally, in the neuronal superposition eyes,

the photoreceptors of neighboring ommatidia that hold converging optical axes interact with the same postsynaptic target to increase sensitivity without sacrificing acuity (Fig.1C; Kirschfeld, 1967). Optical superposition eyes are normally found in nocturnal insects such as moths to increase their sensitivity to light. In contrast apposition eyes, which have better spatial acuity but worse overall sensitivity, can be encountered in diurnal insects as grasshoppers and bees. The neuronal superposition eye, which can combine the benefits of the previous mentioned eye types, is found in dipteran flies (Fig. 1C).

Each ommatidium is composed of two main groups of photoreceptors, the outer and inner group. The outer group, sitting on the borders of each ommatidium, consists of the photoreceptors R1-6. R1-6 have wide rhabdomeres, span the whole ommatidium and express the opsin Rh1. The inner group is composed of the photoreceptors R7 and R8, which are located in the center of each ommatidium. Their rhabdomeres only span half of the ommatidium, with R7 sitting on top of R8. R7 expresses stochastically either the UV sensitive opsin Rh3 or Rh4, whereas R8 express either blue or green absorbing opsins Rh5 & Rh6, respectively. Interestingly, the Rh3 expression in R7 is coupled with the Rh5 expression in R8, as Rh4 is coupled with Rh6, defining two functional subtypes of photoreceptors randomly distributed throughout the fly's eye: *pale* (Rh3/Rh5) which accounts for 30 % of the facets and *yellow* (Rh4/Rh6) for 70 % (Franceschini et al., 1981). R7 and R8 are known to be fundamental for color vision in flies (Gao et al., 2008), but the function of this random distribution is not yet well understood.

As an example, the fruit fly's compound eye has ~700-800 facets per eye with an inter-ommatidial angle of 4.6° , distributed almost over 180° of visual surround. Compared to the visual acuity of the human eye, *Drosophila's* compound eye has a 500 fold lower spacial resolution.

2.3.2 Phototransduction

Invertebrate phototransduction, the process by which light energy is converted into a photoreceptor's electrical response is based, as in vertebrates, on a G-protein signaling cascade. One hallmark of these cascades is their capacity for amplification. This allows invertebrate photoreceptors as well as vertebrate rods to respond with

quantized events (quantum bumps) to single photons (Fig 2B; Yeandle and Spiegler, 1973). Once the absorption of a photon triggered the isomerization of the rhodopsin's (R) 11-*cis* to all-*trans* retinal, the amplification cascade is started (Fig.2C) and producing a depolarization of the invertebrate photoreceptor potential. This is one of the main differences compared to vertebrate photoreceptors, which hyperpolarize in response to an increase in illumination due to a 'dark current' which is turned off by light. Another major difference between vertebrates and invertebrates phototransduction is the dynamics of their response (Fig2B). While in vertebrates any flicker stimulus above 80 Hz is perceived as continuous light, the fly's photoreceptor potential can still follow up to a flicker frequency of more than 300 Hz (Laughlin, 1987). One reason is the different process by which R is regenerated. In *Drosophila*, the activated R, called metharhodopsin (M), is thermo-stable and can be reconverted into R by long-wavelength light. In contrast, vertebrate M has to be phosphorylated several times by the rhodopsin kinase that leads to the binding of arrestin and is followed by its thermal decay. All-*trans* retinal is subsequently shuttled to pigment cells that, in a series of biochemical reactions regenerate it to 11-*cis*-retinal, which subsequently can bind to free opsin within the photoreceptors (for review (Burns and Arshavsky, 2005)). This regeneration strategy is more time consuming. Therefore it limits the temporal resolution of the system more strongly compared with the reversion in *Drosophila* based in red light. Interestingly, this explains the red eye-color of most fly eyes: the retinal screening pigments are transparent to long wavelength light and absorb all other visible wavelength, allowing them to constantly recover back to R by ambient light (for details see Fig.2, reviewed in (Hardie and Raghu, 2001)).

The transduction machinery is located in specialized subcellular compartments of the photoreceptors, the rhabdomeres (Fig2A). Its structure is dictated by the need to maximize the amount of light-absorbing membrane and it is realized by numerous tightly packed microvilli.

Since the brain's capacity to analyze and interpret information is ultimately limited by the input it receives, enhancing the temporal resolution allows insects to compute visual information and perform their acrobatic maneuvers despite their coarse spatial resolution.

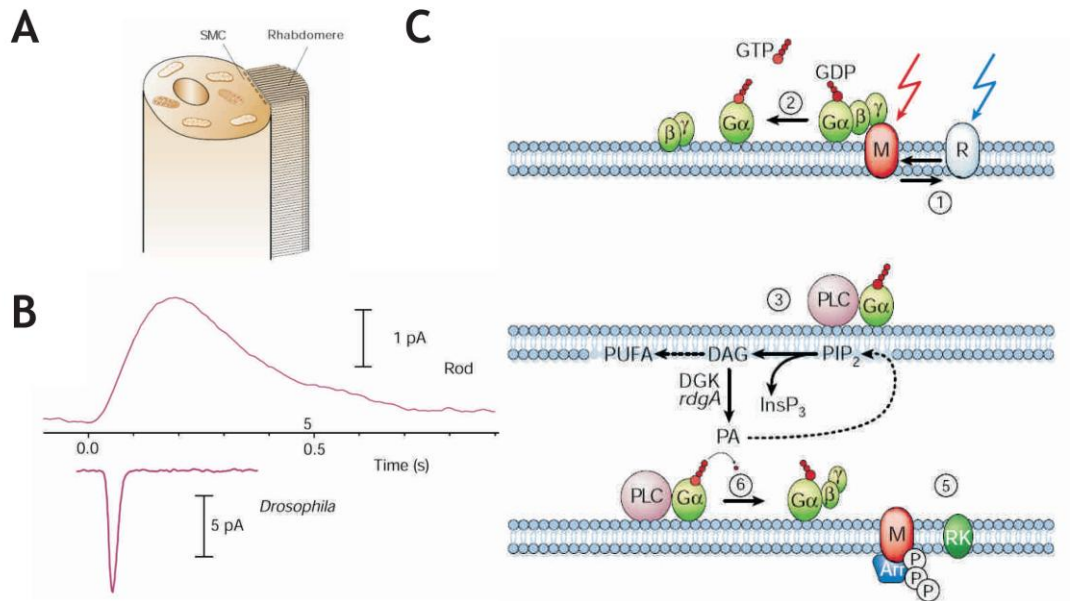


Fig.2. *Drosophila* phototransduction. (A) Photoreceptor in *Drosophila*. The photoreceptor membrane is organized into tightly packed tubular microvilli, each 1-2 μm long and ~ 60 nm in diameter, together forming a 100 μm Rhabdomere. (B) Comparison of quantum-bump kinetics in toad rod outer segment and *Drosophila*. (C) *Drosophila* phototransduction cascade. (1) Invertebrate phototransduction starts, as in vertebrates, when photons are absorbed by the light-sensitive photopigment rhodopsin (R) which photoisomerizes to metarhodopsin (M). (2) M can catalyze the exchange of GDP for GTP on the heterotrimeric G protein (named G_α in *Drosophila* and transducin in vertebrates), dissociation of the GTP-bound α -subunit which subsequently (3) activates the effector enzyme PLC. (4) PLC generates a membrane activated second messenger while hydrolyzing PIP_2 into DAG and InsP_3 , which in turn activate two classes of channels, the TRP and TRPL via an unknown mechanism. DAG is reconverted via a multienzymatic pathway into PIP_2 while (5) M can be inactivated via phosphorylation by rhodopsin kinase (RK) and capped by arrestin, but normally is reactivated by long wave-length light. (6) Finally, G_α is inactivated by the GTPase activity of the G-Protein, leading to re-association with the $G\beta\gamma$ subunits (Modified from Hardie and Raghu (2001)).

2.3.3 The optic lobes

The fly's visual ganglia consist of three successive layers of neuropile, the lamina, medulla and lobula-complex, where the columnar organization reflects the relative position of the ommatidia (Fig. 3A). Therefore, the visual images perceived by the eye are retinotopically projected onto sheets of neuropile such that neighborhood relationships between image points are conserved within the nervous system (Fig 3B). Two chiasmata, one between the lamina and the medulla and another one between the

medulla and the lobula-complex rotate the retinotopic projection along the antero-posterior axis.

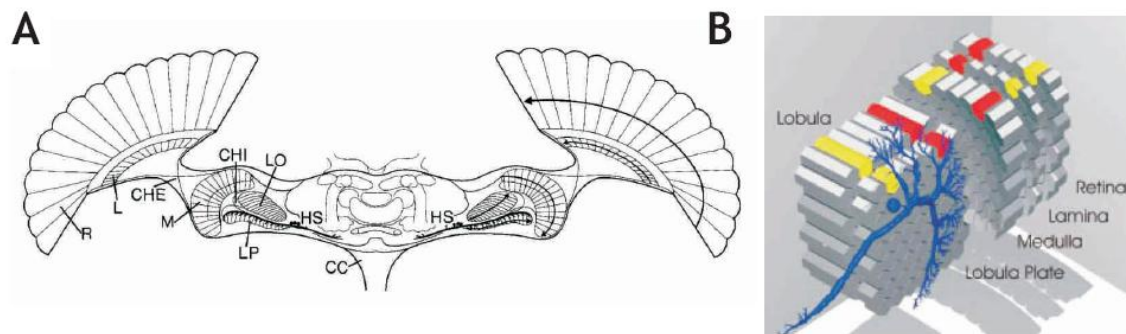


Fig.3. Schematic overview of the visual system of the fly. (A) Dorsal view of the fly's visual system, including the retina (R), the three main neuropils, the lamina (L), the medulla (M), lobula-complex (lobula (L) with lobula plate (LP)), the connective (CC), the inner and outer chiasmata (CHI and CHE, respectively) and an exemplified HS-cell (From Hausen (1982a)). (B) Schematic overview of the columnar organization of the four neuropils. Each layer represents the facets of the retina in a one-to-one fashion leading to a retinotopic projection of the visual surround onto the dendrites of the lobula plate tangential cells (from Borst and Haag (2002)).

In *Drosophila*, each column is thought to be composed of approximately 100 different anatomically described cell types (Fischbach and Dittrich, 1989). With new genetic techniques, so far undescribed cell types are still discovered (Shamprasad Varija Raghu, personal communication). I will briefly focus on the main characteristics of each cell class (for review (Meinertzhagen, 2008)).

Starting from the periphery, as schematically presented in Figure 4, the visual pathway begins with the two previously mentioned groups of photoreceptors. While R1-6 terminate in the lamina (Meinertzhagen and O'Neil, 1991), the inner group, with the photoreceptors R7 & R8, is connected to cells in the medulla. It is known that all photoreceptors use the inhibitory neurotransmitter Histamine (Hardie, 1989), which opens chloride channels encoded by the gene *ort* that mediate a hyperpolarizing current.

The next neuropile, the lamina, constitutes of 5 different lamina monopolar cells, two centrifugal and one T1 cell. Intracellular recordings have been performed in identified L1 and L2 in large flies, showing an inversion and strong high-pass filtering of the signals provided by the photoreceptors (Jaervilehto and Zettler, 1971). All lamina cells have a stereotyped connectivity pattern in the lamina and between

different lamina cells (Meinertzhagen and O'Neil, 1991) and ramify in different layers of the medulla (Takemura et al., 2008), connecting to different medullar interneurons. In the medulla the exact connectivity is less well understood.

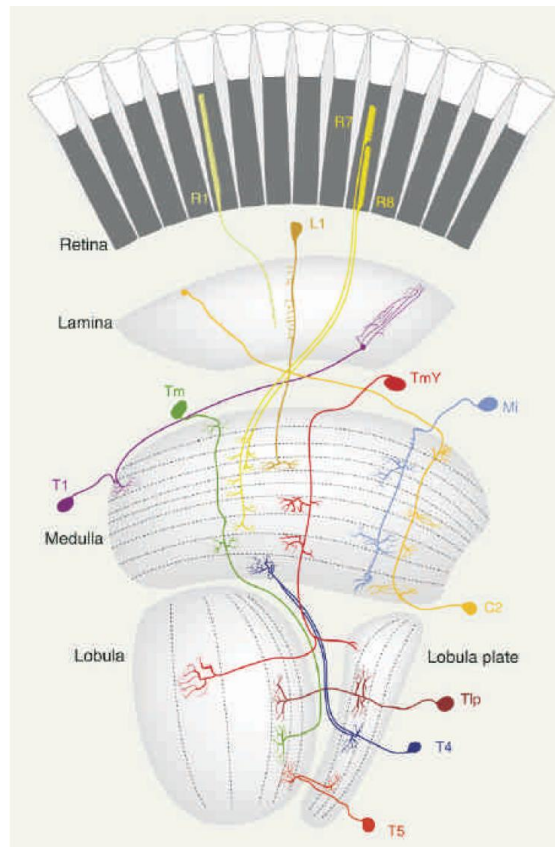


Fig. 4. Columnar cell types in the optic lobes of *Drosophila*. Schematic drawing of characteristic neuronal subtypes of the fly's optic lobe. For clarity, only one type of cell, representative for one distinctive class is presented (from (Borst, 2009), modified after (Fischbach and Dittrich, 1989)).

In the medulla, the columnar cell types can be structurally classified into several classes (Fig. 4). The medulla intrinsic (Mi) cells ramify exclusively in the medullar neuropile whereas transmedulla interneurons (Tm) connect distinct layers of the medulla to the lobula with TmY cells having an additional ramification within the lobula plate. Finally, the bushy T4-cells connect the innermost layer of the medulla with the lobula plate and the bushy T5-cells ramify in the most posterior layer of the lobula as well as in the lobula plate. The latter two subtypes are thought to be the main input elements of the motion sensitive lobula plate tangential cells (see sec. 2.3.4). Thus, T4 and T5 are supposed key-players in motion computations (Bausenwein et al., 1992; Douglass and Strausfeld, 1996).

2.3.4 Motion sensitive interneurons in the lobula plate of large fly species

The lobula plate is a flat structure on the posterior side of the lobula complex. Based on electrophysiological work performed only in big fly species, as *Calliphora vicina* and *Musca domestica*, the lobula plate is thought to represent the “cockpit” of the fly. It is here where the processed motion information is spatially integrated by large motion sensitive tangential cells (LPTCs). LPTCs are a group of 60 neurons, each of which is individually identifiable based on its characteristic anatomy and response properties. Their main response characteristic is that they become excited by motion in their preferred direction (PD) and inhibited by motion in the opposite direction, the so called null direction (ND; Fig. 5).

LPTCs can be grouped functionally into spiking neurons (e.g. H1-6, V1-3), graded potential neurons (CH cells) and neurons with mixed responses (HS, VS and FD-cells). A different criterion for classification is their primary direction of motion sensitivity, vertical (VS and V) or horizontal (H1-6, HS, CH and FD; Fig. 6; reviewed in Borst and Haag, 2002).

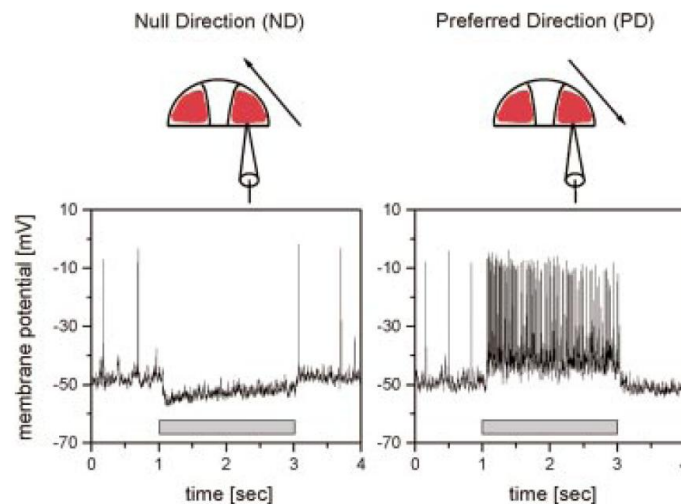


Fig. 5. Intracellular recording of an equatorial horizontal cell (HSE) to moving stimuli. The neuronal response to horizontal grating motion from back-to-front (ND) exhibits a hyperpolarization of the membrane potential (grating movement is represented by the grey line). When the direction of motion is inverted (PD), the cell responds with a strong depolarization superimposed with action potentials of irregular amplitude (From Borst and Haag, 2002).

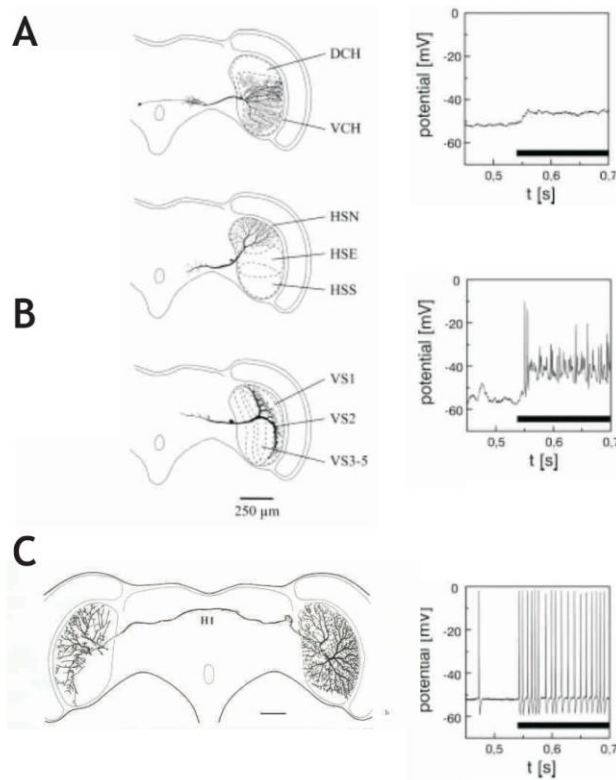


Fig. 6. Functional grouping of LPTCs. (A-C) On the left side, a schematic view on frontal brain sections with different LPTCs. On the right, their primary response properties to motion in their preferred direction (PD; motion stimuli was presented during the black bars). The difference in their functional response properties can be clearly seen from (A) purely graded in CH-cells, (B) over mixed responses in VS- and HS-cells, to (C) spiking in H1 (adapted from (Borst and Haag, 2002; Hausen, 1976)).

Due to the retinotopic organization of the optic lobes, a map of the fly's ipsilateral visual field impinges onto the dendrites of the LPTCs, in such a way that neighboring locations preserve their relative position to each other (Borst and Egelhaaf, 1992; Krapp and Hengstenberg, 1996). Information about local motion, computed by the neurons of the lamina and medulla in an unknown way, is fed onto these neurons via this dendritic input. LPTCs process this incoming information by their interaction in an extensive network composed of ipsilateral and contralateral connections between other LPTCs (reviewed in Borst and Haag, 2002). The whole set of network computations performed by LPTCs is believed to be central for the course control of the fly. Nevertheless, causal evidence in this direction is sparse, but a vast amount of loose correlations has been accumulated. The most interesting ones will be mentioned next. (i) The *Drosophila* mutant *optomotor-blind*^{H31}, where the whole lobula plate is missing, lacks almost all optomotor responses (Heisenberg et al., 1978). Since this might also be attributed to the lack of other neurons than LPTCs, a dysfunctional optic lobe could be expected, making casual interpretations difficult. (ii) Electrical

stimulation of different areas of the lobula plate elicits yaw, lift and landing responses, similar to those elicited by motion stimuli (Blondeau, 1981). In these experiments, the coarse electrical stimulation was rather unspecific and therefore might have activated unknown neurons other than LPTCs. (iii) Finally, the most convincing evidence is based on optomotor responses which led to the postulation of the 'correlation type' motion detector model (Hassenstein and Reichardt, 1952; Hassenstein and Reichardt, 1956; Reichardt, 1957) and that were similarly found in the electric responses of LPTCs (Hausen, 1977; Hausen, 1982a). All together, these results led to the widely believed idea that these neurons are the main link between visual motion computation and optomotor control.

Understanding of the network computations of LPTC has advanced greatly in the last few years in *Calliphora vicina* (Cuntz et al., 2007; Farrow et al., 2005; Farrow et al., 2006; Haag et al., 2007; Haag and Borst, 2004; Haag and Borst, 2005; Wertz et al., 2008). One interesting example of computation within the LPTC network is based on the electrical coupling between VS-cells, a group of 10 LPTCs most sensitive to rotational motion around different axes within the equatorial plane (Krapp and Hengstenberg, 1996). A set of elegant experiments, combining modeling (Cuntz et al., 2007), calcium imaging (Elyada et al., 2009), double recording (Haag and Borst, 2004), ablation experiments (Farrow et al., 2005) and anatomical studies (Haag and Borst, 2005) revealed functional computations performed by the sequentially arranged and electrically coupled VS-cells. VS-cells are sequentially organized in the lobula plate, receive retinotopic input and are gradually more sensitive for optic flow resembling pitch (VS1), roll (VS5) and pitch in the opposite direction (VS10). Due to the electrical coupling in their axonal termini, these cells interpolate the signals of neighboring cells. This computation in turn is used for the robust detection of the fly's actual axis of rotation in natural environment with irregular contrast distribution. For all those reasons this neural network is thought to be pivotal for steering and course correction.

Anatomical studies have shown similarities between the LPTCs found in *Calliphora* (Hausen, 1976) with the ones encountered in *Drosophila* (Rajashekhar and Shamprasad, 2004; Scott et al., 2002). However, functional evidence is fully missing. In the work presented here I closed this gap examining the physiological properties of *Drosophila's* LPTCs.

2.4 The Reichardt detector

Visually guided course control, as a mean to understand the neuronal implementation of a control circuitry, began to be a focus of research when Bernhard Hassenstein and Werner Reichardt started to do a series of elegant experiments using optomotor responses of the beetle *Chlorophanus* as a behavioral measure (Hassenstein and Reichardt, 1952; Fig 7A). These responses represent the animal's tendency to follow the movement of the visual surround to compensate for its mistaken perception of self-motion in the opposite direction. Based on their results Hassenstein and Reichardt proposed a model for motion detection that became known as the 'correlation-type motion detector' or simply the 'Reichardt model' of elementary motion detection. The model starts with the idea that a photoreceptor signal simply becomes modulated in response to a moving object, according to the brightness difference, no matter in what direction the object is moving. Only when at least two photoreceptor signals, displaced along the orientation of image motion, are considered can the direction and the magnitude of motion be derived by an external observer based on the delay of the signals relative to each other (Fig 7B). This is performed by the model mainly by two operations, an asymmetrical temporal filtering and a nonlinear interaction stage where the low-pass filtered (delayed) signal from one image location is multiplied by the high-pass filtered (instantaneous) signal from the neighboring image location (Fig 7B). It is the combination of a temporal delay and a multiplication that allows this type of detector to measure the degree of coincidence between its input channels.

At each image location there exists at least four such subunits with four different orientations: one for rightward, one for leftward, one for downward, one for upward motion. The difference between the output signals of two complementary subunits results in the final detector response. Based on biological evidence, the sum of an array of these detectors is used to simulate the retinotopically arranged Reichardt detectors build by the neuronal layers of the insect visual system (Fig 7C).

This model can account for many of the properties measured in motion driven behaviors, as well as in the electrophysiological responses of LPTCs. In the next paragraphs the most important biological correlates will be discussed.

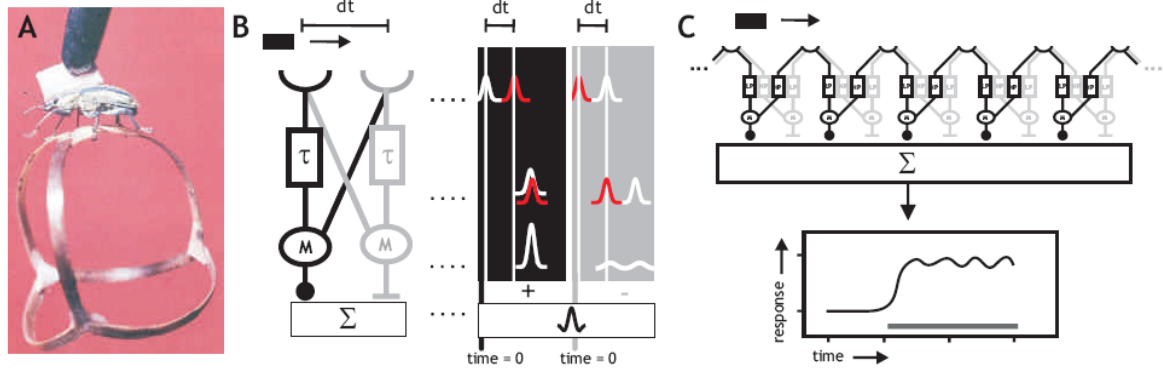


Fig 7. The Reichardt detector model (A). Tethered *Chlorophanus* walking on the Y-maze globe (from Hassenstein, 1991). (B) Basic scheme of a Reichardt detector together with its component responses (right boxes) to a Gaussian luminescence distribution that moves with a constant velocity from left to right. The two mirror symmetric subunits (black and grey subunits) are built up by a delay (τ) and a no-delayed line that are combined in a nonlinear manner (M) and, respectively, subtracted into an integrative unit (Σ). The time of stimulation is indicated for each subunit separately (right boxes). 'dt' is the time needed for the object to move from one photoreceptor to the other. The white and red distributions reflect the delayed and instantaneous signals at each processing step, respectively. At the multiplication step, the black subunit receives the input simultaneously while the grey subunit does it consecutively, enhancing and weakening the input signals respectively. After subtraction of these signals, the final output shows strong direction selectivity. (C) An array of detectors is used to simulate the neural layers between the photoreceptors and tangential cells. The amplitude of the summed responses of all synapses reflects the pattern velocity. Note, that in this case, a high- and a low-pass filter were used for the instantaneous and delayed line, respectively. In the example shown here pattern motion from left to right is called the PD of the motion detector (grating movement is presented by the grey line), while motion in the opposite direction will result in a sign-inverted response. This is called the ND of the detector (adapted from Borst and Haag (2002)).

2.4.1 Experimental evidence

There are three key predictions of the Reichardt detector model that were found in the optomotor response and in the cellular responses of LPTCs:

(i) First of all, the mean response amplitude of elementary motion detectors depends on the structure of the presented visual pattern. For a moving visual grating the response will depend on the spatial wavelength, its contrast and its overall brightness. In particular an increase in velocity will lead to a maximum response. This so called velocity-maximum increases linearly with the spatial wavelength of the pattern, such that the ratio of the spatial wavelength and velocity is constant, i.e. at the same temporal frequency. Such predictable and pattern dependent changes in the

optimal velocity have been recorded in LPTCs (Haag et al., 2004; Fig. 8A) and were similarly found in compensatory optomotor responses of behaving flies (Buchner, 1976; Fermi and Reichardt, 1963; Götz, 1972).

(ii) Second, distinct fingerprints of input from Reichardt detectors to LPTC dendrites can be revealed when local signals instead of integrated large-field responses are analyzed. According to the Reichardt detector, local signals consist of two components, one that is directionally selective and one reflecting the local change in luminance. Such oscillations that reflect the modulation in brightness imposed by the temporal frequency of the moving grating can be measured when a moving grating is presented through a small aperture while recording the axonal membrane potential of an LPTC. Alternatively, as shown in Fig. 8B, a whole field moving grating is presented while recording local calcium fluctuations in fine dendritic tips (Egelhaaf et al., 1989; Haag et al., 2004; Single and Borst, 1998).

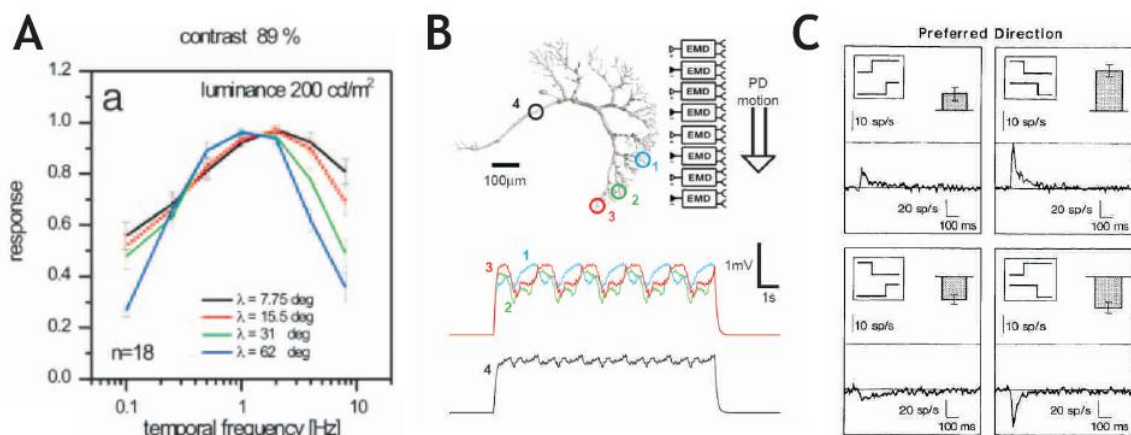


Fig 8. Key evidences for the Reichardt detector model. (A) Temporal frequency tuning recorded from the H1 neuron in the blowfly *Calliphora vicina* using different grating wavelengths λ . An optimal temporal frequency can be seen for all wavelengths presented (adapted from (Haag et al., 2004)). (B; Top) A three dimensional reconstruction of a VS1-cell is used as a compartmental model to predict the spatiotemporal membrane potential distribution upon stimulation with constant visual motion. The neuron is simulated to receive synaptic input from an array of Reichardt detectors. (Bottom) Local membrane potential fluctuation in three dendritic areas indicated by the corresponding colors is shown together with the axonal membrane potential (lower trace). Although the local dendritic potentials consist of a constant response superimposed by temporal modulations of identical frequency but various phase offsets, the axon potential is rather smooth. These modeling results resemble the experimentally recorded dendritic calcium modulations observed in the same neuron (adapted from (Single and Borst, 1998)). (C) Motion-dependent response components as derived from the frequency histogram of four different apparent motion experiments (On-On, Off-Off, Off-On and On-Off) in H1. Note the response

inversion when stimuli were presented with opposing brightness change (bottom two panels; adapted from (Egelhaaf and Borst, 1992))

(iii) Third, using apparent motion experiments, where stepwise changes in local luminance were used to excite the cell, the nonlinearity within in the Reichardt detectors could be experimentally measured. Presenting luminance changes along the preferred direction of H1 (a spiking motion sensitive LPTC), sequences of the same sign (on-on, off-off) produced positive motion responses, while mixed sign sequences (on-off, off-on) resulted in inverted motion responses, as predicted by the model (Egelhaaf and Borst, 1992; Fig. 8C). The logic behind this is based on the assumption that Reichardt detectors perform a true multiplication that is similarly implemented on the cellular level. In mathematical terms an On-response can be stated as +1 and an Off-response as -1. When the mentioned stepwise changes are presented following computations are performed: $+1 \times +1 = +1$; $-1 \times -1 = +1$, $-1 \times +1 = -1$ and $+1 \times -1 = -1$ as seen in the recorded signal of the H1 neuron (Fig 8C).

2.4.2 Biological correlates of the motion computation pathway.

Knowledge about the cellular structure of Reichardt detector is poor and rather speculative. Nevertheless, circumstantial evidence is steadily increasing with new interesting approaches. The known facts will be described next from an anatomical point of view, starting from the outer most retina and ending with LPTCs (for an anatomical overview see section 2.2).

2.4.2.1 Motion detection in the retina

To reveal the relative locations of the Reichardt detector input channels, sophisticated optics were used to present virtual or apparent motion stimuli while recording from H1. Sequential stimulation of single ommatidia (Schuling et al., 1989) or even single photoreceptors (Franceschini et al., 1989; Riehle and Franceschini, 1984) revealed that successive stimulation of photoreceptors R1 and R6 within one single ommatidium is sufficient to elicit directionally selective responses in H1 (Franceschini et al., 1989; Riehle and Franceschini, 1984). In addition, interactions between individual ommatidia separated by up to eight times the inter-ommatidial angle were shown to contribute to the response of the neuron (Schuling et al., 1989).

Evidence that suggests that just the information passed on by R1-R6 is important for motion detection has come from the *Drosophila* mutant *ora* (outer rhabdomere absent) and *sev* (sevenless; Harris et al., 1976; Heisenberg and Buchner, 1977). *sev*, which misses its R7 photoreceptor, exhibits qualitatively normal optomotor behavior, whereas *ora*, which lacks R1-R6, is severely affected (Heisenberg and Buchner, 1977). This leads to the assumption that color vision in *Drosophila* is not primarily involved in motion vision, since R7/R8 are part of the chromatic and R1-R6 of the achromatic system. Further support for this view comes from recent experiments where an equiluminant grating of alternating colored stripes elicited zero optomotor responses (Yamaguchi et al., 2008).

2.4.2.2 Motion detection in the lamina

Exploring the next cellular neuropile, the lamina, four different channels exist that could feed signals from the retina into the motion detection circuitry. There are three lamina monopolar cells, L1 to L3, which receive photoreceptor input from R1-6, but differ with respect to their postsynaptic partner in the medulla and the T1 cell, which receives indirect input from R1-6 via an amacrine cell. Using different cell-specific driver lines for the monopolar cells a series of elegant experiments was performed to dissect their contribution to visual motion detection (Katsov and Clandinin, 2008; Rister et al., 2007). First, the expression of the temperature-sensitive allele of dynamin, called *shibire^{ts}* (Vanderbliek and Meyerowitz, 1991; see also section 2.7), blocked synaptic transmission in L1 and L2. Second, rescuing the transmission from R1-6 onto either L1 or L2, or both, by selectively expressing the histamine receptor encoded by *ort* in a histamine-receptor null mutant. Any effect of a reconstitution or a temperature sensitive block on behavior would indicate sufficiency or necessity of the respective pathway. When such flies were used in an optomotor paradigm, it was shown that L1 and L2 together are necessary and sufficient for motion detection, thus excluding L3 and the amacrine cell-T1 pathway as providing essential input necessary for motion detection. Full redundancy of L1 and L2 was only given at high pattern contrast. At intermediate pattern contrast L1 and L2 seem to mediate motion vision in opposite directions, whereas at very low contrast, both the L1 and L2 pathways were needed for motion detection in any direction. Thus, this study demonstrates the

significance of L1 and L2 as input lines to the visual motion detection circuitry and indicates a differential contribution of L1 and L2.

In *Drosophila*, L2 innervates the lamina neurons L4 in the same cartridge, which reciprocally synapse with two conspicuously backward oriented collaterals onto two L2 neurons in posterior cartridges. Furthermore the L4 neurons are directly connected to all six neighboring L4s (Meinertzhagen and O'Neil, 1991). It has been speculated that this circuitry might be specialized in front-to-back motion (Braitenberg and Debbage, 1974), the prevalent direction in the visual flow-field of fast forward-moving animals. A recent behavioral study used cell specific expression of tetanus neurotoxin light chain (TNT; Sweeney et al., 1995; see also section 2.7) to block chemical synapses. In this study, flies with L4 blocked completely lost optomotor responses but retained wild-type phototactic behavior (Zhu et al., 2009). However, this results are drawn into question by our experiments (Chapter 7).

2.4.2.3 Motion detection in the in the medulla and lobula

Based on the anatomical analysis of horizontal and vertical sensitive LPTCs, four different strata have been found in which these LPTCs extend their dendrites. These layers have also been labeled using the 2-deoxy-glucose (2-DG) method (Buchner et al., 1984), in which flies were fed with a none-degradable radioactive glucose (2-DG) and became stimulated with a moving grating on one eye and a flicker stimulus on the other for 4 hours. Combining the analysis of the layers labeled by 2-DG activity with co-ramification studies of cells located in identical strata of the medulla and lobula revealed the neurons that putatively supply input to the LPTCs. These are the so called bushy T4- and T5-cells that terminate in each of the four strata of the lobula plate (Strausfeld and Lee, 1991). This reasoning led to the proposal of two different cellular pathways from the photoreceptors to the LPTCs (Bausenwein et al., 1990; Strausfeld, 1984; Fig 9). It needs to be emphasized that to date neither physiological nor ultrastructural data exist to solidify these presumptions. The only exception is an electron microscopy study in the blowfly that has unequivocally shown a chemical synapse between an HS-cell dendrite and a columnar T4-cell (Strausfeld and Lee, 1991).

2.4.2.4 Motion detection in the in the lobula plate

The subtraction of local motion detector signals with opposite preferred direction is supposed to be implemented on the dendrites of LPTCs (Borst and Egelhaaf, 1990; Egelhaaf et al., 1990; Gilbert, 1991). This conclusion was drawn from experiments using the GABA-receptor antagonist picrotoxin (Egelhaaf et al., 1990) and current clamp experiments with negative and positive DC current injections (Borst et al., 1995; Borst and Egelhaaf, 1990; Gilbert, 1991) while presenting drifting visual gratings to the fly. According to these studies the subtraction stage of the Reichardt detectors is implemented as a push-pull mechanism, where excitatory cholinergic (Brotz and Borst, 1996) and inhibitory GABAergic (Brotz and Borst, 1996) inputs become spatially integrated on the LPTC dendrites.

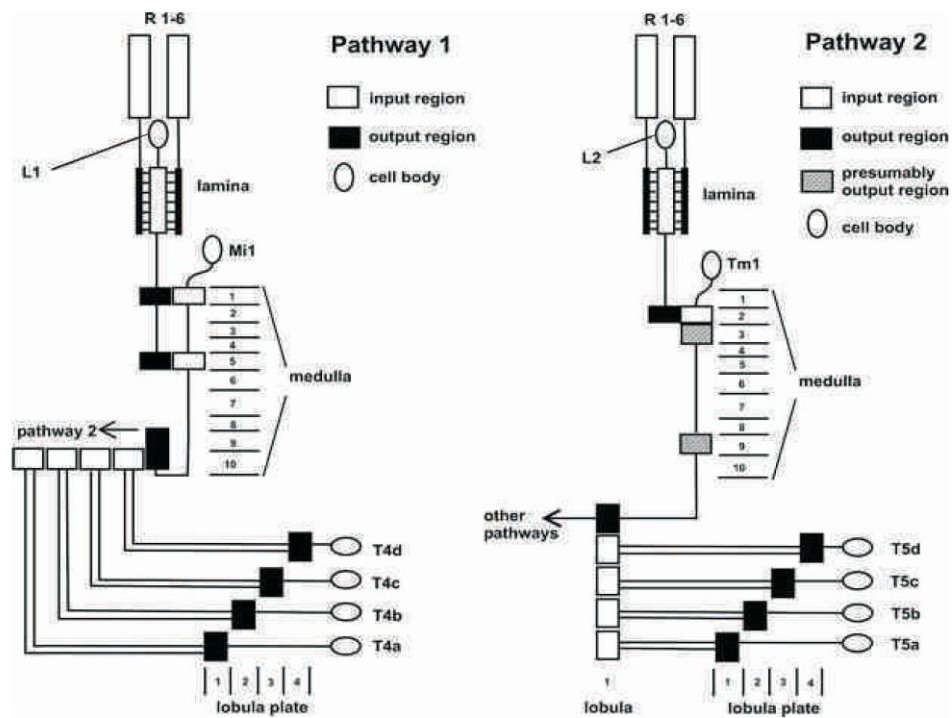


Fig 9. Different proposed pathways for motion vision. One pathway uses the photoreceptors R1-6 that impinge onto the lamina neuron L1. L1 in turn activates the intrinsic medulla neuron Mi1 that synapses onto T4-cells, which then connects to LPTC dendrites. Another potential pathway, which also originates in R1-6, uses the lamina neuron L2. L2 connects to the trans-medulla neuron Tm1, which connects to the most posterior stratum of the lobula. There it contacts T5 cells, which bring the information onto LPTC dendrites (Bausenwein et al., 1992).

2.4.3 Motion computation in other organisms

Directionally selective neurons have been described in the visual cortex of cats (Hubel, 1959; Hubel and Wiesel, 1959), the optic tectum of frogs and pigeons (Lettinger et al., 1959; Matruana and Frenk, 1963), in retinal ganglion (Barlow et al., 1964) and starburst amacrine cells (Euler et al., 2002) of the retina of rabbits, turtles, salamanders and mice and in the area MT (Albright et al., 1984; Dubner and Zeki, 1971) of macaques and many other animals. Intriguingly, the neuronal mechanisms underlying motion detection in these cells appear to be based on different neuronal implementations. Whereas motion sensitivity in the LPTCs is computed by a “Reichardt detector”, motion selectivity in the retina has different fingerprints. The most striking difference is that the nonlinearity described by the true ‘sign’ multiplication is absent. In this case two mechanisms have been proposed: a presynaptic one, based on direction selective starburst amacrine cells (Euler et al., 2002; Hausselt et al., 2007), and a postsynaptic one (Barlow and Levick, 1965; Fried et al., 2002), based on the interplay of inhibitory starburst amacrine cells on postsynaptic direction selective retinal ganglion cells (for review (Fried and Masland, 2007; Wässle, 2004)). Moreover, very recently, a new directionally selective retinal ganglion cell type was described that does not stratify in the starburst amacrine cell layer (Kim et al., 2008), giving rise to the question about the cellular implementation of the motion detection pathway.

The ubiquitous presence of motion selective units in the animal kingdom supports the notion of the fundamental importance of this computation for survival. Nevertheless, the underlying computations are in no case completely understood. Being a computationally precisely described problem and being implemented in relatively ‘simple’ neuronal networks, visual motion detection has emerged as one of the most attractive problems to analyze complex computations in the brain. In this regard, newly developed genetic tools in the mouse retina (Huberman et al., 2009; Kim et al., 2008; Siegert et al., 2009) and in *Drosophila* are opening exciting possibilities in this field of research.

2.5 The genetic armory of *Drosophila melanogaster*

In order to understand the principles of information processing in neural circuits a systematic characterization of the participating cell types and their connections is

required. Even in the optic lobe of big flies, the small size of the constituting interneurons, whose processes can be thinner than 100 nm, and the extremely tight and complex cellular network impeded reliable electrophysiological approaches so far (but see Douglass and Strausfeld, 1995; Douglass and Strausfeld, 1996). One prominent exception has been the LPTCs of big flies like *Calliphora vicina*, which due to their larger size are electrophysiologically approachable (see section 2.3.4). Nevertheless, their input elements and consequently the network interactions involved in the computation of motion information are not understood. To overcome this problem, new genetic approaches in *Drosophila* promise to provide experimental access to such a complex neural system. Using the ability to measure and alter neural activity in genetically determined populations of neurons is expected to reveal the logic of the neural circuits that guide behaviors. In the next paragraph the most important genetic tools available in *Drosophila* will be discussed (reviewed in (Borst, 2009; Luo et al., 2008)).

The “Swiss army knife” of *Drosophila*’s genetic toolbox is the two-component Gal4/UAS-system for targeted transgene expression (Brand and Perrimon, 1993; Fig. 10 top). In this system, a genomic enhancer activates the yeast transcription factor (Gal4) which can activate and amplify the expression of any gene of interest (in Fig. 10 noted as “gene X”) that is under control of the appropriate upstream activating sequence (UAS; Fig. 10 top). This system can be used to identify, activate or inactivate genetically defined cell types, depending on the transgene (“gene X”) expressed. To restrict the expression in an even more defined population of neurons, several tricks have been invented. One is the Split-Gal4 system (Luan et al., 2006), a combinatorial approach in which the DNA-binding domain and the activation domain of Gal4 are expressed under the control of different promoters with partly overlapping expression patterns. Only in those cells where both Gal4 subunits are expressed functional Gal4 is formed. Another approach to reduce the expression pattern is the so called MARCM-system (Lee and Luo, 1999). This system uses induced mitotic recombination between homologous chromosomes to eliminate the Gal4 repressor Gal80 (Lee and Luo, 1999) in order to genetically highlight or express a specific gene in single cells or a small population of neurons. However, the outcome of the recombination is random, confining this technique primarily for anatomical studies. Interestingly, the repressor Gal80 can also be used for a genetic reduction of Gal4-expression. Similar to the Split-Gal4 system, the expression pattern of a specific Gal4 line can be constrained if a partly

overlapping Gal80 expression is superimposed. Finally, the most promising approach that will enable the expression of an exogenous gene in distinct small subset of the adult fly brain has been developed recently. Using a site-specific genomic integration methodology to insert thousands of defined enhancer sequences in the fly's genome, thousands of transgenic fly lines are currently developed to encompass all neurons in the brain in a variety of intersecting patterns (Pfeiffer et al., 2008). Highly specific and reproducible expression patterns will be cardinal for the clean and exact dissection of neuronal circuits the fly brain.

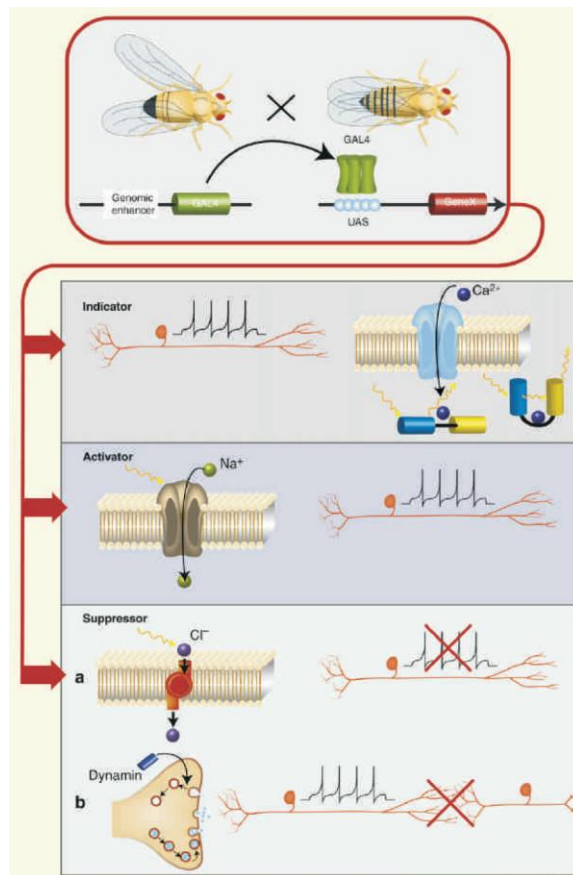


Fig. 10. Genetic toolbox available in *Drosophila*. (top box) The Gal4-UAS-system allows transgenic expression of any gene of choice ('Gene X') in specific populations of neurons. (Top red arrow) Schematic of a ratiometric genetically encoded calcium indicator. This probe allows imaging calcium fluctuations as a read-out for neuronal activity in genetically defined populations of cells. (Middle and lower red arrows) Genetically encoded photosensitive channels can either excite or inhibit neuronal activity when stimulated with light. Disruptors of synaptic release can silence synaptic output in defined populations of cells (from (Borst, 2009)).

Three main transgenic effectors can be used to dissect neuronal circuit functions. The first one is the transgenic expression of a fluorescent protein, such as GFP (Green

Florescent Protein; Chalfie et al., 1994), which allows precise anatomical studies in specified groups of cells(REF). Combining GFP with calcium sensing proteins, like Troponin or Calmodulin (Heim and Griesbeck, 2004; Miyawaki et al., 1997; Nakai et al., 2001), or making GFP pH sensitive (Miesenbock et al., 1998), enabled the use of these probes for imaging of neuronal activity (Reiff et al., 2002; Reiff et al., 2005) and synaptic release (Ng et al., 2002), respectively (Fig 10. top red arrow). To activate or silence neurons, pioneering work has been performed in the last years to develop photosensitive channels (Seki et al., 2007; Szobota et al., 2007; Zemelman et al., 2002; Zemelman et al., 2003; Zhang et al., 2007). These channels can be expressed in defined populations of neurons, allowing functional dissections by light of neuronal circuitries in flies (Lima and Miesenbock, 2005; Schroll et al., 2006; Fig. 10 middle red arrow and bottom red arrow upper insert). Another family of channels that can be activated are the temperature sensitive TRP-channels. These channels react to cold or heat by changing their conductance and thus can influence neuronal activity (Hamada et al., 2008; Peabody et al., 2009). Finally, a set of proteins are known to disrupt synaptic output. The most prominent one is *shibire^{ts}*, a dominant negative temperature sensitive allele of dynamin, which allows synaptic transmission at a permissive temperature and blocks it at around 30 °C (Vanderbliek and Meyerowitz, 1991; Fig. 10. bottom insert). Another widely used disruptor is tetanus neurotoxin light chain (TNT; Sweeney et al., 1995) which cleaves synaptobrevin and thus blocks synaptic transmission irreversibly.

Some interesting behavioral and anatomical studies have already taken advantage of this set of genetic tools to analyze circuit function in the fly's optic lobes (Gao et al., 2008; Katsov and Clandinin, 2008; Raghu et al., 2007; Raghu et al., 2009; Rister et al., 2007; Zhu et al., 2009) and demonstrate the strength of this approaches (see section 2.4.2.2 & results, for review (Borst, 2009)).

2.6 Project goals and achievements

The work presented here aims at expanding the current knowledge of visual information processing in the fly brain. I focus on the fruit fly's motion detection network and the subsequent course control circuitry. For this purpose I took advantage of *Drosophila melanogaster* as a genetic amenable organism. *Drosophila* enables a genetic dissection of defined neuronal circuitries. In doing so, I establish for the first

time an electrophysiological approach to characterize genetically targeted large-field tangential cells in the fruit fly (LPTCs). This allowed me to record the LPTC responses that turned out to be motion sensitive. When presenting motion stimuli to the fly two different groups of LPTCs, the VS- and HS-cells, responded with a depolarizing graded potential shift with superimposed spikelets in their preferred direction and a hyperpolarizing graded shift when presenting motion in the opposite direction. Moreover, their basic response properties satisfy the predictions of the Reichardt detector model. This validates the assumption that in different dipteran flies motion vision is accomplished in similar circuitries and according to common algorithmic rules (Chapter 4 & 6; Jösch et al., 2008; Schnell et al., *submitted*). Furthermore, I analyzed the complex receptive fields of LPTCs by developing a new stimulus paradigm. I found that frontal VS-cells (VS1-VS4) are primarily sensitive to vertical motion and that their maximal responses shift from frontal (VS1) to more lateral (VS4). In contrast, VS5 and in particular VS6 turned out to be more sensitive to rotational stimuli with the center of rotation at 25° and 50° , respectively. HS-cells have their maximal sensitivity in different horizontal planes with the most dorsal HSN being most sensitive to dorsal motion stimuli and the most ventral HSS to ventral stimuli (Chapter 6 & 7; Schnell et al., *submitted*; Jösch et al., in preparation). Moreover, HS- and VS-receptive fields appear to be wider than expected from a scheme that assumes retinotopically organized input. We performed Neurobiotin perfusions of single VS- and HS-cells and found indirect evidence of electrical connections within cells of each group. In essence, this suggests that the expansion of the width of the receptive field arises from electrical coupling. All together, these results open the way for further investigations of specific properties of the network. An obvious example would be the analysis of the molecular key players that mediate the widening of the receptive fields of LPTCs. Moreover, the functional relevance of electric coupling can be analyzed by combining genetic manipulation with behavioral experiments. Thus, the full approach establishes the link between molecules, network function and the animal's behavior. Most importantly, the identification of cells and cellular mechanisms that accomplish visual motion detection will enable us to establish a biophysically realistic model of the Reichardt detector.

In parallel, I contributed important information to two studies that addressed the synaptic organization of LPTCs. Using cell-specific expression of transgenes encoding receptors and presynaptic molecules both either tagged with GFP or a his-tag we found that LPTCs are postsynaptic in the lobula plate and presynaptic in the

protocerebrum. The expression of Acetylcholine- and GABA-receptors on the fine dendritic branches suggests that presynaptic input is provided by excitatory and inhibitory input from motion-sensitive elements with opposite preferred direction. Interestingly, LPTCs receive additional GABAergic input on their axonal termini in the protocerebrum, shaping the output of LPTCs in an unknown way. These functional anatomical studies lay the ground for future compartmental models of the motion detection network (Chapter 3 & 5; Raghu et al., 2007; (Raghu et al., 2009).

Finally, I could improve the electrophysiological technique and optics to record from unlabeled LPTCs. This development allowed me to use the Gal4/UAS system that previously was needed to fluorescently highlight LPTCs, to disrupt presynaptic elements in the lamina without affecting LPTCs. Using targeted expression of tetanus neurotoxin light chain I started blocking synaptic release from specified populations of lamina monopolar cells while recording the responses of LPTCs. Disrupting L1,L2 and L3 caused a complete block of LPTC motion responses. Interestingly, when blocking either L1 or L2, no major difference was found compared with wild-type responses when presenting a moving grating. However, specific response deficits became obvious when moving edges of single contrast polarity were used as visual stimuli instead of gratings. These findings suggest that the visual input stream to the motion detection circuitry is segregated into ON- and OFF-channels, carrying information about increasing or decreasing image contrast separately. Moreover, the segregation of the input channels is in line with a four quadrant multiplication model (Hassenstein & Reichardt, 1956) that challenges the existence of a “true sign” multiplication implemented in the fly’s motion detection circuitry.

In summary, my work paved the way for the cellular and functional analysis of motion vision and course control in *Drosophila*.

3 Manuscript Nr.1

Synaptic Organization of Lobula Plate Tangential Cells in *Drosophila*: GABA-receptors and chemical release sites.

This chapter was published in 2007 in the Journal of Comparative Neurology Volume:
502; Pages: 598-610 by Shamprasad Varija Raghu, Maximilian Jösch,
Alexander Borst & Dierk F. Reiff

Max-Planck-Institute of Neurobiolog
Department of Systems and Computational Neurobiology
Am Klopferspitz 18
D-82152 Martinsried, Germany

Shamprasad Varija Raghu performed and analyzed the experiments concerning the genetic manipulations, immunohistochemistry and anatomy. Maximilian Jösch developed and performed a method to fill single lobula plate tangential cells for immunohistochemic and anatomical analysis. Shamprasad Varija Raghu, Dierk Reiff and Alexander Borst conceived the experiments. Shamprasad Varija Raghu and Dierk Reiff wrote the manuscript.



Abstract

In flies, the large tangential cells of the lobula plate represent an important processing center for visual navigation based on optic flow. While the visual response properties of these cells have been well studied in blowflies, information on their synaptic organization is mostly lacking. Here, we study the distribution of presynaptic release and postsynaptic inhibitory sites in the same set of cells in *Drosophila melanogaster*. Making use of transgenic tools and immunohistochemistry, our results suggest that HS- and VS-cells of *Drosophila* express GABA receptors in their dendritic region within the lobula plate, thus being postsynaptic to inhibitory input there. At their axon terminals in the protocerebrum, both cell types express Synaptobrevin suggesting the presence of presynaptic specializations there. Superimposed on this synaptic polarity, HS- and VS-cell terminals additionally show evidence for postsynaptic GABAergic input. Our findings are in line with the general circuit for visual motion detection and receptive field properties as postulated from electrophysiological and optical recordings in blowflies, suggesting a similar functional organization of lobula plate tangential cells in both species.

Introduction

Self motion of an observer causes the images of the environment to shift on its retina. The resulting distribution of motion vectors in the visual field is called 'optic flow' and represents a rich source of information about the exact type of self motion. Therefore, optic flow information is heavily used for navigation and visual course control. However, before that, visual motion stimuli need to be processed in a number of steps. First, local motion information has to be computed from the time-varying brightness values at each retinal location (Reichardt 1961, 1987; Borst and Egelhaaf, 1989). In a second step, the spatial distribution of the local motion vectors has to be analyzed in order to be indicative for any specific maneuver (Koenderink and van Doorn, 1987).

In flies, the wide field lobula plate tangential cells (LPTCs) present in the posterior part of the third optic neuropil called the 'lobula plate' are specifically tuned for particular optic flow patterns. In *Calliphora vicina*, LPTCs represent a group of about 60 cells per hemisphere each of which can be identified individually due to its characteristic anatomy and visual response properties (Hausen, 1982a, b, 1984; Hengstenberg et al., 1982). Amongst these cells, there exist a group of three cells mostly sensitive to horizontal image motion as occurring during rotation around the fly's vertical body axis called HS-cells, and another set of 10 cells, sensitive to rotation around different axes within the equatorial plane of the fly, called VS-cells (VS1 through 10; Hengstenberg et al., 1982; Krapp and Hengstenberg, 1997). In *Drosophila melanogaster*, different VS- and HS-cells as well as all columnar neurons have been well described on the morphological level (Scott et al., 2002; Fischbach and Dittrich, 1989; Heisenberg et al., 1978; Rajashekhar and Shamprasad, 2004). As in *Calliphora*, the dendrites of the different VS-cells cover rather narrow and overlapping vertical stripes within the lobula plate. However, in contrast to their large cousins, there seem to exist only 6 VS-cell in *Drosophila*, based on the analysis of the Gal4 line 3A (Scott et al., 2002), as opposed to 10 in *Calliphora* (Hengstenberg et al, 1982; Krapp et al., 1998). The HS-system comprises three individually identifiable cells – the northern HSN-, the equatorial HSE- and the southern HSS-cell, in *Drosophila* as well as in *Calliphora* (Hausen, 1982a). The dendrites of these cells cover a rather wide area within the lobula plate, resulting in significant overlap of their dendritic fields (Fischbach and Dittrich, 1989, Scott et al., 2002). Their axons travel medially and terminate in the protocerebrum near the esophagus.

Many visual response characteristics of LPTCs, such as their dependence on pattern properties like velocity, contrast and spatial frequency, are appropriately described by the so-called Reichardt model of local motion detection (Reichardt, 1961, 1987; Egelhaaf et al., 1989; Borst and Egelhaaf, 1989). Reichardt detectors provide a direction-selective signal by correlating the luminance levels in adjacent retinal locations, after they have been temporally filtered in an asymmetric way. At each retinal location this correlation process is done twice in a mirror symmetric way, after which the signals become subtracted from each other. Such detectors are thought to exist along the horizontal as well as along the vertical image axis and to be realized by small-field columnar elements in the medulla and lobula, the second and third neuropil in the fly optic lobe (Buchner et al., 1984; Douglass and Strausfeld, 1995; Brotz and Borst, 1996). Most importantly in the present context, the final stage of local processing, i.e. the subtraction of opposing motion signals, is thought to be represented, together with the spatial integration of local motion signals, within the large LPTC dendrites, by excitatory and inhibitory columnar elements, synapsing onto the dendrites of LPTCs in a retinotopic way (Borst and Egelhaaf, 1990; Borst et al., 1995; Haag et al., 1992; Single et al., 1997; Single and Borst, 2002). However, this type of dendritic input is not sufficient to explain the spatial lay-out of the receptive fields observed in LPTCs. In addition, LPTCs turn out to be heavily connected amongst each other, both within one hemisphere and between both hemispheres, through chemical as well as electrical synapses (Haag and Borst, 2001, 2002, 2003, 2004, 2005). As has been demonstrated by single cell ablation experiments, the width of the receptive fields of VS-cells is substantially enlarged by the input individual VS-cells receive from their neighbors via gap junctions and furthermore shaped by distal VS-cells inhibiting each other mutually (Haag and Borst, 2004; Farrow et al., 2005). Being tuned to specific optic flow patterns directly through the input onto their dendrites, as well as indirectly by their network connectivity with many other tangential cells, LPTCs convey this information onto descending neurons in the protocerebral region, which ultimately control motor neurons for flight and head movements (Gronenberg and Strausfeld, 1990; Gilbert et al., 1995).

Many of the neurons of the motion detection pathway have been characterized in great anatomical (Hausen 1982a, b; Fischbach and Dittrich, 1989; Strausfeld and Bassemir 1985a, b) and physiological details (Douglass and Strausfeld, 1995, 1996; Hengstenberg et al., 1982; Hausen, 1984; Gronenberg and Strausfeld, 1990).

However studies providing direct anatomical evidence for synaptic contacts between these different neurons are relatively sparse. Only three electron microscopic studies have been performed so far on the distribution of chemical synapses on different LPTCs. They provided evidence for chemical synaptic sites on some VS-, HS-, Col A- and CH-cells (Hausen et al., 1980; Gauck et al., 1997) and proved chemical synaptic contact between an HS-cell and the small field columnar T4 cell from the medulla (Strausfeld and Lee, 1991). Interestingly, the analysis of CH-cells revealed that the designation of dendrites and axon terminals as sites of synaptic in- and output, respectively, based on their anatomy and orientation along the assumed visual pathway does not correspond to their functional properties. CH-cell dendrites within the lobula plate possess pre- as well as postsynaptic specializations while their protocerebral ramifications turned out to be purely postsynaptic. Pharmacological and histochemical studies provided evidence for acetyl choline receptors (Sattelle, 1980) and Rdl-type dieldrin resistant GABA receptor subunits (Ffrench-Constant et al., 1990) on the dendrites of LPTCs (Brotz and Borst, 1996; Brotz et al., 2001). However, these studies did not allow to clearly assign the observed antibody stainings to identified single cells, and the protocerebral terminals have not been analyzed.

Drosophila melanogaster offers a number of transgenic tools suitable to precisely address such analysis in individual LPTCs. In the following, we focus our studies on the distribution of chemical synapses in HS- and VS-cells in *Drosophila*. We used the Gal4-UAS system (Brand and Perrimon, 1993) to highlight entire cells and simultaneously target different synaptic marker proteins in VS- and HS-cells. Briefly, the system consists in crossing a Gal4-driver line determining in which cells a given gene shall be expressed with a UAS-reporter line determining which gene is being expressed in these cells. The driver line brings in the yeast transcriptional activator Gal4 (for which no natural recognition sequence exists in wild-type fly strains) under the control of a cell-specific enhancer. The UAS-reporter line houses a transgene cloned right behind a Gal4 responsive, upstream activating sequence (UAS). Only in cells that express Gal4 the transcription of the reporter gene will be activated and the reporter protein will ultimately be expressed. To visualize whole cells or different pre- or postsynaptic sites, indicator flies were used containing the following DNA constructs, all under control of the UAS sequence: i) Whole cells were visualized by using a transmembrane protein (mCD8) fused with the green fluorescent protein (GFP). This construct will be called 'UAS-mCD8-GFP' (Lee and Luo, 1999). ii) To visualize cytoskeletal parts of the cell, we

used the DNA for actin fused to the one coding for green fluorescent protein (GFP). This construct is called 'UAS-actin-GFP' (Verkhusha et al., 1999). iii) To mark presynaptic release sites, we used a fusion protein which consists of the synaptic vesicle protein Synaptobrevin (Trimble et al., 1988; Baumert et al., 1989; DiAntonio et al., 1993) and the monomeric form of the red fluorescent protein mDsRed. This construct is called 'UAS- nSyb-mRed' (see methods). iv). To mark inhibitory postsynaptic sites, we used DNA coding for the Rdl receptor (Ffrench-Constant et al., 1990) fused to a small Hem-Agglutinin (HA) tag against which antibodies were directed to visualize them. This construct is called 'UAS- Rdl-HA' (Sa'nchez-Soriano et al., 2005). Small number and single cell clones expressing different combinations of these UAS-reporters were generated by Mosaic Analysis using a Repressible Cell Marker (MARCM, Lee and Luo, 1999). The technique is described in great detail elsewhere. In brief, MARCM relies on the ubiquitous co-expression of Gal80 which represses Gal4-UAS-mediated gene expression. However, the gene encoding Gal80 can be eliminated from dividing cells by heat-induced recombinatory events between the homologous chromosomes. As a result, a small subset or only a single cell of the primary enhancer - Gal4 pattern will execute the UAS-controlled reporter expression. Alternatively, single cells were stained by intracellular dye injection. Both methods were combined with antibody stainings against the inhibitory neurotransmitter GABA. As a result, the present study suggests distinct inhibitory postsynaptic sites on the dendrites of both VS- and HS-cells. In contrast to CH-cells in *Calliphora*, neither VS- nor HS-cells show any signs of presynaptic specializations within their dendrites within the lobula plate as revealed by the mentioned techniques and laser scanning confocal microscopy. The axon terminals of *Drosophila* VS- and HS-cells, however, show evidence for both pre and postsynaptic sites. Thus these cells likely receive chemical input from both the lobula plate and the protocerebral region. The chemical output of both cell types, as revealed on the non-EM level, is strictly confined to the protocerebral element of these cells. These findings about the particular polarity and distribution of inhibitory input to VS- and HS-cells will be discussed in the functional context of visual motion detection, receptive field properties and visual course control.

Materials and methods

Fly culture. *Drosophila melanogaster* were grown on standard corn medium at 25 °C, 12:12 hours dark: light cycle and 60 % humidity. For all experiments flies were kept in 30 ml - vials containing ~ 10 ml food. All flies behaved entirely normal. The flies did not show any obvious deficits and thus no specific tests were done.

Molecular biology, fly strains and MARCM analysis. We used the Gal4-UAS system to direct gene expression to defined populations of neurons within the *Drosophila* brain (Brand and Perrimon, 1993). The previously described (Scott et al., 2002) enhancer trap line Gal4-3A (kindly provided by M. Heisenberg, Wuerzburg) was crossed to the following UAS-reporter fly lines: UAS-mCD8-GFP (Lee and Luo, 1999, kindly provided by L. Luo, Stanford), UAS-actin-GFP (Verkhusha et al., 1999, kindly provided by H. Oda, Kyoto, Japan), UAS-Rdl-HA (Sańchez-Soriano et al., 2005, kindly provided by A. Prokop, Manchester) and UAS-nSyb-mRed. UAS-nSyb-mRed flies were generated as follows: the cDNA of neuronal synaptobrevin (nSyb, DiAntonio et al., 1993, cDNA kindly provided by D. Deitcher, Ithaca, New York) was amplified via PCR. The stop codon was removed and a 3' EcoRI and 5' NotI site was added. Monomeric DsRed (mRed, Campbell et al., 2002, cDNA kindly provided by R.E. Tsien, San Diego) was amplified introducing a 3' NotI and a 5' XbaI site. Both cDNAs were subcloned into the pUAST-vector (Brand and Perrimon, 1993) such that mRed was fused to the C-terminal end of nSyb. Transgenic flies were generated via standard techniques using P-element mediated germ line transfection (Spradling and Rubin, 1982). For all our experiments an x-chromosomal UAS-nSyb-mRed insertion was used.

Female experimental flies in which the full Gal4-3A expression pattern was employed had the following genotypes: UAS-nSyb-mRed/+; UAS-mCD8-GFP/+; Gal4-3A/+ (Coexpression of mCD8-GFP and nSyb-mRed), +/+; UAS-mCD8-GFP/UAS-Rdl-HA; Gal4-3A/+ (Coexpression of mCD8-GFP and Rdl-HA) and +/+; UAS-actin-GFP/UAS-Rdl-HA; Gal4-3A/+ (Coexpression of actin-GFP and Rdl-HA).

Restricted Gal4-3A expression patterns were created by clonal analysis using the MARCM technique (Lee and Luo, 1999). We generated female experimental flies of the genotype hs-FLP, UAS-mCD8-GFP/ UAS-nSyb-mRed; FRT^{40A}/FRT^{40A}, tubP-Gal80; Gal4-3A/+. For the induction of mitotic recombination eggs were collected at one hour

intervals. The emerged larvae were exposed to heat shocks (45 to 60 minutes in a 37 °C water bath) two and three days after hatching. A fluorescence stereomicroscope (Leica MZ16FA) was used to select three to five day old flies that showed GFP and mRed expression.

Immunohistochemistry. Female flies three to five days after eclosion were dissected. Their brains were removed and fixed in 4 % paraformaldehyde for 30 minutes at room temperature. Subsequently, the brains were washed for 45 - 60 minutes in PBT (phosphate buffered saline (pH 7.2) including 1 % Triton X-100). For antibody staining, the samples were further incubated in PBT including 2 % normal goat serum (Sigma Aldrich, G9023) and primary antibodies (1: 200, overnight at 4 °C). Antibodies were removed by several washing steps (5 x 20 minutes in PBT) and secondary antibodies were added (1: 200, overnight at 4°C). A 5 x 20 minutes washing protocol (PBT) was followed by final washing steps in PBS (5 x 20 minutes). The stained brains were mounted in Vectashield (Vector Laboratories, Burlingame) and analyzed by confocal microscopy (see below).

The following primary and secondary antibodies were used in the present study. *Primary antibodies:* Alexa Fluor 488 rabbit anti-GFP-IgG (catalog number-A-21311, lot number-37766A, Molecular Probes; Huang et al., 2005; Reiff et al., 2005), monoclonal rat anti-HA (catalog number-11867423, lot number-11928100, Roche; Sa'nchez-Soriano et al., 2005) and polyclonal rabbit anti-GABA (Catalog number-ab8891, lot number-99876, Abcam; Papay et al., 2006; Buijs et al., 1987). The specificity of Alexa Fluor 488 rabbit anti-GFP-IgG antibody was tested in brain tissues from UAS-mCD8-GFP flies and that of rat anti-HA antibody in UAS-Rdl-HA flies in the absence of the Gal4-driver. The GABA antibody was raised in rabbit by immunizing with GABA-glutaraldehyde-lysine conjugates. The specificity of this antibody was tested in the rat brain previously (Buijs et al., 1987). As a control for specificity of this antibody, *Drosophila* brains were incubated with GABA antibody that was preabsorbed with GABA-glutaraldehyde-BSA\GABA-glutaraldehyde-lysine conjugates as described by Buijs et al. (1987). The results from all control experiments for the primary antibodies are illustrated in the supplementary Fig.1. *Secondary antibodies:* Alexa Fluor 568 goat anti-rat-IgG (catalog number-A11077, lot number-40136A, Molecular Probes), Alexa Fluor 405 goat anti-rabbit-IgG (catalog number-A31556, lot number-37764A, Molecular Probes).

Intracellular dye filling. UAS-GCaMP1.3 (Reiff et al., 2005) expressing flies (driven by Gal4-DB331, kindly provided by R. Stocker, Fribourg) were used to target LPTCs for intracellular dye injection. GCaMP1.3 was chosen for its detectable but low fluorescence level at resting intracellular calcium. These flies were decapitated and the cut heads were fixed in a layer of two-component glue (UHU Plus, UHU GmbH & Co. KG, Baden, Germany) with the facet eyes looking downward into the glue. After hardening of the glue (~2 min) the specimen were covered with Ringer solution and the cuticle at the backside of the fly's head was removed using sharp needles (Neolus, Gx3/4" 0,4 x 20 mm). This procedure allowed direct access to the brain and protease XIV (E.C.3.4.24.31, Sigma, Steinheim, Germany) treatment (1 mg / ml) to partially digest the neurolemma. After two minutes the protease solution was replaced by protease free Ringer solution including several washing steps. Finally the main tracheal branches were removed. Dye fillings were performed using quartz electrodes (QF 100-60-10, Sutter Instrument) pulled on a laser puller (P-2000, Sutter Instrument). Electrodes were filled with a 10 mM Alexa Fluor 594 solution (A10442, Invitrogen GmbH) and backfilled with 2 M KAc / 0,5 M KCl solution. Impaled cells were loaded by negative current pulses for few seconds. Subsequently, the brains were fixed in 4 % PFA for 30 min and antibody staining was performed as described.

Microscopy and Data Analysis. Serial optical sections were taken at 0.5 μm intervals with 1024 x 1024 and 512 x 512 pixel resolution using confocal microscopes (LEICA TCSNT and LEICA SP2) and oil-immersion 40X- (n.a. = 1.25), 63X- (n.a. = 1.4) and 100X- (n.a. = 1.4) Plan-Apochromat objectives. In most cases, coronal sections were taken from the posterior side of the brain. For Figure 1c, horizontal sections were taken in the dorsal region of the brain. The individual confocal stacks were analyzed using Image J (NIH, U.S.A) and Amira 3.1 (Zuse Institute Berlin (ZIB), Berlin) software. The size, contrast and brightness of the resulting images were adjusted with Photoshop® CS (Adobe Systems, San Jose, CA).

Results

The Gal4-3A expression pattern

In the present study we expressed different transgenes in VS- and HS-cells in the *Drosophila* brain. In a first series of experiments the basic expression pattern of Gal4-3A (Scott et al., 2002) was analyzed in female flies (UAS-mCD8-GFP/UAS-mCD8-GFP; Gal4-3A/+). The fluorescence of the membrane tagged marker mCD8-GFP was enhanced by antibody staining against GFP (see methods). This was done to highlight the complete cell population included in the Gal4-3A expression pattern. A widespread GFP-expression was found in the different layers of the optic lobe including the medulla (M), lobula (L) and lobula plate (LP; Fig.1). However, due to their massive GFP expression six VS- and three HS-cells stand out from the surrounding fluorescence and could be easily identified based on a previous anatomical description (Scott et al., 2002; Fig. 1 a and b, arrowheads). Different VS-cells lie serially with their overlapping dendrites stretching out along the dorsal-ventral axis of the lobula plate (Fig. 1 a). Their axons extend to the posterior slope in the peri-esophageal region (Fig. 1 d) where they bifurcate and give rise to two vertically oriented main branches. These vertical branches have few side branches projecting laterally. Anterior to the VS-cells, all three HS-cells, HSN, HSE and HSS (Fig. 1 b) described in *Calliphora* and *Musca* were found in the *Drosophila* lobula plate, as previously shown by Fischbach and Dittrich (1989) and Scott et al. (2002). The dendrites of the HS-cells cover the dorsal (HSN), medial (HSE) and ventral (HSS) parts of the lobula plate (Fig. 1 b).

A horizontal cross section of the optic lobe illustrating the expression pattern of the Gal4-3A driver line is shown in Figure 1 c. At least two distinct layers can be observed in the lobula plate. Dendrites of different VS-cells occupy the posterior layers of the lobula plate whereas HS-cell dendrites occupy the anterior most layers (Fig 1 c). This is in agreement with several different antibody stainings from Brotz et al. (2001) and activity dependent labeling patterns obtained with radioactive labeled 2-deoxy-Glucose (Buchner et al., 1984). Buchner et al. (1984) could further separate the VS- and HS- dendritic layers in layers preferentially responding to the preferred- or null-direction of a moving visual stimulus. In Fig.1 c, the different columnar neurons that are included in the Gal4-3A expression pattern might obscure such a subdivision.

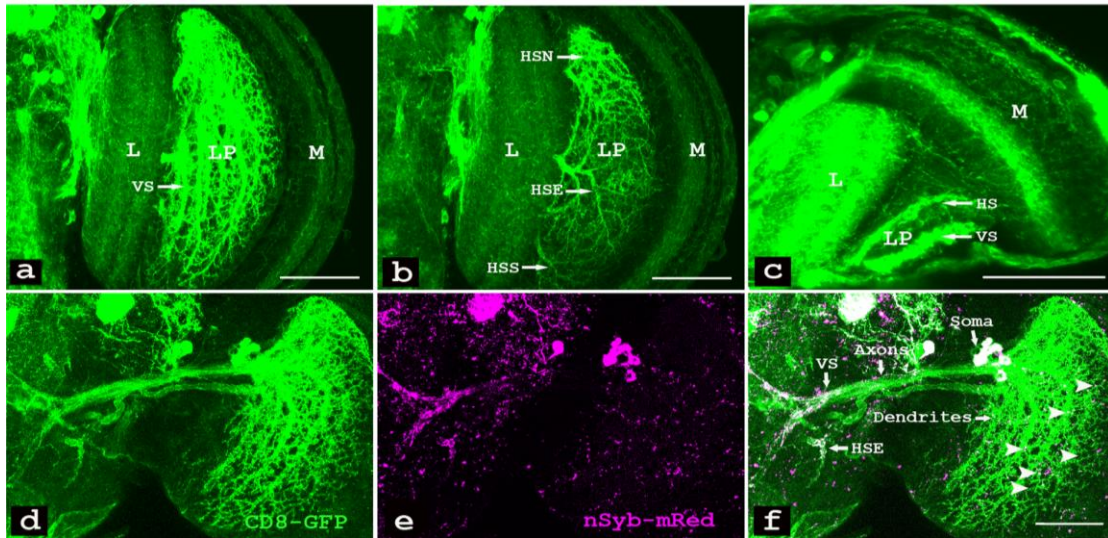


Fig 1. Expression pattern of the enhancer trap line Gal4-3A. Membrane tagged GFP (UAS-mCD8-GFP, green, a-c) and neuronal Synaptobrevin-mRed (UAS-nSyb-mRed, magenta, d-f) were coexpressed in the optic lobe of *Drosophila melanogaster*. **a:** Collapsed image of the posterior part of the optic lobe taken from a frontal view. Expression was found in the medulla (M), lobula (L), lobula plate (LP) and the central brain. In the posterior part of the lobula plate six serially arranged VS-cells extend their overlapping dendrites. **b:** similarly generated frontal view of the anterior lobula plate. Three HS-cells can be identified, the dendrites of HSN, HSE and HSS cover the dorsal, medial and ventral part of the lobula plate, respectively. **c:** Collapsed image of the optic lobe taken from a horizontal view. Dendrites of VS-cells occupy the posterior layer whereas dendrites of HS-cells occupy the anterior most layer of the lobula plate. Gal4-3A driven expression can also be seen in many columnar neurons in the medulla and lobula. **d-f:** Different VS- and HS-cells show coexpression of mCD8-GFP and nSyb-mRed. The fluorescent protein mRed fused to neuronal synaptobrevin labels synaptic vesicles and thus the presumed sites of activity dependent chemical signal transmission. It is important to notice that expression was also driven in a large number of unidentified columnar cells. **d:** Frontal view of the posterior part of the lobula plate. Expression of mCD8-GFP outlines the morphology of different VS-cells. Protocerebral projections of VS-cells travel dorsally and terminate in the dorsal protocerebrum where they bifurcate into two vertical branches from which many lateral branches arises. An HSE-cell projection travels more ventrally to the protocerebrum. **e:** Same section as **d**. Expression of nSyb-mRed shows the presumed chemical output synapses of all cells included in the Gal4-3A expression pattern. **f:** Overlay of (d) and (e). nSyb-mRed expression is most pronounced at the protocerebral ramifications of the VS- and HS-cells. A subtle level of nSyb-mRed expression can also be seen in the dendritic region of the investigated LPTCs (e and arrowheads in f). nSyb-mRed was also found on LPTC cell bodies and cells of the central brain. Image a, b and c are maximum intensity projections of 20, 22 and 40 images, respectively. Images d, e and f are maximum intensity projections of 48 images each. Individual image were taken every 0.5 μm along the z-axis, scale Bar: 50 μm .

Protocerebral projections of VS- and HS-cells express markers for output synapses

To identify possible regions of synaptic output within VS- and HS-cells, we generated UAS-neuronal Synaptobrevin-mRed flies (see methods). Neuronal Synaptobrevin (nSyb; Trimble et al., 1988; Baumert et al., 1989) is a small synaptic vesicle membrane protein with a conserved N-terminal cytoplasmic domain and a small, highly variable, luminal domain to which mRed was fused. nSyb was chosen as it represents a widely used marker for presynaptic vesicles across different species due to its high level of conservation from mammals to *Drosophila* (Sudhof et al., 1989; DiAntonio et al., 1993). In this construct, the fluorescent protein mRed (Campbell et al., 2002) is used to visualize nSyb. Flies co-expressing nSyb-mRed and mCD8-GFP under the control of the Gal4-3A driver line were used (UAS-nSyb-mRed/+; UAS-mCD8-GFP/+; Gal4-3A/+). The assumed axonal terminals of all VS-cells were found to be located in close proximity to each other within the protocerebrum. Here, they showed a high level of nSyb-mRed. This observation strongly suggests that the protocerebral projections act as the actual sites of axonal output (Fig. 1d-f). nSyb-mRed localization was most pronounced at sites where the axon terminals bifurcate into two vertical branches. The protocerebral terminals of HS- cells revealed a similar expression pattern (Fig. 1d-f) suggesting that these cells, too, have output synapses in the protocerebral region.

MARCM analysis identifies protocerebral projections as sole expression sites of presynaptic markers in VS-cells

We did a clonal analysis of small numbers of cells in order to unambiguously allocate the nSyb-mRed staining. This was necessary as nSyb-mRed could have been expressed in the different compartments of the LPTCs or in columnar and central neurons that are included in the Gal4-3A expression pattern (Fig.1). MARCM allowed us to co-express mCD8-GFP and nSyb-mRed (hs-FLP, UAS-mCD8-GFP / UAS-nSyb-mRed; FRT^{40A}/FRT^{40A}, tubP-Gal80; Gal4-3A/+) in individual VS- or HS-cells, or small groups of clonally related cells, in an otherwise unlabeled tissue (Lee and Luo, 1999). Mitotic recombination was induced at 37 °C at different developmental larval stages. Different time intervals for the heat shock were tested to generate clones. We succeeded in generating only very few single VS-cell clones. The success rate was below 1 %. Only three clones were found in a total of about 400 brains. Both single

cell VS-clones (VS2, Fig. 2a-d; VS6, Fig. 2e -h) showed nSyb-mRed exclusively localized to the axon terminal. The subtle level of nSyb-mRed observed in the presumed dendritic area of both VS- and HS-cells within the lobula plate (Fig. 1f, arrowheads) was almost completely eliminated. The few remaining nSyb-mRed spots within the lobula plate (Fig. 2b, f) did not colocalize within the mCD8-GFP labeled dendrites. The axon terminal of the VS2-cell bifurcates into two vertical branches with few laterally projecting side branches that showed prominent nSyb-mRed accumulation (Fig. 2c, arrows). Similarly nSyb-mRed was localized to the fine terminal branches of the protocerebral VS6-projection (Fig. 2g). The only other site of nSyb-mRed expression in HS- and VS-cells was the soma (Fig. 2c, g and k) which most likely refers to protein biosynthesis. We generated 3D- reconstructions based on the detected mCD8-GFP fluorescence of the VS2- and the VS6-cell (from confocal image stacks using iso-surface rendering; Amira 3.1). We overlaid the obtained cells to the nSyb-mRed fluorescence and erased all nSyb-mRed fluorescence outside the reconstructed cells (Fig. 2d and h). This procedure accentuates that (a) the dendrites of the VS-cells showed no expression of nSyb-mRed and (b) all staining within the VS-cells, beside the soma, is found in the protocerebral axon terminal.

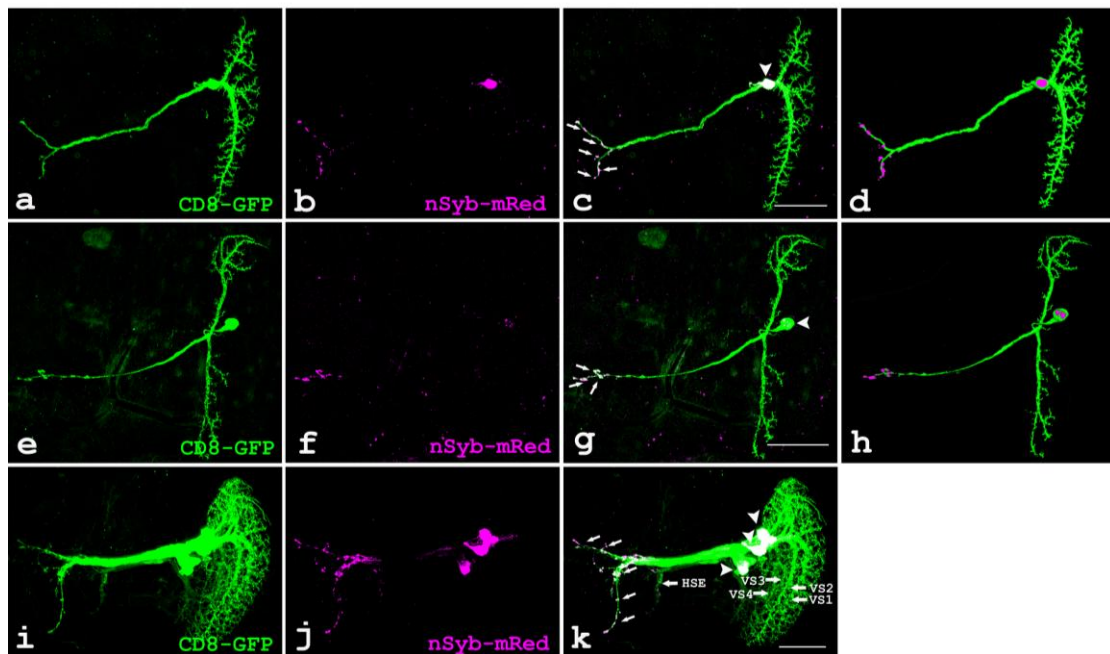


Fig 2. Elimination of expression in the central brain and in columnar elements allows the unambiguous localization of fluorescently labeled Synaptobrevin and suggests chemical output synapses on VS- and HS-cell ramifications in the protocerebrum. MARCM clones of different VS-cells and one HSE-cell were generated that coexpress membrane tagged GFP (green) and nSyb-mRed

(magenta). **a-d**: VS2-single cell clone, **e-h**: Single cell clone of a VS6-cell, **i-j**: multicellular clones. **a**, **e** and **i**: mCD8-GFP allows the identification of (a) a single VS2-cell, (e) a single VS6-cell and (i) a single HSE-cell and a multicellular clone of different VS-cells (VS1, VS2, VS3, VS4) based on their morphology. **b**, **f** and **j**: nSyb-mRed expression labels the presumed presynaptic sites on (b) the VS2-cell, (f) the VS6-cell and (j) the HS-clone and the multicellular VS-clone. **c**, **g** and **k**: overlay of mCD8-GFP and nSyb-mRed expression. nSyb-mRed is found at the axon terminal (arrows) and in the somata (arrowheads). In single or small number cell clones there is no staining colocalizing to the dendrites. **d** and **h**: Isosurface 3D-view of (d) the VS2-cell and (h) the VS6-cell including colocalizing nSyb-mRed only. Images **a**, **b**, **c** represents maximum intensity projections of 40 images. **e**, **f**, **g** are build of 50 images and **i**, **j**, **k** are build of 46 images (z-distance 0.5 μm , scale bar: 50 μm).

In the MARCM experiments described above, the probability for successful induction of mitotic recombination was extremely low. We increased the duration and number of the heat-shock(s) to more frequently generate MARCM clones. However, this only resulted in the generation of a brain including two clones amongst them one was multicellular (Fig. 2i-k). The VS-clone included 4 cells (VS1, VS2, VS3 and VS4) and the HS-clone was a single HSE-cell, that was only weakly stained. The dendrites of the VS-cells lie serially to each other with the VS1-dendrite occupying the outermost region of the lobula plate. The protocerebral terminals are arranged in close proximity. The dendrite of the HSE-cell covered the medial part of the lobula plate. nSyb-mRed localization in these 5 cells was identical to our description in the single cell clones. In summary, the analysis of single and multicellular clones of different VS-cells and an HSE-cell indicates that output synapses of these cells are exclusively localized to the tips of the protocerebral projections. This result allows to designate these processes as chemical output region. The nSyb-mRed expression observed within the lobula plate results from columnar elements presynaptic to VS- and HS-cells that are included in the Gal4-3A expression pattern (Fig. 1).

Dendritic tips and central projections of all VS-cells show evidence for inhibitory input synapses

In the next series of experiments, we studied the localization of presumed inhibitory postsynaptic sites within VS- and HS-cells. Based on a series of experiments performed in *Calliphora* (Borst and Egelhaaf, 1989; Borst et al, 1995; Single et al, 1997), inhibitory postsynaptic sites were expected to be located on LPTC dendrites of *Drosophila*, too. Their distribution was analyzed by expression of an HA- tagged

GABA receptor subunit, called Rdl. Rdl receptors form insecticide (Dieldrin) resistant, picrotoxin (PTX) sensitive GABA-gated chloride channels (Ffrench-constant et al., 1993; Zhang et al., 1995). The distribution of these receptors has been addressed by antibody staining in different layers of the optic lobes of *Calliphora* (Brotz et al., 2001). However, no information about single identified cells was given and the antibody is no longer available. Thus, we used flies of the genotype UAS-mCD8-GFP/+; UAS-Rdl-HA/+; Gal4 3A/+ driving expression of both mCD8-GFP and HA-tagged Rdl (Sańchez-Soriano et al., 2005). Anti-HA antibody staining served to fluorescently label the tagged receptors (see methods). Rdl-HA (magenta, Fig. 3a -f) localized to the assumed dendrites of all VS-cells within the lobula plate. The GFP fluorescence shown in green outlines the cell membrane of VS-cells in Figure 3. HA-Rdl was concentrated at the fine terminal tips of the dendrites (Fig. 3a - f, arrows). Thus, the dendritic tips likely represent the sites of most prominent inhibitory synaptic input. Only a subtle level of Rdl-HA expression was observed in the primary and secondary shafts of the dendrites (Fig. 3a-f). This was approved in experiments where the sometimes rather weak mCD8-GFP expression was replaced by actin-GFP. Compared to mCD8-GFP, actin-GFP labeled the dendritic tips more clearly. An example from a VS1- cell is shown in Figure 3g – i. Using these flies (+/+; UAS-act-GFP/UAS-Rdl-HA; Gal4 3A/+) we confirmed the localization of Rdl receptors to the dendritic tips. In addition we proved the absence of processes from columnar elements that might have expressed the detected Rdl-HA. This is most obvious in the shown overlay (Fig. 3i). The inhibitory GABAergic receptors and the absence of nSyb-mRed on VS-cells arborizations in the lobula plate show that these cells have their dendrites here.

In the same set of experiments, the protocerebral projections of different VS-cells were examined for Rdl-HA expression (+/+; UAS-mCD8-GFP/+; UAS-Rdl-HA/+; Gal4 3A/+). From the region where each axon terminal bifurcates to their tips, a high level of Rdl-HA expression was observed (Fig. 3j - l). The intensity of the Rdl-HA staining in this region was even more pronounced than the one observed in the dendritic region. Individual axon terminals could, however, not be identified in this image due to the significant overlap of their processes. However, analysis of individual confocal images of 0.5 μm thickness (data not shown) suggests that Rdl-HA expression in this region can be assigned to all six VS-cells highlighted by the Gal4-3A driver line. These experiments suggest a large number of inhibitory synaptic inputs impinging onto VS-cell axon terminals within the protocerebral region.

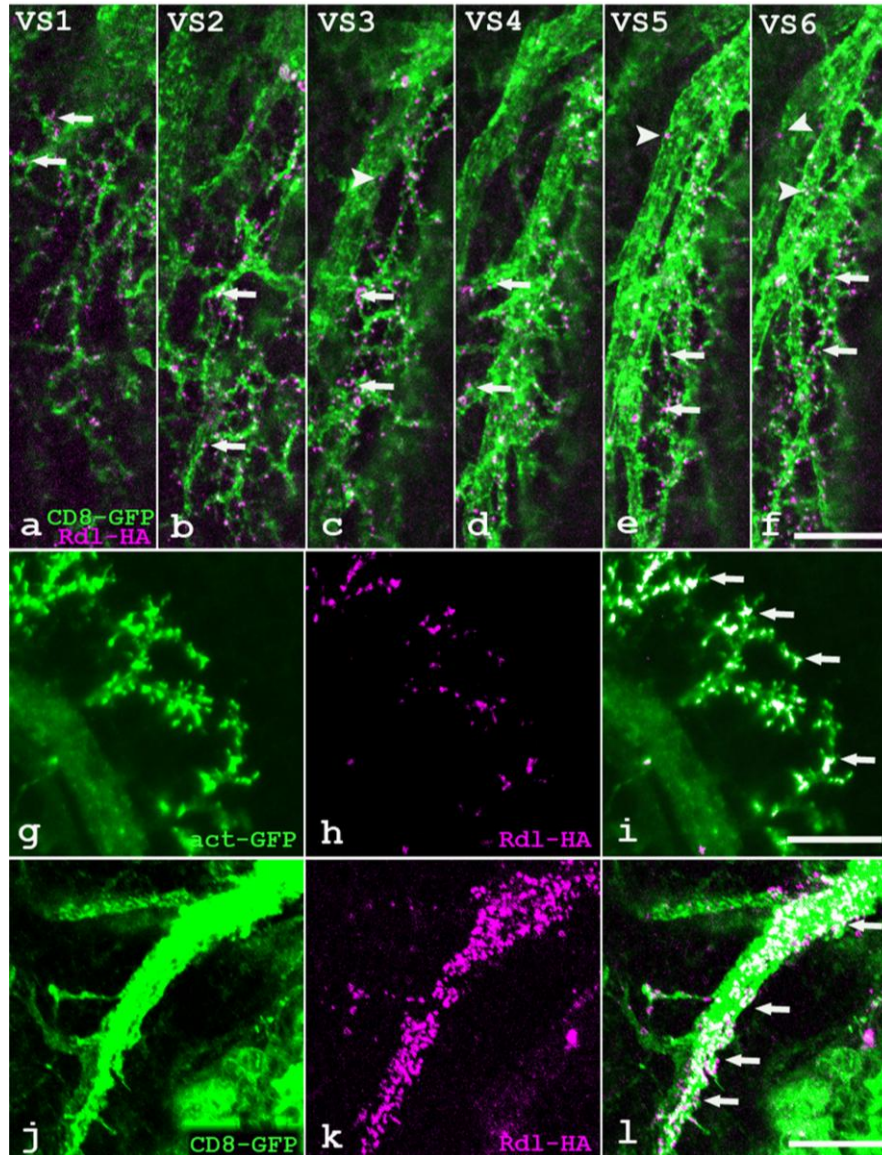


Fig 3. Distribution of Rdl-type GABA receptors on VS-cells. Gal4-3A was used to drive coexpression of tagged GFP (green, UAS-mCD8-GFP or UAS-actin-GFP) and HA-tagged Rdl-type GABA receptors (magenta, UAS-Rdl-HA). **a-f**: coexpression of mCD8-GFP and Rdl-HA on the dendrites of VS-cells. The dendritic branches of all six VS-cells express Rdl-HA. Only a subtle level of Rdl-HA was observed in the primary and secondary shafts (arrowheads in (c), (e) and (f)). Most receptor protein is localized to the tips of the dendrites (arrows). **g-i**: Close-ups of dorsal dendritic branches show the localization of Rdl receptors to the very tips of the dendrites. In these experiments Rdl-HA (h) was co-expressed to actin-GFP (g). The overlay is shown in (i). **j-l**: Protocerebral projections of VS-cells are visualized by mCD8-GFP expression (j) and show massive Rdl-HA accumulation (k). This is also shown in the overlay (l) of both channels (arrows). The panels (a – f), (g- i) and (j-l) are maximum intensity projections of 3, 5 and 6 images, respectively. Individual images were separated by 0.5 μ m in z-direction. Scale bar: 10 μ m in (a-i) and 20 μ m (j-l). HA-tagged Rdl receptors were visualized by Alexa 568 and antibody staining (see methods).

Dendritic tips and central projections of the HSE-cell show evidence for inhibitory input synapses

One of the horizontally sensitive neurons, an HSE-cell, was examined for the distribution of the Rdl-HA protein. Flies co-expressing mCD8-GFP and Rdl-HA (UAS-mCD8-GFP/+; UAS-Rdl-HA/+; Gal4 3A/+) were used for this analysis. Similar to the VS-cells, our data suggests that HSE is postsynaptic to inhibitory GABAergic input in the lobula plate (Fig. 4a – c). Rdl-HA localization was mostly confined to terminal branches of the dendrite (Fig. 4c, arrows). The protocerebral projection of the HSE-cell showed Rdl-HA staining (Fig. 4d - f, arrows in 4f) as well. Processes from columnar elements or central neurons can not be seen (Fig.4) and nSyb-mRed was localized to the protocerebral part only (Fig. 2k). Compared to the expression level observed in VS-cells the HSE cell showed a lower abundance of Rdl receptors. Nevertheless, these results indicate inhibitory synaptic input impinging on the HSE-dendrite in the lobula plate as well as on its axonal terminal. In HSS- and HSN-cells experiments on GABAergic postsynaptic sites were not conclusive due to the very low expression level of Rdl-HA and mCD8-GFP (data not shown).

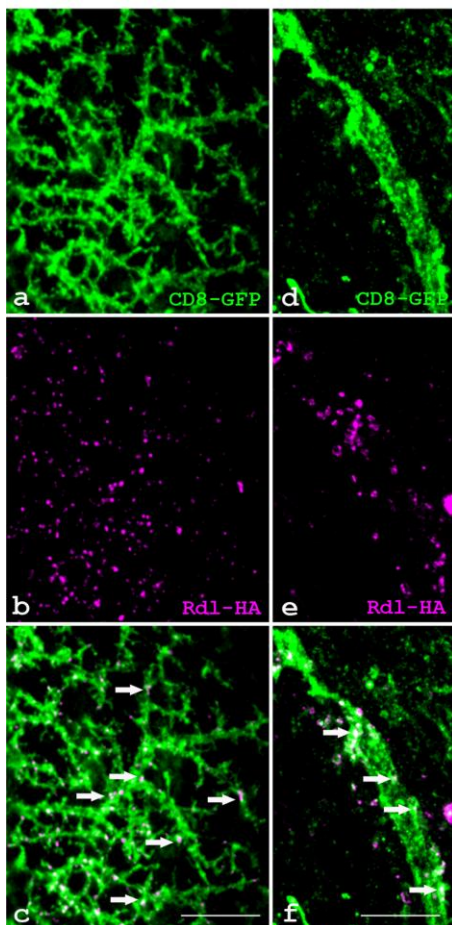


Fig 4. Distribution of Rdl-type GABA receptors on an HSE-cell. Gal4-3A was used to drive coexpression of tagged GFP (green, UAS-mCD8-GFP) and HA-tagged Rdl-type GABA receptors (magenta, UAS-Rdl-HA). **a-c:** All dendritic branches of the HSE-cell show Rdl-HA expression. **a:** mCD8-GFP outlines the morphology of the HSE-dendrite. **b:** Rdl-HA immunolabeling. **c:** Overlay of (a) and (b): Rdl-localization on the HSE-dendrite suggests inhibitory postsynaptic sites that were mostly found at the fine terminal endings (arrows). **d-f:** Protocerebral ramification of an HSE-cell. **d:** mCD8-GFP and **e:** Rdl-HA expression. **f:** The overlay of (d) and (e) shows Rdl-HA expression (arrows) indicative of inhibitory input from neighboring neurons or processes. The panels (a – c) and (d - f) are maximum intensity projections of 5 and 3 images, respectively. Individual images were separated by 0.5 μ m in z-direction. Scale bar: 20 μ m in (a-c) and 15 μ m in (d-f). HA-tagged Rdl-receptors were visualized by Alexa 568 and antibody staining (see methods).

Indications for GABAergic input onto LPTCs

Our analysis of probable inhibitory postsynaptic synapses within VS- and HS-cells using Rdl-HA might disregard other GABA-receptor subtypes (Harvey et al., 1994; Henderson et al., 1993) that could be expressed on the same cells. To complement our findings we set out to investigate the corresponding distribution of presynaptic GABAergic terminals impinging onto these LPTCs. Different VS- and HS-cells were filled with the red fluorescent dye Alexa-Fluor 594 by intracellular injection. Subsequently, the brain was stained using an antibody against GABA (see methods). In Figure 5, such an analysis of the GABAergic input on the dorsal part of a single VS3-cell is illustrated. The GABA-immunoreactivity (green) can be located in the surroundings of a dendritic branch (magenta, Fig. 5a). In Figure 5b, a close-up of the area marked by the white box in Figure 5a is shown. A yz-view (using 'voltex' and 'orthoslice' plug-ins of Amira 3.1) along the yellow line in Figure 5b shows that the green GABA profiles make contacts closely juxtaposed to the dendritic surface. Similar analysis of the VS-axon terminals (Fig. 5d,e) and corresponding yz-views showed that the green GABA profiles make contacts closely juxtaposed to the axonal surface (Fig. 5f).

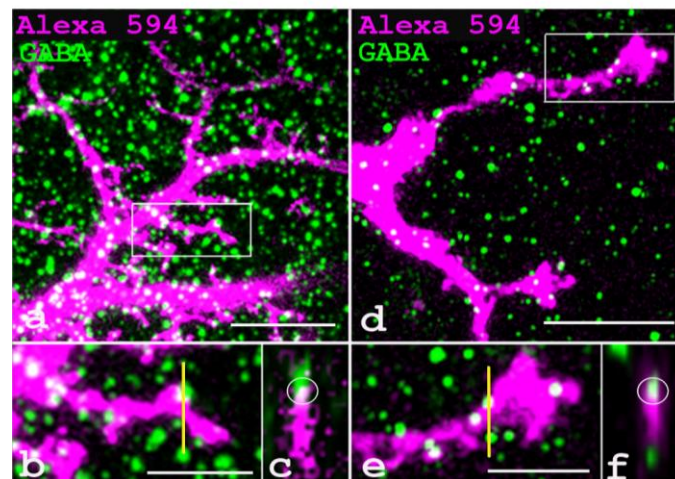


Fig 5. Single VS3-cell filled with Alexa-Fluor 594 (magenta) in an anti-GABA (green) immunolabeled brain. a: GABAergic input is visible in the surrounding of the VS3-dendrite. Many of the GABA-positive profiles are closely juxtaposed to the dendrite. As a result of the projection of 6 images into a single plane some profiles appear to be superimposed. **b:** close up of a small dendritic branch marked by the white box in (a). **c:** yz-view along the section marked by the yellow vertical line in (b). The yz-view shows that GABAergic profiles are closely juxtaposed to the dendrites but not localized within the dendrite. **d-e:** similar investigation of the immunolabeled GABA-profiles in the protocerebral projection of the VS3-cell. **d:** VS3-terminal filled with Alexa-Fluor 594 and GABA-

immunoreactive profiles (green) in its surrounding **e**: close up of the region marked by the white box in (d). **f**: yz-view along the section marked by the yellow vertical line in (e). The yz-view shows that GABAergic profiles are closely juxtaposed to the protocerebral VS3-projection but not localized within it. Dorsal is left in a-c and up in d-f. Images a, b, d and e are maximum intensity projections of 6 images (0.5 μm sections). Scale bar: 10 μm in (a, d) and 5 μm in (b, e).

We did similar GABA-stainings and analysis on brains that contained individual Alexa filled HS-cells. A dendritic branch (Fig.6a-c) and an axonal terminal of an HSE-cell are shown. As in VS-cells, but less pronounced, presynaptic GABA is closely juxtaposed to the dendrite and the axon, respectively.

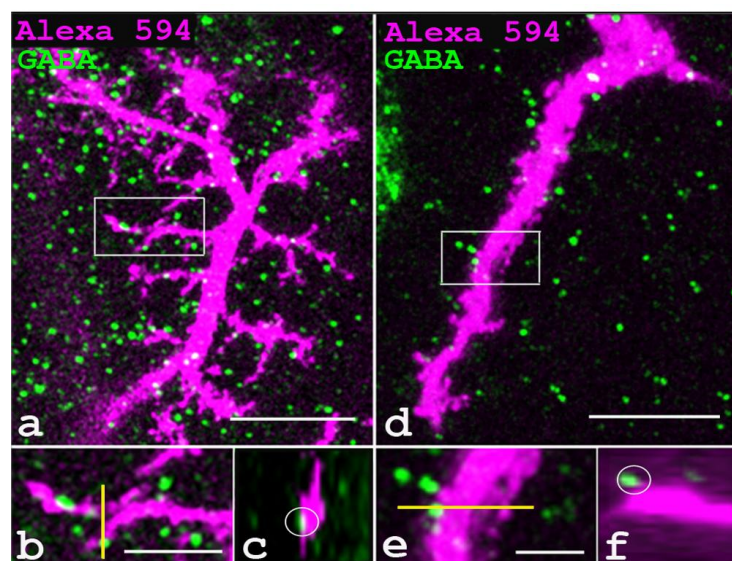


Fig 6. Single HSE-cell filled with Alexa-Fluor 594 (magenta) in an anti-GABA (green) immunolabeled brain. a: GABAergic immunoreactivity is visible in the surrounding of the HSE-dendrite and individual GABA-positive profiles are closely juxtaposed suggesting presynaptic sites of GABAergic input. **b:** close up of a small dendritic HSE-branch marked by the white box in (a). **c:** The yz-view along the section marked by the yellow vertical line in (b) shows that GABAergic profiles are closely juxtaposed to the dendrites but not localized within it. **d-e:** similar investigation of the immunolabeled GABA-profiles in the protocerebral projection of the HSE-cell. **d:** HSE-terminal filled with Alexa-Fluor 594 and GABA-immunoreactive profiles (green) in its surrounding **e**: close up of the region marked by the white box in (d). **f:** yz-view along the section marked by the yellow horizontal line in (e). The yz-view shows that GABAergic profiles are closely juxtaposed to the protocerebral HSE-projection but not localized within it. Dorsal is left. Images a, b, d and e are the maximum intensity projection of 6 images displaced by 0.5 μm in z-direction. Scale Bar: 10 μm in a, d and 5 μm in b, e.

Discussion

Connectivity of VS- and HS-cells in the fly visual system

The synaptic organization and polarity of VS- and HS-cells within their local environment provides important information about their function and integration into the motion detection circuitry (Hausen, 1982a, b; reviewed in Borst and Haag, 2002). Using *Drosophila* as a model organism we investigated the distribution of genetically labeled synaptic proteins on VS- and HS-cells and confirmed our findings by immunolabeling of genetically unmanipulated synapses. Focusing on GABAergic receptors, the inhibitory transmitter GABA (Meyer et al., 1986) itself and Synaptobrevin as a marker for presynaptic vesicles we provide evidence for a centripetal flow of information. High resolution confocal light microscopy of fluorescently labeled pre- and postsynaptic proteins suggests that both cell types extend their elaborated dendrites within the lobula plate where they harbor postsynaptic specializations only. Both cell types send long processes to the central brain. At the proximal end of these processes the highly specific and well characterized synaptic vesicle associated protein Synaptobrevin (Trimble et al., 1988; Baumert et al., 1989; Sudhof et al., 1989; DiAntonio et al., 1993) is expressed suggesting the presence of presynaptic chemical synapses at the protocerebral terminal. Superimposed to this centripetal flow of information we found evidence for additional inhibitory input impinging on their axon terminals. Our conclusions were drawn from the following findings: (a) Rdl-type GABA receptors were detected on the tips of all VS- and HS-cell dendrites in the lobula plate (Fig. 3 and 4) and the cognate transmitter GABA was shown to be juxtaposed to the dendrites (Fig. 5 and 6). The juxtaposed GABA is indicative of inhibitory release from columnar elements (Buchner et al., 1984; Douglass and Strausfeld, 1995; Brotz and Borst, 1996) impinging on LPTC dendrites as predicted by a Reichardt-model (Reichardt, 1961, 1987). (b) Synaptobrevin was exclusively localized at the terminals of the protocerebral projections suggesting that information is passed onto neurons that are postsynaptic to VS- and HS-cells in the protocerebrum (Gronenberg and Strausfeld, 1990; Gilbert et al. 1995; Chan et al. 1998). The neurotransmitter of this connection still needs to be determined. However, based on immunohistochemical experiments we can exclude GABA, as GABA is located strictly outside and juxtaposed but not within individual visualized VS- and HS-cell terminals (Fig. 5 and 6). (c) Rdl-type GABA receptors were

localized to HS- and in particular VS-cell axon terminals (Fig. 3) which is in agreement with the juxtaposed GABA-staining (Fig. 5 and 6). This newly described evidence for inhibitory input to the axon terminals provides new insights to the anatomical basis of the spatial lay out of receptive fields in these cells (Haag and Borst, 2001, 2002, 2003, 2004, 2005). Experiments on CH-cells demonstrated that the designation of axons and dendrites without such information can be misleading. In *Calliphora*, the lobula plate branches of CH-cells possess both post- and presynaptic specializations and its protocerebral part proved to be exclusively postsynaptic (Gauck et al., 1997). These findings have important functional implications as CH-cells receive their entire dendritic input via electric synapses from neighboring ipsilateral HS-cell dendrites (Haag and Borst, 2002; Farrow et al., 2003) and receive additional input on their protocerebral projections from the H2 neuron (Hausen, 1984; Haag and Borst, 2001). Based on these results dendritic image processing and the generation of increased motion contrast could be simulated (Cuntz et al., 2003). Our data on synapse distribution on VS- and HS-cells will contribute to similar studies in these neurons.

Genetic methods for the analysis of synaptic connectivity

The use of the Gal4-UAS system (Brand and Perrimon, 1993) in *Drosophila* allowed the precise light microscopic localization of identified synaptic proteins that characterize pre- and inhibitory postsynaptic sites. This information was used to pinpoint the localization of chemical synapses on identified VS- and HS-cells. As elegant as the technique is one has to be aware of the fact that ultimate prove of functional synapses would require an in depth analysis on both the EM and the electro-/optophysiological level. Based on our approach, individual cells or small numbers of neurons could be analyzed when Gal4-UAS was part of the MARCM technique (Lee and Luo, 1999). As a common principle, both strategies enable the coexpression of two reporter proteins. Thus, individual cells can be identified by their overall morphology and specific synaptic proteins can be labeled simultaneously within the same cells using different marker molecules. In this approach, all obtained information is imperatively coupled to a particular cell. Comparable specificity could not be achieved so far in any of the electron microscopic (Pierantoni, 1976; Hausen et al., 1980), anatomical (Hausen 1982a, b; Fischbach and Dittrich, 1989; Strausfeld and Bassemir 1985a, b), immunohistochemical (Brotz et al. 2001) or pharmacological (Brotz and Borst, 1996) studies. We overcame this problem by combining standard genetic techniques for

whole cell labeling (UAS-mCD8-GFP, Lee and Luo, 1999; UAS-actin-GFP, Verkhusha et al., 1999) with the expression of HA-tagged Rdl-type GABA-receptors (UAS-Rdl-HA, Sa'nchez-Soriano et al., 2005) or fluorescently labeled Synaptobrevin (see methods). Only few studies applied a comparable coexpression of differentially labeled proteins so far (Otsuna and Ito, 2006). The obtained sparse staining allowed to unequivocally allocate even highly abundant proteins like nSyb to subcellular compartments of identified cells (Fig. 1-4). In comparison, even antibody stainings of less abundant proteins resulted in a massive fluorescence signal in the surrounding tissue. Decisions on colocalization versus juxtaposition of labeled protein on individual highlighted cells could only be made in small regions and thin sections (Fig. 5 and 6). Also we were limited by the availability of specific antibodies. These problems can elegantly be bypassed by coexpression studies using MARCM. However, a number of limitations of this method have to be considered. First, it can only be used to express labeled proteins whose native unlabeled equivalents have previously been demonstrated on the cells of interest. For Rdl-receptors (Ffrench-Constant et al., 1990) this was shown in several studies in different fly-species (Brotz and Borst, 1996; Brotz et al., 2001) and neuronal Synaptobrevin (Trimble et al., 1988; Baumert et al., 1989) is a widely used marker for synaptic vesicles in basically all species investigated so far including *Drosophila* (Sudhof et al., 1989; DiAntonio et al., 1993). Second, a quantitative interpretation of the obtained staining can not be made. The expression level of the labeled protein depends on the efficacy of the expression system and the protein will eventually compete with the intrinsic unlabeled protein for translation and localization. Third, fluorescent proteins tend to form multimeric complexes. Thus, aggregates might form that disrupt proper protein trafficking and localization (Otsuna and Ito, 2006). We avoided this problem by fusing nSyb to monomeric DsRed (Campbell et al., 2002) instead of the original tetrameric DsRed (Verkhusha et al., 2001). The resulting construct nSyb-mRed localized in a similar way to the widely used nSyb-GFP (Ito et al., 1998; Estes et al., 2000) and was ideally suited to study presynaptic vesicle release sites in GFP-labeled neurons.

Evidence for exclusively postsynaptic VS- and HS-cell dendrites in the lobula plate

The detailed anatomical and physiological investigations in the past twenty years suggested that VS- and HS-cells are postsynaptic in the lobula plate and presynaptic in the protocerebrum (Hausen, 1982a, b, 1984; Hengstenberg et al., 1982; Fischbach

and Dittrich, 1989; Strausfeld and Bassemir, 1985 a, b; Gronenberg and Strausfeld, 1990; Douglas and Strausfeld, 1995, 1996). However, the physiological and immunohistochemical characterization of these cells and of their local connections in the lobula plate and protocerebrum is still incomplete. Only a few EM-studies provided evidence for chemical postsynaptic sites on VS- and HS-cell dendrites in the lobula plate. None of these studies showed evidence for vesicle release sites (Hausen et al., 1980; Strausfeld and Lee, 1991). These results are in accordance with the presence of postsynaptic receptors (Fig. 3 and 4) and the absence of vesicle associated Synaptobrevin (Fig. 1 and 2) on VS- and HS-cell dendrites. Theoretical arguments for their function as dendrites came from the pioneering work of Reichardt and Hassenstein (Reichardt, 1961) and the following detailed foundation of Reichardt detectors as minimal circuits for the computation of local motion vectors (Reichardt 1961, 1987; Borst and Egelhaaf, 1989; Egelhaaf et al., 1989). According to this model such local motion signals become spatially summed on the elaborated dendrites of direction-selective VS- and HS-cells within the lobula plate. In this model GABAergic input to Rdl receptors on the dendrites is of particular importance as mirror symmetrical subunits of the Reichardt detector (half-detectors with opposite preferred direction) generate opposing motion signals. The superposition of excitatory and inhibitory synaptic currents in VS- and HS-cell dendrites would correspond to the subtraction of the half-detector output signals in the Reichardt model. This mechanism provides information about the direction of image motion at each retinal location. Although further details about the cellular implementation of Reichardt detectors are still elusive, a lot of evidence has been accumulated that such an algorithm is indeed at work (Borst and Egelhaaf, 1990; Borst et al., 1995; Borst et al., 2005; Haag et al., 1992; Haag et al., 2004; Single et al., 1997; Single and Borst, 2002). The found Rdl receptor localization strongly suggests that Reichardt detectors impinge on the very tips of VS- (Fig.3g-i) and HS-cell dendrites (Fig. 4c). By this way a retinotopic map of local motion information is retained that will be lost during the spatial integration of simultaneous inputs. The most striking evidence for such a scenario comes from local dendritic calcium measurements (Single and Borst, 1998; Haag et al., 2004). In these experiments local calcium signals from dendritic tips were shown to consist of a DC component indicative of the direction of image motion superimposed by modulations reflecting the temporal change of local luminance. These modulations become eliminated when integrated and measured in lower order branches as the local

modulations are shifted in phase due to the spatial separation of the local inputs along the axes of image motion.

In the main dendritic branches calcium accumulates via voltage activated calcium channels (Egelhaaf and Borst, 1995; Single and Borst 1998, 2002) whereas in dendritic tips, additional calcium influx occurs through nicotinic cholinergic receptors (Single and Borst, 2002). These findings strongly suggest that ARD-type cholinergic receptors (Brotz et al., 2001) will be found in close proximity to the shown Rdl receptors on the tips of VS- and HS-cells. However, this remains to be proven.

Similarly, the identity of the columnar neurons providing excitatory and inhibitory input to the LPTCs is not known. Two main groups of columnar neurons, the T4 and T5 cells, were proposed to constitute the basic input to LPTCs (reviewed in Borst and Haag, 2002). This view is based on the following evidence: T4 and T5 cells exist in four different subtypes per column each ramifying in one of the four different layers of the lobula plate (Fischbach and Dittrich, 1989). The same four layers were labeled by activity dependent uptake of 2-deoxy-glucose (Buchner et al., 1984) during visual motion presentation. Furthermore, Strausfeld and Lee (1991) showed the existence of a chemical synapse between a T4 and an HS-cell dendrite. In the light of these findings genetic labeling techniques will be very useful to clarify those columnar neurons that provide synaptic input to the LPTCs in the lobula plate.

Evidence for inhibitory input to VS- and HS-cell axon terminals in the protocerebrum

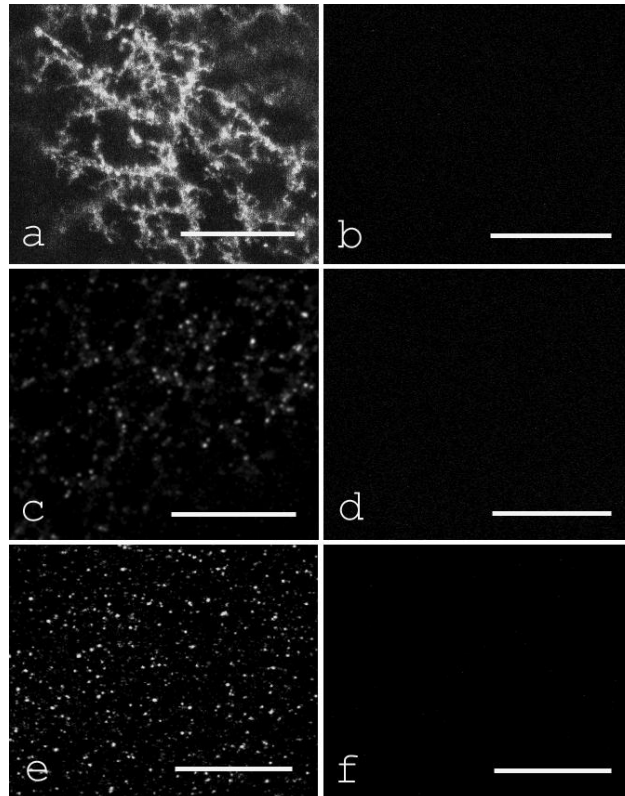
In flies, visually guided flight maneuvers and course control rely heavily on the output of VS- and HS-cells. This is reflected in the fact that, in the protocerebrum, both cell types convey information about optic flow onto descending neurons that in turn connect to motoneurons controlling neck and flight muscles (Gronenberg and Strausfeld, 1990; Strausfeld and Gronenberg 1990; Gronenberg et al., 1995; Chan et al., 1998, Haag and Borst, 2005). The complex receptive fields of VS- and HS-cells are the product of retinotopically organized columnar input and various network interactions between them. Thus, their output is shaped by both, signals impinging directly onto their dendrite as well as by signals processed and communicated by other LPTCs (Haag and Borst,

2003, 2004) reaching them, indirectly, onto their dendrite or axon terminal. Some of these LPTC-LPTC interactions are brought about by electrical interactions. E.g. Farrow et al. (2005) showed that the horizontal extension of the receptive field of VS-cells in *Calliphora* is enlarged by electric synapses between ipsilateral neighboring VS-cells. Similarly, the firing rate of H2-cells in response to rotational optic flow becomes scaled by electric axonal-axonal coupling to the HSE-cell of the contralateral side of the brain (Farrow et al., 2006). Furthermore, ipsilateral dendrites can be electrically coupled to provide a blurred and enlarged representation of the stimulus as mentioned before for HS- and CH-cells (Haag and Borst, 2002; Farrow et al., 2003).

In the current context, physiological evidence for chemical interactions between LPTCs is of particular interest. In flies, evidence for chemical axon-axonal interactions is still rare and to our knowledge there is no report on inhibitory input to the terminals of HS-cells so far. Possible connections might originate from the heterolateral V2-, H2- and H4-cell (Strausfeld et al., 1995) as these neurons are GABAergic and provide colocalizing ramifications in the protocerebrum. In this study, no evidence was given for connections between single identified cells. However, unspecified postsynaptic sites on HS-cell terminals were described in *Musca* (Strausfeld and Bassemir, 1985b). Taken together, the functional implication of Rdl receptor localization on HS-axon terminals remains to be analyzed. The situation is more conclusive when the tuning of VS-cells to rotational flow fields is considered. VS-cells with lateral receptive fields become strongly excited by downward motion in the center of their receptive field and are excited by upward motion in the frontal part of their receptive field (Krapp et al., 1998). The anatomical basis of this finding is unknown. If frontal VS-cells were connected to an unknown inhibitory interneuron that releases GABA on lateral VS-cells, release from inhibition could explain this finding. Besides the fact that VS-cells with frontal receptive fields become hyperpolarized by upward motion presented in the center of their receptive fields, evidence for such a release from inhibition is rather weak. Injection of negative current in VS1 and simultaneous recording of VS7-10 (Haag and Borst, 2004) showed no clear depolarization of the membrane potential in VS7-10. However, in the same set of experiments, a sign reversal of positive current injections was observed: positive injection into VS1 caused simultaneous hyperpolarization in VS7-10 and vice versa (Haag and Borst, 2004). Such sign reversal and inhibition cannot be mediated via electrical coupling. Thus, there is clear evidence for inhibitory chemical coupling between VS-cells via unknown other neurons.

The Rdl receptors on the VS-cell axons discovered in this study could mediate this inhibition. Future work will allow to further untangle the circuitry and to derive a generic model of flow-field processing and visual course control in flies.

Supplementary Material



Supplementary Fig 1. Specificity of immunolabeling with GFP-, HA- and GABA-antibodies. For each antibody both images were taken at similar conditions and intensities. **a:** Dendritic region of an HSE cell (genotype: +/+; UAS-mCD8-GFP/+; Gal4-3A/+) stained with Alexa Fluor 488 rabbit anti-GFP antibody. Only the GFP-expressing HSE cell is recognized by the antibody. **b:** negative control: no immunoreactivity is detected in the same brain area in the absence of the Gal4-driver (genotype: +/+; UAS-mCD8-GFP/+; +/+ stained with Alexa Fluor 488 rabbit anti-GFP antibody). **c:** Dendritic region of an HSE cell (genotype: +/+; UAS-Rdl-HA/+; Gal4-3A/+) stained with monoclonal rat anti-HA antibody and Alexa Fluor 568 goat anti rat IgG. Only the Rdl-HA-expressing HSE cell is recognized by the antibody. **d:** negative control: no immunoreactivity is detected in the same brain area in the absence of the Gal4-driver (genotype: +/+; UAS-Rdl-HA/+; +/+ stained with monoclonal rat anti-HA antibody and Alexa Fluor 568 goat anti rat IgG). **e:** Anti-GABA immunoreactivity in the lobula of a *Drosophila* wild type fly. The polyclonal rabbit anti-GABA and Alexa Fluor 568 goat anti rabbit IgG (catalog number-A11011, lot number-84E2-1, Molecular Probes) labeled individual spots similar to the ones that were detected juxtaposed to LPTC in Figure 5 and 6. **f:** no staining could be observed in the same brain

area when the GABA-antibody was preabsorbed with GABA-glutaraldehyde-BSA conjugates, same antibodies used as in (e). Scale Bar: 20 μ m

Acknowledgements

We are grateful to Wolfgang Essbauer and Christian Theile for excellent technical assistance, to Thomas Hendel and Bettina Schnell for comments on the manuscript. We thank Yong Choe for discussion and comments, Liqun Luo, Andreas Prokop, Martin Heisenberg for providing flies and Roger Tsien for providing DNA.

References

- Baumert, M., P. R. Maycox, F. Navone, P. De Camilli, and R. Jahn (1989) Synaptobrevin: an integral membrane protein of 18,000 daltons present in small synaptic vesicles of rat brain. *EMBO J.* 8:379-384
- Borst, A., and M. Egelhaaf (1989) Principles of visual motion detection. *Trends Neurosci.* 12:297-306
- Borst, A., and M. Egelhaaf (1990) Direction selectivity of fly motion-sensitive neurons is computed in a two-stage process. *Proc. Natl. Acad. Sci. USA* 87: 9363-9367
- Borst, A., M. Egelhaaf, and J. Haag (1995) Mechanisms of dendritic integration underlying gain control in fly motion-sensitive interneurons. *J. Comput. Neurosci.* 2: 5-18
- Borst, A., and J. Haag (2002) Neural networks in the cockpit of the fly. *J. Comp. Physiol.* 188: 419-437
- Borst, A., Flanagan, V.L. and H. Sompolinsky (2005) Adaptation without parameter change: Dynamic gain control in motion detection. *Proc. Natl. Acad. Sci. USA* 102:6172-6176
- Brand, A. H., and N. Perrimon (1993) Targeted gene expression as a means of altering cell fates and generating dominant phenotypes. *Development* 118:401-415
- Brotz, T. M., and A. Borst (1996) Cholinergic and GABAergic receptors on fly tangential cells and their role in visual motion detection. *J. Neurophysiol.* 76:1786-1799
- Brotz, T. M., E. D. Gundelfinger, and A. Borst (2001) Cholinergic and GABAergic pathways in fly motion vision. *BMC Neuroscience* 2:1
- Buchner, E., S. Buchner, and I. Bulthoff (1984) Deoxyglucose mapping of nervous activity induced in *Drosophila* brain by visual movement. *J. Comp. Physiol. A* 155:471-483
- Buijs, R. M., E. H. S. van Vulpen and M. Geffard (1987) Ultrastructural localization of GABA in the supraoptic nucleus and neural lobe. *Neuroscience* 20:347-355
- Campbell, R.E., O. Tour, A. E. Palmer, P. A. Steinbach, G. S. Baird, D. A. Zacharias, and R. Y. Tsien (2002) A monomeric red fluorescent protein. *Proc. Natl. Acad. Sci. U S A* 99:7877-7882
- Chan, W. P., F. Prete, and M. H. Dickinson (1998) Visual input to the efferent control system of a fly's "gyroscope". *Science* 280:289-292
- Cuntz, H., J. Haag, and A. Borst (2003) Neural image processing by dendritic networks. *Proc. Natl. Acad. Sci. U S A* 100:11082-85
- DiAntonio, A., R. W. Burgess, A. C. Chin, D. L. Deitcher, R. H. Scheller, and T. L. Schwarz (1993). Identification and characterization of *Drosophila* genes for synaptic vesicle proteins. *J. Neurosci.* 13:4924-4925

- Douglass, J. K., and N. J. Strausfeld (1995) Visual motion detection circuits in flies: peripheral motion computation by identified small-field retinotopic neurons. *J. Neurosci.* 15:5596-5611
- Douglass, J. K., and N. J. Strausfeld (1996) Visual motion detection circuits in flies: parallel direction- and non-direction-sensitive pathways between the medulla and lobula plate. *J. Neurosci.* 16:4551-4562
- Egelhaaf, M., A. Borst, and W. Reichardt (1989) Computational structure of a biological motion detection system as revealed by local detector analysis in the fly's nervous system. *J. Opt. Soc. Am. A* 6:1070-1087
- Egelhaaf, M., and A. Borst (1995) Calcium accumulation in visual interneurons of the fly: stimulus dependence and relationship to membrane potential. *J. Neurophysiol.* 73:2540-2552
- Estes, P.S., G. L. Ho, R. Narayanan, and M. Ramaswami (2000) Synaptic localization and restricted diffusion of a *Drosophila* neuronal synaptobrevin--green fluorescent protein chimera in vivo. *J. Neurogenet.* 13:233-55
- Farrow, K., J. Haag, and A. Borst (2003) Input organization of multifunctional motion-sensitive neurons in the blowfly. *J. Neurosci.* 23:9805-9811
- Farrow, K., A. Borst, and J. Haag (2005) Sharing receptive fields with your neighbors: Tuning the vertical system cells to wide field motion *J. Neurosci.* 25: 3985-3993
- Farrow, K., J. Haag and A. Borst (2006) Nonlinear, binocular interactions underlying flow field selectivity of a motion-sensitive neuron. *Nat. Neurosci.* 9:1312-1320
- Ffrench-Constant, R. H., R. T. Roush, D. Mortlock, and G. P. Dively (1990) Isolation of dieldrin resistance from field populations of *Drosophila melanogaster* (Diptera: Drosophilidae). *Econ. Entomol.* 83:1733-1737
- Ffrench-Constant, R. H., T. A. Rocheleau, J. C. Steichen, and A. E. Chalmers (1993) A point mutation in *Drosophila* GABA receptor confers insecticide resistance. *Nature* 363:449-451
- Fischbach, K. F., and A. P. M. Dittrich (1989). The optic lobe of *Drosophila melanogaster*. I. A Golgi analysis of wild-type structures. *Cell Tissue Res.* 258:441-475
- Gauck, V., M. Egelhaaf, and A. Borst (1997) Synapse distribution on VCH, an inhibitory, motion-sensitive interneuron in the fly visual system. *J. Comp. Neurol.* 381:489-499
- Gilbert, C., W. Gronenberg, and N. J. Strausfeld (1995) Oculomotor control in calliphorid flies: Head movements during activation and inhibition of neck motor neurons corroborate neuroanatomical predictions. *J. Comp. Neurol.* 361:285-297
- Gronenberg, W., and N. J. Strausfeld (1990) Descending neurons supplying the neck and flight motor of Diptera: physiological and anatomical characteristics. *J. Comp. Neurol.* 302:973-991
- Gronenberg, W., J. J. Milde, and N. J. Strausfeld (1995) Oculomotor control in calliphorid flies: organization of descending neurons to neck motor neurons responding to visual stimuli. *J. Comp. Neurol.* 361:267-84
- Haag, J., M. Egelhaaf, and A. Borst (1992) Dendritic integration of motion information in visual interneurons of the blowfly. *Neuroscience Letters* 140: 173-176
- Haag, J., and A. Borst (2001) Recurrent network interactions underlying flow-field selectivity of visual interneurons. *J. Neuroscience* 21: 5685-5692
- Haag, J., and A. Borst (2002) Dendro-dendritic interactions between motion-sensitive large-field neurons in the fly. *J. Neuroscience* 22: 3227-3233
- Haag, J., and A. Borst (2003) Orientation tuning of motion-sensitive neurons shaped by vertical-horizontal network interactions. *J. Comp. Physiol. A* 189: 363-370

- Haag, J., and A. Borst (2004) Neural mechanism underlying complex receptive field properties of motion-sensitive interneurons. *Nature Neuroscience* 7: 628-634
- Haag, J., W. Denk, and A. Borst (2004) Fly motion vision is based on Reichardt detectors regardless of the signal-to-noise ratio. *Proc. Natl. Acad. Sci. U S A* 101:16333-16338
- Haag, J., and A. Borst (2005) Dye-coupling visualizes networks of large-field motion-sensitive neurons in the fly. *J.Comp.Physiol. A* 191: 445-454
- Harvey, R. J., B. Schmitt, I. Hermans-Borgmeyer, E. D. Gundelfinger, H. Betz, and M. G. Darlison (1994) Sequence of a *Drosophila* ligand-gated ion-channel polypeptide with an unusual amino-terminal extracellular domain. *J. Neurochem.* 62: 2480-2483
- Hausen, K., K. Wolburg-Buchholz, and W. A. Ribi (1980) The synaptic organization of visual interneurons in the lobula complex of flies. *Cell Tissue Res.* 208:371-387
- Hausen, K. (1982a) Motion sensitive interneurons in the optomotor system of the fly. I. The horizontal cells: structure and signals. *Biol.Cybern.* 45:143-156
- Hausen, K. (1982b) Motion sensitive interneurons in the optomotor system of the fly. II. The horizontal cells: receptive field organization and response characteristics. *Biol. Cybern.* 46:67-79
- Hausen, K. (1984) The lobula-complex of the fly: structure, function and significance in visual behaviour. In: Ali MA (ed) *Photoreception and vision in invertebrates*. Plenum Press, New York, pp 523-559
- Heisenberg, M., R. Wonneberger, and R. Wolf (1978) optomotor-blindH31 *Drosophila* mutant of the lobula plate giant neurons. *J.Comp.Physiol. A* 124:287-296
- Henderson, J. E., D. M. Soderlund, and D. C. Knipple (1993) Characterization of a putative gamma-aminobutyric acid (GABA) receptor beta subunit gene from *Drosophila melanogaster* *Biochem Biophys Res. Commun.* 193:474-82
- Hengstenberg, R., K. Hausen, and B. Hengstenberg (1982) The number and structure of the giant vertical cells (VS) in the lobula plate on the blowfly *Calliphora erythrocephala*. *J.Comp.Physiol. A* 149:163-177
- Huang, Z., K. Zang, and L. F. Reichardt (2005) The origin recognition core complex regulates dendrite and spine development in postmitotic neurons. *J. Cell Biol.* 170:527-35
- Ito, K., K. Suzuki, P. Estes, M. Ramaswami, D. Yamamoto, and N. J. Strausfeld (1998) The organization of extrinsic neurons and their implications in the functional roles of the mushroom bodies in *Drosophila melanogaster* Meigen. *Learn. Mem.* 5:52-77
- Koenderink, J.J., and A. J. van Doorn (1987) Facts on optic flow. *Biol.Cybern.* 56: 247 -254
- Krapp, H. G., and R. Hengstenberg (1997) A fast stimulus procedure to determine local receptive field properties of motion-sensitive visual interneurons. *Vision Res.* 37:225-34
- Krapp, H.G., Hengstenberg, B. and Hengstenberg R. (1998) Dendritic structure and receptive-field organization of optic flow processing interneurons in the fly. *J. Neurophysiol.* 79:1902-1917
- Lee, T., and L. Luo (1999) Mosaic analysis with a repressible cell marker for studies of gene function in neuronal morphogenesis. *Neuron* 22:451-461
- Meyer, E. P., C. Matute, P. Streit, and D. R. Nässel (1986) Insect optic lobe neurons identifiable with monoclonal antibodies to GABA. *Histochemistry* 84:207-216
- Otsuna, H., and K. Ito (2006) Systematic analysis of the visual projection neurons of *Drosophila melanogaster*. I. Lobula-specific pathways. *J. Comp. Neurol.* 497:928-58
- Papay, R., R. Gaivin, A. Jha, D. F. McCune, J. C. McGrath, M. C. Rodrigo, P. C. Simpson, V. A. Doze, and D. M. Perez (2006) Localization of the mouse alpha1A-adrenergic receptor (AR) in the brain: alpha1AAR is expressed in neurons, GABAergic interneurons, and NG2 oligodendrocyte progenitors. *J. Comp. Neurol.* 497:209-22

- Pierantoni, R. (1976) A look in the cockpit of the fly. The architecture of the lobula plate. *Cell Tissue Res.* 171:101-122.
- Rajashekhar, K. P., and V. R. Shamprasad (2004) Golgi analysis of tangential neurons in the lobula plate of *Drosophila melanogaster*. *J. Biosci.* 29: 93-104
- Reichardt, W. (1961) Autocorrelation, a principle for the evaluation of sensory information by the central nervous system. In: Rosenblith WA (ed) *Sensory communication*. MIT Press/Wiley, New York, pp 377-390
- Reichardt, W. (1987) Evaluation of optical motion information by movement detectors. *J. Comp. Physiol. A* 161:533-547
- Reiff, D. F., A. Ihring, G. Guerrero, E. Y. Isacoff, M. Jösch, J. Nakai, and A. Borst (2005) In vivo performance of genetically encoded indicators of neural activity in flies. *J. Neurosci.* 25:4766–4778
- Sattelle, D. B. (1980) Acetylcholine receptors of insects. In: *Advances in Insect Physiology*. Academic Press, London, New York 15: 215-315
- Sanchez-Soriano, N., W. Bottenberg, A. Fiala, U. Haessler, A. Kerassoviti, E. Knust, R. Lohr, and A. Prokop (2005) Are dendrites in *Drosophila* homologous to vertebrate dendrites?. *Dev. Biol.* 288:126-38
- Scott, E. K., T. Raabe, and L. Luo (2002) Structure of the vertical and horizontal system neurons of the lobula plate in *Drosophila*. *J. Comp. Neurol.* 454:470-481
- Single, S., J. Haag, and A. Borst (1997) Dendritic computation of direction selectivity and gain control in visual interneurons. *J. Neurosci.* 17: 6023-6030
- Single, S. and A. Borst (1998) Dendritic integration and its role in computing image velocity. *Science* 281:1848-50.
- Single, S., and A. Borst (2002) Different mechanisms of calcium entry within different dendritic compartments. *J. Neurophysiol.* 87:1616-1624
- Spradling, A. C., and G. M. Rubin (1982) Transposition of cloned P elements into *Drosophila* germ line chromosomes. *Science* 218:341-347
- Strausfeld, N. J., and U. K. Bassemir (1985a) Lobula plate and ocellar interneurons converge onto a cluster of descending neurons leading to neck and leg motor neuropil in *Calliphora erythrocephala*. *Cell Tissue Res.* 240:617-640
- Strausfeld, N. J., and U. K. Bassemir (1985b) The organization of giant horizontal-motion-sensitive neurons and their synaptic relationships in the lateral deutocerebrum of *Calliphora erythrocephala* and *Musca domestica*. *Cell Tissue Res.* 242:531–550
- Strausfeld, N. J., and W. Gronenberg (1990) Descending neurons supplying the neck and flight motor of Diptera: organization and neuroanatomical relationships with visual pathways. *J. Comp. Neurol.* 302:954-972
- Strausfeld, N. J., and J. K. Lee (1991) Neuronal basis for parallel visual processing in the fly. *Vis. Neurosci.* 7:13-33
- Strausfeld, N. J., A. Kong, J. J. Milde, C. Gilbert, and L. Ramaiah (1995) Oculomotor control in Calliphorid flies: GABAergic organization in heterolateral inhibitory pathways. *J.Comp.Neurol.* 361:298–320
- Sudhof, T. C., M. Baumert, M. S. Perin, and R. Jahn (1989) A synaptic vesicle membrane protein is conserved from mammals to *Drosophila*. *Neuron* 2:1475-81
- Trimble, W. S., D. M. Cowan, and R. H. Scheller (1988) VAMP-1: a synaptic vesicle-associated integral membrane protein. *Proc. Natl. Acad. Sci. U S A* 85:4538-42
- Verkhusha, V. V., S. Tsukita, and H. Oda (1999) Actin dynamics in lamellipodia of migrating border cells in the *Drosophila* ovary revealed by a GFP-actin fusion protein. *FEBS Lett.* 445:395-401

Verkhusha, V. V., H. Otsuna, T. Awasaki, H. Oda, S. Tsukita, and K. Ito (2001) An enhanced mutant of red fluorescent protein DsRed for double labeling and developmental timer of neural fiber bundle formation. *J. Biol. Chem.* 276:29621-29624

Zhang, H. G., H. J. Lee, T. Rocheleau, R. H. ffrench-Constant, and M.Y. Jackson (1995) Subunit composition determines picrotoxin and bicuculline sensitivity of *Drosophila* gamma-aminobutyric acid receptors. *Mol. Pharmacol.* 48:835-840

4 Manuscript Nr.2

Response Properties of Motion-Sensitive Visual Interneurons in the Lobula Plate of *Drosophila melanogaster*.

This chapter was published in March 2008 in *Current Biology*, Volume 18, 368-374;
by Maximilian Jösch, Johannes Plett, Alexander Borst and Dierk F. Reiff.

Max-Planck-Institute of Neurobiolog
Department of Systems and Computational Neurobiology
Am Klopferspitz 18
D-82152 Martinsried, Germany

Maximilian Jösch developed the methodology to record from lobula plate tangential cell in vivo and performed and analyzed the experiments. Johannes Plett developed the LED-stimulus device. Maximilian Jösch , Dierk Reiff and Alexander Borst conceived the experiments. Dierk Reiff, Maximilian Jösch and Alexander Borst wrote the manuscript.



Summary

The crystalline-like structure of the optic lobes of the fruit fly *Drosophila melanogaster* has made them a model system to study neuronal cell fate determination, axonal path finding and target selection. For functional studies, however, the small size of the constituting visual interneurons has presented a formidable barrier so far. We have overcome this problem by establishing *in vivo* whole cell recordings [1] from genetically targeted visual interneurons of *Drosophila*. Here, we describe the response properties of six motion-sensitive large-field neurons in the lobula plate that form a network consisting of individually identifiable, directionally-selective cells most sensitive to vertical image motion (VS-cells [2,3]). Individual VS-cell responses to visual motion stimuli exhibit all the characteristics that are indicative for presynaptic input from elementary motion detectors of the correlation-type [4,5]. Different VS-cells possess distinct receptive fields that are arranged sequentially along the eye's azimuth, corresponding to their characteristic cellular morphology and position within the retinotopically organized lobula plate. In addition, lateral connections between individual VS-cells cause strongly overlapping receptive fields that are wider than expected from their dendritic input. Our results suggest that motion vision in different dipteran fly species is accomplished in similar circuitries and according to common algorithmic rules. The underlying neural mechanisms of population coding within the VS-cell network and of elementary motion detection, respectively, can now be analyzed by combining electrophysiology and genetic intervention in *Drosophila*.

Results and Discussion

Motion vision in the *Drosophila* visual system has been considered an ideal model system to address the fundamental rules of information processing in neural networks. This notion is based on genetic amenability that meets a crystalline-like organization of the neural lattice. Moreover, experiments can be guided by a conceptually much advanced theoretical background: precisely defined visual stimuli are being used in experiments [6] that can be fed into a well established computational model [4]. Following the latter idea, cellular responses of giant motion-sensitive cells within the lobula plate of large flies have been extensively analyzed [7]. However, these experiments were at some point limited by the lack of elaborated genetic tools in large flies, whereas in *Drosophila* similar experiments were so far hampered by difficulties in recording from identified neurons in the intact animal during visual stimulation. Inspired by the detailed findings in large flies, we focused on experiments suitable to address recent as well as classical aspects of visual motion detection such as direction-selectivity and orientation tuning (Fig.1), recently described receptive field organization and computations within the VS-cell network [8-10] (Fig.2) and various hallmarks of the correlation-type model of motion detection (Figs.3,4). We reproduced these findings in *Drosophila* and demonstrate that it is now possible to combine functional cellular approaches with the rich repertoire of genetic techniques as established in many other studies. This combination promises important insights into the neural circuitry underlying elementary motion detection in columnar neurons of the second visual ganglion, the medulla, as well as information processing within the VS-cell network of the lobula plate.

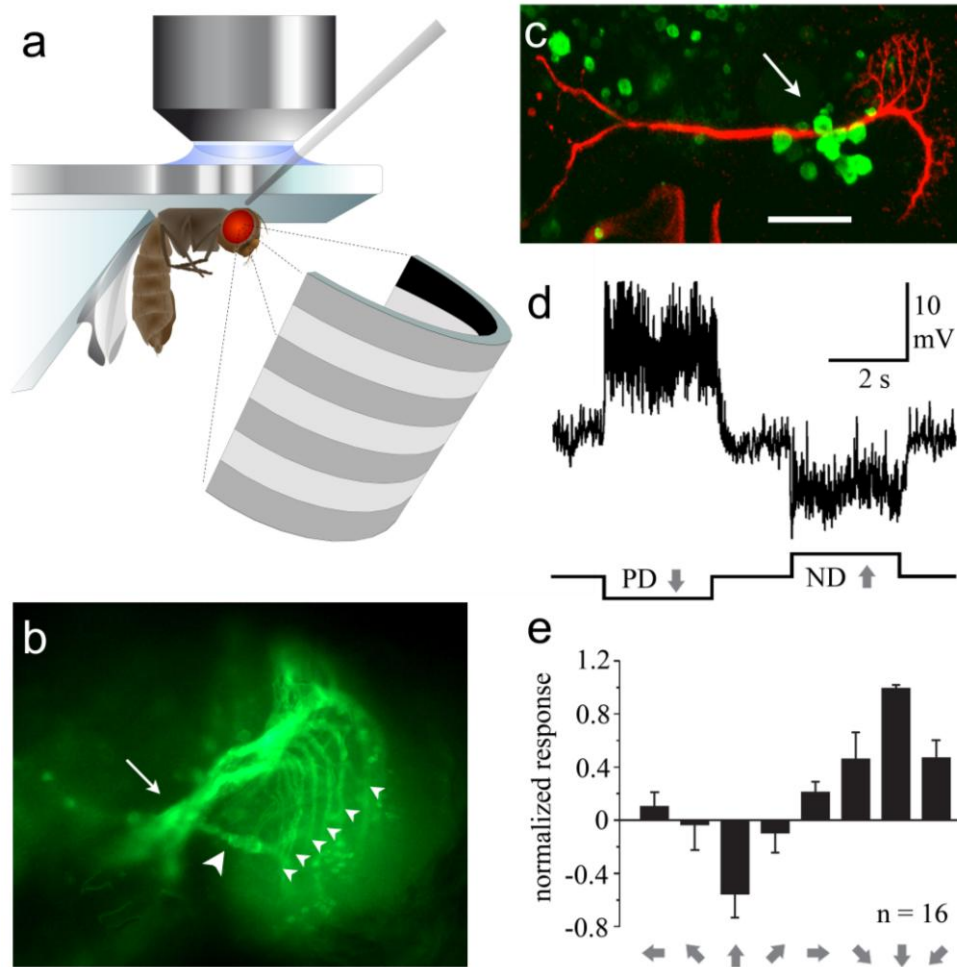


Figure 1 Whole cell patch clamp recordings from genetically labeled visual interneurons in the lobula plate. (A) Schematic drawing of the fly preparation including recording electrode and stimulus presentation in the ventral field of view. (B) View on a *in vivo* preparation of a fly expressing a cytosolic fluorescent marker in a population of lobula plate tangential cells (*DB331-Gal4* \rightarrow *UAS-Yellow Cameleon 3.3*; wide field epifluorescence image). 6 VS-cells (VS1-VS6) can be identified with their dendrites (small white arrowheads) and axons (white arrow). The dendrite of the HSS-cell is also visible (large white arrowhead). However, HS-cells are mostly hidden by the more superficial VS-cells. (C) View of the lobula plate of an experimental animal immediately after recording of a VS1-cell. The expression of a different green fluorescent marker (*DB331-Gal4* \rightarrow *UAS-mcD8-TN-XL-8aa*, see supplemental material) highlights mostly the somata of LPTCs (white arrow) and a few other cells. The recorded cell was perfused with Alexa 568 (red, see methods; collapsed confocal image stack; scale bar: 25 μ m; VS-1 soma removed during withdrawal of the patch pipette). (D) The recorded membrane potential of the VS1-cell shown in (C) displays direction selective responses. Grating motion is indicated by the bottom black line (large field sinusoidal horizontal grating, $\lambda = 50^\circ$ and $v = 50^\circ / \text{sec}$; E) Orientation tuning of *Drosophila* VS-cells. 16 recorded VS-cells (VS1-VS4), each being most sensitive to stimulation along the vertical axis were averaged. The grating, same as in (D), moved into eight different directions indicated by the grey arrows. Data and error bars represent mean \pm SEM.

Whole Cell Patch Recordings Reveal Six Motion Sensitive *Drosophila* VS-cells (VS1-VS6).

Recently it has been shown that individual neurons in *Drosophila* are accessible to whole cell patch-clamp recording [1]. Following this approach we report the first single unit recordings of motion sensitive, individually identified *Drosophila* visual interneurons (Fig. 1A, see methods). Since the preparation prevents the use of high contrast providing optics (like differential interference contrast), we used the Gal4-UAS system [11] and water immersion optics to fluorescently target a small population of tangential cells within the third visual ganglion of the optic lobe, the lobula plate (*DB331-Gal4* \rightarrow *UAS-YC3.3*; Fig. 1B). Based on their morphological similarities to the corresponding lobula plate tangential cells in *Calliphora* [7,12,13] these neurons have previously been characterized in fruit flies as 3 HS- (HSS-cell: large white arrowhead) and 6 more posterior VS-cells (small white arrowheads) [2,3,14,15]. *Drosophila* VS-cells extend their closely intermingled axonal projections (Fig. 1B, white arrow) to the central brain and possess large dendrites that span large parts of the lobula plate tangentially. The six VS-cell dendrites tile the lobula plate sequentially (Fig. 1B, white arrowheads; see also Figs. 1C, 2B) with partially overlapping dendritic fields.

In a first set of experiments we investigated direction selectivity and orientation tuning in the six anatomically described *Drosophila* VS-cells. We added a red fluorescent dye to the intracellular solution and directed the electrode towards green fluorescent cells. Stable whole cell patch-clamp recordings were only feasible from cell bodies, but cell bodies were not clearly visible in neurons that expressed cytosolic YC3.3 (Fig. 1B). Thus we facilitated visually guided patch-clamp recordings by expression of a green fluorescent marker (*DB331-Gal4* \rightarrow *UAS-mCD8-TN-XL-8 α* ; see supplementary information) that predominantly highlights somata (Fig. 1C). Using this marker, recordings were obtained from more than 100 VS-cells all individually identified from dye fills subsequent to the recording (Fig. 1C; see methods). VS-cells revealed an input resistance of 30-40 M Ω , a resting potential of about -45 mV (-55 mV when corrected for the liquid junction potential) and showed spontaneous fast membrane fluctuations even in the absence of moving visual stimuli. During the presentation of vertically moving periodic gratings (velocity $v = 50^\circ/\text{sec}$, spatial wavelength $\lambda = 44^\circ$, as seen by the fly) all VS-cells exhibited directionally selective responses, such as shown for a VS1-cell (Fig. 1D, Fig. S1). Upward motion (ND = null direction) and downward motion

(PD = preferred direction) of a periodic horizontal grating elicited a graded hyperpolarization and depolarization of the membrane potential, respectively, superimposed by small action potentials of irregular amplitude that can likely be attributed to TTX-sensitive fast voltage-activated sodium currents as their main source (Fig. S2). These fast events were reduced in frequency and amplitude during upward motion and increased during downward motion (Fig. 1D, Fig. S1). Presentation of large field grating motion in eight different directions and 4 different orientations separated by 45° (Fig. 1E) revealed that all six VS-cell types were indistinguishably sensitive to large field stimuli moving along the vertical axis of the animal, thus the responses of different VS-cell types were pooled ($n = 16$, $v = 25^\circ/\text{sec}$, $\lambda = 25^\circ$).

Receptive Field Organization and Evidence for a *Drosophila* VS-cell network.

Because the fly visual system is organized retinotopically, the visual surround is mapped onto the individual VS-cell dendrites by their connections to presynaptic columnar elements [15]. Six VS-cells (VS1-VS6) have consistently been described in *Drosophila* [2,3,14,15] and each facet eye looks at $\sim 180^\circ$ elevation and $\sim 180^\circ$ azimuth [16]. Estimating a dendritic overlap of 50% between adjacent cells, each cell is supposed to sample local motion detectors from maximally about 60° along the azimuth and almost 180° elevation. However, the architecture of the receptive fields might be more complex as shown in *Calliphora* where the visual surround is indeed mapped onto the ten VS-cell dendrites in precisely this way, yet the extent of the VS-cell receptive fields along the azimuth is much broader [8,17,18]. This prompted us to analyze how vertical motion in different areas of the visual surround of the fly is represented by the six *Drosophila* VS-cells. A small bar of 6° width was moved up- and downwards in the ventral field of view from 0° to -50° ventrally at 28 different positions along the azimuth from -60° on the contralateral side to $+105^\circ$ on the ipsilateral side ($0^\circ = \text{frontal}$; Fig. S3). The mean normalized response (PD minus ND) of each cell at each position of the moving bar was averaged for VS-cells of the same cell type ($n = 4, 6, 9, 5, 5, 2$ cells, respectively, for VS1-VS6). Dye fills allowed unequivocal identification of different VS-cells (Fig. 2A) based and on their distinct dendritic branching pattern [2,3]. Plotting the normalized responses for each cell type (Fig. 2B) as a function of the azimuth shows that i) each *Drosophila* VS-cell type possesses its distinct receptive field, ii) the receptive field centers of the different VS-cells are sequentially arranged along the azimuth with VS1 being most frontal and

VS6 most lateral (Fig. 2B). Note, however, that we could not characterize the receptive field in the dorsal part of the eye due to the arrangement of the fly in the recording setup (Fig. 1A). iii) The receptive fields of VS-cells cover more than 100° of visual space along the azimuth (half-width of about 80°) which is much wider than expected (see above). Only the position of the receptive field center is determined by the position of the dendrite while the width of their receptive fields seems to be affected by other factors, too.

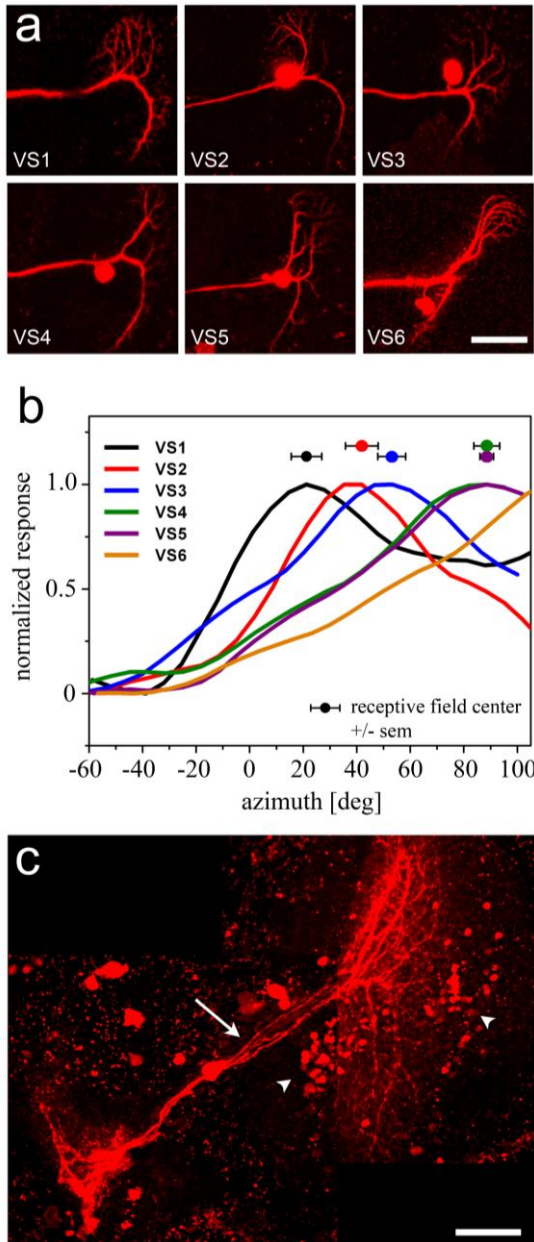


Figure 2 Receptive fields of the six *Drosophila* VS-cells (VS1-VS6) (A) Alexa 568, loaded via the patch pipette, enabled reliable identification of the recorded VS-cell type (VS1 - VS6; collapsed confocal image stacks, scale bar: 25 μ m). (B) Average receptive fields of VS1 - VS6 (mean \pm SEM). The centers of the different VS-cell types are sequentially arranged along the azimuth showing a surprisingly large overlap. Note that, for VS6, the center is located outside (posterior) of the stimulated area. (C) Dye coupling of neighboring VS-cells. A single, genetically labeled (*DB331-Gal4* \rightarrow *UAS-mCD8-TN-XL-8aa*) VS6-cell was perfused with a mixture of Alexa-568 (red) and Neurobiotin via the patch pipette. The spread of Neurobiotin (detected by staining with Streptavidin-Alexa-568, in red) to at least four neighboring VS-cells reveals an intensity gradient with distant cells being stained more faintly. 4 - 5 VS-cell axons (white arrow) and two clusters of small cell bodies from unidentified columnar neurons (white arrowheads) are stained (scale bar 50 μ m). Comparable results were obtained from all types of VS-cells in 15 independent experiments.

The width and overlap of VS-cell receptive fields as described in *Calliphora* [8,9,17,18] might represent a common organization principle for dipteran VS-cells.

According to this view, VS-cells partially inherit their receptive fields from their immediate VS-cell neighbors. The emerging VS-cell network is endowed with intricate computational properties [10,19] where electrical synapses to neighboring VS-cells play a key role. We investigated possible electric coupling in *Drosophila* VS-cells indirectly by perfusion of an individual VS-cell with a mixture of two different dyes, Alexa 568 and Neurobiotin, loaded via the same patch pipette (Fig. 2C). As in all other experiments Alexa 568 never spread to other cells but remained restricted to the recorded one. This allowed the immediate identification of the patched neuron. After fixation and labeling of Neurobiotin via Streptavidin-Alexa 568, the diffusion of Neurobiotin to other neurons within the lobula plate or the lateral protocerebrum was detected in all trials (n = 15, all types of VS-cells analyzed). Typically, Neurobiotin labeled the immediate neighbors of the perfused VS-cell. In Figure 2C the axons and basal dendrites of 4 VS-cells neighboring to the patched VS6-neuron are strongly labeled (white arrow) and additional labeling was observed in cell bodies within the cortex of the lobula plate (white arrowheads). Thus, VS-cells in *Drosophila* show dye coupling providing indirect evidence for electric coupling between neighboring VS-cells as the basis for their large receptive fields [20].

Computational Structure of the Presynaptic Motion Detection Circuitry

Directionally selective responses in insects are computed locally and in parallel from the changing retinal brightness distribution [4,5,21] by correlating, at each image location, the brightness values as derived from neighboring photoreceptor signals after asymmetric temporal filtering. Doing this twice in a mirror-symmetrical fashion and subtracting the output signals of both subunits leads to a fully directional output signal. As a hallmark of such a computation, the response of the animal to a drifting sine grating is expected to show a velocity optimum, which is a linear function of the pattern wavelength resulting in a constant temporal frequency optimum. This has been found to hold true in behavioral experiments on the beetle *Chlorophanus* [21], the honeybee *Apis* [22], the housefly *Musca* [23,24] as well as in *Drosophila* [6,25,26]. Subsequent work in the blowfly *Phaenicia* and *Calliphora* confirmed that, amongst other predictions of the Reichardt model [27,28], this response feature is fully retained, too, in large-field motion-sensitive neurons in the lobula plate [29,30]. Thus we measured the velocity dependence at different spatial wavelengths presenting sine gratings at spatial wavelength $\lambda = 44^\circ$ and 22° , respectively, that drifted downward for three

seconds at various speeds. Plotting the normalized mean response as a function of pattern velocity revealed a response optimum at $44^\circ/\text{sec}$ for the large and at $22^\circ/\text{s}$ for the small wavelength pattern (Fig. 3A). When plotted as function of the temporal frequency (Fig. 3B), both curves coincide with the same response optimum at 1 Hz. This finding makes a strong argument for elementary motion detectors of the correlation-type providing input to VS-cells in *Drosophila*.

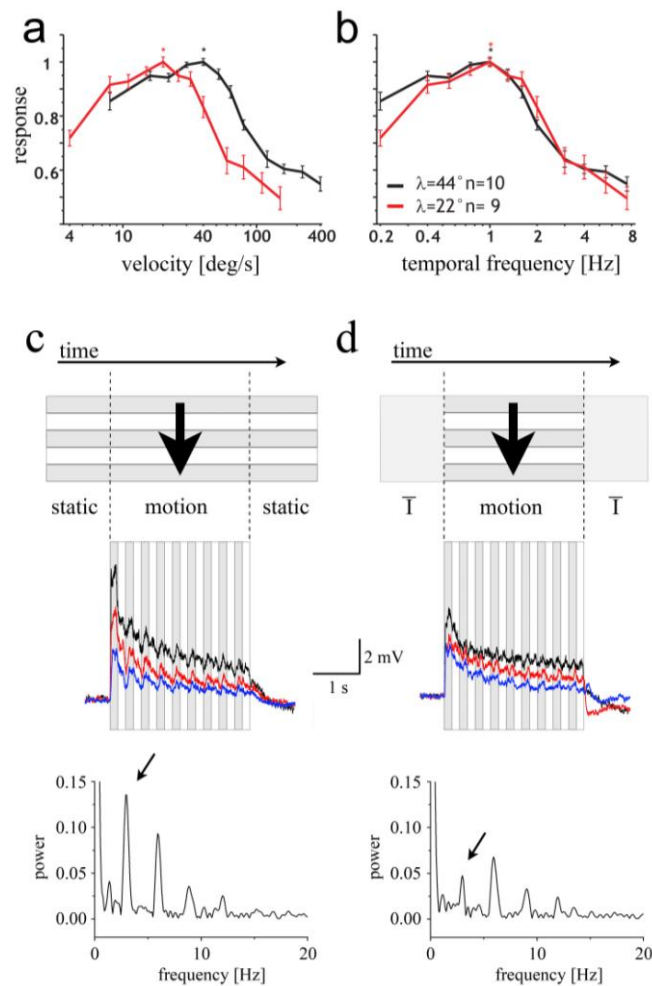


Figure 3 Velocity tuning (A, B) and step-responses (C, D) of *Drosophila* VS-cells. (A) Normalized responses of VS-cells to PD- motion are plotted against the velocity of the stimulus using two different sine wave stimuli (red: $\lambda = 22^\circ$, black: $\lambda = 44^\circ$). At each stimulus velocity the first 500 ms of the recording trace after motion-onset were normalized to the maximum response. Each cell was measured at least 4 times for each stimulus condition, asterisk indicate the maximum of the mean response. Data of VS1-VS4 cells are averaged, $n = 9$ and 10 cells, respectively, mean \pm SEM. (B) Same data as in A, but plotted as a function of the temporal frequency (velocity divided by the pattern wavelength). (C) After motion onset VS-cells exhibit characteristic oscillations that are imposed by the temporal frequency of the moving grating ($\lambda = 50^\circ$, 3 Hz, indicated by the grey stripes in the background) if the still grating was already present before the onset of motion. A periodic square-wave grating was presented, after 4 seconds the grating started to move abruptly at a constant velocity of $150^\circ / \text{s}$ ($f_t = 3$ Hz). Experiments were performed at constant mean luminance with 85 % (black), 28 % (red) and 14 %

(blue) pattern contrast. The relative magnitude of the oscillations increased with decreasing pattern contrast. **(D)** Only weak oscillations are detectable in the VS-cell response if the still grating prior the onset of constant motion is replaced by an equiluminant homogeneous screen (stimulus contrast as in C). Bottom panels in c and d show Fast Fourier Transforms (FFT) of the mean response of all experiments in (C) and (D). FFT revealed a 3 fold higher power at the temporal frequency of the pattern (3 Hz, black arrow) when a static grating was presented prior to motion onset as compared to a homogeneous screen (cell types VS1-VS4 averaged, $n = 8$ cells; 8 to 20 sweeps / cell).

Characteristic step-response transients elicited by the abrupt onset of motion represent another key feature of the presynaptic motion detection circuitry [31,32]. In *Calliphora* this step-response consists of initial transient oscillations followed by a plateau-like steady state response. The initial oscillations are imposed by the frequency of brightness changes of the pattern and do not reflect intrinsic oscillatory dynamics of the neural circuitry. However, both components depend on features of the visual stimulus itself and precisely match model calculations based on a correlation-type detector model [33]. We analyzed step-responses in VS-cells of *Drosophila* (Fig. 3C). Prior to the onset of grating motion, either an identical stationary grating ($\lambda = 50^\circ$, Fig. 3C) or an isoluminant homogeneous screen (Fig. 3D) was presented to the flies. After 4 seconds the grating started moving abruptly at a velocity of $150^\circ/\text{s}$ corresponding to a temporal frequency of 3 Hz which allowed detection of several oscillation cycles. With both types of pre-stimulus conditions experiments were performed at 85, 28 and 14 % pattern contrast (black, red and green recording traces, respectively, in Fig. 3C and D). When starting from a stationary grating, the response oscillated at 3 Hz (Fig. 3C). The oscillations lasted for several seconds and their amplitude depended on the pattern contrast: with increasing contrast the oscillations were damped more quickly and gave way to the underlying steady-state response. When a homogeneous green screen was presented before the onset of grating movement (Fig. 3D), the oscillations tended to have much smaller amplitudes. Small remaining oscillations can most likely be attributed to the limited spatial resolution of the LED arena. As expected, under these conditions the steady-state component showed a similar positive dependence on pattern contrast. The responses of all experiments were used to calculate the power spectra of the recordings taken at both pre-stimulus conditions (lower panels in Figs. 3C and 3D). With the grating presented prior to motion VS-cell responses oscillated with three-fold higher power at the fundamental frequency of the moving grating (3 Hz) compared to the homogeneous screen as starting condition. These results are in line with the step-responses measured in *Calliphora* tangential cells [32] and can be precisely simulated in a correlation-type model of elementary motion detection that

includes two temporal filters [33]. Adaptation of the time-constant of a high-pass filter in the cross-arms of the detector can fully reproduce these results whereas other models or versions of motion detectors fail.

One prerequisite of a directionally selective neuron is its capability to encode the direction of image motion independent of the sign of contrast. We investigated this property by presenting either a black bar moving on a white background or a white bar moving on a black background (Fig. 4A). In the different VS-cell types upward and downward motion of the bar was always reported by hyperpolarization and depolarization of the membrane potential, respectively, independent of the sign of contrast. As a further test for the Reichardt-model, we studied the contrast dependence of the VS-cell response. Due to the multiplication of luminance values, a quadratic contrast dependence of individual correlation-type motion detectors is expected in principle [27]. However, as analyzed in all species so far, such a quadratic contrast dependence is found for small contrasts only (contrast < 10 %); for higher contrast levels, the response strongly saturates [6,34]. We observed a similar saturation nonlinearity in *Drosophila* VS-cells when flies were stimulated with a periodic grating drifting at 1 Hz temporal frequency at four different contrast levels (10, 40, 75 and 100 %). The response increased with increasing pattern contrast and showed clear signs of saturation at high luminance contrast (Fig.4B). In agreement with behavioral studies on the optomotor response in *Drosophila* [6], the half-maximum response was reached at about 24 % luminance contrast.

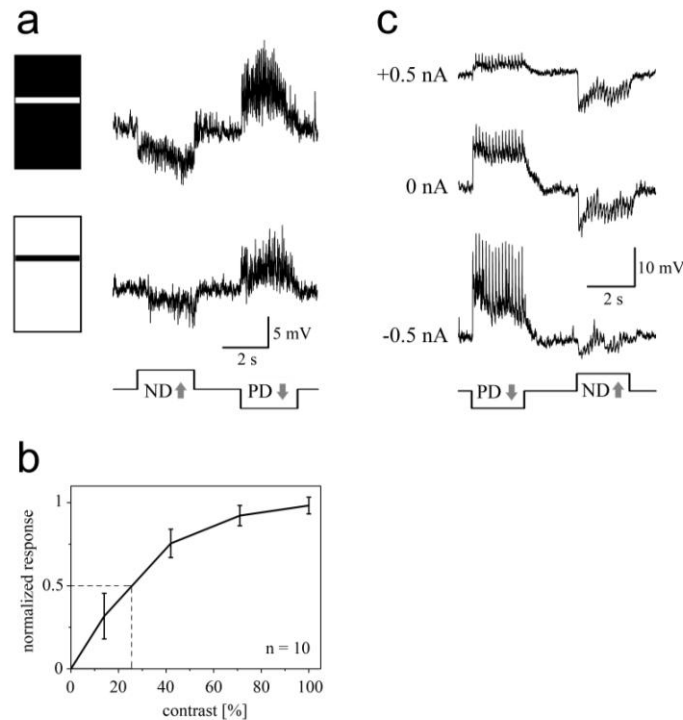


Figure 4 Further response characteristics of VS-cells. (A) A white bar in front of a black background (upper trace) and a black bar in front of a white background (lower trace) were moving up and down. Under both conditions the direction of the moving bar was reported similarly by the membrane potential during upward and downward motion, respectively, independent of the sign of contrast. (B) A periodic grating ($\lambda = 25^\circ$) was moved at constant speed and a temporal frequency of 1 Hz. The normalized response of VS-cells increases with increasing pattern contrast and exhibited a saturation characteristic with a half-maximum response at 24 % pattern contrast ($n = 10$, mean \pm SEM). (C) Recording traces of a VS-cell in current clamp during PD- and ND-motion reveal that responses evoked by grating motion depend on the magnitude and polarity of the injected current. Current was injected permanently (+ 0.5, 0 and -0.5 nA) while the pattern moved upward or downward. Grating motion is indicated by the black line underneath the traces. In (A) and (C) 14 and 10 cells, respectively, were analyzed, in all panels data was pooled from VS1-VS4).

Last we elucidated the final step in local motion detection, i.e. the subtraction of local motion detectors with opposite preferred direction. If this subtraction stage was presynaptic to the dendrites of VS-cells (alternative 1), a single type of fully directional input would be expected. The synaptic transmitter release of this input would be up- and down-regulated according to preferred or null direction motion. If the subtraction stage was realized on the dendrites of VS-cells themselves (alternative 2), two types of inputs with opposite preferred direction should provide inhibitory and excitatory input to the VS-cell dendrites, respectively. One can decide between these two alternatives in various ways, all of which have been done in tangential cells of

Calliphora, and all of which provide evidence for the latter situation [35-37]. We recorded from VS-cells in current clamp mode and injected DC- current while presenting periodic grating motion in preferred and null direction (Fig. 4C). If alternative 1 holds true, injection of constant current should affect both preferred and null direction response similarly by shifting the membrane potential away from the synaptic reversal potential. If, however, alternative 2 is realized, hyperpolarizing the postsynaptic cell should decrease the null direction response by reducing the driving force and, at the same time, increase the preferred direction response by increasing the driving force. Injection of depolarizing current would cause the opposite. Injection of -0.5 nA eliminated the hyperpolarization during null direction motion completely while the preferred direction response became larger. Depolarizing current injection of + 0.5 nA increased the amplitude of the null direction motion response whereas the amplitude of the graded depolarization and the small action potentials during preferred direction motion was decreased. These findings provide evidence that VS-cells in *Drosophila* receive input from two types of local, motion-sensitive elements: one excitatory tuned to downward motion, one inhibitory tuned to upward motion. Thus, in terms of the computational structure described above, the subtraction stage of the correlation-type motion detector is implemented as a push-pull mechanism between excitatory and inhibitory inputs on the dendrites of VS-cells in *Drosophila*.

In summary, we established *Drosophila melanogaster* as a model system for the cellular analysis of visual motion detection and provide the first account on *Drosophila* VS-cell response properties. By reproducing knowledge in *Drosophila* VS-cells that was originally obtained in large flies like *Calliphora* we suggest that (i) uniform neural mechanisms of visual motion processing exist across different dipteran species, (ii) *Drosophila* qualifies for the analysis of population coding within the VS-cell network, and (iii) *Drosophila* allows to unravel the neural implementation of elementary motion detection in columnar neurons of the medulla. This can be achieved by combining the expression of genetic tools allowing to activate or inactivate neural function [38,39] in genetically targeted columnar neurons while recording from VS-cells during visual stimulation.

Experimental procedures

Flies. Flies were raised on standard cornmeal-agar medium at a 12 h light / 12 h dark cycle, 25°C and 60 % humidity. We used female experimental flies, one day post- eclosion. The DB331-Gal4 line (kindly provided by R. Stocker, Fribourg, Switzerland) was used to express Gal4 mostly in tangential cells and a few unidentified columnar neurons. UAS-YC3.3 was used in Figure 1B to highlight entire cells by cytosolic expression of the reporter molecule. In all other experiments UAS-mCD8-TN-XL-8aa was used to predominantly stain cell bodies (see supplemental material).

Preparation. Flies were anesthetized on ice and waxed on a Plexiglas holder using bee wax. The head was bent down to expose the caudal backside of the head (Fig.1A) and the extended proboscis was fixed. Occasionally wax was put on the thorax and parts of the contra lateral eye to stabilize the preparation. Aluminum foil with a hole of ~ 1-2 mm sustained by a ring shaped metal holder was placed on top of the fly such that thorax and head tightly fitted into the hole. The aluminum foil separated the upper wet part (covered with ringer solution [1]) of the preparation from the lower dry part. The foil was aligned to the most dorsal ommatidia located in the dorsal rim area. Water immersion optics was used from above and visual patterns (see below) were presented to dry and intact facette eyes. A small window was cut into the backside of the head and during mild protease treatment (protease XIV, E.C.3.4.24.31, Sigma, Steinheim, Germany; 1 mg / ml, max 3 min) the neurolemma was partially digested and the main tracheal branches and fat body were removed. The protease was rinsed off carefully and replaced by ringer solution. A ringer-filled cleaning electrode (tip ~ 4 µm) was used to remove the extracellular matrix and to expose the VS-cell somata for recording.

Visually guided whole cell recording. Genetically labeled green fluorescent VS-cell somata covered by ringer solution [1] were approached with a patch electrode filled with a red fluorescent dye (intracellular solution as in [40]; containing additional 5 mM Spermine and 30 µM Alexa-Fluor-568-hydrazide-Na, Molecular Probes, adjusted to pH = 7.3). Recordings were established under visual control using a 40X water immersion objective (LumplanF, Olympus), a Zeiss Microscope (Axiotech vario 100, Zeiss, Oberkochen, Germany), fluorescence excitation (100 W fluorescence lamp, heat

filter, neutral density filter OD 0.3; all from Zeiss, Germany) and a dual band filter-set (EGFP / DsRed, Chroma Technology, Rockingham, USA). During the recordings the fluorescence excitation was shut off to prevent blinding of the fly. 5-7 M Ω patch-electrodes (thin wall, filament, 1.5 mm, WPI, Florida, USA) were pulled on a Sutter-P97 (Sutter Instrument Company, CA, USA). A reference electrode (Ag-AgCl) was immersed in the extra cellular saline (pH 7.3, 1.5 mM CaCl₂, no sucrose). Signals were recorded on an NPI BA-1S Bridge Amplifier (NPI Electronics GmbH, Tamm, Germany), low-pass filtered at 3 kHz and digitized at 10 kHz via a digital-to-analog converter (PCI-DAS6025, Measurement Computing, Norton, MA, USA) using Matlab (Vers. 7.3.0.267, Mathworks Inc., USA). After the recording, several images of each Alexa-filled LPTC were taken at different depths along the z-axis (HQ-filter-set Alexa 568, Chroma Technology, Rockingham, USA) using a CCD camera (Spot Pursuit 1.4 Megapixel, Visitron Systems GmbH, Puchheim, Germany). These images allowed anatomical identification of the recorded cell based on their characteristic branching patterns. Additionally, cells were digitized by confocal fluorescence microscopy (see next section). The precise position of the fly's head was controlled using the deep pseudo-pupil technique [41]. Deviations of more than 5° were corrected during the data analysis.

Confocal microscopy. Serial optical sections were taken from recorded VS-cells in the intact preparation using a Leica confocal microscope (TCSNT, Leica) and a 40X water-immersion objective (LUMPlanF, Olympus). Images were taken at 1 μ m intervals and 1024 x 1024 pixel resolution. Size, contrast and brightness of the resulting image stacks were adjusted using ImageJ (<http://rsb.info.nih.gov/ij>).

Neurobiotin coupling. VS-cells were targeted and perfused using patch electrodes as described above. 3 % Neurobiotin (Vector Labs, Burlingame) was added to the intracellular solution. Neurobiotin and Alexa Fluor 568 were co-injected using \pm 0.5 nA current pulses for up to 10 min. For initial identification the perfused individual VS-cell was imaged using the fluorescence microscope and CCD-camera described above. For Streptavidin staining, brains were fixed in 4 % PFA (40 min), washed in PBT (45 – 60 min; PBT: PBS, including 1 % Triton X-100, pH 7.2) and incubated in PBT including 2 % normal goat serum (Sigma Aldrich, St. Louis, MO; G9023). Streptavidin Alexa Fluor 568 conjugate (Invitrogen) was added at 1:100 overnight (4°C). Streptavidin was removed by several washing steps (5 x 20 minutes in PBT) and followed by final

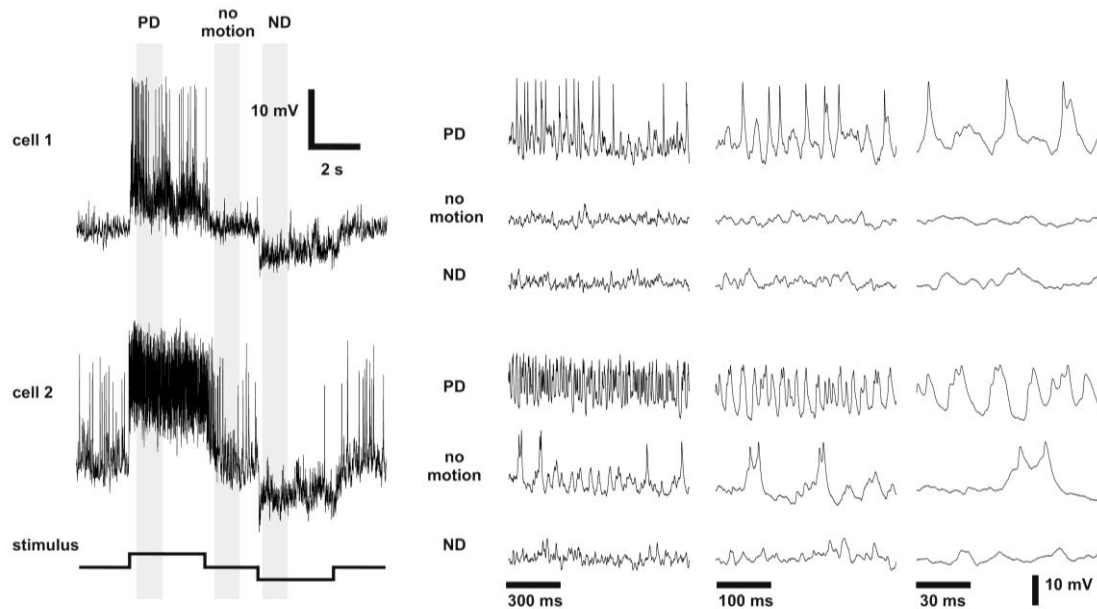
washing steps in PBS (5 x 20 minutes). The stained brains were mounted in Vectashield (Vector Laboratories, Burlingame, CA) and analyzed by confocal microscopy. Perfusion of a single VS-cell never resulted in more than one Alexa-568 filled cell. Only after labeling of Neurobiotin using Streptavidin-Alexa-568 conjugate other cells lighted up. The second red label was used to prevent spectral overlap with the green fluorescence of genetically labeled neurons.

Visual stimulation. Two custom built LED arenas allowed refresh rates of up to ~ 550 Hz and 16 intensity levels. They covered 170° (1.9° resolution) and 180° (3.2° resolution) of the horizontal visual field, respectively. The LED arenas were engineered and modified based on the open source information of the Dickinson Laboratory (www.its.caltech.edu/~mreiser/panels.html). The first LED array consists of seven by four individual TA08-81GWA dot matrix displays (Kingbright, City of Industry, CA, USA) each harboring eight by eight individual green (568 nm) LEDs. The second arena consists of eleven by eight BM-10288MD dot matrix displays each again housing eight by eight green (568 nm) LEDs. In both implementations each dot matrix display is controlled by an ATmega168 microcontroller (Atmel, San Jose, CA, USA) combined with a ULN2804 line driver (Toshiba America Inc, NY, USA) acting as a current sink. All panels are in turn controlled via an I²C interface by an ATmega128 (Atmel, San Jose, CA, USA) based main controller board which reads in pattern information from a compact flash (CF) memory card. Matlab (Vers. 7.3.0.267, Mathworks Inc., USA) was used for programming and generation of the patterns as well as for sending the serial command sequences via RS-232 to the main controller board. The luminance range of the stimuli was $0,5 - 8 \text{ cd} / \text{m}^2$ for investigation of step-responses and $0 - 8 \text{ cd} / \text{m}^2$ in all other experiments.

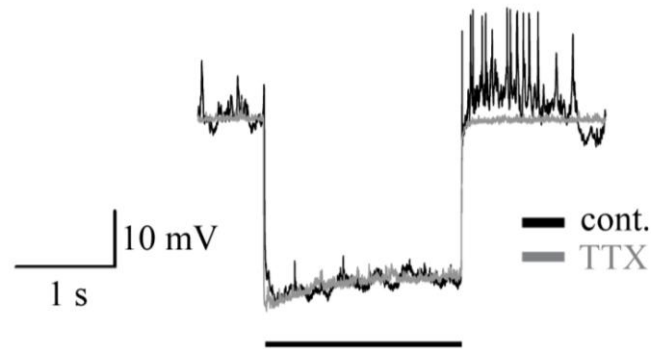
Data analysis. Data were acquired and analyzed using the data acquisition and analysis toolboxes of Matlab (Vers. 7.3.0.267, The Mathworks, USA). Receptive fields were calculate by binning the responses of single VS-cells to vertical stimulation ($\sim 5^\circ$ elevation / $\sim 6^\circ$ azimuth) and subtracting the mean response during null direction from the mean response during preferred direction motion. The data of each individually identified cell was normalized to the maximum response. The projection of the receptive field on the azimuth was calculated for each VS-cell individually by averaging the binned responses at the different elevations at each position along the

azimuth. Contrast was calculated as $(I_{\max} - I_{\min}) / (I_{\max} + I_{\min})$ with an absolute I_{\min} and I_{\max} of 0 and 8 cd / m², respectively.

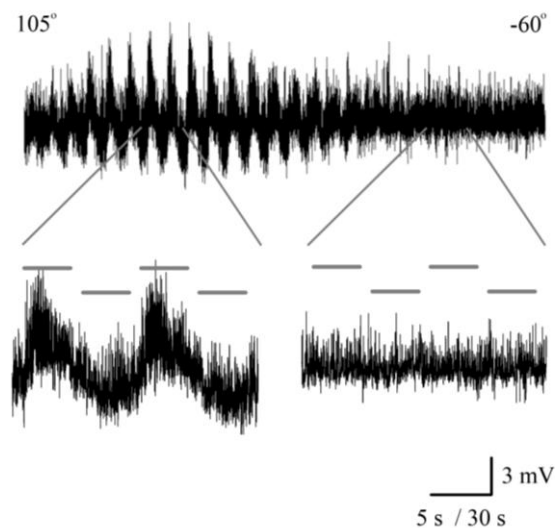
Supplementary Material



Supplementary Figure S1 Recording traces of two VS-cells during presentation of a periodic sinusoidal grating (0.2 – 8 cd / m²). The time-course of the membrane potential relative to the direction of grating motion designates both neurons as directionally selective prototypic VS-cells similar to the ones described in large flies. All recorded cells exhibited a depolarization during constant downward grating motion (preferred-direction, PD) and a hyperpolarization during constant upward grating motion (null-direction, ND). However, there were differences from cell to cell in the rate at which fast membrane fluctuations of irregular amplitude occur. In one type of cells (cell 1) spike-like events are basically absent if a still grating is presented (no motion) and during PD-motion fast membrane fluctuations are easily detectable that are superimposed on the steady-state depolarization (see close-ups to the right). The other type of cells is represented by cell 2. Spike-like events are highly abundant even in the absence of grating motion. During PD-motion a more pronounced steady-state membrane potential depolarization is exhibited during which individual spike-like potential deflections are not easily detectable (see close-ups to the right). During ND-motion fast membrane potential fluctuations were almost completely suppressed in both types of cells. Both types were observed at similar abundance and did not correlate with the specific VS-cell type. Grating motion is indicated by the black line underneath the recording traces to the right. Sections of the recording traces at the time marked by the grey stripes are shown at increasingly finer time-scale in the panels to the right. It has to be mentioned that in big flies membrane potential fluctuations have been shown to be dependent on the mean brightness [11]. However, in our experiments this parameter was not changed.



Supplementary Figure S2 Active membrane properties in *Drosophila* VS-cells involve TTX-sensitive fast voltage-activated sodium currents. To investigate if such currents are among the ionic repertoire of *Drosophila* VS-cells, -1 nA current was injected for two seconds (indicated by the black bar) turning the membrane potential more negative by additional 30 mV. Then, the neuron was released from hyperpolarization. All this was done without visual stimulation. The black recording trace shows that the fast membrane potential fluctuations are reduced during hyperpolarization. Immediately after being released from negative current, the neuron generated a series of high frequency rebound spikes that can be considered intrinsic in origin and that were blocked by application of TTX onto the lobula plate (grey recording trace). Thus, TTX-sensitive fast voltage-activated sodium currents are likely to be a main source of the irregular amplitude high-frequency events. This interpretation would further corroborate the idea of common mechanisms and pathways of visual motion detection in Dipteran flies [26-28]. Nonetheless we have to consider that the complete block of all fast membrane potential fluctuations by TTX might include blocking of action potentials in columnar elements that provide input to VS-cells (TTX: 500 nM on the lobula plate, grey trace, n = 6; 10 μ l of a 25 μ M TTX-ringer solution were added to 0,5 ml ringer in the bath).



Supplementary Figure S3 Analysis of receptive field width. Five minutes of a recording of a VS3-cell are shown. During the experiment increasingly depolarizing and hyperpolarizing responses are elicited

during PD- and ND-motion, respectively, as the bar moves into the center of the receptive field (upper trace). These potential deflections disappear again as the bar reaches more frontal positions (see close ups, left trace: receptive field center; right trace: off-center). A horizontal bar of 6° width was moved upward (ND) and downward (PD) from vertically 0° to -50° at successive horizontal positions within the ventral field of view. The horizontal positions ranged from ipsilateral +105° posterior to contralateral -60°.

UAS-mCD8-TN-XL-8aa: On its N-terminus the low-affinity calcium indicator TN-XL (Mank et al., 2006) was fused to the transmembrane domain mCD8, on its C-terminus a short Glycin-linker was used to connect TN-XL to six aminoacids known to bind to the PDZ domain of mint. The inspiration for the cloning of this construct came from an article by Maximov & Bezprozvanny (2002) where the authors describe the targeting of N-type voltage gated calcium channels in hippocampal neurons. The authors describe a binding motif of only 6 aminoacids (DQDHWG) located at the C-terminus of the $\alpha 1B$ subunit. In their account this motif was sufficient to cause specific targeting of a mCD4-GFP construct to axons and presynaptic terminals of hippocampal neurons in culture. We used this idea to clone a synaptically targeted version of TN-XL. However, axonal targeting was not retained in transgenic flies and the calcium sensitivity of the reporter was essentially lost. Instead, at low to medium expression levels mCD8-TN-XL-8aa highlights somata efficiently when expressed in neurons of transgenic flies. The protein seems to be trapped in the endoplasmatic reticulum. Although initially unintended we made use of this expression pattern as somata were much brighter compared with an UAS-GFP-nls construct. In our experiments we used a chromosomal insertion on the third chromosome. These flies were crossed to the DB331-Gal4 driver. Even flies homozygous for the driver line and the UAS-construct were behaving normally and no obvious differences could be observed compared with wt-flies.

Supplementary Reference

Mank M, Reiff DF, Heim N, Friedrich MW, Borst A, Griesbeck O (2006) A FRET-based calcium biosensor with fast signal kinetics and high fluorescence change. *Biophys. J.* 90: 1790-1796.

Maximov A, Bezprozvanny I (2002) Synaptic targeting of N-type calcium channels in hippocampal neurons. *J. Neurosci.* 22: 6939-6952.

Acknowledgements

We greatly thank Rachel Wilson for her initial help on whole cell recordings and encouragement, Michael Reiser for advice on the LED-arena, Wolfgang Essbauer, Christian Theile and the MPI workshop for excellent technical support, Robert Schorner for artwork, Yong Choe and Juergen Haag for many helpful suggestions, Bettina Schnell for comments on the manuscript, Alexandra Ihring for the generation of

transgenic flies, Thomas Hendel and all members of the Borst Lab for discussion and help on data analysis and Reinhardt Stocker for providing the DB331-Gal4 line. This work was supported by the Max-Planck-Society and by an HFSP grant to K. Ito, A. Borst and B. Nelson.

References

1. Wilson RI, Turner GC, Laurent G (2004) Transformation of olfactory representations in the *Drosophila* antennal lobe. *Science* 303: 366-370.
2. Scott EK, Raabe T, Luo L (2002) Structure of the vertical and horizontal system neurons of the lobula plate in *Drosophila*. *J Comp Neurol* 454: 470-481.
3. Raghu SV, Jösch M, Borst A, Reiff DF (2007) Synaptic organization of lobula plate tangential cells in *Drosophila*: γ -aminobutyric acid receptors and chemical release sites. *J Comp Neurol* 502: 598-610.
4. Reichardt W (1961) Autocorrelation, a principle for the evaluation of sensory information by the central nervous system. In: Rosenblith WA (ed). *Sensory communication*. MIT Press/Wiley, New York. pp. 377-390.
5. Borst A, Egelhaaf M (1989) Principles of visual motion detection. *Trends Neurosci* 12: 297-306.
6. Götz KG (1964) Optomotorische Untersuchungen des visuellen Systems einiger Augenmutanten der Fruchtfliege *Drosophila*. *Kybernetik* 2: 77-92.
7. Borst A, Haag J (2002) Neural networks in the cockpit of the fly. *J Comp Physiol* 188: 419-437.
8. Haag J, Borst A (2004) Neural mechanism underlying complex receptive field properties of motion-sensitive interneurons. *Nature Neurosci* 7: 628-634.
9. Farrow K, Borst A, Haag J (2005) Sharing receptive fields with your neighbors: Tuning the vertical system cells to wide field motion *J Neurosci* 25: 3985-3993.
10. Cuntz H, Haag J, Foerstner F, Segev I, Borst A (2007) Robust coding of flow-field parameters by axo-axonal gap junctions between fly visual interneurons. *Proc Natl Acad Sci USA* 104: 10229-10233.
11. Brand AH, Perrimon N (1993) Targeted gene expression as a means of altering cell fates and generating dominant phenotypes. *Development* 118: 401-415.
12. Hausen K (1982) Motion sensitive interneurons in the optomotor system of the fly. I. The horizontal cells: structure and signals. *Biol Cybern* 45: 143-156.
13. Hengstenberg R, Hausen K, Hengstenberg B (1982) The number and structure of the giant vertical cells (VS) in the lobula plate on the blowfly *Calliphora erythrocephala*. *J Comp Physiol A* 149: 163-177.
14. Heisenberg M, Wollenberger R, Wolf R (1978) Optomotor-blind^{H31} – a *Drosophila* mutant of the lobula plate giant neurons. *J Comp Physiol* 124: 287-296.
15. Fischbach KF, Ditttrich APM (1989). The optic lobe of *Drosophila melanogaster*. I. A Golgi analysis of wild-type structures. *Cell Tissue Res* 258: 441-475.
16. Buchner E, Buchner S, Buelthoff I (1984) Deoxyglucose mapping of nervous activity induced in *Drosophila* brain by visual movement. *J Comp Physiol A* 155: 471-483.
17. Krapp HG, Hengstenberg B, Hengstenberg R (1998) Dendritic structure and receptive-field organization of optic flow processing interneurons in the fly. *J Neurophysiol* 79: 1902-1917.
18. Haag J, Wertz A, Borst A (2007): Integration of lobula plate output signals by DNOVS1, an identified premotor descending neuron. *J Neurosci* 27: 1992-2000.
19. Weber F, Eichner H, Cuntz H, Borst A (2008) Eigenanalysis of a neural network for optic flow processing. *New J Physics*, 10: 015013 (21pp).

20. Haag J, Borst A (2005) Dye-coupling visualizes networks of large-field motion-sensitive neurons in the fly. *J Comp Physiol A* 191: 445-454.
21. Hassenstein B, Reichardt W (1956) Systemtheoretische Analyse der Zeit-, Reihenfolgen- und Vorzeichenbewertung bei der Bewegungspertzeption des Rüsselkaefers *Chlorophanus*. *Z Naturforschung* 11b: 513-524.
22. Kunze P (1961) Untersuchung des Bewegungsehens fixiert fliegender Bienen. *Z. vergl. Physiol.* 44: 656-684.
23. Fermi G, Reichardt W (1963) Optomotorische Reaktionen der Fliege *Musca domestica*. Abhängigkeit der Reaktion von der Wellenlänge, der Geschwindigkeit, dem Kontrast und der mittleren Leuchtdichte bewegter periodischer Muster. *Kybernetik* 2:15-28.
24. Eckert H (1973) Optomotorische Untersuchungen am visuellen System der Stubenfliege *Musca domestica* L. *Kybernetik* 14: 1-23.
25. Heisenberg M (1972) Comparative behavioral studies on two visual mutants of *Drosophila*. *J Comp Physiol* 80: 119-136.
26. Buchner E, Götz KG, Straub C (1978) Elementary detectors for vertical movement in the visual system of *Drosophila*. *Biol Cybernetics* 31: 235-242.
27. Egelhaaf M, Borst A, Reichardt W (1989) Computational structure of a biological motion detection system as revealed by local detector analysis in the fly's nervous system. *J Opt Soc Am A* 6: 1070-1087.
28. Single S, Borst A (1998) Dendritic integration and its role in computing image velocity. *Science* 281: 1848-50.
29. Eckert H (1980) Functional properties of the H1-neurone in the third optic ganglion of the blowfly, *Phaenicia*. *J.Comp.Physiol.* 135:29-39.
30. Haag J, Denk W, Borst A (2004) Fly motion vision is based on Reichardt detectors regardless of the signal-to-noise ratio. *Proc Natl Acad Sci USA* 101: 16333-16338.
31. Egelhaaf M, Borst A (1989) Transient and steady-state response properties of movement detectors. *J Opt Soc Am A* 6: 116-127.
32. Reisenman C, Haag J, Borst A (2003) Adaptation of response transients in fly motion vision. I: Experiments. *Vis Res* 43: 1292-1307.
33. Borst A, Reisenman C, Haag J (2003) Adaptation of response transients in fly motion vision. II: Model studies. *Vis Res* 43: 1309-1322.
34. Harris RA, O'Carroll DC, Laughlin SB (2000). Contrast gain reduction in fly motion adaptation. *Neuron* 28: 595-606.
35. Borst A, Egelhaaf M (1990) Direction selectivity of fly motion-sensitive neurons is computed in a two-stage process. *Proc Natl Acad Sci USA* 87: 9363-9367.
36. Gilbert C (1991). Membrane conductance changes associated with the response of motion sensitive insect visual neurons. *Z.Naturforsch.* 45c:1222-1224.
37. Egelhaaf M, Borst A, Pilz B (1990). The role of GABA in detecting visual motion. *Brain Res.* 509: 156-160.
38. Thum AS, Knapek S, Rister J, Dierichs-Schmitt E, Heisenberg M, Tanimoto H (2006) Differential potencies of effector genes in adult *Drosophila*. *J Comp Neurol* 498: 194-203.
39. Miesenboeck G, Kevrekidis IG (2005) Optical imaging and control of genetically designated neurons in functioning circuits. *Annu Rev Neurosci* 28: 533-63.
40. Wilson RI, Laurent G (2005) Role of GABAergic inhibition in shaping odor-evoked spatio-temporal patterns in the *Drosophila* antennal lobe. *J Neurosci* 25: 9069-9079.

5 Manuscript Nr. 3

Synaptic Organization of Lobula Plate Tangential Cells in *Drosophila*: DA7 Cholinergic Receptors.

This chapter was published in January 2009 in the Journal of Neurogenetics Volume 23; Pages:200-209; by Shamprasad Varija Raghu¹, Maximilian Jösch¹, Stephan Sigrist², Alexander Borst¹, Dierk F. Reiff^{1,*}

1 Dept of Systems and Computational Neurobiology
Max-Planck-Institute of Neurobiology
Martinsried, Germany

2 Rudolf-Virchow-Zentrum
Wuerzburg, Germany

* Corresponding Author

Shamprasad Varija Raghu performed and analyzed the experiments concerning the genetic manipulations, immunohistochemistry and anatomy. Maximilian Jösch performed the electrophysiological and pharmacological experiments. Stephan Sigrist contributed with genetic constructs. Shamprasad Varija Raghu, Maximilian Jösch, Dierk Reiff and Alexander Borst conceived the experiments. Dierk Reiff wrote the manuscript.



Abstract

The nervous system of seeing animals derives information about optic flow in two subsequent steps. First, local motion vectors are calculated from moving retinal images, second the spatial distribution of these vectors is analyzed on the dendrites of large downstream neurons. In dipteran flies, this second step relies on a set of motion-sensitive lobula plate tangential cells (LPTCs) that have been studied in great detail in large fly species. Yet, studies on neurons that convey information to LPTCs and neuroanatomical investigations that enable a mechanistic understanding of the underlying dendritic computations in LPTCs are rare. We investigated the subcellular distribution of nicotinic acetylcholine receptors (nAChRs) on two sets of LPTCs, VS and HS cells in *Drosophila melanogaster*. We describe that both cell types express D α 7-type nAChR subunits specifically on higher order dendritic branches, similar to the expression of GABA receptors. These findings support a model in which directional selectivity of LPTCs is achieved by the dendritic integration of excitatory, cholinergic and inhibitory, GABA-ergic input from local motion detectors with opposite preferred direction. Nonetheless, whole cell recordings in mutant flies without D α 7 nAChRs revealed that direction selectivity of VS and HS cells is largely retained. In addition, mutant LPTCs were responsive to acetylcholine and remaining nAChR receptors were labeled by α -bungarotoxin. These results in LPTCs with genetically manipulated excitatory input synapses suggest a robust cellular implementation of dendritic processing that warrants direction selectivity. The underlying mechanism that ensures appropriate nAChR mediated synaptic currents and the functional implications of separate sets or heteromultimeric nAChRs can now be addressed in this system.

Introduction

Self motion of an animal causes shifting images of the environment on the retina. Photoreceptors report these time-varying local brightness values to a relatively small neural network of downstream neurons that compute local motion vectors according to the correlation-type detector model (Hassenstein & Reichardt, 1956; Reichardt, 1961; Borst & Egelhaaf, 1989). The underlying computations involve asymmetric temporal filtering and multiplication of the input from two neighboring photoreceptors. This process is done twice, once in each of the two mirror symmetrical subunits with opposite preferred direction. The output of the two subunits is subtracted which results in a directional selective response. Interestingly, the cellular composition of this network and the biophysical implementation of the underlying computations are still largely unknown.

The output of large arrays of local motion detectors has to be processed in a second step to obtain information about optic flow. The latter is an important prerequisite for successful navigation. This last step is accomplished by analysis of the spatial distribution of local motion vectors (Koenderink & van Doorn, 1987). Studies in dipteran flies have shown that this spatio-temporal analysis of local motion vectors takes place in the posterior division of the third neuropile of the fly optic lobe, the lobula plate (reviewed in Borst & Haag, 2002). Here, about 60 individually identifiable motion sensitive neurons reside, the Lobula Plate Tangential Cells (LPTCs). Different LPTC exhibit distinct visual responses and are tuned to particular optic flow patterns (Hengstenberg, 1982; Hausen, 1982a; Hausen, 1982b; Krapp & Hengstenberg, 1996; Borst & Haag, 1996; Haag, Theunissen, & Borst, 1997; Krapp, Hengstenberg, & Hengstenberg, 1998; Haag, Vermeulen, & Borst, 1999). Their tuning results in first place from the columnar input to their dendrites as described above. As a result LPTCs of the vertical system (VS) are most sensitive to vertical motion and rotations around different axes within the equatorial plane of the animal. LPTCs of the horizontal system (HS) are tuned to horizontal motion and thus to rotations around the vertical body axis. However, the receptive field properties of VS and HS cells become further modified by numerous connections between LPTCs of the same or different type that reside in the ipsi- and contralateral lobula plate (Farrow, Haag, & Borst, 2003; Haag & Borst, 2004; Haag & Borst, 2005; Farrow, Borst, & Haag, 2005; Farrow, Haag, & Borst, 2006). The axons of both cell types represent important output

elements of the lobula plate. They travel medially and terminate in the lateral protocerebrum (Hengstenberg, Hausen, & Hengstenberg, 1982; Hausen, 1982a; Scott, Raabe, & Luo, 2002; Raghu, Jösch, Borst, & Reiff, 2007) where they synapse on dendrites of descending neurons (Haag, Wertz, & Borst, 2007; Wertz, Borst, & Haag, 2008). The latter instruct motoneurons that control neck and flight muscles (Gronenberg & Strausfeld, 1990). Thus, visual control of flight maneuvers is accomplished.

In *Drosophila melanogaster*, different HS and VS cells as well as most of the columnar neurons have been well described based on their morphology (Heisenberg, Wonneberger, & Wolf, 1978; Fischbach & Dittrich, 1989; Scott et al., 2002; Rajashekar & Shamprasad, 2004; Raghu et al., 2007). The HS system comprises three individually identifiable cells, the northern, equatorial and southern HSN, HSE and HSS cell that are similarly present in large flies and *Drosophila*. Their dendritic fields cover a wide dorsal, equatorial, and ventral area within the lobula plate, respectively, with significant overlap. Only recently the first electric response properties of neurons within the *Drosophila* lamina (Zheng et al., 2006) and of *Drosophila* VS cells (Jösch, Plett, Borst, & Reiff, 2008) have been reported, too. Consistent with anatomical studies the functional investigation of the VS cell system in *Drosophila* revealed six VS cells as compared to 10 in *Calliphora* (Hausen, 1982a; Scott et al., 2002; Raghu et al., 2007; Jösch et al., 2008). *Drosophila* VS cells exhibit directional selective responses and possess distinct receptive fields. Their receptive field centers are arranged sequentially along the eye's azimuth, corresponding to the serial positioning of their partially overlapping dendrites within the retinotopically organized lobula plate. The dendrites themselves stretch out along the dorsal-ventral axis of this neuropile, similar to the dendrites of HS cells. Experimental evidence suggests that the dendrites of both cell types receive direct input from two different arrays of antagonistic local, motion-sensitive elements with opposite preferred direction. Such antagonistic detector arrays exist for both the horizontal and the vertical axis, respectively (Borst & Egelhaaf, 1990; Brotz & Borst, 1996; Brotz, Gundelfinger, & Borst, 2001). Yet, their cellular identity has still not been revealed but some evidence goes in favor of the bushy T cells, T4 and T5 (Buchner, Buchner, & Bülthoff, 1984; Fischbach et al., 1989). Only a single study has shown evidence for chemical synapses between an HS cell dendrite and a columnar T4 cells from the medulla (Strausfeld & Lee, 1991).

Nevertheless, individual VS cell responses in large flies (Haag, Denk, & Borst, 2004) and *Drosophila* (Jösch et al., 2008) exhibit all the characteristics that are indicative of presynaptic input from antagonistic elementary motion detectors of the correlation type. With respect to the computational structure of the correlation detector (Reichardt, 1961), the final subtraction stage and spatial integration of the output of local motion detectors with opposite preferred direction seems to be implemented on the LPTC dendrites. In such a push-pull model excitatory and inhibitory synapses form the input to LPTC dendrites (Borst et al., 1990; Gilbert, 1991; Borst, Egelhaaf, & Haag, 1995). Pharmacological and histochemical studies on the distribution of dipteran acetylcholine receptors (Sattelle, 1980; Schuster, Phannavong, Schroder, & Gundelfinger, 1993; Hess, Merz, & Gundelfinger, 1994; Jonas, Phannavong, Schuster, Schroder, & Gundelfinger, 1994; Chamaon, Schulz, Smalla, Seidel, & Gundelfinger, 2000; Fayyazuddin, Zaheer, Hiesinger, & Bellen, 2006) and Rdl-type diethyltrinitrophenyl-resistant GABA receptor subunits (French-Constant, Roush, Mortlock, & Dively, 1990) on the dendrites of LPTCs (Brotz et al., 1996; Brotz et al., 2001) suggest that these antagonistic inputs are cholinergic and GABAergic, respectively. However, a detailed description of the subcellular distribution of the cognate receptors on LPTC dendrites is still missing.

Here we extend a recent study on the synaptic organization and subcellular distribution of inhibitory GABA receptors (Raghu et al., 2007) on *Drosophila* LPTCs and describe the subcellular distribution of excitatory D α 7 nicotinic cholinergic receptors (nAChRs) on the same set of cells. D α 7 nAChR subunits belong to a family of ten different nAChR genes in *Drosophila* that encode the subunits D α 1-7 and D β 1-3. In the prototypic nAChR five subunits of the same or different type assemble to one pentameric ligand-gated cation channel (Sattelle et al., 2005; Jones, Brown, & Sattelle, 2007). These nAChR channels are key players for fast excitatory neurotransmission in the central nervous system of insects (Leech & Sattelle, 1993). Only little is known about the interplay of subunit composition and electric channel properties (see discussion).

We used genetic, immunohistochemical and electrophysiological techniques and describe that D α 7 receptor subunits are exclusively located on higher order branches of VS and HS cell dendrites. In the absence of D α 7 receptor subunits direction selectivity of VS cells was largely retained. This finding suggests the existence of

remaining nAChRs which was corroborated by α -bungarotoxin labeling. The remaining nAChRs represent either a separate set of nAChRs that do not involve D α 7 subunits or alternatively, nAChRs that are functional in the absence of D α 7 expression. In both cases a regulatory mechanism can be assumed that compensates for the loss of the D α 7 nAChR subunit and warrants direction selectivity in cells with genetically manipulated excitatory input synapses.

Materials and Methods

Flies and fly culture.

Flies were raised on standard corn medium at 25 °C and 60 % humidity. Female flies 3-5 days after eclosion were used in all experiments. The enhancer trap lines Gal4-DB331 (Jösch et al., 2008) and Gal4-3A (Scott et al., 2002) were kindly provided by R. Stocker (Fribourg, Switzerland) and M. Heisenberg (Wuerzburg, Germany), respectively, and used to drive expression in LPTCs. The D α 7 knock out fly line PD Δ Y6 (Fayyazuddin et al., 2006) was kindly provided by Hugo Bellen (Texas, USA). UAS-D α 7-GFP flies were generated by PCR amplification of the D α 7 open reading frame from a pAc5.1A D α 7 construct (gift of Amir Fayyazuddin and Hugo Bellen) using the primers 5' GAGGGACCAGTTTTCATATC 3' and 5' GAGCCTCGAGCTTCGCTTACGGGAAAATGAAATGCG 3' and additional XhoI site 6 bp after the end of the open reading frame. After digesting the PCR product with NotI and XhoI the fragment was subcloned into pKS. The EGFP tag was inserted after G442 using primer extension PCRs including a duplex linker, using the native HindIII and the XhoI site. Finally the tagged construct was transferred into the pUAST vector using NotI and XhoI. Detailed protocols and primer sequences for extension PCR on request. Female experimental flies of the following genotypes were used for immunohistochemistry: Gal4-DB331/+; UAS-mCD8-GFP/+; +/+; Gal4-DB331/+; UAS-mCD8-DsRed/+; UAS-D α 7-GFP/+, PD Δ Y6; UAS-mCD8-GFP; Gal4-3A. Electrophysiology was performed on: PD Δ Y6; UAS-mCD8-GFP; Gal4-3A and corresponding control flies +/+; mCD8-GFP/cyo; 3A-Gal4/3A-Gal4.

Immunohistochemistry

The brains of female flies were excised, fixed in 4 % Paraformaldehyde for 30 minutes and incubated in phosphate-buffered saline (PBS) including 1 % Triton X-100 (PBT) for 45-60 minutes. The brains were further incubated in PBT with 2 % normal goat serum (Sigma Aldrich, St. Louis, MO) for one hour. The primary antibodies Alexa Fluor 488 rabbit anti-GFP-IgG (A-21311, Molecular Probes, Eugene, OR) or monoclonal rat anti-mCD8 (MCD0800, Caltag laboratories) were added (1:200) overnight at 4 C and removed by a series of washing steps in PBT. The secondary antibody Alexa Fluor 568 goat anti-rat-IgG (A11077, Molecular Probes) was added (1:200) overnight at 4° C and removed by further washing steps in PBT for a total of 60-90 minutes. Subsequent to a final washing step in PBS for 45-60 minutes the stained brains were mounted in Vectashield (Vector Laboratories, Burlingame, CA) and analyzed by confocal microscopy. For antibody staining of D α 7 receptor subunits (rat anti-D α 7, kindly provided by Hugo Bellen, Texas, USA; Fayyazuddin et al., 2006) the brains were fixed either in ice cold 4 % PFA for 5 minutes or in ice cold PFA-Lysine-Periodate (PLP) fixative (Mclean and Nakane, 1974) for 20 minutes. PFA and PLP fixed brains were washed in 1X PBT and 0.4X PBT, respectively. Further processing was performed as described above. α -bungarotoxin-Alexa 647 (B35450, Molecular Probes) staining was performed at room temperature (1:100, diluted with 1X Tris Buffer Saline, TBS) without fixation for 60-90 minutes. Subsequently the brains were washed 3-4 times in 1XTBS with 15 minutes intervals. The stained brains were mounted in Vectashield and immediately analyzed by confocal microscopy. All steps were done at room temperature unless otherwise stated.

Electrophysiology

Visually guided whole cell recordings from highlighted LPTCs (genotypes see above) were performed as described recently (Jösch et al., 2008). For visual stimulation large-field visual square gratings (spatial wavelength $\lambda = 25$ deg, velocity $\lambda = 25$ deg/sec) were presented to the eyes of the flies. In the pharmacological experiments the brains were perfused with ringer (Wilson et al. 2004) at a constant speed of 3 ml/min. Whole cell recordings were established in Calcium containing ringer and visually evoked control responses were recorded. Then the ringer was changed to zero Calcium solution with 20 mM Magnesium. In this solution the visually evoked responses

were monitored until they disappeared completely. LPTCs were then stimulated by perfusion of ringer (zero Calcium, 20 mM Magnesium) with additional 1 mM acetylcholine for several seconds.

Data Analysis

Serial optical sections were taken at 0.5 μm intervals with 1024 x 1024 pixel resolution using confocal microscopes (LEICA TCSNT and SP2-UV) and oil-immersion 40X- (NA = 1.25), 63X- (NA = 1.4) and 100X- (NA = 1.4) Plan-Apochromat objectives. In all cases, frontal (coronal) sections were taken from the posterior side of the brain. The individual confocal stacks were analyzed using Image J (NIH, U.S.A). The size, contrast and brightness of the resulting images were adjusted with Photoshop® CS (Adobe Systems, San Jose, CA).

Results

We investigated the subcellular distribution of D α 7 cholinergic receptor subunits on LPTCs and their contribution to direction selectivity of *Drosophila* LPTCs. In a first set of experiments we used a subunit specific antibody against D α 7 cholinergic receptor subunits (Fayyazuddin et al., 2006) in flies with genetically labeled fluorescent (UAS-mCD8-GFP) VS and HS cells (GAL4-DB331 (Raghu et al., 2007; Jösch et al., 2008) or Gal4-3A (Scott et al., 2002; Raghu et al., 2007)). Both Gal4 lines drive expression in six VS cells and three HS cells of the adult *Drosophila* brain. The dendrites of these VS and HS cells cover wide areas within the lobula plate where they receive input from numerous columnar elements from presumably the medulla and the lobula (Fischbach et al., 1989; Strausfeld et al., 1991).

Immunolabeling provides evidence for excitatory cholinergic input to the dendritic tips of VS and HS cells.

We analyzed the distribution of D α 7 immunoreactivity on VS and HS cells. The antibody staining against D α 7 (Fayyazuddin et al., 2006) in brains of female flies (Gal4-DB331/+; UAS-mCD8-GFP/+; +/+) required slight modification of the published protocol (see Materials and Methods). The used D α 7 antibody recognized the cytoplasmic loop between the transmembrane domains M3 and M4 of the D α 7 subunit. Since this loop varies for different nAChR subunits, the used antibody is highly specific (Fayyazuddin et al., 2006). The fluorescence of the transgenically expressed membrane tagged marker mCD8-GFP was enhanced by a green fluorescent antibody against GFP (see Materials and Methods). The green fluorescence labels the different VS cells that lie serially, with their overlapping dendrites stretching out along the dorsal-ventral axis of the lobula plate (Fig 1 a, arrows). Figure 1 a-c shows that D α 7 immunoreactivity (magenta) is exclusively localized on the dendrites of the different VS cells (arrows in 1 a-c). High magnification images, such as the dorsal dendritic branch of a VS1 cell (Figure 1 d-e) reveal D α 7 immunolabeling that is almost exclusively localized to the dendritic tips (Fig 1 d-e). These experiments suggest a large number of D α 7 excitatory synaptic inputs impinging onto the fine dendritic tips of VS cells.

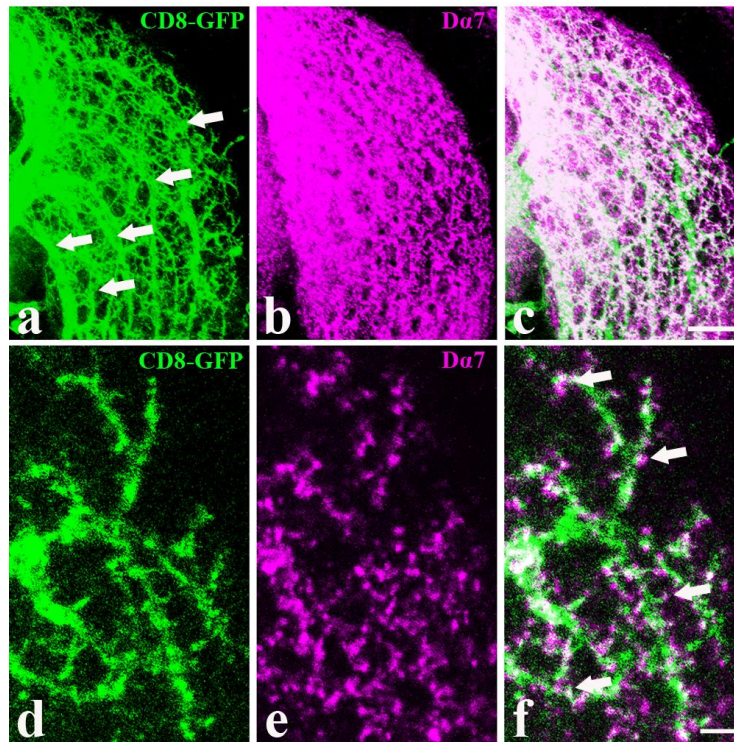


Figure 1. Localization of D α 7 immunoreactivity in VS cells of the adult fly visual system. Confocal image stacks show Gal4-DB331 driven expression of membrane tagged GFP in dendrites of all VS cells in green and D α 7 immunolabeling in magenta. **a-c**: Collapsed confocal image stack (frontal sections) of the posterior lobula plate (slightly posterior to the HS cell layer). mCD8-GFP outlines the six VS cells VS1-VS6. The different VS cells lie serially, with their overlapping dendrites stretching out along the dorsal-ventral axis of the lobula plate (arrows, in a). There is prominent D α 7 immunoreactivity in the area covered by the dendritic branches of all six VS cells (overlay of both channels in c). **d-e**: The close up of a small dendritic branch of a VS1 cell shows that D α 7 immunoreactivity is specifically localized to the dendritic tips (arrows). Similar results were obtained for all branches of all VS cells. The required PLP fixation resulted in only moderate preservation of the tissue. The shown images represent maximum intensity projections of 12 and 2 images in a-c and d-f, respectively. Individual images were separated by 0.5 μ m in z-direction. Scale Bar = 20 μ m in a-c and 2 μ m in d-f.

Similar experiments were done to address the distribution of D α 7 immunoreactivity (magenta) on the dendrites of the three different HS cells (green; Fig 2a-f). The dendrites of the HS cells (Fig 2a, arrows) lie anterior to the ones of the VS cells and can thus be separated. They cover the dorsal (HSN), medial (HSE) and ventral (HSS) part of the lobula plate (arrows in Fig 2a). D α 7 immunolabeling (Fig. 2b) can be located to the dendrites of HSN, HSE and HSS cells. A close up of a dorsal part of an HSE cell (2d-e, arrows) suggests that also in HS cells the cholinergic excitatory synapses are specifically localized on the fine dendritic tips.

In summary, immunolabeling of endogenous D α 7 nAChR subunits suggests that D α 7 is expressed in LPTCs and specifically localized to fine dendritic tips of VS and HS cells. However, in these experiments the texture of particularly thin terminal structures (Fig. 1 and 2) was slightly distorted due to the PLP fixation required for the use of the D α 7 antibody.

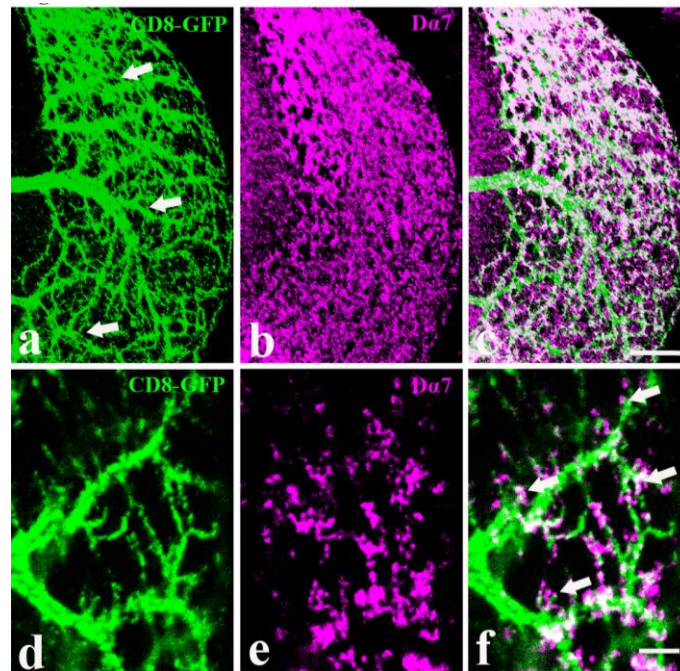


Figure 2. Localization of D α 7 immunoreactivity in HS cells of the adult fly visual system. Confocal image stacks show Gal4-DB331 driven expression of membrane tagged GFP in dendrites of all three HS cells in green and D α 7 immunolabeling in magenta. **a-c**: Collapsed confocal image stack (frontal sections) of the posterior lobula plate anterior to the VS cell layer. mCD8-GFP outlines the dendrites of HSN, HSE and HSS that cover the dorsal, medial and ventral part of the lobula plate, respectively. There is prominent D α 7 immunoreactivity in the area covered by the dendritic branches of all HS cells (overlay of both channels in c). **d-e**: The close up of a dorsal dendritic branch of an HSE cell shows that D α 7 immunoreactivity is specifically localized to the dendritic tips (arrows). Similar results were obtained for all branches of all HS cells. The required PLP fixation resulted in only moderate preservation of the tissue. The shown images represent maximum intensity projections of 14 and 2 images in a-c and d-f, respectively. Individual images were separated by 0.5 μ m in z-direction. Scale Bar = 20 μ m in a-c and 4 μ m in d-f.

D α 7-GFP is located to the fine dendritic tips of VS and HS cells.

We bypassed the problem of moderate preservation of PLP-fixed tissue by analyzing the Gal4-driven expression of a GFP-tagged D α 7 receptor subunit (see Material and

Methods) in genetically labeled LPTCs (*Gal4-DB331/+; UAS-mCD8-DsRed/+; UAS-Da7-GFP/+*) and PFA-fixed tissue. The fluorescence signal of both DsRed labeled cells and Da7-GFP was enhanced further by staining with DsRed and GFP antibodies, respectively (see Materials and Methods). Membrane tagged DsRed revealed the anatomy of entire VS and HS cells (magenta, Fig 3 and 4) whereas Da7-GFP (green, arrows, Fig 3 and 4) was exclusively localized to the terminal dendritic tips of both cell types. This is even more evident in the close ups of VS dendrites (Fig3e-j; with very subtle Da7-GFP expression on the primary dendritic shafts). Similar results were obtained for all three HS cells, HSN, HSE and HSS (Fig 4a-c). Again, the expression of Da7-GFP was confined to the fine dendritic tips. These results are in line with the immunolabeling of the endogenous Da7 protein and suggest that cholinergic excitatory columnar elements impinge directly onto the terminal dendritic tips of VS and HS cells within the lobula plate.

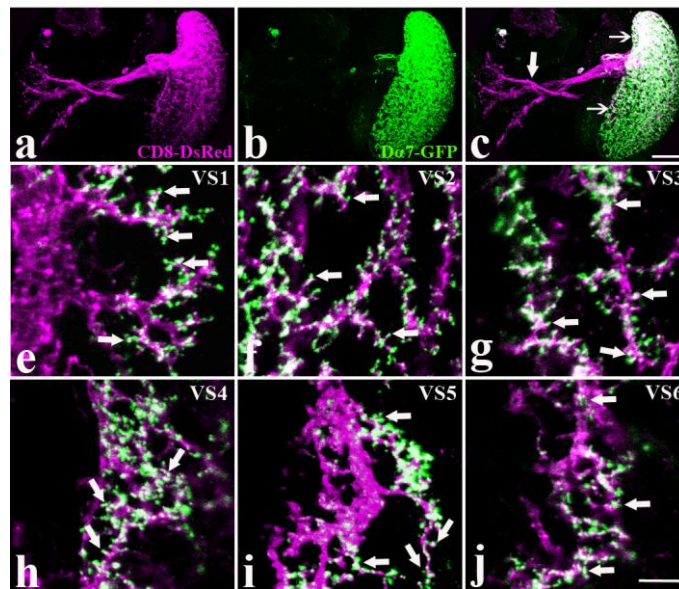


Figure 3. GFP-tagged Da7 nAChRs are exclusively localized on dendritic tips of all six VS cells. Confocal image stacks show *Gal4-DB331* driven expression of membrane tagged DsRed (magenta) and Da7-GFP (green) in the dendrites of all VS cells (frontal sections of the posterior lobula plate and the lateral protocerebrum) **a**: mCD8-DsRed labels all VS cells. Some HS cells, in particular their axonal projections to the lateral protocerebrum are also visible in this image collection. The protocerebral projections of VS cells travel dorsally and bifurcate into two vertical branches in the protocerebral region. **b**: same section as in **a** but recorded in the green channel. Da7-GFP is strongly expressed in the entire dendritic region of the VS cells within the lobula plate. **c**: Overlay of **a** and **b**. There is no expression of Da7-GFP in the protocerebral projections. **e-j**: Da7-GFP is strictly localized to the fine dendritic tips of VS1-VS6. In these experiments fine structures were preserved by PFA fixation. **a-c**:

Maximum intensity projection of 32 images, scale bar = 40 μm . e-j: Maximum intensity projections of 6, 3, 3, 2, 3 and 2 images, scale bar = 5 μm . Individual images were separated by 0.5 μm in z-direction. The protocerebral projections of VS and HS cells that extend to the posterior slope in the peri-oesophageal region (Fig 3a, thick arrow in 3c, Fig 5a-e) show no detectable D α 7-GFP fluorescence (Fig 5a). This finding is not questioned by the fact that individual protocerebral terminals are closely intermingled and could not be identified in isolation. Similarly, the protocerebral projections of the horizontally sensitive neurons HSN and HSE showed no sign of D α 7-GFP expression (Fig 5b and c). The analysis of protocerebral projections of VS and HS cells was complemented by antibody staining of endogenous D α 7 protein (Fig 5d-e). We found D α 7 immunoreactivity in the peri-oesophageal region but the analysis of individual confocal images of 0.5 μm thickness revealed no evidence for the presence of D α 7 receptor subunits on the protocerebral projections (Fig 5d-e, arrows) of VS and HS cells.

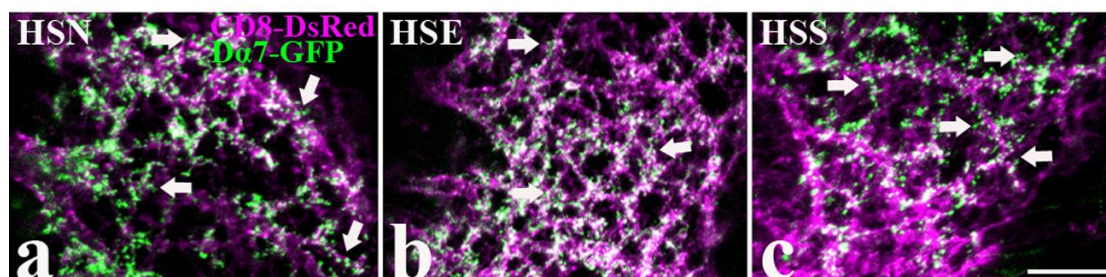


Figure 4. GFP-tagged D α 7 nAChRs are exclusively localized on dendritic tips of all three HS cells. Membrane tagged DsRed (magenta) and D α 7-GFP (green) label all three HS cells (Gal4-DB-331). The confocal images of dendrites of **a**: HSN, **b**: HSE and **c**: HSS show, that distinct spots of green D α 7-GFP are specifically localized to the dendritic tips of HS cells. Maximum intensity projection of 4, 4 and 10 images in a, b and c, respectively. Individual images were separated by 0.5 μm in z-direction. Scale bar = 10 μm .

In summary, the first set of experiments identified endogenous D α 7 protein on LPTCs, however with slightly limited preservation of the tissue. Nevertheless its localization could be assigned to the very distal dendritic branches. In this second set of experiments, the subcellular distribution of endogenous D α 7 protein was corroborated by a transgenic expression analysis. The transgenic expression of GFP-labeled D α 7 subunits allowed for the use of PFA for tissue fixation and thus for detecting D α 7 nAChRs on the finest dendritic tips of VS and HS cells.

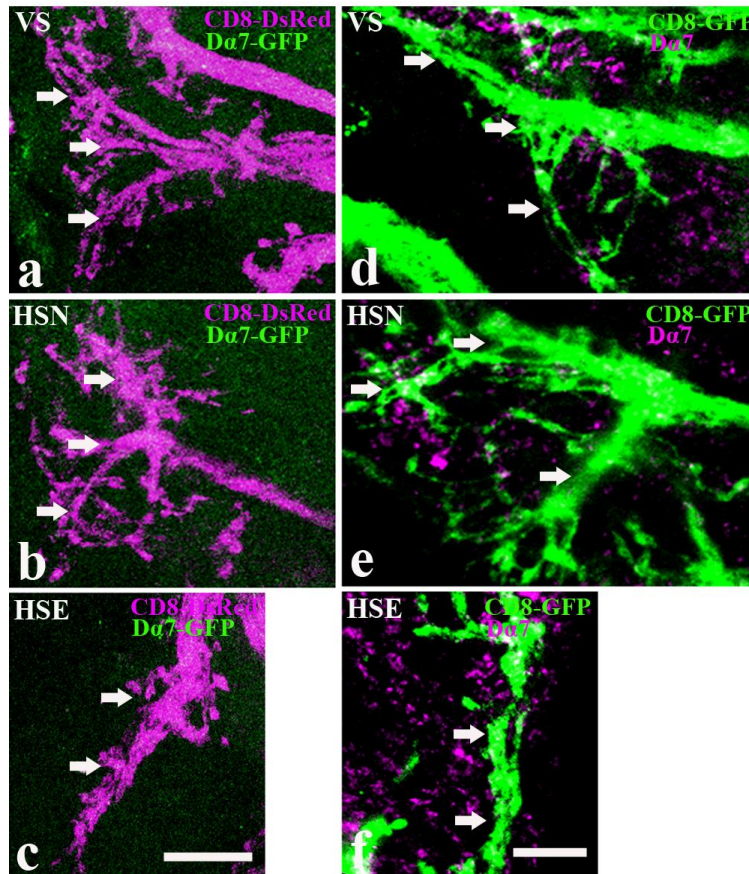


Figure 5. Da7 nAChRs are not expressed on the protocerebral branches of VS and HS cells. a-c: Transgenic expression of Da7-GFP (green) combined with mCD8-DsRed (magenta) expression. **d-f:** Immunolabeling of Da7 nAChRs (magenta) combined with mCD8-GFP (green) expression. The protocerebral part of VS and HS cells is free of the cholinergic receptor subunit. Protocerebral projections of VS cells (a and d), HSN (b and e) and HSE (c and f) are shown in this complementary approach. Maximum intensity projections of 7, 5, and 9 images are shown in a, b and c, respectively. In d – f very few white dots can be seen that are a result of the maximum intensity projections of several images (2, 5 and 6 images in d, e and f, respectively). Visual inspection of individual images of 0.5 μ m thickness showed that Da7 immunoreactivity was always outside of the labeled LPTC processes. Individual images were separated by 0.5 μ m in z-direction. Scale bar = 20 μ m in a-c and 10 μ m in d-f.

Direction selectivity of VS cells is retained in the absence of Da7.

Da7 mutant flies lack almost the entire ligand-binding domain, the transmembrane domain M1 and a part of the pore-lining helix M2. The giant fiber mediated escape behavior is disrupted in these flies due to defective cholinergic neurotransmission onto the giant fiber neurons (Fayyazuddin et al., 2006). The highly abundant expression of Da7 receptor subunits in all optic neuropiles (Fayyazuddin et al., 2006) and the dendritic tips of motion sensitive LPTCs (Fig.1 - 5) suggests a role in motion processing.

We made a first attempt to address the specific requirement of the D α 7 nAChR subunit by whole cell recording in live animals during visual stimulation (Jösch et al., 2008). VS cells were targeted for whole cell recording in D α 7 mutant flies (Fig. 6a and b) using Gal4-3A driven expression of UAS-mCD8-GFP (P Δ EY6/ P Δ EY6; mCD8-GFP/Cyo; Gal4-3A/+). The immunolabeling in Figure 6a and 6b shows that the D α 7 antigen was reduced to background level in D α 7- flies. Nevertheless, whole cell patch clamp recordings revealed no obvious defects in the motion responses of mutant flies compared to the responses of wild type flies (Jösch et al., 2008). All recorded VS cells in D α 7- flies (n = 7) reported the movement of a large field visual periodic grating with directional selective responses. These responses were indistinguishable from what we observed in a previous study (Fig. 6c). Upward and downward motion elicited a graded hyperpolarization and depolarization, respectively, the latter superimposed with spike like events.

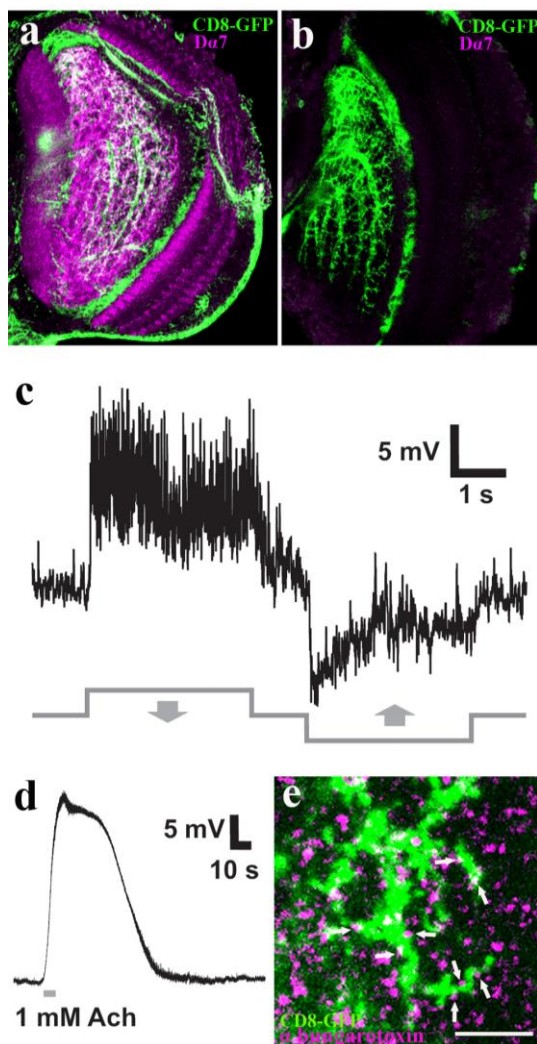


Figure 6. Directional selective responses are largely retained in D α 7 mutant flies. D α 7 immunoreactivity in the optic lobe in control (a) and D α 7 mutant flies (b). D α 7 immunoreactivity (magenta) is completely absent in D α 7 mutant flies. Membrane tagged GFP (green) driven by Gal4-3A was used to target VS and HS cells for whole cell recording. c: VS cells in flies that are mutant for D α 7 exhibit canonical directional-selective responses (n = 7). A periodic visual grating was moved at a temporal frequency of 1 Hz in front of the fly's eye. d: VS cells in a D α 7 mutant flies respond to acetylcholine in preparations with blocked synaptic transmission (see methods). 1mM acetylcholine elicited strong depolarizations of up to 30 mV that returned to baseline after removal of the drug (n = 3). e: α -bungarotoxin-alexa 647 labeling (magenta) in D α 7 mutant flies. The higher order branch of a dorsal VS1 dendrite (Gal4-3A driven mCD8-GFP in green) shows that α -bungarotoxin-alexa 647 staining is localized to the dendritic tips (arrows, scale bar = 3 μ m). Maximum intensity projections of 6 images separated by 0.5 μ m in z in a and b and of 4 images separated by 0.35 μ m in z in e.

Next we asked if VS cells in D α 7- flies are still responsive to cholinergic input from columnar neurons. This was analyzed by decoupling of VS cells from their chemical input and direct pharmacological stimulation with ACh. VS cells were isolated from their presynaptic chemical input by perfusion with ringer that contained zero Calcium and 20 mM Magnesium, an ionic composition that blocks synaptic transmission (Brotz, Egelhaaf, & Borst, 1995). After switching to the zero-Calcium high-Magnesium ringer the visually evoked responses disappeared completely. However, short pulses of 1 mM Ach evoked immediate, strong depolarization up to 30 mV (Fig. 6d). The depolarization returned to baseline in the absence of ACh. This experiment was performed on three different cells in three different animals, each time with the same outcome. Remaining nAChRs with functional binding sites were labeled with fluorescent α -bungarotoxin (Fig. 6e).

In the experiments described in the first two paragraphs of our results D α 7 nAChRs were shown to possess neuroanatomical characteristics of a molecular key-player in the dendritic integration of large field visual motion. However, this last set of experiments revealed that flies without the gene for D α 7 nAChR subunits still form nAChRs on LPTC dendrites that are responsive to ACh and that bind α -bungarotoxin. Moreover, direction selectivity in these genetically manipulated LPTCs was retained. These findings suggest a surprisingly robust cellular implementation of the underlying dendritic computations: altered subunit composition in the excitatory input channel appears largely compensated to warrant proper motion vision.

Discussion

We investigated the subcellular distribution of the D α 7 nAChR subunit on large field motion sensitive HS and VS cells of the *Drosophila* lobula plate. Two complementary approaches were used, immunolabeling (Fayyazuddin et al., 2006) of endogenous D α 7 protein (Fig 1, 2 and 5) and Gal4-UAS driven D α 7-GFP (Fig 3, 4 and 5) expression. Both methods showed that D α 7 is specifically localized to the fine dendritic tips of VS and HS cells as revealed by confocal microscopy. This finding further supports the idea that the dendritic tips of these cells play a key role in the analysis of optic flow. Large arrays of directionally selective columnar elements would then impinge directly onto these dendrites (Borst et al., 1990). Thus, retinotopically organized excitatory cholinergic and inhibitory GABAergic input from local motion detectors with opposite preferred direction would be summed up to unequivocally derive the direction of large field image motion and optic flow (Borst et al., 1990; Brotz et al., 1996; Brotz et al., 2001). Such an arrangement is consistent with physiological experiments in large fly species (Borst et al., 1990; Borst et al., 1995) as well as with recent current injection experiments in *Drosophila* (Jösch et al., 2008) and has been interpreted as a biophysical means to implement a velocity gain control mechanism. Histochemical studies showed the expression of nAChRs (Sattelle, 1980; Jonas, Major, & Sakmann, 1993; Schuster et al., 1993; Hess et al., 1994; Chamaon et al., 2000; Fayyazuddin et al., 2006) and Rdl-type GABA receptor subunits (ffrench-Constant et al., 1990; Enell, Hamasaka, Kolodziejczyk, & Nassel, 2007) in different regions of the optic lobe. Moreover, on the subcellular level, we recently demonstrated that RDL-type GABA receptors are similarly localized to the dendritic tips of VS and HS cells in *Drosophila* (Raghu et al., 2007). The localization of D α 7 subunits presented here corroborates this model. However, our experiments in D α 7- flies suggest, that the excitatory input is more complex. Direction selectivity of VS and HS cells was retained in D α 7- flies and α -bungarotoxin sensitive nAChRs were still present (Fig.6). Such α -bungarotoxin sensitive nAChRs might for instance involve ARD subunits (Schloss, Hermans-Borgmeyer, Betz, & Gundelfinger, 1988). Thus, visual motion detection and LPTCs in *Drosophila* represent an ideal model system to study the functional implications of nAChR subunit composition.

In the central nervous system of insects nAChRs are key players for fast excitatory neurotransmission (Leech et al., 1993). Structurally, they assemble to pentameric membrane protein complexes. The different genes can give rise to receptor assemblies with distinct functional properties, however little is known about their physiology in *Drosophila* in vivo. About ten different nAChRs have been described in *Drosophila* so far (Jonas et al., 1993; Schuster et al., 1993; Hess et al., 1994; Chamaon et al., 2000; Chamaon, Smalla, Thomas, & Gundelfinger, 2002; Wegener, Hamasaka, & Nassel, 2004; Sattelle et al., 2005; Fayyazuddin et al., 2006). It was suggested that pentameric complexes are formed that consist of either ALS(D α 1) & SBD & D α 2, or D α 3 & ARD, or ARD & SBD (Chamaon et al., 2000; Chamaon et al., 2002). More recently, D α 5, D α 6 and D α 7 were added to the nAChR subunit arsenal present in *Drosophila* (Grauso, Reenan, Culetto, & Sattelle, 2002). In vertebrates D α 5–7 were shown to form homomeric receptors, but to our knowledge no information is currently available for *Drosophila*.

Our experiments on D α 7- flies allow several interpretations that are not mutual exclusive. D α 7 subunits might form homomeric nAChRs, an interpretation that might be suggested by data from vertebrates. In this case another type or several other types of nAChRs are expressed on the VS and HS cell dendrites. Alternatively, D α 7 subunits could contribute to homomeric and heteromeric or only heteromeric nAChRs. In any case the functional compensation for the absence of D α 7 comes as a surprise and opens the way for detailed functional studies that are build on the combination of a predictive computational model of visual motion detection, whole cell recording and genetic manipulation in *Drosophila*.

Acknowledgments

We thank Wolfgang Essbauer and Christian Theile for excellent technical assistance. We are grateful to Martin Heisenberg, Liqun Luo, Nung Jan, Hugo Bellen, Amir Fayyazuddin and Reinhard Stocker for providing flies and antibodies. This work was supported by the Max-Planck-Society and by a Human Frontier Science Program (HFSP) grant to K. Ito, A.B., and B. Nelson.

Abbreviations

ACh: acetylcholine

GABA: gamma-aminobutyric-acid

LPTCs: lobula plate tangential cells

nAChR: nicotinic acetylcholine receptor

VS: vertical system

HS: horizontal system

References

Borst, A. & Egelhaaf, M. (1989). Principles of visual motion detection. *Trends in Neurosciences*, 12, 297-306.

Borst, A. & Egelhaaf, M. (1990). Direction selectivity of fly motion-sensitive neurons is computed in a two-stage process. *Proceedings of the National Academy of Science USA*, 87, 9363-9367.

Borst, A., Egelhaaf, M., & Haag, J. (1995). Mechanisms of dendritic integration underlying gain control in fly motion-sensitive interneurons. *Journal of Computational Neuroscience*, 2, 5-18.

Borst, A. & Haag, J. (1996). The intrinsic electrophysiological characteristics of fly lobula plate tangential cells :I. Passive membrane properties. *Journal of Computational Neuroscience*, 3, 313-336.

Borst, A. & Haag, J. (2002). Neural networks in the cockpit of the fly. *J.Comp Physiol A Neuroethol.Sens.Neural Behav.Physiol*, 188, 419-437.

Brotz, T. M. & Borst, A. (1996). Cholinergic and GABAergic receptors on fly tangential cells and their role in visual motion detection. *Journal of Neurophysiology*, 76, 1786-1799.

Brotz, T. M., Egelhaaf, M., & Borst, A. (1995). A preparation of the blowfly (*Calliphora erythrocephala*) brain for in vitro electrophysiological and pharmacological studies. *Journal of Neuroscience Methods*, 57, 37-46.

Brotz, T. M., Gundelfinger, E. D., & Borst, A. (2001). Cholinergic and GABAergic pathways in fly motion vision. *BMC.Neurosci.*, 2, 1.

Buchner, E., Buchner, S., & Bülthoff, I. (1984). Deoxyglucose mapping of nervous activity induced in *Drosophila* brain by visual movement. *Journal of Comparative Physiology A*, 155, 471-483.

Chamaon, K., Schulz, R., Smalla, K. H., Seidel, B., & Gundelfinger, E. D. (2000). Neuronal nicotinic acetylcholine receptors of *Drosophila melanogaster*: the alpha-subunit $\alpha 3$ and the beta-type subunit ARD co-assemble within the same receptor complex. *FEBS Lett.*, 482, 189-192.

Chamaon, K., Smalla, K. H., Thomas, U., & Gundelfinger, E. D. (2002). Nicotinic acetylcholine receptors of *Drosophila*: three subunits encoded by genomically linked genes can co-assemble into the same receptor complex. *J.Neurochem.*, 80, 149-157.

Enell, L., Hamasaka, Y., Kolodziejczyk, A., & Nassel, D. R. (2007). gamma-Aminobutyric acid (GABA) signaling components in *Drosophila*: immunocytochemical localization of GABA(B) receptors in relation to the GABA(A) receptor subunit RDL and a vesicular GABA transporter. *J.Comp Neurol.*, 505, 18-31.

Farrow, K., Borst, A., & Haag, J. (2005). Sharing receptive fields with your neighbors: tuning the vertical system cells to wide field motion. *J.Neurosci.*, 25, 3985-3993.

Farrow, K., Haag, J., & Borst, A. (2003). Input organization of multifunctional motion-sensitive neurons in the blowfly. *Journal of Neuroscience*, 23, 9805-9811.

Farrow, K., Haag, J., & Borst, A. (2006). Nonlinear, binocular interactions underlying flow field selectivity of a motion-sensitive neuron. *Nat.Neurosci.*, 9, 1312-1320.

Fayyazuddin, A., Zaheer, M. A., Hiesinger, P. R., & Bellen, H. J. (2006). The nicotinic acetylcholine receptor $\alpha 7$ is required for an escape behavior in *Drosophila*. *PLoS.Biol.*, 4, e63.

- French-Constant, R. H., Roush, R. T., Mortlock, D., & Dively, G. P. (1990). Isolation of dieldrin resistance from field populations of *Drosophila melanogaster* (Diptera: Drosophilidae). *J.Econ.Entomol.*, 83, 1733-1737.
- Fischbach, K. F. & Dittrich, A. P. M. (1989). The optic lobe of *Drosophila melanogaster*. I. A Golgi analysis of wild-type structure. *Cell Tissue and Research*, 258, 441-475.
- Gilbert, C. (1991). Membrane conductance changes associated with the response of motion sensitive insect visual neurons. *Zeitschrift fuer Naturforschung*, 45c, 1222-1224.
- Grauso, M., Reenan, R. A., Culetto, E., & Sattelle, D. B. (2002). Novel putative nicotinic acetylcholine receptor subunit genes, *Dalpha5*, *Dalpha6* and *Dalpha7*, in *Drosophila melanogaster* identify a new and highly conserved target of adenosine deaminase acting on RNA-mediated A-to-I pre-mRNA editing. *Genetics*, 160, 1519-1533.
- Gronenberg, W. & Strausfeld, N. J. (1990). Descending neurons supplying the neck and flight motor of diptera: Physiological and anatomical characteristics. *Journal of Comparative Neurology*, 302, 973-991.
- Haag, J. & Borst, A. (2004). Neural mechanism underlying complex receptive field properties of motion-sensitive interneurons. *Nat.Neurosci.*, 7, 628-634.
- Haag, J. & Borst, A. (2005). Dye-coupling visualizes networks of large-field motion-sensitive neurons in the fly. *J.Comp Physiol A Neuroethol.Sens.Neural Behav.Physiol*, 191, 445-454.
- Haag, J., Denk, W., & Borst, A. (2004). Fly motion vision is based on Reichardt detectors regardless of the signal-to-noise ratio 3. *Proc.Natl.Acad.Sci.U.S.A*, 101, 16333-16338.
- Haag, J., Theunissen, F., & Borst, A. (1997). The intrinsic electrophysiological characteristics of fly lobula plate tangential cells: II. active membrane properties. *Journal of Computational Neuroscience*, 4, 349-369.
- Haag, J., Vermeulen, A., & Borst, A. (1999). The Intrinsic Electrophysiological Characteristics of Fly Lobula Plate Tangential Cells: III. Visual Response Properties. *Journal of Computational Neuroscience*, 7, 213-234.
- Haag, J., Wertz, A., & Borst, A. (2007). Integration of lobula plate output signals by DNOVS1, an identified premotor descending neuron. *J.Neurosci.*, 27, 1992-2000.
- Hassenstein, B. & Reichardt, W. (1956). Systemtheoretische Analyse der Zeit-, Reihenfolgen- und Vorzeichenbewertung bei der Bewegungsperzeption des Rüsselkäfers *Chlorophanus*. *Zeitschrift fuer Naturforschung*, 11b, 513-524.
- Hausen, K. (1982a). Motion sensitive interneurons in the optomotor system of the fly. I. The Horizontal Cells: Structure and signals. *Biological Cybernetics*, 45, 143-156.
- Hausen, K. (1982b). Motion sensitive interneurons in the optomotor system of the fly. II. The Horizontal Cells: Receptive field organization and response characteristics. *Biological Cybernetics*, 46, 67-79.
- Heisenberg, M., Wonneberger, R., & Wolf, R. (1978). Optomotor-blind (H31) - a *Drosophila* mutant of the lobula plate giant neurons. *Journal of Comparative Physiology*, 124, 287-296.
- Hengstenberg, R. (1982). Common visual response properties of giant vertical cells in the lobula plate of the blowfly *Calliphora*. *Journal of Comparative Physiology A*, 149, 179-193.
- Hengstenberg, R., Hausen, K., & Hengstenberg, B. (1982). The number and structure of giant vertical cells (VS) in the lobula plate of the blowfly *Calliphora erythrocephala*. *Journal of Comparative Physiology A*, 149, 163-177.
- Hess, N., Merz, B., & Gundelfinger, E. D. (1994). Acetylcholine receptors of the *Drosophila* brain: a 900 bp promoter fragment contains the essential information for specific expression of the *ard* gene in vivo. *Federation of European Biochemical Societies*, 346, 135-140.
- Jösch, M., Plett, J., Borst, A., & Reiff, D. F. (2008). Response properties of motion-sensitive visual interneurons in the lobula plate of *Drosophila melanogaster*. *Current Biology*, 18, 1-7.
- Jonas, P., Major, G., & Sakmann, B. (1993). Quantal components of unitary EPSCs at the mossy fibre synapse on CA3 pyramidal cells of rat hippocampus. *Journal of Physiology*, 472, 615-663.
- Jonas, P. E., Phannavong, B., Schuster, R., Schroder, C., & Gundelfinger, E. D. (1994). Expression of the ligand-binding nicotinic acetylcholine receptor subunit D alpha 2 in the *Drosophila* central nervous system. *J.Neurobiol.*, 25, 1494-1508.

- Jones, A. K., Brown, L. A., & Sattelle, D. B. (2007). Insect nicotinic acetylcholine receptor gene families: from genetic model organism to vector, pest and beneficial species. *Invert.Neurosci.*, *7*, 67-73.
- Koenderink, J. J. & van Doorn, A. J. (1987). Facts on optic flow. *Biological Cybernetics*, *56*, 247-254.
- Krapp, H. G., Hengstenberg, B., & Hengstenberg, R. (1998). Dendritic Structure and Receptive-Field Organization of Optic Flow Processing Interneurons in the Fly. *Journal of Neurophysiology*, *79*, 1902-1917.
- Krapp, H. G. & Hengstenberg, R. (1996). Estimation of self - motion by optic flow processing in single visual interneurons. *Nature*, *384*, 463-466.
- Leech, C. A. & Sattelle, D. B. (1993). Acetylcholine receptor/channel molecules of insects. *EXS*, *63*, 81-97.
- Raghu, S. V., Jösch, M., Borst, A., & Reiff, D. F. (2007). Synaptic organization of lobula plate tangential cells in *Drosophila*: gamma-aminobutyric acid receptors and chemical release sites. *J.Comp Neurol.*, *502*, 598-610.
- Rajashekhar, K. P. & Shamprasad, V. R. (2004). Golgi analysis of tangential neurons in the lobula plate of *Drosophila melanogaster*. *J.Biosci.*, *29*, 93-104.
- Reichardt, W. (1961). Autocorrelation, a principle for the evaluation of sensory information by the central nervous system. In W.A.Rosenblith (Ed.), *Sensory Communication* (pp. 303-317). New York, London: The M.I.T. Press and John Wiley & Sons.
- Sattelle, D. B. (1980). In *Advances in Insect Physiology*. (pp. 215-315). Academic Press, London, New York.
- Sattelle, D. B., Jones, A. K., Sattelle, B. M., Matsuda, K., Reenan, R., & Biggin, P. C. (2005). Edit, cut and paste in the nicotinic acetylcholine receptor gene family of *Drosophila melanogaster*. *BioEssays*, *27*, 366-376.
- Schloss, P., Hermans-Borgmeyer, I., Betz, H., & Gundelfinger, E. D. (1988). Neuronal acetylcholine receptors in *Drosophila*: the ARD protein is a component of a high-affinity alpha-bungarotoxin binding complex. *EMBO J.*, *7*, 2889-2894.
- Schuster, R., Phannavong, B., Schroder, C., & Gundelfinger, E. D. (1993). Immunohistochemical localization of a ligand-binding and a structural subunit of nicotinic acetylcholine receptors in the central nervous system of *Drosophila melanogaster*. *J.Comp Neurol.*, *335*, 149-162.
- Scott, E. K., Raabe, T., & Luo, L. (2002). Structure of the vertical and horizontal system neurons of the lobula plate in *Drosophila*. *J.Comp Neurol.*, *454*, 470-481.
- Strausfeld, N. J. & Lee, J. K. (1991). Neuronal basis for parallel visual processing in the fly. *Visual Neuroscience*, *7*, 13-33.
- Wegener, C., Hamasaka, Y., & Nassel, D. R. (2004). Acetylcholine increases intracellular Ca²⁺ via nicotinic receptors in cultured PDF-containing clock neurons of *Drosophila*. *J.Neurophysiol.*, *91*, 912-923.
- Wertz, A., Borst, A., & Haag, J. (2008). Nonlinear integration of binocular optic flow by DNOVS2, a descending neuron of the fly. *J.Neurosci.*, *28*, 3131-3140.
- Zheng, L., de Polavieja, G. G., Wolfram, V., Asyali, M. H., Hardie, R. C., & Juusola, M. (2006). Feedback network controls photoreceptor output at the layer of first visual synapses in *Drosophila*. *J.Gen.Physiol.*, *127*, 495-510.

6 Manuscript Nr.4

Processing of horizontal optic flow in three visual interneurons of the *Drosophila* brain

This chapter has been submitted to the Journal of Neuroscience by Bettina Schnell, Maximilian Jösch, Friedrich Förstner, Shamprasad Varija Raghun, Kei Ito[#], Alexander Borst & Dierk F. Reiff

MPI for Neurobiology

Dept. of Systems and Computational Neurobiology

Martinsried, Germany

[#] Center for Bioinformatics

Institute of Molecular and Cellular Biosciences

Tokyo, Japan.

Bettina Schnell performed electrophysiological experiments, the neurobiotin fills and analyzed the data. Maximilian Jösch performed the “blind” patch electrophysiological experiments, analyzed this data and trained B. Schnell. Friedrich Förstner performed the anatomical reconstructions, Shamprasad Varija Raghun performed the histological experiments. Kei Ito supplied flies. Bettina Schnell, Dierk Reiff and Alexander Borst conceived experiments. Bettina Schnell and Dierk Reiff wrote the manuscript.



Abstract

Motion vision is essential for navigating through the environment. Due to its genetic amenability, the fruit fly *Drosophila* has served for long as a model organism for studying optomotor behavior as elicited by large-field horizontal motion. However, the neurons underlying this behavior have not been studied in *Drosophila* so far. Here we report whole-cell recordings from three types of cells, two were genetically labeled and the third was recorded “blindly”. Their shape and position precisely match the three cells of the horizontal system (HSN, HSE and HSS) in *Drosophila* described only anatomically so far. HS-cells are tuned to large field horizontal motion in a direction-selective way: they become excited by front-to-back motion and inhibited by back-to-front motion in the ipsilateral field of view. The response properties of HS-cells like contrast and velocity dependence are in accordance with the correlation type model of motion detection. Neurobiotin injection revealed extensive coupling among ipsilateral HS-cells and additional coupling to tangential cells that have their dendrites in the contralateral hemisphere of the brain. This connectivity scheme accounts for the layout of their receptive fields and explains their sensitivity to ipsilateral as well as to contralateral motion. In all these respects, *Drosophila* HS-cells are similar to their counterparts in the blow fly *Calliphora*. However, we also found substantial differences between *Drosophila* and *Calliphora* HS-cells with respect to their dendritic structure and connectivity. In summary, our study provides important information for the further dissection of the circuitry mediating optomotor responses by combining genetics, physiology and behavior.

Introduction

To navigate safely through the environment flies rely heavily on visual motion information (Borst and Haag, 2002). Once airborne, they use the characteristic flow-fields caused by their self-motion to correct for deviations from a straight flight path. The precision and reliability of these so-called optomotor responses combined with the small size of their brain make flies an ideal organism to study the underlying neural circuitry (Götz, 1964; Heisenberg et al., 1978; Chan et al., 1998; Frye and Dickinson, 2001; Egelhaaf et al., 2003).

Detailed anatomical maps describing the cell types of the optic lobes (Strausfeld, 1976; Fischbach and Dittrich, 1989; Scott et al., 2002) are at hand. In the blow fly *Calliphora*, about 60 motion sensitive neurons, the so called Lobula Plate Tangential Cells (LPTCs) are supposed to be the main output elements that convey information about large- and small-field motion onto descending neurons to ultimately control head movement and locomotion (Gronenberg and Strausfeld, 1990; Gilbert et al., 1995; Chan et al., 1998).

To analyze neuronal function different approaches were pursued in big and small flies. In *Calliphora* the response properties of LPTCs have been characterized in greatest detail by intracellular recording (Borst and Haag, 2002). Among them, cells of the vertical system (VS) respond preferentially to vertical motion (Hengstenberg et al., 1982) and motion elicited by rotation around an axis in the horizontal plane of the animal (Krapp et al., 1998). Horizontal system- (HS) cells respond to translation (Hausen, 1982a; Hausen, 1982b) and rotational motion around the vertical axis of the fly (Krapp et al., 2001). Their tuning to specific optic flow fields can be explained by dendritic input from opposing arrays of local motion detectors built from columnar elements (Borst and Egelhaaf, 1990; Single and Borst, 1998; Jösch et al., 2008; Raghu et al., 2007; Raghu et al., 2009) as well as input from other LPTCs (Haag and Borst, 2004; Haag and Borst, 2007; Elyada et al., 2009; Haag and Borst, 2008; Farrow et al., 2006; Farrow et al., 2005).

In *Drosophila*, mainly genetic techniques have been used to disrupt parts of the circuitry and to compare the behavior of wild type and mutant flies (Götz, 1964; Götz, 1965; Heisenberg and Buchner, 1977; Heisenberg, 1972). This approach also allows

studying columnar neurons presynaptic to LPTCs that, even in large flies, escaped from a rigorous electrophysiological analysis because of their small size.

Recent studies on the behavior of wild type (Tammero et al., 2004; Duistermars et al., 2007; Mronz and Lehmann, 2008; Fry et al., 2009) and transgenic *Drosophila* with certain types of columnar neurons blocked (Rister et al., 2007; Katsov and Clandinin, 2008; Zhu et al., 2009) provided new insights into motion vision and optomotor behavior. However, these studies also revealed the limitations of behavioral experiments as read-out for the functional role of a specific class of neurons. Moreover, the interpretation of studies in *Drosophila* relies heavily on physiological data from large flies as a functional description of LPTCs in *Drosophila* is only available for VS-cells (Jösch et al., 2008).

We close this gap by characterizing the response properties of the three HS-cells in *Drosophila* that are supposed to mediate yaw turning behavior. HS-cells are tuned to large field horizontal motion and match the predictions of a correlation detector model. Their complex receptive fields, contrast dependence and velocity tuning corroborate findings on HS-cells in *Calliphora*. Compared to large flies however, their dendritic structure and connectivity to other LPTCs are different.

Materials and Methods

Flies

Flies were raised on standard cornmeal-agar medium with a 12 hr light / 12 hr dark cycle, 25 °C, and 60 % humidity. We used female experimental flies, one day after eclosion. The line NP 0282 (NP consortium) expresses Gal4 in two of the three HS-cells (HSN and HSE, Fig. 1A) and in unidentified neurons of the central brain. UAS-mCD-GFP was used to highlight entire cells by cytosolic expression of the reporter molecule. UAS-mCD8-TN-XL-8aa (Jösch et al., 2008) was used to predominantly stain cell bodies.

Visually Guided Whole-Cell Recording

Patch-clamp recordings were performed as described previously (Jösch et al., 2008). Flies were anesthetized on ice and waxed on a Plexiglas holder. The head was bent down to expose the caudal backside of the head, and the extended proboscis was

fixed. Aluminum foil with a hole of ~1–2 mm sustained by a ring-shaped metal holder was placed on top of the fly and separated the upper wet part (covered with ringer solution (Wilson et al., 2004)) of the preparation from the lower dry part. Water-immersion optics was used from above; visual patterns (see below) were presented to dry and fully intact facet eyes. A small window was cut into the backside of the head, and during mild protease treatment (protease XIV, E.C.3.4.24.31, Sigma, Steinheim, Germany; 2 mg/ml, max 4 min), the neurolemma was partially digested and the main tracheal branches and fat body were removed. The protease was rinsed off carefully and replaced by ringer solution. A ringer-filled cleaning electrode was used to remove the extracellular matrix and to expose the HS-cell somata for recording.

Genetically labeled green fluorescent HS-cell somata were approached with a patch electrode filled with a red fluorescent dye (intracellular solution (Wilson and Laurent, 2005) containing additional 5 mM Spermine and 30 mM Alexa-Fluor-568-hydrazide-Na, Molecular Probes, adjusted to pH = 7.3). Recordings were established under visual control with a 40x water-immersion objective (LumplanF, Olympus), a Zeiss Microscope (Axiotech Vario 100, Zeiss, Oberkochen, Germany), fluorescence excitation (100 W fluorescence lamp, heat filter, neutral-density filter OD 0.3; all from Zeiss, Germany), and a dual-band filter set (EGFP/DsRed, Chroma Technology, Vermont, USA). During the recordings, the fluorescence excitation was shut off to prevent blinding of the fly. Patch electrodes of 6–8 M Ω resistance (thin wall, filament, 1.5 mm, WPI, Florida, USA) were pulled on a Sutter- P97 (Sutter Instrument Company, California, USA). A reference electrode (Ag-AgCl) was immersed in the extracellular saline (pH 7.3, 1.5 mM CaCl₂, no sucrose). Signals were recorded on a NPI BA-1S Bridge Amplifier (NPI Electronics GmbH, Tamm, Germany), low-pass filtered at 3 kHz, and digitized at 10 kHz via a digital-to-analog converter (PCI-DAS6025, Measurement Computing, Massachusetts, USA) with Matlab (Vers. 7.3.0.267, Mathworks, Massachusetts, USA). After the recording, several images of each Alexa-filled LPTC were taken at different depths along the z-axis (HQ-filter set Alexa-568, Chroma Technology, USA) with a CCD camera (Spot Pursuit 1.4 Megapixel, Visitron Systems GmbH, Puchheim, Germany).

Immunohistochemistry

Female flies were dissected three to five days after eclosion. Their brains were removed and fixed in 4 % paraformaldehyde for 30 minutes at room temperature.

Subsequently, the brains were washed for 45 - 60 minutes in PBT (phosphate buffered saline (pH 7.2) including 1 % Triton X-100). For antibody staining, the samples were incubated in PBT including 2 % normal goat serum (Sigma Aldrich, G9023) for 1 hour at room temperature followed by incubation with primary antibodies (1: 200, overnight at 4 °C). Primary antibodies were removed by several washing steps (5 x 20 minutes in PBT) and secondary antibodies were added (1: 200, overnight at 4 °C). The samples were further washed with PBT (3 x 20 minutes) followed by final washing steps in PBS (3 x 20 minutes). The stained brains were mounted in Vectashield (Vector Laboratories, Burlingame) and analyzed by confocal microscopy (see below). The following primary and secondary antibodies were used: Alexa Fluor 488 rabbit anti-GFP-IgG (A-21311, Molecular Probes), Mouse anti-Dlg (4F3, Developmental Studies Hybridoma Bank (DSHB) and Alexa Fluor 594 goat anti-mouse IgG (A11005, Molecular Probes).

Confocal Microscopy & reconstruction

Serial optical sections were taken at 0.5 μm intervals with 1024 x 1024 pixel resolution using confocal microscopes (LEICA TCSNT) and oil-immersion 40x (n.a. = 1.25) or 63x Plan-Apochromat objectives. The individual confocal stacks were analyzed using Image J (NIH, U.S.A) software. The size, contrast and brightness of the resulting images were adjusted with Photoshop® CS (Adobe Systems, San Jose, CA). Cells were manually traced using previously described custom written software (Cuntz et al., 2008) resulting in detailed cylinder models. Lobula plate volumes were reconstructed manually by outlining their outer borders in each slice and sampling surface meshes. Cylinder and volume models were visualized using the Blender animation system (<http://www.blender.org>).

Neurobiotin Staining

VS cells were targeted and perfused with patch electrodes as described above. 2 - 4 % Neurobiotin (Vector Labs, Burlingame) was added to the intracellular solution. Neurobiotin and Alexa Fluor-568 were coinjected via ± 0.2 nA current pulses for up to 10 min. For initial identification, the perfused individual HS-cell was imaged with the fluorescence microscope and CCD camera as described above. Staining against Neurobiotin with Streptavidin Alexa Fluor-568 conjugate (Invitrogen, 1:100) was performed as described above, except that whole fly heads were fixed in 4 % PFA (2 h) before dissection in PBS. Perfusion of a single HS cell never resulted in more than

one Alexa-568-filled cell. Only after labeling of Neurobiotin with Streptavidin- Alexa-568 conjugate did other cells light up. The second red label was used to prevent spectral overlap with the green fluorescence of genetically labeled neurons.

Visual Stimulation

For visual stimulation a custom built LED arena was used based on the open-source information of the Dickinson Laboratory (<http://www.dickinson.caltech.edu/PanelsPage>). Our arena consists of 15 by 8 TA08-81GWA dot matrix displays (Kingbright, California, USA), each harboring 8 by 8 individual green (568 nm) LEDs, covering 170° in azimuth and 85° in elevation of the fly's visual field with an angular resolution of about 1.4° between adjacent LEDs. The arena is capable of frame rates above 600 fps with 16 intensity levels. To measure the velocity tuning and contrast dependency of HS-cells precisely, patterns were generated in which four consecutive frames were used to define one image. This resulted in 64 equidistant intensity levels available per pixel. Each dot matrix display is controlled by an ATmega644 microcontroller (Atmel, California, USA) that obtains pattern information from one central ATmega128 based main controller board, which in turn reads in pattern information from a compact flash (CF) memory card. For achieving high frame rates with a system of this size, each panel controller was equipped with an external AT45DB041B flash memory chip for local pattern buffering. Matlab was used for programming and generation of the patterns as well as for sending the serial command sequences via RS-232 to the main controller board and local buffering. The luminance range of the stimuli was 0-8 cd/m².

Data Analysis

Data were acquired and analyzed with the data acquisition and analysis toolboxes of Matlab. Receptive fields were calculated by binning the responses of single HS-cells to horizontal stimulation (~5.7° elevation and ~5.7° azimuth) and subtracting the mean response during null direction from the mean response during preferred direction motion. The data of each individually identified cell were normalized to the maximum response. The projection of the receptive field on the azimuth was calculated for each HS cell individually by averaging the binned responses at the different azimuth at each position along the elevation. Contrast was calculated as $(I_{\max} - I_{\min}) / (I_{\max} + I_{\min})$. For analyzing the velocity dependence the mean of the first 500 ms after onset of PD motion was taken.

Results

Based on anatomical similarity to the three horizontally sensitive LPTCs in blow flies (Hausen, 1982a; Hausen, 1982b), the horizontal system of *Drosophila* has been proposed to consist of the three giant output neurons HSN, HSE and HSS (Heisenberg et al., 1978; Fischbach and Dittrich, 1989). The dendrites of these cells reside in a thin anterior layer of the lobula plate (Fig. 1A) where they cover the dorsal, middle and ventral part of this retinotopically organized neuropile, respectively (Heisenberg et al., 1978; Scott et al., 2002). Their axons project centrally to the lateral protocerebrum where they are supposed to synapse onto descending neurons (Eckert and Meller, 1981; Haag et al., 2007) and thus to control optomotor turning responses induced by horizontal optic flow.

We performed the first *in-vivo* whole cell recordings from the somata of HS-cells and characterized their response properties during large field visual motion (Fig. 1B). In the first series of experiments reproducible recordings from identified cells were enabled using the NP 0282 Gal4 driver line. At the level of the Lobula Plate, NP 0282 specifically labels HSN and HSE (Fig. 1A). Despite the lack of HSS, NP 0282 was chosen to express a green fluorescent marker that highlights the soma (Jösch et al., 2008) of HSN and HSE under the fluorescence microscope. The recording electrode was visualized by adding a red fluorescent dye to the electrode solution which allowed directing the electrode under visual guidance towards the green cell bodies. Thus, during the recording, the cells became perfused with the red dye and the recorded signals could be assigned to the specific cell type. In these recordings, HS-cells exhibited a resting membrane potential of about -55 mV (corrected for liquid junction potential) and an input resistance of 10-20 M Ω (n = 25). At rest, all recorded HS cells showed small and rapid spontaneous membrane fluctuations of high frequency (Fig 1C).

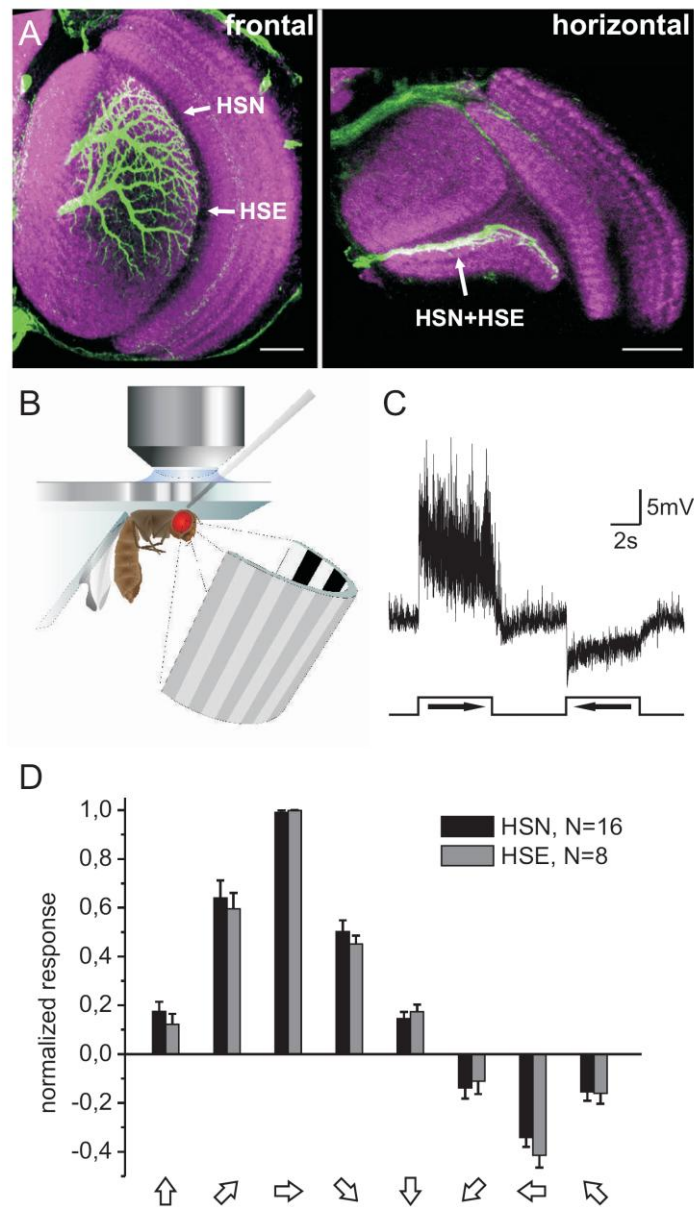


Figure 1. Basic response properties of HS-cells in *Drosophila*. (A) The Gal4-line NP0282 drives expression of the fluorescent marker mCD8-GFP in two neurons of the lobula plate. Based on their anatomy and on comparable neurons in large dipteran flies these neurons were previously described as the northern (HSN) and equatorial (HSE) cells of the *Drosophila* HS-system. Their dendrites cover large overlapping areas (frontal section) in a thin anterior layer (horizontal section) of the lobula plate (scale bars 25 μ m). Reliable whole cell recordings from these neurons were done by fluorescent labeling of their soma only (see methods). (B) Scheme of the recording setup and preparation of the fly under the fluorescence microscope. In the lower dry half of the preparation the fly is looking at moving patterns presented on a LED arena. (C) Canonical response of an HSN-cell plotted against time. A vertical sine grating ($\lambda = 42.5^\circ$) moving horizontally (temporal frequency = 1 Hz) elicits a directionally selective response. Large field rotation with an ipsilateral front-to-back component (preferred direction, PD) elicits a strong depolarization. Motion in the opposite direction (null direction, ND) elicits a strong hyperpolarization of the membrane potential. Small, fast membrane fluctuations increase in size during

PD-motion. (D) Directional tuning. Plotted is the mean response amplitude during 5s grating motion (same stimulus as in (C)) in four different orientations and a total of eight different directions. HSN and HSE respond strongest to horizontal motion. Error bars indicate SEM.

HSN- and HSE are tuned to horizontal motion in a direction-selective way.

When stimulated with a large-field sine grating moving front-to-back in front of the ipsilateral eye (including an area of back-to-front motion in the contralateral eye), HS-cells canonically exhibited a graded depolarization superimposed by spike-like events (Fig. 1C). Motion in the opposite direction led to a hyperpolarization of the membrane potential and a reduction of the fast spike-like events. Presentation of sine gratings moving in four different orientations and a total of eight different directions revealed a strong directional tuning of both HSN and HSE (black and grey bars, respectively, Fig.1D) to large field horizontal motion, similar to their counterparts in *Calliphora*. Ipsilateral front-to-back motion elicited the strongest activation (preferred direction, PD) and back-to-front motion the strongest inhibition (null direction, ND). Typically, ND responses were smaller in amplitude than PD responses. Diagonal motion led to weaker responses and almost no responses were elicited by vertical motion in either direction. Thus, HS-cells in *Drosophila* are tuned to large field horizontal motion in a directional selective way.

HS-cell responses suggest input from correlation-type motion detectors

According to the correlation-type model for elementary motion detection (Reichardt, 1961; Borst and Egelhaaf, 1989), motion information is extracted from the retinal image by a multiplicative interaction of luminance signals from two neighboring receptors after delaying one of them in time. Large field directional selectivity of LPTCs can then arise from spatial integration of input from two arrays of such detectors, one excitatory and the other inhibitory, that compute local motion information with opposite preferred direction (Single et al., 1997; Single and Borst, 1998; Raghu et al., 2007; Raghu et al., 2009; Jösch et al., 2008). The output of such a correlation-type model has certain features that we tested for in HS-cell responses. These features are the appearance of a velocity optimum (Fig.2A), the dependency of this velocity optimum on the spatial wavelength of the moving grating (Fig.2B), the

dependence of the response on the magnitude of contrast (Fig.2C) and the independence of the sign of contrast (Fig.2D). To characterize the velocity dependence of HS-cells in response to PD motion, we presented sine gratings of 22° or 44° spatial wavelength (inset Fig.2A) at nine different velocities (Fig.2A). For both patterns the HS-cell response increased non-linearly, exhibited a maximum response at an angular velocity of $22^\circ/s$ and $44^\circ/s$, respectively, and declined at higher velocities (Fig. 2A). For both patterns this resulted in a maximal response at around 1 Hz (velocity [deg/s] divided by spatial wavelength [deg]) which represents the so called temporal frequency optimum, a hallmark of the correlation-type detector model (Fig. 2B).

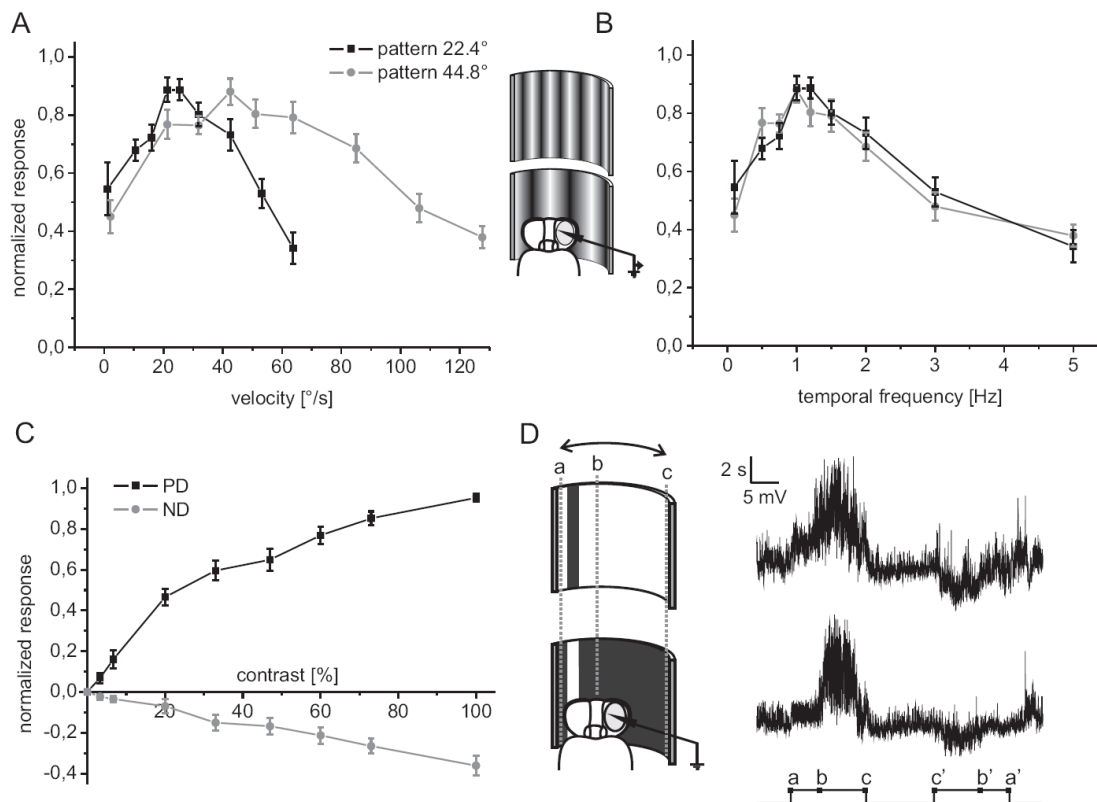


Figure 2. HSN and HSE responses match the predictions of a correlation-type motion detector. (A) Velocity dependence. Two sine gratings of different spatial wavelength ($\lambda = 22.4^\circ$ and $\lambda = 44.8^\circ$) moving at nine different velocities elicited a velocity optimum that depended on the spatial wavelength of the pattern. Plotted is the mean response during the first 500 ms after onset of PD motion, normalized to the maximal response for each fly. $N = 10$ for each grating, error bar: SEM. (B) Constant temporal frequency optimum of 1 Hz. Same data as in (A) plotted against the temporal frequency ($tf = \text{velocity} / \lambda$). (C) Contrast dependence. Square wave gratings ($\lambda=34^\circ$) of different contrast moving in PD or ND ($tf = 1$ Hz) were presented. Plotted is the mean response during 5s of motion normalized to the maximal response of each HS-cell. Response amplitudes increase with contrast, but exhibit saturation. $N = 19$, error bars: SEM. (D) Independence of the sign of contrast. Example trace of an HS-cell responding to a light bar on a dark background and a dark bar on a light background moving in PD and ND (width of

the bar: 8.5° , maximal contrast). The direction of motion is reported by the membrane potential independent of the sign of contrast. a , b and c and a' , b' and c' mark the time points, at which the bar occupied the respective positions indicated in the schematic drawing. Note that HS-cells respond to motion on the contralateral side (a to b and b' to a') as well. Ipsilateral motion elicited stronger responses (b to c and c' to b').

The dependency of the response on the magnitude of contrast was shown by presenting square-wave gratings (spatial wavelength: 34°) of different contrast ranging from 3.3 to 100 % which were moving at a constant velocity of $34^\circ/\text{sec}$ (Fig.1C). For both PD and ND motion the response amplitudes increased with pattern contrast and PD responses saturated at higher contrast (Fig. 2C). Furthermore, the correlation-type motion detector reports the direction of movement independent of the sign of contrast. In accordance with this prediction, a moving dark bar on a light background or a moving light bar on a dark background evoked depolarizing PD responses for front-to-back motion and hyperpolarizing ND responses for back-to-front motion (Fig. 2D). In these experiments a still bar was presented to the contralateral field of view, began to move at time (a), entered the ipsilateral field of view at time (b), continued its way and stopped at a lateral position at time (c). From there it moved back by reversing the sequence c' , b' and a' (Fig. 2D). Regressive motion of the bar through the contralateral visual field of view elicited a depolarizing response, which was, however, smaller than that caused by ipsilateral progressive motion (see below). Taken together, the response properties of HS-cells are indicative of presynaptic computations according to the correlation-type model of motion detection.

HS-cells of one hemisphere have strongly overlapping, binocular receptive fields

The environment, as scanned by the ipsilateral compound eye, is mapped retinotopically onto the columnar elements that are supposed to provide the synaptic input to the giant HS-cell dendrites in the lobula plate (Strausfeld, 1984; Braitenberg, 1970). As a consequence of this layout, the position and the branching pattern of an HS-cell within the lobula plate (Fig. 3A) should be predictive of its ipsilateral receptive field (Hausen, 1982a; Hausen, 1982b). We reconstructed the dendritic trees of 10 HSN and HSE cell pairs from confocal image stacks of GFP-labeled cells to analyze the dendritic structure in detail. One example is shown in Figure 3A. The dendrites of HSN and HSE cover the dorsal and equatorial part of the lobula plate, respectively,

with the size of the dendritic spanning field of HSE being about 1.5 times larger than that of HSN (data not shown). The overlap of their dendritic spanning fields is very large, that of HSE covers on the average about 90 % of that of HSN. A dendritic branch of HSE reaches even close to the dorsal most boundary of HSN (Fig. 3A). Any deviation of the receptive field from this anatomical map can possibly be attributed to input from neurons other than the columnar ones.

We analyzed the receptive fields of HSN and HSE by presenting a small bar (5.6° high and 1.4° wide) moving front-to-back and back-to-front at different positions subtending 170° along the azimuth and about 85° of elevation. We binned the response within a time window that corresponded to motion of about 5.6° along the azimuth, and plotted the normalized response amplitudes (PD - ND) in false color code against the position of the bar on the arena (Fig. 3B). As the arena is only curved in the horizontal direction, the size of the bar as stated above is only valid for the equatorial position and appeared slightly smaller to the fly in the dorsal and ventral part of the visual field. Our analysis revealed that HSN- and HSE-cells in *Drosophila* have large receptive fields that cover at their largest extent over 60° of elevation and the entire stimulated area covered by the arena along the azimuth (170°). They are most sensitive to motion at positions corresponding to their dendritic trees in the Lobula Plate, which is dorsal for HSN and equatorial for HSE (Fig. 3A and B). In contrast to *Calliphora* (Hausen 1982b), however, HSE in *Drosophila* seems to be maximally sensitive in the lateral visual field and not in the frontal one.

To estimate the amount of overlap between the receptive fields of HSN and HSE, a threshold of 25 % of the maximal response was set. The areas, where the responses of HSN, HSE or both cells exceeded this threshold, were colored differently. Based on this criterion, the receptive fields of ipsilateral HSE and HSN overlap by about 70 to 80 % (Fig. 3D). In particular the receptive field of HSN reaches nearly as far ventrally as that of HSE. Small variations of the threshold led to qualitatively similar results in several preparations. The huge overlap of the receptive fields of HSN and HSE corresponds in part to the huge overlap of their dendritic trees stated above. However, the lack of dendritic branches of HSN in the ventral area indicates that the ventral extension of the receptive field of HSN can not be explained by direct input to the dendrite (compare Fig. 3A and B).

Another interesting feature of the receptive fields of HSN and HSE is their sensitivity to contralateral motion (Fig. 2D). We presented moving square-wave gratings in either the ipsilateral or the contralateral part of the visual field to investigate this in further

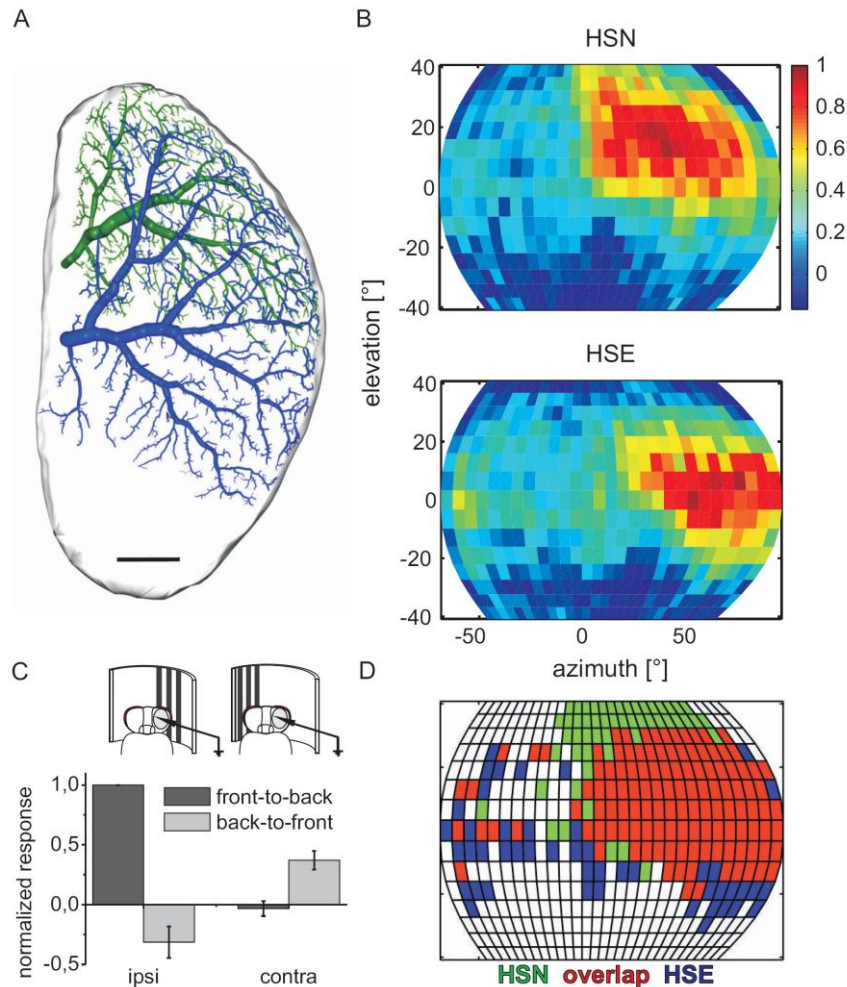


Figure 3 Dendritic structure and receptive fields of HSN and HSE. (A) Reconstruction of the dendritic arborization of HSN and HSE in the lobula plate. The overlapping dendrites of both cells were reconstructed from confocal sections of GFP-labeled cells. (B) Receptive fields of HSN and HSE. Plotted are response amplitudes (PD-ND) elicited by a small local bar moving horizontally at different elevations normalized to the maximal response. HSN and HSE share a large part of their receptive field and are most responsive to motion covered by their own dendritic trees in the lobula plate (that is more dorsal for HSN and equatorial for HSE). The ipsilateral receptive fields are much larger than expected from the area covered by their dendrites and the cells also respond to contralateral motion. $N = 4$ for HSE and $N = 7$ for HSN. (C) Sensitivity to contralateral motion. Square wave gratings ($\lambda = 22.4^\circ$) were presented in either the contra- or the ipsilateral visual field as shown in the schematic drawing (sparing the frontal region of binocular overlap). Contralateral back-to-front motion elicited a weak depolarization of the membrane potential in HS-cells and a strong depolarization in response to ipsilateral front-to-back motion. $N = 6$, error bar: SEM. (D) Overlap of the receptive fields. The amount

of overlap between the receptive fields of HSN and HSE was estimated by applying a threshold of 25 % of the maximal response in (B). Areas, where the response amplitude of HSN and HSE exceeded this threshold are plotted in red; areas where only HSN or HSE responses reach the threshold are plotted in green and blue, respectively. Compare to the much smaller overlap of the dendritic trees in (A).

detail. The pattern covered about 56° in azimuth and 85° in elevation. To prevent stimulation of the area of binocular overlap (Heisenberg and Wolf, 1984), the pattern was displaced by $\pm 15^\circ$ with respect to the frontal gaze of the fly (Fig. 3C). Motion in front of the ipsilateral eye elicited canonical PD and ND responses i.e. a depolarization for front-to-back and a hyperpolarization for back-to-front motion. Contralateral back-to-front motion, however, elicited a robust depolarization whereas contralateral front-to-back motion did not elicit a noticeable response. Thus, HSN and HSE are tuned to rotational panoramic motion stimuli as they arise from rotation of the animal around the vertical body axis. Very importantly, their sensory input is not confined to the retinotopically organized columnar neurons that impinge onto their dendritic tree.

In the course of our experiments we occasionally recorded from genetically unlabeled HS-cells in different genotypes that represented control situations. The recordings of these cells were indistinguishable from our previous recordings of labeled HSE and HSN and included recordings from HSS-cells that were not highlighted by the Gal4-driver in the previous experiments. We characterized the receptive fields in further detail by presenting in addition to the horizontally moving bar (see above) a local bar moving vertically. From the responses to local horizontal and vertical motion we calculated response vectors that indicate by their orientation the local preferred direction and by their length the strength of the response. All local vectors together constitute the optic flow field of a given HS-cell (Fig. 4). All three HS-cells exhibited a slight vertical sensitivity. HSN and to a weaker extent HSE depolarize in response to upward motion in the fronto-dorsal and fronto-equatorial part of their receptive fields. HSS shows a similar sensitivity to upward motion in a more ventro-lateral position. Similar to HSN, the receptive field of HSS overlaps quite strongly with that of HSE.

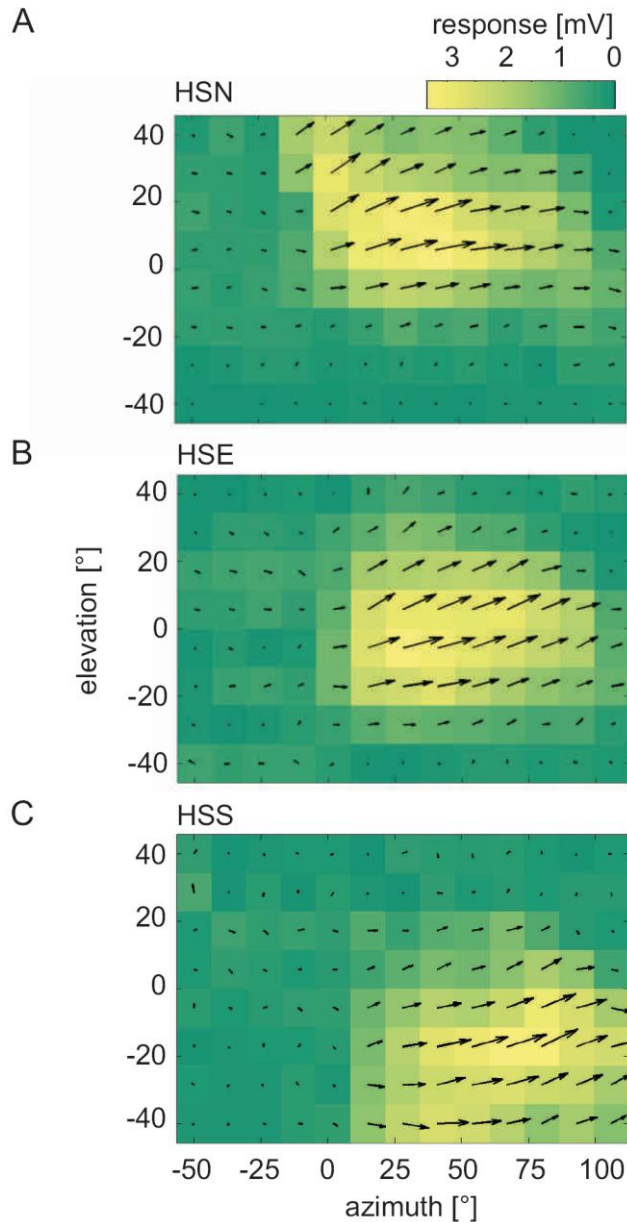


Figure 4. Vector fields of HSN (A), HSE (B) and HSS (C).

Local preferred direction and response strength of all three HS-cells are indicated by the orientation and lengths of the motion vectors (arrows). The strength of the response is in addition indicated by a heat map. Vectors were calculated by subtracting PD- and ND-responses to small bars moving either horizontally or vertically at different positions (compare Figure 3). Similar to HSN and HSE the maximum sensitivity in the ventral receptive field of HSS corresponds to the area occupied by its dendritic tree in the lobula plate (not shown). As the other HS-cells, HSS responds mainly to horizontal motion. However, all HS-cells show a slight sensitivity to upward motion in mostly the center of their receptive field. All responses from HSS ($n = 6$) and HSE ($n = 9$) were recorded 'blind' from unlabeled cells. HSN vector maps were calculated from the local responses of labeled ($n = 4$) and unlabeled cells ($n = 1$).

Dye-coupling suggests that HS-cells are central to a complex network of electrically coupled neurons.

In *Calliphora* complex receptive fields of VS- and HS-cells arise from electric coupling to other LPTCs (Haag and Borst, 2002; 2004; Cuntz et al., 2007). We investigated whether this holds also true for HS-cells in *Drosophila*. For that purpose, Neurobiotin, a molecule sufficiently small to pass Innexin-based gap junctions, was added to the intracellular solution in the recording electrode. Perfusion with Alexa-568 allowed for immediate identification of the recorded neuron. Later, the spread of Neurobiotin was

detected by staining with Streptavidin-coupled to Alexa-568 (Jösch et al., 2008). As the initially perfused free Alexa-568 never stained other cells except the injected one, we concluded that fluorescence after streptavidin-Alexa-568 labeling in other cells is due to direct or indirect coupling via electrical synapses to the recorded cell (Fig. 5).

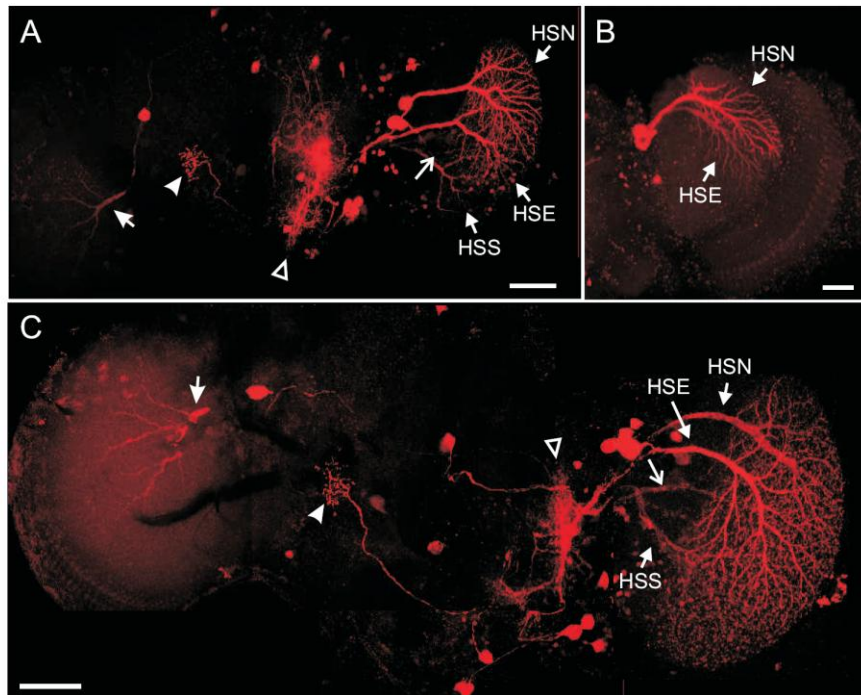


Figure 5. Spread of Neurobiotin within the HS-circuitry. The spread of Neurobiotin, which can pass through Innexin junctions, provides indirect evidence for electric coupling among HS- and other cells. Neurobiotin was injected in either HSE (A) or HSN (B) and (C) and visualized with Streptavidin coupled to a red fluorescent dye. Co-staining was detected in: neighboring HS-cells (indicated in (A) to (C)), unidentified ipsilateral descending neurons (open triangle), cells projecting to the contralateral protocerebrum where HS-cell axons terminate (arrowheads in (A) and (C)), contralateral LPTCs (filled arrows in (A) and (C)) and occasionally in unidentified fibers in the same lobula plate (open arrows in (A) and (C)). The figure shows composites of maximum intensity projections of confocal image stacks taken from neighboring regions of the brain. Scale bars 50µm.

When we injected Neurobiotin into either HSN (Fig. 5A, B) or HSE (Fig. 5C), one or both of the remaining HS-cells were typically labeled. In contrast to similar experiments in *Calliphora* (Haag and Borst, 2005), no CH-cells were found to be colabeled. From this observation we conclude that HS-cells in *Drosophila* are directly coupled with each other. Nevertheless, we observed additional staining in fibers other than the three HS-cells in the same lobula plate (Fig. 5A and C). Unfortunately the staining was too weak to enable unequivocal identification of these processes. In these

two cases (Fig. 5A and C) the arborization of an LPTC in the contralateral lobula plate was also labeled that might belong to the unidentified ipsilateral processes mentioned before. This cell represents a possible candidate neuron to provide the contralateral input to HS-cells described above (Fig. 2 and 3). In addition, HS-cells were extensively coupled to descending neurons (Fig. 5A and C) that could not be identified individually. One frequently labeled neuron has a prominent arborization on the contralateral side and probably connects the output region of HS-cells of both hemispheres (arrowhead in Fig. 5A and B). Taken together, HS-cells are at the centre of a complicated network of electrically coupled neurons. This network comprises descending neurons, HS-cells and LPTCs so far unidentified in *Drosophila* from the same and the contralateral hemisphere. The columnar input to the ipsilateral dendrite and the electric coupling to the LPTC network are likely sufficient to explain the entire receptive fields of the HS-cells.

Discussion

Drosophila reacts to horizontally drifting retinal images with compensatory yaw-torque responses thought to stabilize straight flight segments (Heisenberg and Wolf, 1984). The giant HS-cells in the lobula plate are thought to play a key role in the control of this behavior. However, their exact role remains elusive. Patch-clamp recordings in *Drosophila*, an animal that allows for genetic manipulation and behavioral analysis, were only established recently (Wilson et al., 2004) and physiological data from HS-cells were so far not available. We used the Gal4/UAS-system (Brand and Perrimon, 1993) to fluorescently label two of the three HS-cells, HSN and HSE, which allowed for the investigation of their basic anatomy (Fig. 1 and 3) and targeting for reliable recordings from the soma (Fig. 1 - 3); neighboring HSS-cells were recorded without the use of genetic labeling (Fig. 4). Hence, we describe the response characteristics of all three giant neurons of the HS-system in *Drosophila*, their directional selective output, receptive field organization and network interactions.

Basic response properties of *Drosophila* HS-cells.

Concerning their basic response properties, HS-cells in *Drosophila* are largely similar to their counterparts in *Calliphora* (Hausen, 1982a; Hausen, 1982b). They respond to

horizontal motion with graded membrane potential changes in a directional selective way (Fig. 1). Their responses are indicative of input from elementary motion detectors of the correlation-type (Fig. 2). This is suggested by responses being independent of the sign of contrast and by exhibiting a velocity optimum that linearly depends on the spatial wavelength of the moving periodic grating. Such a dependency results in a single temporal frequency optimum and is a characteristic feature of presynaptic computations according to the correlation-type detector model (Reichardt, 1961; Borst and Egelhaaf, 1989). The temporal frequency optimum of 1 Hz (Fig. 2) precisely matches the results from our previous account on *Drosophila* VS-cells (Jösch et al., 2008) and findings from H1-cells in *Calliphora* (Haag et al., 2004). However, recordings from HS-cells in *Calliphora* resulted in slightly higher values of 2 – 5 Hz (Hausen, 1982b), suggesting differences between the two fly species. The quadratic dependence of the response on the contrast predicted by a correlation-type detector model is generally found only in the low contrast range (Buchner, 1984). At higher contrasts, responses saturate probably due to a gain control mechanism (Fig. 2) in elementary motion detectors. However, the cellular implementation of elementary motion detectors is still an open question in the field.

Anatomical layout of HS-cell dendrites and receptive fields.

The image of the environment is represented by retinotopically organized columnar maps in the optic lobes (Strausfeld, 1976; Braitenberg, 1970; Strausfeld, 1984). Within this arrangement, the dendrites of HSN and HSE occupy large, highly constant areas in the lobula plate. However, the overlap of their dendrites is much larger in *Drosophila* (Fig. 2A; Heisenberg et al., 1978) than in *Calliphora* (Hausen, 1982a). Such differences in LPTC- anatomy and number have been described among dipteran flies and were linked to their flight style and behavior (Buschbeck and Strausfeld, 1997; Nordstrom et al., 2008).

The area covered by the dendrites of HSN, HSE and HSS correspond to the centers of large dorsal, equatorial and ventral receptive fields, respectively. Yet, the ipsilateral receptive field, in particular of HSN, exceeds the area occupied by its dendrite in the lobula plate significantly (Fig. 3B). In addition, HSN and HSE are also sensitive to contralateral motion. These receptive fields of HS-cells can be explained by assuming 1) dendritic input from local motion detectors, 2) electric coupling to neighboring HS-

cells and 3) input from contralateral neurons tuned to regressive motion. The evidence for this input organization is discussed below.

(1) Ipsilateral columnar input.

The excitatory and inhibitory responses of HS-cells suggest that *Drosophila* HS-cells inherit their main response characteristics from two specific classes of elementary motion half-detectors with opposite preferred direction (Borst and Egelhaaf, 1990; Borst et al., 1995; Single and Borst, 1998). Further evidence for this scheme comes from the localization of excitatory cholinergic and inhibitory GABAergic synapses on the dendritic tips of VS- and HS-cells in *Drosophila* (Raghu et al., 2007; Raghu et al., 2009) and the simultaneous integration of excitatory and inhibitory input with separate reversal potentials during grating motion (Jösch et al., 2008). Possible input elements might be the bushy T4- and T5-cells (Strausfeld, 1976; Bausenwein and Fischbach, 1992).

The retinotopic arrangement of the detectors is further supported by our finding that HS-cells respond to local motion stimuli with a strong preference for horizontal motion. Moreover, gradual changes in local PD with a bias to upward motion were observed in the dorsofrontal (HSN and HSE) and ventrolateral (HSS) margins of the receptive field (Fig. 4). Sensitivity to vertical motion in parts of the receptive field was also reported for HS-cells in *Calliphora* and was attributed to the arrangement of the ommatidial lattice in the corresponding parts of the eye (Hausen, 1982b). This most likely holds true also for *Drosophila* (Heisenberg and Wolf, 1984). HS-cells in *Drosophila* were not coupled to any of the vertically sensitive LPTCs although connections between HSN and lateral VS-cells (Haag and Borst, 2005) were reported in *Calliphora*. However, in *Calliphora* these connections are supplied via the dCH cell (Haag and Borst, 2007) and CH-cells could not be found in *Drosophila*.

(2) Coupling to neighboring HS-cells.

Direct electric coupling between neighboring HS-cells or via descending neurons is suggested by the spread of Neurobiotin (Fig. 5) and provides the most plausible explanation for the observed broad ipsilateral receptive fields (Fig. 3 and 4). A similar ipsilateral coupling has been found in the VS-cell network in *Drosophila* (Jösch et

al., 2008) and within and between the HS- and VS-system of *Calliphora* (Haag and Borst, 2004; Farrow et al., 2005; Haag and Borst, 2007) where lateral connections are thought to be responsible for the large receptive fields and, hence, the robustness of the response against inhomogeneous contrast distribution in the image (Cuntz et al., 2007). Moreover, HS-cells in *Calliphora* are coupled to each other only indirectly via the dorsal and ventral CH-cell (Haag and Borst, 2002; Cuntz et al., 2003), which receive graded input from HS-cells. In response to large-field motion, CH-cells in turn inhibit so-called figure detection neurons, thereby tuning them to small-field motion (Warzecha et al., 1993; Cuntz et al., 2003; Egelhaaf, 1985; Haag and Borst, 2002). It is unclear how *Drosophila* solves this problem. The fact that CH-cells were never detected in our experiments matches their absence in any of the Gal4 screens and any of the detailed anatomical descriptions reported so far in *Drosophila* (Fischbach and Dittrich, 1989). The weakly stained fibers next to HS-cells (Fig. 5) in the ipsilateral lobula plate could not be identified due to their weak Neurobiotin labeling. The very strong and reliable coupling of HS- and CH-cells in *Calliphora* makes it unlikely that these weakly stained fibers represent processes of *Drosophila* CH-cells. They could rather belong to the heterolateral projecting neurons (see below).

(3) Input from neurons with contralateral receptive fields.

In addition to two sources of ipsilateral input, we find sensitivity to contralateral back-to-front motion in HSN and HSE (contralateral sensitivity of HSS was not systematically analyzed). The heterolateral projecting LPTCs detected in the Neurobiotin injection (Fig. 4A and C) are good candidates to provide this input. They might correspond to either H1 or H2, two heterolateral spiking neurons that provide input to HS-cells in *Calliphora* (Haag and Borst, 2001; Hausen, 1982a; Hausen, 1982b; Horstmann et al., 2000). Both cells have their dendrites in the contralateral lobula plate where they respond to back-to-front motion with an increase in spike frequency. The axonal arborization of H1 is in the contralateral lobula plate. H2 axons project to the output region of HS-cells in the contralateral protocerebrum where they build electric contacts with HS-cells. Due to the many other labeled cells and relatively weak labeling of the heterolateral neurons we could not determine if Neurobiotin labeled H1, H2 or even both.

Behavioral relevance

HS-cells are supposed to be key-players for the control of optomotor turning responses elicited by horizontal motion. This notion is mostly based on the observation that electrical responses of HS-cells in *Calliphora* and optomotor torque responses in *Musca* and *Drosophila* show a similar dependence on spatial features of moving visual stimuli (Götz and Buchner, 1978; Hausen, 1982a; Hausen, 1982b; Reichardt and Egelhaaf, 1988; Hausen and Wehrhahn, 1989). In addition, elimination of the HS-system in *Musca* by laser ablation (Geiger and Nässel, 1981) and the *omb* mutation (largely missing HS-cells and many other LPTCs and columnar neurons absent) in *Drosophila* (*omb*, Heisenberg et al., 1978) lead to severe deficits in the execution of yaw optomotor responses.

We found that HS-cells in *Drosophila* are similarly tuned to binocular rotational motion around the vertical body axis (Fig. 3). Their responses exhibit a similar dependency on features of the stimulus as optomotor yaw-torque responses, in particular a temporal frequency optimum of about 1 Hz (Fig. 2A and B; Götz, 1964; Buchner, 1984). Thus, our experiments corroborate their functional contribution to compensatory turning behavior. This consent, however, is somewhat questioned by recently published behavioral experiments that report an optimum response between 5 and 10 Hz (Duistermars et al., 2007; Fry et al., 2009). At this frequency, however, HS-cell responses (Fig. 2) and previously measured yaw-torque (Götz, 1964) were reduced to less than half of the maximal response. It remains speculative if this discrepancy can be attributed to differences in the stimulus presentation.

Further measurements are required to investigate if HS-cells in *Drosophila* also encode information about the structure of the visual surround during translational motion, as is suggested from experiments in blowflies (Boeddeker and Egelhaaf, 2005; Kern et al., 2005). Also, lateral expansion stimuli need to be analyzed as they were reported to elicit larger optomotor responses than rotational ones (Tammero et al., 2004; Duistermars et al., 2007). In summary, HS-cell output very likely feeds into multisensory neural circuits that control different behaviors of the fly (Frye and Dickinson, 2001; Frye and Dickinson, 2004).

Concluding remarks

HS-cells in *Drosophila* and large dipteran flies have largely similar response properties indicative of a correlation-type motion detector model. However, we describe substantial differences in the organization of the neural circuitry for the detection of horizontal optic flow. The overlap and relative size of ipsilateral HS-cell dendrites is larger in *Drosophila*. CH-cells, that link the HS- and VS-system in *Calliphora* and that are key elements of a circuitry dedicated to the detection of small moving objects, were not found in *Drosophila*. In addition, *Drosophila* HS-cells exhibit a lower temporal frequency optimum than their counterparts in *Calliphora*. These differences might reflect adaptations to different lifestyles, as the basic response properties of large-field motion-sensitive neurons seem to match differences in flight style (O'Carroll et al., 1996). Our functional and anatomical characterization of the HS-cell circuitry in *Drosophila* can now serve to dissect (a) the presynaptic motion detection circuitry and (b) the exquisite control mechanism of compensatory optomotor responses by combining genetic manipulation of neuronal function with physiological recording and behavioral analysis.

Acknowledgements

We greatly thank Wolfgang Essbauer, Christian Theile and the MPI workshop for excellent technical support, Johannes Plett for the design of the LED arena, Robert Schorner for artwork, and Juergen Haag, Erich Buchner as well as the other members of the Borst department for discussion. This work was supported by the Max-Planck-Society, and by an HFSP grant to K. Ito, A. Borst and B. Nelson.

Reference List

- Bausenwein B, Fischbach K-F (1992) Activity labeling patterns in the medulla of *Drosophila melanogaster* caused by motion stimuli. *Cell Tissue Res* 270: 25-35.
- Boeddeker N, Egelhaaf M (2005) A single control system for smooth and saccade-like pursuit in blowflies. *Journal of experimental biology* 208: 1563-1572.
- Borst A, Egelhaaf M (1989) Principles of visual motion detection. *Trends Neurosci* 12: 297-306.
- Borst A, Egelhaaf M (1990) Direction selectivity of fly motion-sensitive neurons is computed in a two-stage process. *Proc Natl Acad Sci USA* 87: 9363-9367.

- Borst A, Egelhaaf M, Haag J (1995) Mechanisms of dendritic integration underlying gain control in fly motion-sensitive interneurons. *J Computat Neurosci* 2: 5-18.
- Borst A, Haag J (2002) Neural networks in the cockpit of the fly. *J Comp Physiol A Neuroethol Sens Neural Behav Physiol* 188: 419-437.
- Braitenberg V (1970) Ordnung und Orientierung der Elemente im Sehsystem der Fliege. *Kybernetik* 7: 235-242.
- Brand AH, Perrimon N (1993) Targeted gene expression as a means of altering cell fates and generating dominant phenotypes. *Development* 118: 401-15.
- Buchner E (1984) Behavioural analysis of spatial vision in insects. In: *Photoreception and vision in invertebrates* (Ali MA, ed), pp 561-621. New York, London: Plenum Press.
- Buschbeck EK, Strausfeld NJ (1997) The relevance of neural architecture to visual performance: phylogenetic conservation and variation in dipteran visual systems. *J Comp Neurol* 383: 282-304.
- Chan WP, Prete F, Dickinson MH (1998) Visual input to the efferent control system of a fly's "gyroscope". *Sci* 280: 289-292.
- Cuntz H, Forstner F, Haag J, Borst A (2008) The morphological identity of insect dendrites. *PLoS Comput Biol* 4: e1000251.
- Cuntz H, Haag J, Borst A (2003) Neural image processing by dendritic networks. *Proc Natl Acad Sci U S A* 100: 11082-11085.
- Cuntz H, Haag J, Forstner F, Segev I, Borst A (2007) Robust coding of flow-field parameters by axo-axonal gap junctions between fly visual interneurons. *Proc Natl Acad Sci U S A* 104: 10229-10233.
- Duistermars BJ, Chow DM, Condro M, Frye MA (2007) The spatial, temporal and contrast properties of expansion and rotation flight optomotor responses in *Drosophila*. *J Exp Biol* 210: 3218-3227.
- Eckert H, Meller K (1981) Synaptic structures of identified, motion-sensitive interneurons in the brain of the fly, *Phaenicia*. *Verh Dtsch Zool Ges* 1981: 179.
- Egelhaaf M (1985) On the neuronal basis of figure-ground discrimination by relative motion in the visual system of the fly. II. Figure-Detection Cells, a new class of visual interneurons. *Biol Cybern* 52: 195-209.
- Egelhaaf M, Boddeker N, Kern R, Kretzberg J, Lindemann JP, Warzecha AK (2003) Visually guided orientation in flies: case studies in computational neuroethology. *J Comp Physiol A Neuroethol Sens Neural Behav Physiol* 189: 401-409.
- Elyada YM, Haag J, Borst A (2009) Different receptive fields in axons and dendrites underlie robust coding in motion-sensitive neurons. *Nat Neurosci* 12: 327-332.
- Farrow K, Borst A, Haag J (2005) Sharing receptive fields with your neighbors: tuning the vertical system cells to wide field motion. *J Neurosci* 25: 3985-3993.
- Farrow K, Haag J, Borst A (2006) Nonlinear, binocular interactions underlying flow field selectivity of a motion-sensitive neuron. *Nat Neurosci* 9: 1312-1320.
- Fischbach KF, Dittrich APM (1989) The optic lobe of *Drosophila melanogaster*. I. A Golgi analysis of wild-type structure. *Cell Tissue Res* 258: 441-475.
- Fry SN, Rohrseitz N, Straw AD, Dickinson MH (2009) Visual control of flight speed in *Drosophila melanogaster*. *J Exp Biol* 212: 1120-1130.
- Frye MA, Dickinson MH (2001) Fly flight: a model for the neural control of complex behavior. *neuron* 32: 385-388.
- Frye MA, Dickinson MH (2004) Closing the loop between neurobiology and flight behavior in *Drosophila*. *Curr Opin Neurobiol* 14: 729-736.
- Geiger G, Nässel DR (1981) Visual orientation behaviour of flies after selective laser beam ablation of interneurons. *Nature* 293: 398-399.
- Gilbert C, Gronenberg W, Strausfeld NJ (1995) Oculomotor control in calliphorid flies: head movements during activation and inhibition of neck motor neurons corroborate neuroanatomical predictions. *J Comp Neurol* 361: 285-297.
- Götz KG (1964) Optomotorische Untersuchungen des visuellen Systems einiger Augenmutanten der Fruchtfliege *Drosophila*. *Kybernetik* 2: 77-92.

- Götz KG (1965) Die optischen Übertragungseigenschaften der Komplexaugen von *Drosophila*. *Kybernetik* 2: 215-221.
- Götz KG, Buchner E (1978) Evidence for one-way movement detection in the visual system of *Drosophila*. *Biol Cybern* 31: 243-248.
- Gronenberg W, Strausfeld NJ (1990) Descending neurons supplying the neck and flight motor of diptera: Physiological and anatomical characteristics. *J Comp Neurol* 302: 973-991.
- Haag J, Borst A (2001) Recurrent network interactions underlying flow-field selectivity of visual interneurons. *J Neurosci* 21: 5685-5692.
- Haag J, Borst A (2002) Dendro-dendritic interactions between motion-sensitive large-field neurons in the fly. *J Neurosci* 22: 3227-3233.
- Haag J, Borst A (2004) Neural mechanism underlying complex receptive field properties of motion-sensitive interneurons. *Nat Neurosci* 7: 628-634.
- Haag J, Borst A (2005) Dye-coupling visualizes networks of large-field motion-sensitive neurons in the fly. *J Comp Physiol A Neuroethol Sens Neural Behav Physiol* 191: 445-454.
- Haag J, Borst A (2007) Reciprocal inhibitory connections within a neural network for rotational optic-flow processing. *Front Neurosci* 1: 111-121.
- Haag J, Borst A (2008) Electrical coupling of lobula plate tangential cells to a heterolateral motion-sensitive neuron in the fly. *J Neurosci* 28: 14435-14442.
- Haag J, Denk W, Borst A (2004) Fly motion vision is based on Reichardt detectors regardless of the signal-to-noise ratio. *Proc Natl Acad Sci U S A* 101: 16333-16338.
- Haag J, Wertz A, Borst A (2007) Integration of lobula plate output signals by DNOVS1, an identified premotor descending neuron. *J Neurosci* 27: 1992-2000.
- Hausen K (1982a) Motion sensitive interneurons in the optomotor system of the fly. I. The Horizontal Cells: Structure and signals. *Biol Cybern* 45: 143-156.
- Hausen K (1982b) Motion sensitive interneurons in the optomotor system of the fly. II. The Horizontal Cells: Receptive field organization and response characteristics. *Biol Cybern* 46: 67-79.
- Hausen K, Wehrhahn C (1989) Neural circuits mediating visual flight control in flies. I. Quantitative comparison of neural and behavioral response characteristics. *J Neurosci* 9: 3828-3836.
- HEISENBERG M (1972) Comparative Behavioral Studies on 2 Visual Mutants of *Drosophila*. *J Comp Physiol* 80: 119-8.
- Heisenberg M, Buchner E (1977) The role of retinula cell types in visual behavior of *Drosophila melanogaster*. *J Comp Physiol* 117: 127-162.
- Heisenberg M, Wolf R (1984) *Vision in Drosophila*. Berlin, Heidelberg, New York, Tokyo: Springer.
- Heisenberg M, Wonneberger R, Wolf R (1978) Optomotor-blind (H31) -a *Drosophila* mutant of the lobula plate giant neurons. *J Comp Physiol* 124: 287-296.
- Hengstenberg R, Hausen K, Hengstenberg B (1982) The number and structure of giant vertical cells (VS) in the lobula plate of the blowfly *Calliphora erythrocephala*. *J Comp Physiol A* 149: 163-177.
- Horstmann W, Egelhaaf M, Warzecha AK (2000) Synaptic interaction increase optic flow specificity. *Eur J Neurosci*: 2157-2165.
- Jösch M, Plett J, Borst A, Reiff DF (2008) Response properties of motion-sensitive visual interneurons in the lobula plate of *Drosophila melanogaster*. *Current Biology* 18: 1-7.
- Katsov AY, Clandinin TR (2008) Motion processing streams in *Drosophila* are behaviorally specialized. *neuron* 59: 322-335.
- Kern R, van Hateren JH, Michaelis C, Lindemann JP, Egelhaaf M (2005) Function of a fly motion-sensitive neuron matches eye movements during free flight. *PLoS Biol* 3: e171.
- Krapp HG, Hengstenberg B, Hengstenberg R (1998) Dendritic structure and receptive-field organization of optic flow processing interneurons in the fly. *J Neurophysiol* 79: 1902-1917.
- Krapp HG, Hengstenberg R, Egelhaaf M (2001) Binocular contributions to optic flow processing in the fly visual system. *J Neurophysiol* 85: 724-734.

- Mronz M, Lehmann FO (2008) The free-flight response of *Drosophila* to motion of the visual environment. *J Exp Biol* 211: 2026-2045.
- Nordstroem K, Barnett PD, Moyer DM, I, Brinkworth RS, O'Carroll DC (2008) Sexual dimorphism in the hoverfly motion vision pathway. *Curr Biol* 18: 661-667.
- O'Carroll D, Bidwell NJ, Laughlin SB, Warrant EJ (1996) Insect motion detectors matched to visual ecology. *Nature* 382: 63-66.
- Raghu SV, Jösch M, Borst A, Reiff DF (2007) Synaptic organization of lobula plate tangential cells in *Drosophila*: gamma-aminobutyric acid receptors and chemical release sites. *J Comp Neurol* 502: 598-610.
- Raghu SV, Jösch M, Sigrist SJ, Borst A, Reiff DF (2009) Synaptic Organization of Lobula Plate Tangential Cells in *Drosophila*: $\alpha 7$ Cholinergic Receptors. *J Neurogenet* DOI: 10.1080/01677060802471684.
- Reichardt W (1961) Autocorrelation, a principle for the evaluation of sensory information by the central nervous system. In: *Sensory Communication* (Rosenblith WA, ed), pp 303-317. New York, London: The M.I.T. Press and John Wiley & Sons.
- Reichardt W, Egelhaaf M (1988) Properties of individual movement detectors as derived from behavioural experiments on the visual system of the fly. *Biol Cybern* 58: 287-294.
- Rister J, Pauls D, Schnell B, Ting CY, Lee CH, Sinakevitch I, Morante J, Strausfeld NJ, Ito K, Heisenberg M (2007) Dissection of the peripheral motion channel in the visual system of *Drosophila melanogaster*. *neuron* 56: 155-170.
- Scott EK, Raabe T, Luo LQ (2002) Structure of the vertical and horizontal system neurons of the lobula plate in *Drosophila*. *Journal of Comparative Neurology* 454: 470-481.
- Single S, Borst A (1998) Dendritic integration and its role in computing image velocity. *Sci* 281: 1848-1850.
- Single S, Haag J, Borst A (1997) Dendritic computation of direction selectivity and gain control in visual interneurons. *J Neurosci* 17: 6023-6030.
- Strausfeld NJ (1976) *Atlas of an insect brain*. Berlin, Heidelberg: Springer.
- Strausfeld NJ (1984) Functional neuroanatomy of the blowfly's visual system. In: *Photoreception and vision in invertebrates* (Ali MA, ed), pp 483-522. Plenum Publishing Corporation.
- Tammero LF, Frye MA, Dickinson MH (2004) Spatial organization of visuomotor reflexes in *Drosophila*. *J Exp Biol* 207: 113-122.
- Warzecha AK, Egelhaaf M, Borst A (1993) Neural circuit tuning fly visual interneurons to motion of small objects. I. Dissection of the circuit by pharmacological and photoinactivation techniques. *J Neurophysiol* 69: 329-339.
- Wilson RI, Laurent G (2005) Role of GABAergic inhibition in shaping odor-evoked spatiotemporal patterns in the *Drosophila* antennal lobe. *J Neurosci* 25: 9069-9079.
- Wilson RI, Turner GC, Laurent G (2004) Transformation of olfactory representations in the *Drosophila* antennal lobe. *Science* 303: 366-70.
- Zhu Y, Nern A, Zipursky SL, Frye MA (2009) Peripheral visual circuits functionally segregate motion and phototaxis behaviors in the fly. *Curr Biol* 19: 613-619.

7 Manuscript Nr.5

Contribution of different lamina cells to the fly motion detection circuitry

This chapter will be submitted within the next few weeks by Maximilian Jösch, Shamprasad Varija Raghu, Dierk F. Reiff & Alexander Borst.

MPI for Neurobiology

Dept. of Systems and Computational Neurobiology

Martinsried, Germany

Maximilian Jösch performed the electrophysiological experiments and analyzed the data. Shamprasad Varija Raghu performed the anatomical analysis. Maximilian Jösch, Dierk Reiff and Alexander Borst conceived experiments. Maximilian Jösch wrote the manuscript.



Abstract

Motion vision is a major function of all visual systems, yet the underlying neural mechanisms and circuitries are still elusive. In the fruit fly *Drosophila melanogaster* photoreceptor signals from R1-6 split into parallel pathways in the first optic neuropile, the lamina¹. Lamina cells are known not to be directionally selective², whereas a few synapses downstream in the lobula plate, a group of large field neurons respond to visual motion in a directionally selective way³. In between, direction selectivity is being computed by an unknown network of elementary motion detectors. In order to address the cellular implementation of the circuitry computing directional selectivity, we performed whole cell recordings from lobula plate neurons in flies where we disrupted the chemical output from lamina cells L1 and L2. When presenting a grating drifting either horizontally or vertically, we found that the motion response was reduced strongly by blocking L1, and moderately by blocking L2. Interestingly, when using a drifting Off-edge (bright-to-dark transition) instead of a grating, the response was completely abolished when either L1 or L2 was blocked. Thus, both L1- and L2-cells seem to be necessary for the detection of moving Off-edges arguing for an interaction between these cells in order to provide the signal specific for brightness decrease. Our results support a segregation of luminance information into On- and Off-pathways prior to motion computation, as postulated in a cellular model of elementary motion detection, the 'four quadrant multiplier'⁴.

Manuscript

Directional selective cells are found in a vast number of animals and brain regions, ranging from the retina of rabbits⁵ to the visual cortex of macaque⁶. The responses of these cells can serve different tasks like object detection based on relative motion, as well as orientation and course control based on optic flow analysis⁷. In flies, such motion-sensitive neurons, the lobula plate tangential cells, are found in the caudal part of the third neuropile of the optic lobe, the lobula plate³. Their characteristic morphology and response properties have made them an excellent model system for the study of motion processing⁷. Lobula plate tangential cells have been demonstrated to receive input from an array of local motion detectors of the Reichardt-type^{8,9}. In its minimal form, one Reichardt detector consists of two mirror-symmetrical subunits both receiving input from the same two neighboring photoreceptors. In each subunit, the luminance level derived from one photoreceptor is low-pass filtered and becomes subsequently multiplied with the instantaneous signal derived from the neighboring photoreceptor. The results of both multipliers are then subtracted giving rise to a fully directional output signal. Despite the precise specifications of the computational steps of motion detection, the neural mechanisms and circuitry presynaptic to the lobula plate tangential cells have escaped so far from a detailed analysis. This is due to the small size of the constituting neurons and the high complexity of their neural architecture. We set out to elucidate the cellular implementation starting from the most outer neuropile, the lamina. For this purpose, we combined electrophysiological recordings of lobula plate tangential cells with genetic intervention of presynaptic elements (Fig 1 a&b).

Each lamina cartridge comprises five different monopolar cells, two centrifugal cells and one T1 cell (Fig. 1c). In this study we focused on lamina cells L1, L2 and L4, speculated to be the main input elements for motion vision¹⁰⁻¹³. We used several enhancer-lines with distinct expression in different populations of lamina monopolar cells (Fig 1d). One line had targeted expression in L1 (Split-Glu), three lines in L2 (Split-Cha; *ort^{C3}-Gal4*; 21-D), one line in L1, L2 and L3 (*ort^{C2}-Gal4*) and one line in L4 (*Ln-Gal4*). Unfortunately, the expression pattern in the optic lobes of these enhancer lines also included other medullar cell populations (Fig. 1d), a fact that has to be kept in mind for further interpretations. To monitor the effects of the genetic manipulation of targeted populations of first-order interneurons, we focused on two previously

characterized groups of lobula plate tangential cells, the VS- (Vertical Sensitive)⁹ and

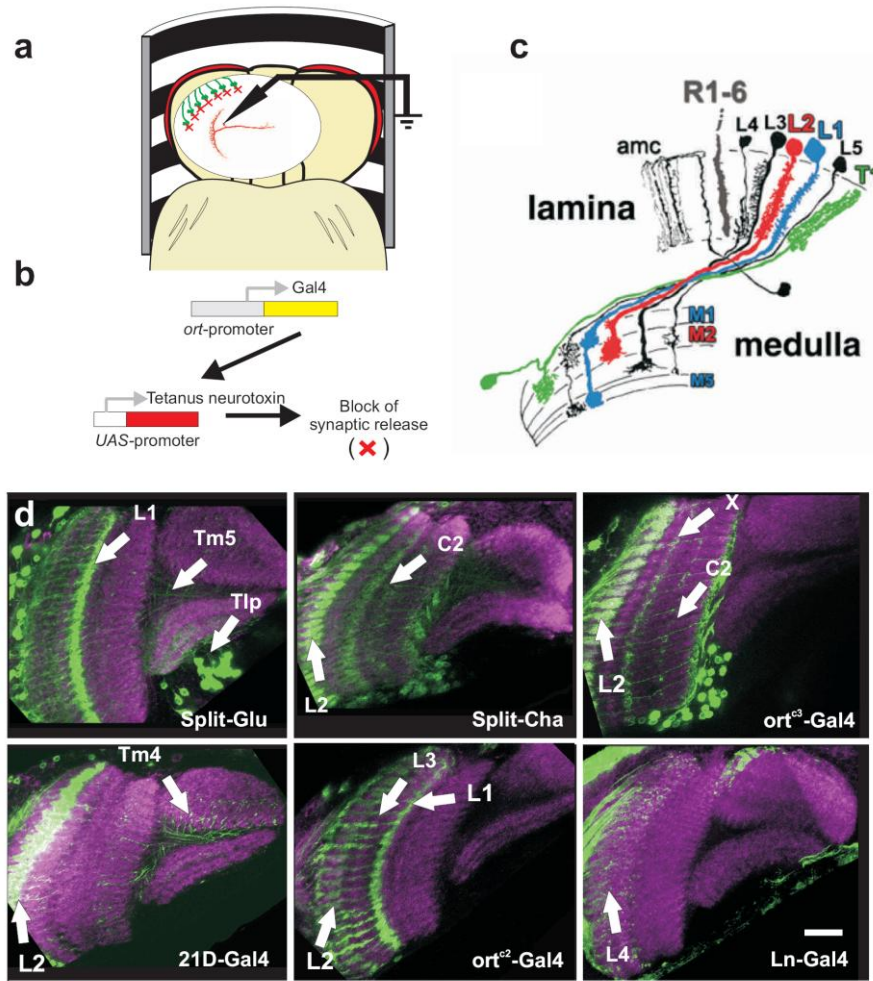


Fig. 1. Combined electrophysiological and neurogenetic approach. (a) Schematic drawing of a fly preparation, including visual stimulus device. A recording electrode is pointing towards a red dye-filled VS cell. A tetanus neurotoxin block of synaptic release in a population of lamina cells (represented by the green neuronal terminals) is shown by red crosses (b) The Gal4/UAS system is used to express TNT under enhancement of e.g. the *ort*-promoter region. (c) Schematic drawing of different laminar cell populations (taken from¹⁰). (d) GFP expression pattern in the optic lobes of the different Gal4 lines used in this study. Specified layers are visible in the medulla, representing the output regions of different lamina cells. Note the expression of other neuronal populations. X denotes an unidentified cell type (Scale bar 10 μ m).

HS-cells (Horizontal Sensitive)¹⁴. *Drosophila's* VS- and HS-cells are two morphologically defined groups of cells preferentially sensitive to vertical and horizontal motion, respectively. Exceptionally, VS5 and specially VS6 are tuned to rotational flow fields with their center of rotation at around 25 ° and 50 ° azimuth (Suppl. Fig 1). Their main response mode is to be excited by motion stimuli in their preferred direction (PD) by a graded depolarization of their membrane potential superimposed with spikelets.

Motion stimuli in the opposite direction (null direction, 'ND') elicit a graded hyperpolarization^{9,14} (Fig. 2a). While recording from VS- and HS-cell we took advantage of the Gal4/UAS system¹⁵ to specifically disrupt the input elements through directed tetanus neurotoxin light chain (TNT)¹⁶ expression (Fig 1c). TNT cleaves synaptobrevin suppressing vesicle release and thus silencing chemical synapses irreversible (Fig 1b&c). To optimize the parameters needed to disrupt synaptic release via TNT we characterized the block of photoreceptors and lamina monopolar cell output (Supp. Material, Supp. Fig. 2). We observed a dramatic change in the effectiveness depending on the temperature in which the flies were reared (Sup. Fig. 2). These results contradict the idea that different kinds of neuronal specific synaptobrevins, a TNT cleavable and a non-cleavable one, are localized in different populations of neurons in *Drosophila*¹⁷ and rather argue for a temperature depended ubiquitous neuronal block via TNT (Supp. Material).

We next analyzed the role of each input channel to motion processing. In a first series of experiments, we used a moving sine grating to stimulate the cells ($\lambda = 22^\circ$, temporal frequency = 1 Hz, mean luminance = 4 cd / m²). Blocking L1 strongly reduced the grating response, both for motion in the preferred as well as in the null direction (Fig 3a, left; Fig. 3b). Blocking L2 induced a more subtle effect. When the output of L2 was disrupted with the Split-Cha line, a moderate reduction in the response sensitivity could be seen at all contrast levels (Fig. 3a, second from left; Fig. 3b). When using the *ort*^{C3} line a subtle effect was visible only at low contrast levels (Fig. 3a, third from left; Fig. 3b). However, disrupting L2 via the 21D-line showed no significant effect (Supp. Fig 3). These flies (21D→UAS-TNT) had to be raised at a permissive temperature of 25 °C (Supp. Material). At this temperature a decrease of the TNT efficacy is expected and thus can explain the lack of any effect. We further investigated the input channels for motion detection by blocking the group of lamina monopolar cells L1, L2 and L3 with the *ort*^{C2}-Gal4 line (Fig 1d). These flies showed an almost 100% block of motion responses in lobula plate tangential cells, even at the highest pattern contrast (Fig. 3a, right; Fig 3b). To further constrain the analysis of the input elements we tried to block L1 and L2 specifically, taking advantage of lines previously used in behavioral studies^{10,18}. Unexpectedly, the most specific laminar cell enhancer lines were lethal when combined with TNT at the optimal block temperature (Supp. Table 1), making further analysis impossible. We suspect that this lethality is

due to an optic lobe unspecific expression pattern in other tissue. Interestingly, we also

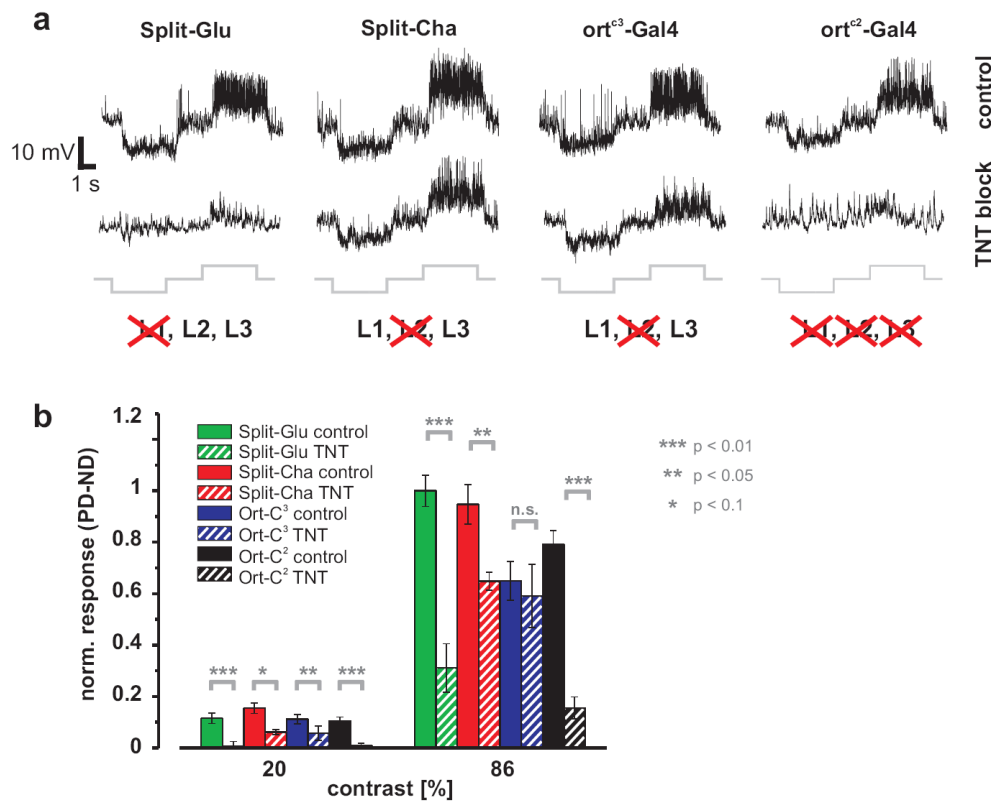


Fig. 3. Contrast dependency. (a) Recorded membrane potentials of different VS cells recorded in the specified genotypes. Responses to a large field sine-grating ($\lambda = 22^\circ$, $v = 22^\circ/s$). The top traces are the control flies; the bottom traces the experimental flies. Grating motion is represented by the bottom grey lines. (b) Normalized mean responses (PD-ND) of all analyzed fly genotypes. (Split-Cha: exp. flies $n = 19$; control flies $n = 6$; *ort^{C3}*: exp. $n = 7$; control $n = 7$; Split-Glu: exp. $n = 8$; control $n = 6$.)

noticed that *ort^{C2}*-Gal4 flies combined with TNT showed wild type responses if recorded directly after hatching (data not shown). This is indicative for a late expression start of the *ort*-promoter and points out that the effects described are not due to developmental defects induced by TNT¹⁷, but rather to a synaptic block of the specified lamina monopolar cell types tested.

A grating stimulus is composed of many simultaneously moving dark-to-bright (On-edge) and bright-to-dark transitions (Off-edge; Fig. 3a). We therefore investigated if the lamina monopolar cells might be involved in the analysis of either one of those motion inputs. We found that by blocking either L1 or L2, VS- and HS-cells revealed a strong reduction to motion sensitivity towards On-edge motion (Fig 3b). These results are in line with the reduction of the contrast dependencies to moving grating (Fig 2b). Most interestingly, motion responses to Off-edge stimuli were completely abolished in

the L1- and two L2-lines tested (Fig 3b). These findings demonstrate that both L1

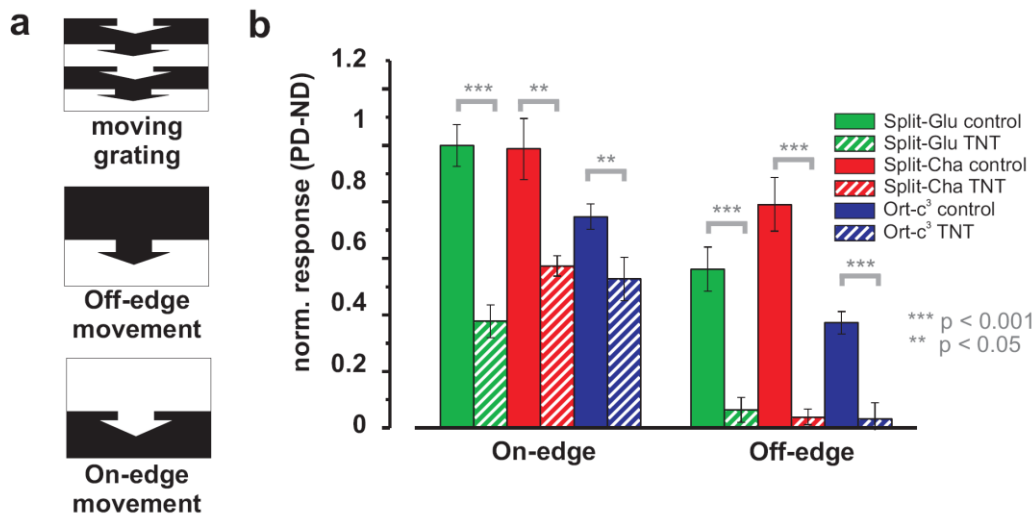


Fig. 3. On- and Off-edge motion detection. (a) Schematic example of the stimulus used. A grating, a dark edge (Off-edge) and a bright edge (On-edge) are moving downwards. (b) Normalized mean responses of truly directional stimuli (PD-ND stimuli) of to either a moving on- or off-edge stimuli (Split-Cha control n = 7, Split-Cha x TNT n = 23, ort^{c3} control n = 7, ort^{c3} x TNT n = 6, Split-Glu control n = 7, Split-Glu x TNT n = 11)

and L2 cells are necessary for the detection of Off-motion, suggesting a possible interaction between the two cells. In concordance with these findings, we could also measure a statistically significant reduction to Off-edge motion responses using the third L2 Line (21D; Suppl. Fig 4a&b). Our data indicate that at 25 °C, the combination of 21D-Gal4 and TNT could only elicit a partial block of the L2 synapses, resulting in an incomplete block of the Off-responses. Interestingly, if the experimental flies were raised at room temperature, no reduction in their Off-responses to moving gratings could be seen (Suppl. Fig. 4a, striped bar), supporting the notion of a temperature sensitive block.

Finally, we tested the possible involvement of the laminar neuron L4 that had been speculated to be specialized in front-to-back motion processing¹³. A recent behavioral study found, using cell specific TNT expression, that flies in which L4 cells were blocked using the Ln-Gal4 line, completely lose optomotor responses but retain wild-type phototactic behavior¹⁸. In line with these results, we found that motion responses in VS and HS cells were completely abolished (Fig 4a). The conspicuous absence of any light responses let us perform ERG experiment to see if the transmission from photoreceptors to laminar monopolar cells was affected. At stimulation frequencies equal to the temporal frequency of maximal motion responses, i.e. 1 Hz, the lamina transients were

undetectable (Fig 4b). This suggests a strong block of photoreceptor's output. We therefore carefully reexamined the expression pattern and found expression in the photoreceptors (Fig 4c). This shows that the absence of motion vision (Fig. 4a) is due to a disruption at the photoreceptor output synapse and not due to the specific contribution of L4 to motion processing.

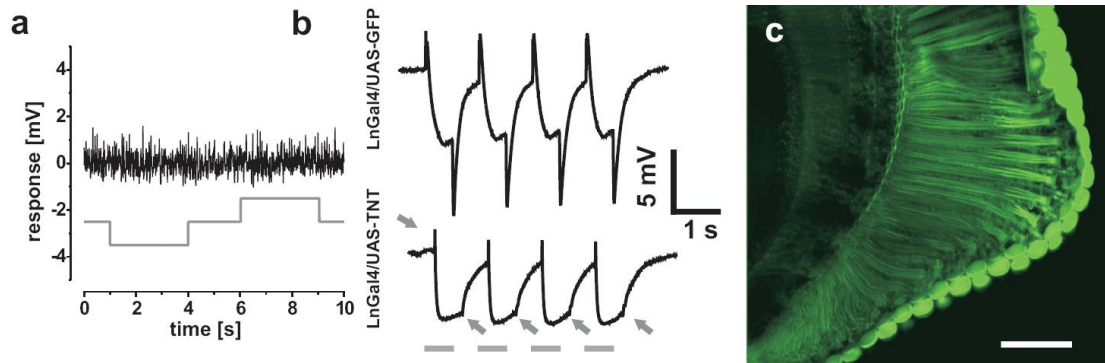


Fig. 4. TNT expression under the Ln-Gal4 line disrupts photoreceptor output. (a) Mean motion responses to vertical sine grating of Ln-G114 → TNT flies (n=10; grating motion is represented by the bottom grey line). (b) ERG of flashes presented at the same temporal frequency as the motion stimuli (1 Hz). Representative responses of control (upper traces) and experimental (lower traces) flies. A complete ablation, especially of the light off lamina peaks are observed (see arrows). (c) Ln-Gal4 expression pattern in the flies' retina (Ln-Gal4 → UAS-GFP). The photoreceptor boundaries of each Ommatidium of R1-6 can be clearly distinguished.

Based on anatomical studies, two pathways were proposed to be involved in motion processing^{11,12}. The first uses L1 and the second L2 to feed information into the motion detection circuitry. Several behavioral studies have approached this question with different neurogenetic approaches^{10,18,19}. The results of these studies have been contradictory proposing different roles for the pathways mentioned above. Our experimental results show that the simultaneous block of L1, L2 & L3 completely abolishes motion sensitive responses in lobula plate tangential cells, indicating that these cells provide input to the motion detection circuitry. Therefore we suggest that the absence of any optomotor effect measured in a previous behavioral study¹⁸ was due to suboptimal experimental constraints, since these flies were kept at room temperature. In addition, the main conclusion presented by another behavioral study¹⁰ says that at intermediate contrast L1 and L2 mediate motion vision in opposite directions: the L1 pathway mediates front-to-back and the L2 pathway back-to-front motion. In our L1 or L2 blocking experiments the response of VS- and HS-cells to moving gratings only showed reduced contrast sensitivity. Therefore, our findings are

not in accordance that L1 and L2 mediate opposing unidirectional motion detection. Taken together, behavioral responses are the result of motion processing and a wide range of additional computations. In contrast, the direct measurement of the VS- and HS-cell responses primarily represents the output of the motion processing circuitry and consequently allows a more precise description of the motion sensitive inputs. We speculate that the complexity of behavior superimposed with the unspecific expression patterns of the mentioned Gal4 lines outside the optic lobes are the main causes for differences between our results and previous behavioral studies.

Finally, our data suggest a segregation of motion pathways that are involved in the detection of moving patterns with either increase (On) or decrease (Off) luminance (Fig 4b). In this respect, an electrophysiological study performed in the fly *Calliphora vicina* has shown that adjacent luminance steps of opposing polarity interact producing a motion sensitive response²⁰. This data is indicative for the absence of previously suggested separate Reichardt detectors specialized in On- and Off-motion detection²¹, since a clear interaction of On- and Off-stimuli was measured. These results led to the hypothesis that the luminance polarity transmitted by each arm of the Reichardt detector is conserved and being further processed by a sign-correct multiplication²⁰. If this interaction is accomplished by a synaptic interaction between two neurons, a postsynaptic signal should be enhanced when both presynaptic inputs either simultaneously increase (On) or decrease (Off). To the best of our knowledge, no corresponding synaptic mechanism has ever been described to accomplish this. However, if the brightness increments or decrements are represented in separate On- and Off-channels, each one carrying positive signals only, the synaptic mechanism underlying such an interaction is less complex, only requiring a supralinear input-output relationship. To fully mimic a sign-corrected multiplication, four subunits take care of all possible combinations between the On- and Off- input channels ('Four quadrant multiplier⁴'). Our results are in line with such a four quadrant multiplication model, giving the first experimental indication for the input implementation to the motion detection circuitry. The future understanding of this implementation and the subsequent processing of the signals in the medulla will be key for the complete cellular description of motion processing in flies.

Materials

Flies.

Flies were raised on standard cornmeal-agar medium at a 12 h light / 12 h dark cycle, 25°C and 60 % humidity. We used female experimental flies, one day post-eclosion. For the TNT Experiments, flies were raised at a 12 h light / 12 h dark cycle at 29°C. The *ortC2-Gal4*, *ortC3-Gal4*, *ortC1-3-GAL4AD*; + ; *cha-Gal4DBD* (denoted as Split-Cha) and *vGlut-dVP16AD/CyO*; *ortC2-Gal4DBD/TM3* (denoted as Split-Glu) lines were kindly provided by Chi-Hon Lee²². The *c202-Gal4*, *21D-Gal4* and *6298-Gal4* lines were kindly provided by J. Rister¹⁰. *Ln-Gal4* was kindly provided by M. Fry¹⁸. The *Rh1-Gal4* lines were obtained from Bloomington Stock center (Stock Nr. 8688 and 8691).

Preparation.

Flies were anesthetized on ice and waxed on a Plexiglas holder using bee wax. The dissection of the cuticula and exposure of the brain lobula plate was performed as in⁹. A ringer-filled cleaning electrode (tip ~ 4 µm) was used to remove the extra cellular matrix and to expose the LPTC somata for recording, which were recognized by their permanent location next to a prominent tracheal branch.

Whole cell recording.

VS- and HS-cell somata covered by ringer solution²³ were approached with a patch electrode filled with a red fluorescent dye (intracellular solution as in⁹). Recordings were established under visual control using a 40X water immersion objective (LumplanF, Olympus), a Zeiss Microscope (Axiotech vario 100, Zeiss, Oberkochen, Germany), illumination (100 W fluorescence lamp, hot mirror, neutral density filter OD 0.3; all from Zeiss, Germany). To enhance tissue contrast, we used two polarization filters, one located as an excitation filter and the other as an emission filter, with slight deviation on their polarization plane. For eye protection, we additionally used a 420 nm LP filter on the light path. For further details of the setup, see⁹.

Electroretinogram

Female flies were briefly anesthetized by cooling and were then attached to a holder with wax, which was also used to immobilize head and legs. ERGs were obtained by placing an indifferent (reference) glass microelectrode in the thorax and a recording

glass microelectrode just beneath the cornea of the stimulated eye. Both were filled with *Drosophila* Ringer's solution. Recordings were performed at room temperature. As stimulus device we used the LED arena with either all panels off or all on at maximal intensity.

Confocal microscopy.

Serial optical sections were taken from recorded VS-cells in the intact preparation using a Leica confocal microscope (TCSNT, Leica) and a 40X water-immersion objective (LUMPlanF, Olympus). Images were taken at 1 μm intervals and 1024 x 1024 pixel resolution. Size, contrast and brightness of the resulting image stacks were adjusted using ImageJ (<http://rsb.info.nih.gov/ij>).

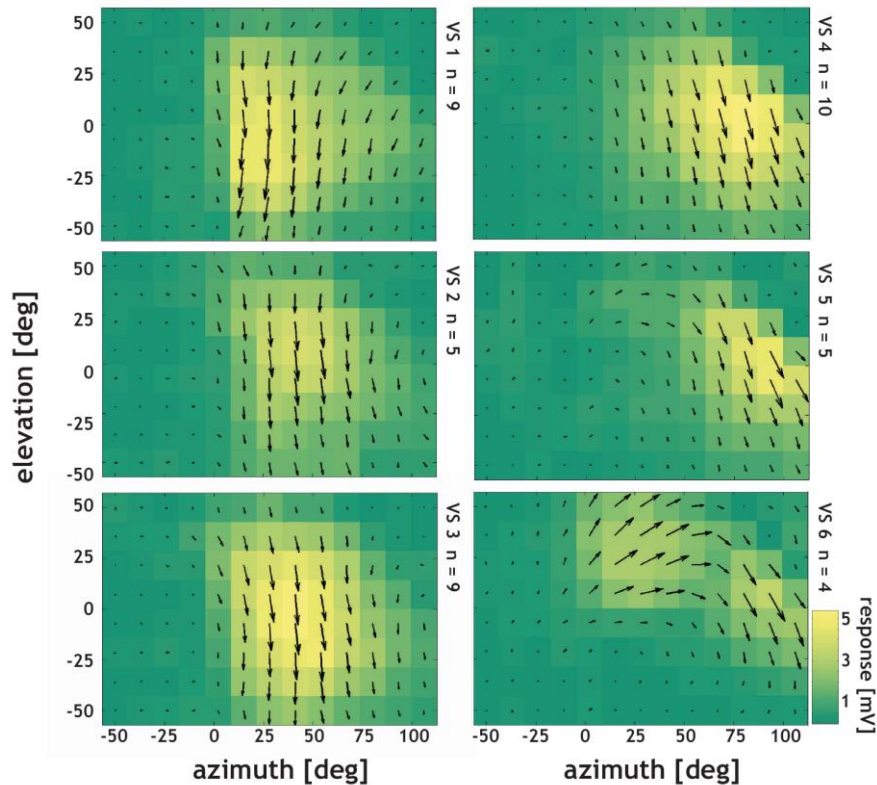
Visual stimulation.

A custom-built LED arena covered $\sim 170^\circ$ (1.9° resolution) of the horizontal and $\sim 100^\circ$ (1.8° resolution) vertical visual field, allowing refresh rates of up to 600 Hz with 16 intensity levels. The spectral peak of the LEDs was at 568nm and the luminance range of the stimuli were between 0 – 8 cd / m^2 . For technical details see ⁹.

Data analysis.

Data was acquired and analyzed using the data acquisition and analysis toolboxes of Matlab (The Mathworks, USA). Receptive fields were calculate as in¹⁴. The contrast was calculated as $(I_{\text{max}} - I_{\text{min}}) / (I_{\text{max}} + I_{\text{min}})$ with an absolute I_{min} and I_{max} of 0.5 and 8 cd / m^2 , respectively. The contrast responses was defined as the difference between the average response of the preferred and null-motion direction during a 2 s stimulation of a square grating ($\lambda = 22^\circ$) at 1 Hz temporal frequency. On- and Off-responses were defined as the difference between the mean response during the complete movement of the moving edge and the 500ms average potential prior stimulation. The difference between the responses during preferred- and null-motion direction was plotted.

Supplementary Material

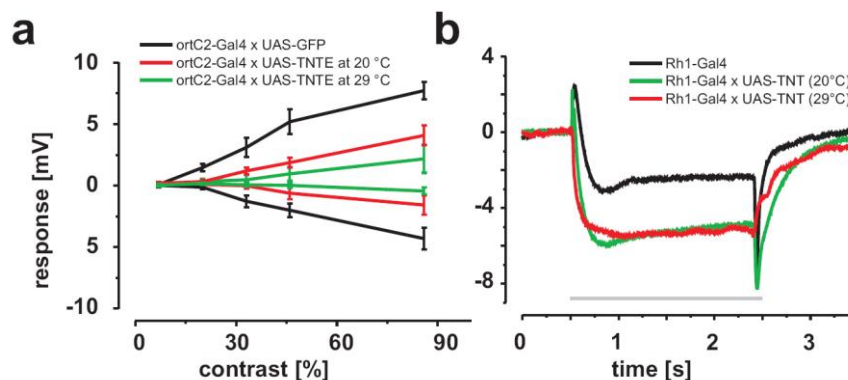


Supp. Fig. 1. Receptive field properties of VS cells. Average receptive fields of VS1 – VS6 recorded from control flies. Normalized vector plots show the maximal direction sensitivity of each cell at each point in space. The underlying color-map represents the magnitude of the responses at each given point.

Temperature sensitivity of TNT

A previous study has suggested that different kinds of neuronal specific synaptobrevins, a TNT cleavable and a non-cleavable one, are localized in different populations of neurons in *Drosophila*¹⁷. Since this argumentation could invalidate our results, we retested this hypothesis and characterized the optimal parameters needed to disrupt synaptic release via TNT expression. We found a change in the effectiveness depending on the expression level and the expression onset of the driver lines, but most dramatically on the temperature in which the flies were reared. We expressed TNT in photoreceptors R1-6 using the enhancer line Rh1-Gal4 and tested the strength of the photoreceptor block by electroretinogram (ERG)²⁴ recordings. The fly's ERG represents the summed extracellular components of the photoreceptor and the transient lamina membrane potential peaks, which are visible at the onset and offset of the

stimuli. Flies that were held at 20 °C for five days only showed a reduction of the lamina responses and an increase of the DC component, suggesting a partial block of photoreceptor terminals. However, when rearing these flies at 29 °C for two days, the lamina transients were completely abolished indicating a strong temperature sensitivity of the disruptor (Supp. Fig 2a). These results contradict the hypothesis of a second non-cleavable isoforms of synaptobrevin supposed to be present in photoreceptors. We further investigated the TNT disruptor using the *ort^{C2}*-Gal4 line that contains the lamina monopolar cells L1, L2 and L3 in its expression pattern, finding a temperature sensitive block of motion responses (Supp. Fig. 2b).



Supp. Fig. 2. Quantitative analysis of TNT block. (a) ERG of *Rh1-Gal4* and *Rh1-Gal4*→UAS-TNTE flies. A complete reduction of the lamina cell responses was observed after holding the flies for 3 days at 29 °C (red trace). If the flies were held at 20 °C for 5 days, only subtle changes in the lamina peak kinetics and the DC component could be observed (green trace). (b) Contrast dependencies of control (*ort^{C2}*-Gal4 → UAS-GFP), experimental flies held at 20 °C (*ort^{C2}*-Gal4 → UAS-TNTE) and at 29 °C (A3). A strong reduction in the contrast dependency was observed at higher temperatures (mean +/- SEM).

TNT induced lethality

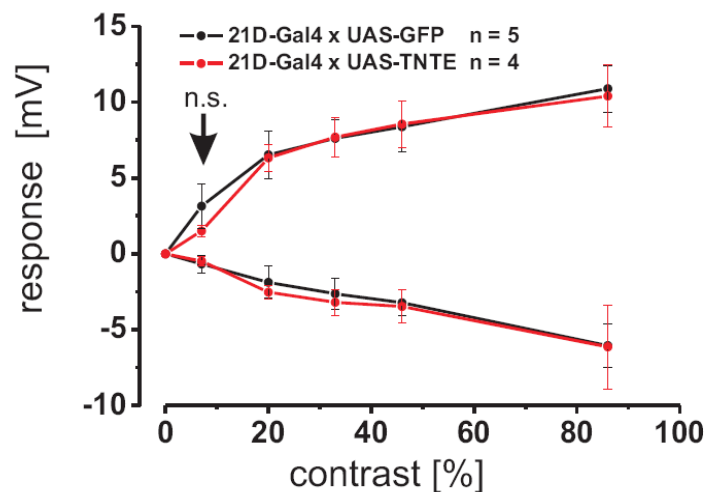
We controlled for a possible developmental effect co-expressing the temperature sensitive variant of the Gal4 repressor Gal80. In this configuration, Gal80 should repress the expression of TNT at 20 °C and enable it at 30 °C. In this scenario, the same viability was seen for all enhancer lines tested apart of C155 (Supp. Table 1). C155 has a strong expression in the complete central nervous system. When crossed to TNT, experimental embryos appear to develop normally prior hatching from the egg. However, no larva was seen hatching from any egg probably due to dysfunctional nervous system. We think that due to the high expression level and wide expression

pattern of C155 the suboptimal TNT parameters can still disrupt enough neuronal tissue.

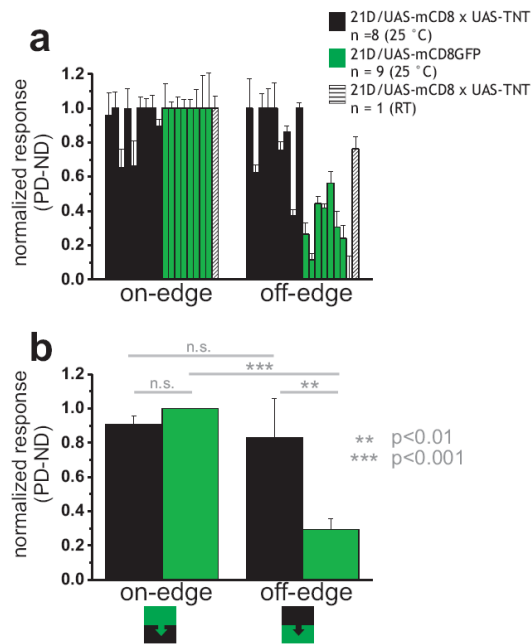
For the direct TNT expression experiments, flies were held at the mentioned temperatures during the complete development. Interestingly, young viable flies hold at 20 °C died after few days when increasing the incubation temperature to 29 °C, enforcing the idea of the temperature sensitivity of TNT. For the Gal80 repression experiments, the experimental flies were reared first at 20 °C and after pupal hatch, incubated at 29 °C (see Supp. Table 1).

genotypes	expression pattern in LMC	other expressions in the optic lobes	UAS-TNT 20 °C	UAS-TNT 29 °C	UAS-TNT; tub-Gal80ts 20 °C	UAS-TNT; tub-Gal80ts 29 °C
6289	L1 & L2	Tm cells	viable	lethal	viable	lethal
21D	L2	Tm4	viable	lethal	viable	lethal
c202	L1	?	viable	lethal	viable	lethal
c155	whole CNS	whole CNS	lethal	lethal	viable	lethal
ort ^{c3}	L2	C2 and one unkown	viable	viable	viable	viable
ort ^{c2}	L1, L2 & L3	-	viable	viable	viable	viable
Split-cha	L2	C2	viable	viable	viable	viable
Split-glu	L1	Tm5, Tlp	viable	viable	viable	viable
Ln-Gal4	primarily L4	week L2 and L5 cells	viable	viable	viable	viable

Supp. Table 1. Viability of different driver lines with TNT.



Supp. Fig 3. Contrast dependence of 21D-Gal4 line. Contrast dependency of both control and experimental flies to moving gratings ($\lambda = 22^\circ$, $\nu = 1$ Hz). A not significant tendency was observed at the lowest contrast level during PD stimulation (experimental flies $n = 5$ / control flies $n = 5$).



Supp. Fig 4. On- and Off-edge motion detection of 21D-Gal4 line. (a) Normalized responses of each control (21D-Gal4→UAS-GFP) and experimental (21D-Gal4 → UAS-TNTE) fly (mean +/- SEM). **(b)** Average responses of both groups (mean +/- SEM). A significant reduction of the off-edge motion responses could be observed in the TNT experiments (experimental flies n = 8/ control flies n = 9).

Reference List

1. Meinertzhagen, I.A. & O'Neil, S.D. Synaptic organization of columnar elements in the lamina of the wild type in *Drosophila melanogaster*. *J. Comp Neurol.* 305, 232-263 (1991).
2. Gilbert, C., Penisten, D.K. & Devoe, R.D. Discrimination of Visual-Motion from Flicker by Identified Neurons in the Medulla of the Fleshfly *Sarcophaga-Bullata*. *Journal of Comparative Physiology A-Sensory Neural and Behavioral Physiology* 168, 653-673 (1991).
3. Hausen, K. Functional characterization and anatomical identification of motion sensitive neurons in the lobula plate of the blowfly *Calliphora erythrocephala*. *Z. Naturforsch.* 31c, 629-633 (1976).
4. Hassenstein, B. & Reichardt, W. Systemtheoretische Analyse der Zeit-, Reihenfolgen- und Vorzeichenauswertung bei der Bewegungspertzeption des Rüsselkäfers *Chlorophanus*. *Z. Naturforsch.* 11b, 513-524 (1956).
5. Barlow, H.B., Hill, R.M. & Levick, W.R. Retinal Ganglion Cells Responding Selectively to Direction + Speed of Image Motion in Rabbit. *Journal of Physiology-London* 173, 377-& (1964).
6. Dubner, R. & Zeki, S.M. Response Properties and Receptive Fields of Cells in An Anatomically Defined Region of Superior Temporal Sulcus in Monkey. *Brain Research* 35, 528-& (1971).
7. Borst, A. & Haag, J. Neural networks in the cockpit of the fly. *J. Comp Physiol A Neuroethol. Sens. Neural Behav. Physiol* 188, 419-437 (2002).
8. Reichardt, W. Sensory Communication. Rosenblith, W.A. (ed.), pp. 303-317 (The M.I.T. Press and John Wiley & Sons, New York, London, 1961).

9. Jösch,M., Plett,J., Borst,A. & Reiff,D.F. Response properties of motion-sensitive visual interneurons in the lobula plate of *Drosophila melanogaster*. *Curr. Biol.* 18, 368-374 (2008).
10. Rister,J. *et al.* Dissection of the peripheral motion channel in the visual system of *Drosophila melanogaster*. *Neuron* 56, 155-170 (2007).
11. Buchner,E., Buchner,S. & Bühlhoff,I. Deoxyglucose mapping of nervous activity induced in *Drosophila* brain by visual movement. *J. Comp. Physiol. A* 155, 471-483 (1984).
12. Bausenwein,B., Dittrich,A.P.M. & Fischbach,K.F. The optic lobe of *Drosophila melanogaster*. II. Sorting of retinotopic pathways in the medulla. *Cell Tissue Res.* 267, 17-28 (1992).
13. Braitenberg V. & Debbage,P. Regular Net of Reciprocal Synapses in Visual System of Fly, *Musca-Domestica*. *Journal of Comparative Physiology* 90, 25-31 (1974).
14. Schnell B. *et al.* Processing of horizontal optic flow in three visual interneurons of the *Drosophila* brain. *submitted* (2009).
15. Brand,A.H. & Perrimon,N. Targeted Gene-Expression As A Means of Altering Cell Fates and Generating Dominant Phenotypes. *Development* 118, 401-415 (1993).
16. Sweeney,S.T., Broadie,K., Keane,J., Niemann,H. & Okane,C.J. Targeted Expression of Tetanus Toxin Light-Chain in *Drosophila* Specifically Eliminates Synaptic Transmission and Causes Behavioral Defects. *Neuron* 14, 341-351 (1995).
17. Rister,J. & Heisenberg,M. Distinct functions of neuronal synaptobrevin in developing and mature fly photoreceptors. *Journal of Neurobiology* 66, 1271-1284 (2006).
18. Zhu,Y., Nern,A., Zipursky,S.L. & Frye,M.A. Peripheral Visual Circuits Functionally Segregate Motion and Phototaxis Behaviors in the Fly. *Current Biology* 19, 613-619 (2009).
19. Katsov,A.Y. & Clandinin,T.R. Motion processing streams in *Drosophila* are behaviorally specialized. *Neuron* 59, 322-335 (2008).
20. Egelhaaf,M. & Borst,A. Are there separate ON and OFF channels in fly motion vision? *Vis. Neurosci.* 8, 151-164 (1992).
21. Franceschini,N., Riehle,A. & Le Nestour,A. Facets of vision. Stavenga,D.G. & Hardie,R.C. (eds.), pp. 360-390 (Springer-Verlag, Berlin,Heidelberg,1989).
22. Gao,S.Y. *et al.* The Neural Substrate of Spectral Preference in *Drosophila*. *Neuron* 60, 328-342 (2008).
23. Wilson,R.I., Turner,G.C. & Laurent,G. Transformation of olfactory representations in the *Drosophila* antennal lobe. *Sci* 303, 366-370 (2004).
24. Wulff,V.J. & Jahn,T.L. The Electroretinogram of *Cynomya*. *Anatomical Record* 96, 506-507 (1946).

8 Discussion

In this work, a series of electrophysiological, neuroanatomical and neurogenetical experiments were conducted to pursue the question of the cellular implementation of motion vision and course control in the fly. A new electrophysiological approach was developed in *Drosophila melanogaster* which, in combination with *Drosophila's* rich repertoire of genetic techniques, represents the foundation for the dissection of the fly's visual processing circuitries.

8.1 Introduction of *Drosophila* as a model organism for the analysis of the motion detection circuitry

Morphological studies of columnar interneurons of the lamina and medulla in *Drosophila* have shown similarities to their anatomically characterized counterparts in other dipteran flies (Fischbach and Dittrich, 1989; Strausfeld, 1976). Similar observations have been made while comparing the morphology of LPTCs, suggesting an analogous functional role across fly species (Rajashekhar and Shamprasad, 2004; Scott et al., 2002, Hausen, 1976). Though, much larger inter-species variance has been reported at the level of LPTCs than at the level of columnar interneurons (Buschbeck and Strausfeld, 1996; Buschbeck and Strausfeld, 1997). However, physiological evidence for this assumption was missing. To close this gap an electrophysiological technique to reliably record from genetically targeted visual interneurons of the lobula plate of *Drosophila* was designed and implemented. Thereby, two prominent groups of large-field neurons were analyzed for the first time, the "vertical sensitive" (VS; Chapter 4; Jösch et al., 2008) and "horizontal sensitive" (HS) cells (Chapter 6; Schnell et al. submitted). Based on this studies, I could show that (1) uniform neuronal mechanisms of visual motion processing exist across different dipteran species, (2) *Drosophila* qualifies for the analysis of population coding within the LPTC networks and finally (3) *Drosophila* allows the combined electrophysiological and neurogenetical dissection of the cellular implementation of the elementary motion detector as well as the functional dissection of the LPTC-network.

8.2 Basic response properties of VS- and HS-cells.

The main basic responses of *Drosophila's* VS- and HS-cell closely resemble the ones described in bigger fly species (Chapter 2, Sec. 2.3.4). VS-cells are excited by whole field motion in downward direction (Chapter 5, Fig 1; Jösch et al., 2008), while HS-cells by ipsilateral front-to-back motion (Chapter 6, Fig 1). Whole field motion stimuli along their preferred direction elicit a depolarization of their membrane potential superimposed with spike-like events. In contrast, when presenting motion stimuli in the opposite direction the cells strongly hyperpolarize.

8.3 Fingerprints of computations according to the Reichardt detector model of visual motion detection.

To use *Drosophila* as a model organism for the cellular understanding of motion vision, a validation of the knowledge acquired in the last 30 years in this field in bigger flies is of great interest (Borst et al., 2003; Götz 1972, 1973, Haag et al., 2004; Hassenstein and Reichardt, 1956; Hausen, 1976; Reisenman et al., 2003). Therefore I investigated if the characteristics predicted by the Reichardt detector model can be found in the responses of *Drosophila's* LPTCs. As described previously (Chapter 2, section 2.3), the Reichardt detector is based on a multiplicative interaction of asymmetrically filtered luminance values measured by neighboring photoreceptors. Doing this twice in a mirror-symmetric fashion and subtracting the output signal of both subunits leads to a fully directional output signal (Chapter 2, section 2.4; Hassenstein and Reichardt, 1956). Intriguingly, I found that the motion responses of LPTCs in *Drosophila* fulfill all predictions of the Reichardt detector.

One hallmark of the Reichardt detector is its' temporal frequency optimum: When stimulated by a drifting sine grating, the responses are predicted to be maximal at a certain velocity. For different spatial wavelength of the stimulus, different velocity optima should arise. This velocity optima in turn behave in such a way that when divided by the spatial wavelength of the stimulus, a constant temporal frequency in Hz appears for all spatial wavelengths presented. This is the case for *Drosophila's* VS- (Chapter 4, Fig. 3A&B; Jösch et al., 2008) and HS-cells (Chapter 6, Fig 2A&B, these experiments were performed by Bettina Schnell). In both cell populations, the temporal-frequency optimum coincides at 1 Hz. Interestingly, as shown in behavioral

experiments by Karl Götz in the 60's, the maximal optomotor response in a tethered flying *Drosophila* is found at the very same contrast frequency (Götz, 1964). Thus, our experiments are in line with a functional contribution of these cells to the execution of compensatory turning behavior. This result, however, is drawn into question by recently published behavioral studies that report an optimum response at 5-10 Hz (Duistermars et al., 2007; Fry et al., 2009). In my experiments, VS- and HS-cells miss substantial graded responses at grating motion stimulation of temporal frequency of 10 Hz. The experiments performed by K. Götz show that at stimulation frequencies of 10 Hz the response strength is reduced to less than half in both flying and walking *Drosophila* (Götz, 1964; Götz and Wenking, 1973). It remains speculative if the different optima can be attributed to differences in the stimulus presentation like maximal frame rates and spatial resolutions of the used stimulus devices.

Another prediction of the multiplicative interaction of the Reichardt model is that directional selective neurons encode image motion independent of the sign of contrast. This was proven to be the case for VS (Chapter 4, Fig 4A; Jösch et al., 2008) as well as for HS-cells (Chapter 6, Fig. 2D; Schnell et al., submitted). In addition, motion perception is strongly depended on the contrast of the moving object. We measured a strong dependence of the LPTC responses on the contrast of the stimuli. In this respect, the Reichardt detector has a quadratic dependence to contrast. However, I found in line with previous behavioral experiments in *Drosophila* (Buchner, 1984), that this dependence can only be measured at low contrast levels. At higher contrast, the responses saturate probably due to a gain control mechanism in elementary motion detectors (Chapter 4, Fig. 4B & Chapter 6, Fig. 2C; Jösch et al., 2008).

Finally, I tested the last step of local motion detection, the subtraction of both mirror symmetric subunits. I recorded from VS-cell during visual stimulation while injecting negative or positive DC currents. My results show that DC current injections changed the driving force for both subunits independently, suggesting that two types of inputs with opposite direction provide inhibition and excitation to VS-cell dendrites (Chapter 4, Fig. 4C).

In summary, the characteristics of the recorded responses can be described by a Reichardt detector model. These findings set the framework for further neurogenetic studies that aim to elucidate the cellular implementation of this algorithmic model.

8.4 The VS-cell network in *Drosophila*.

Drosophila VS-cell network is composed of at least 6 individually identifiable, directionally selective cells. Each morphologically classified VS-cell type possesses a distinct receptive field sequentially arranged along the azimuth, with VS1 being most sensitive to frontal and VS6 to lateral stimuli (Chapter 4, Fig 2B; Jösch et al., 2008). The organization of their dendritic arborization is in concordance with their receptive field properties. When analyzing their optic-flow fields a clear sensitivity to vertical motion can be observed for the most frontal VS1, VS2, VS3 and VS4 cells. In contrast, VS5 and specially VS6 seem to respond strongest to rotational motion at 25 ° and 50 ° azimuth, respectively (Chapter 7, Fig. S. 1; Jösch et al., 2008).

As in the blowfly *Calliphora*, the receptive fields in *Drosophila* are wider than expected from their retinotopic input. In the blowfly, a sequentially arranged electrical coupling between VS-cells was found to be responsible for this observation (Farrow et al., 2005; Haag and Borst, 2004). Consistent with these findings, we found evidence for electrical coupling of VS-cells in *Drosophila* too (Chapter 4. Fig. 2C; Jösch et al., 2008). In concordance with these results, we also observed a very strong immunolabeling of innexin 8, an insect gap-junction protein. Innexin 8, also known as *shakB*, co-localizes with the axonal termini of VS- and HS-cells (data not shown). In VS-cells, this particular wiring has been proposed to be essential for the fly's course control. It performs a linear interpolation between their output signals, leading to a robust representation of the axis of rotation even in the presence of textureless patches of the visual surround (Cuntz et al., 2007). In *Drosophila*, the majority of VS cells are less rotationally tuned than *Calliphora*'s. Only VS5 and VS6 appear to have rotational flow-fields (Chapter 7. Fig. S1). Nevertheless, the similarity of both network connections suggests a common computational principle which still has to be tested in behavior. This appears now to be possible by genetically targeting the gap-junction molecule innexin 8. We are currently trying to use diverse RNA interference molecules to down-regulate specifically the electrical coupling between VS-cells only. This should allow testing this coupling electrophysiologically and in behavior.

8.5 *Drosophila's HS cell network*

The results of my work and the work of Bettina Schnell in our lab showed that *Drosophila's* HS-cell network is composed of 3 individually identifiable, directionally selective cells, most sensitive to front-to-back motion on their ipsilateral side. Their dendritic fields strongly overlap, with HSN being more dorsal, HSE equatorial (Chapter 4, Fig. 3A) and HSS ventral (Scott et al., 2002). As for the VS-cells, the columnar organization of the medullar elements that provide input to the HS-cell dendrites in the lobula plate are retinotopically organized. Interestingly, the overlap of their dendritic spanning fields is very large, e.g. that of HSE covers on the average about 90 % of that of HSN (Chapter 6, Fig. 3A). This feature can also be observed in the receptive field of the HSN-, HSE- and HSS-cell (Chapter 4, Fig. 4), where HSN has a strong dorsal, HSE, equatorial and HSS ventral sensitivity. The major overlap of the receptive fields also matches their dendritic morphology (Chapter 4, Fig3). Another interesting aspect is their sensitivity to contralateral motion (Chapter 4, Fig. 2A). HS-cells respond to contralateral back-to-front motion with a depolarization of their membrane potential. The opposite is found on the ipsilateral side, where front-to-back motion elicits a depolarization. This data altogether suggests that HS cells are tuned to rotational panoramic motion stimuli.

Performing Neurobiotin perfusion of single HS-cells and tracing the dye in the LPTC-circuit, coupling was observed indicating electrical connections (experiments performed by B. Schnell). Here two interesting facts were learned. The contralateral back-to-front sensitivity probably arises from either H1 or H2 like cells (Chapter 6, Fig 6). As already described in *Calliphora*, both cells have dendrites in the contralateral lobula plate and respond to back-to-front motion with an increase in the spiking frequency (Haag and Borst, 2001; Hausen, 1982a; Hausen, 1982b; Horstmann et al., 2000). Due to the relatively weak labeling of the heterolateral neurons and the vast amount of other labeled cells, no precise classification could be done so far. Second, HS-cells in *Drosophila* appear to be directly coupled via gap junction and not, as described in *Calliphora*, via CH-cells (Haag and Borst, 2002; Chapter 6, Fig 6). In *Calliphora* this coupling is important, since CH-cells inhibit the so-called figure detection neurons (Egelhaaf, 1985) and thereby tune them to small-field motion (Cuntz et al., 2003). It is unclear how *Drosophila* solves this problem.

8.6 Synaptic organization of LPTCs in the *Drosophila* brain

To understand the implementation of a circuit it is important to assess the exact location of the inputs it receives. Together with Shamprasad Varija Raghu, we took a close look at the synaptic organization of the VS- and HS-cells characterized electrophysiologically in my previously mentioned studies. We found that both, VS- and HS-cells receive GABAergic and acetylcholinergic inputs on their dendritic tips. This was shown by two complementary approaches: First, via immunolabeling of endogenous acetylcholine-receptor subunit $D\alpha 7$ (Chapter 5, Fig. 1&2; Raghu et al., 2009) and the neurotransmitter GABA (Chapter 3, Fig. 5&6). Second, via transgenic expression of labeled $D\alpha 7$ subunits (Chapter 5, Fig. 3&4; Raghu et al., 2009) and the Rdl-type GABA-receptors (Chapter 3, Fig. 3; Raghu et al., 2007). Our results are in accordance with the subtractive step of the Reichardt detector model previously described in big fly species (Borst and Egelhaaf, 1990; Egelhaaf et al., 1990; Gilbert, 1991), which is also implemented as a push-pull mechanism between excitatory and inhibitory inputs on the dendrites of *Drosophila*'s LPTCs (Chapter 4, Fig.4C; Jösch et al., 2008).

Regarding the excitatory component, it is known that nicotinic acetylcholine receptors (nAChR) are key players for fast excitatory neurotransmission in the central nervous system of insects (Leech and Sattelle, 1993). Consequently we tried to take advantage of the expression of the $D\alpha 7$ -nAChR subunit in the optic lobes and recorded from VS-cells in $D\alpha 7$ -knock-out flies. Surprisingly, no major differences to WT motion responses were found (Chapter 5, Fig. 6; Raghu et al., 2009). To test if other acetylcholine-receptor subunit might functionally compensate for the missing $D\alpha 7$ -nAChR subunit, we performed a pharmacological investigation. We found that $D\alpha 7$ -knock-out flies strongly react to acetylcholine and that Alexa-647 labeled α -bungorotoxin still co-localizes with the dendritic tips of VS-cells in the mutant flies. nAChR are composed of pentameric protein complexes of different subunits (Tomizawa and Casida, 2001). Different subunit compositions can give rise to receptor assemblies with distinct functional properties; however little is known about their physiology in *Drosophila in vivo*. One study has already used the same approach to disrupt the acetylcholinergic signaling in the giant-fiber mediated escape behavior (Fayyazuddin et al., 2006). Thus, our finding suggests an unexpected mechanism in motion vision that compensate for the absence of the widely expressed $D\alpha 7$ -subunit.

Concerning GABAergic inhibitory input onto VS- and HS-cells, an additional input region on the axonal termini was found (Chapter 3, Fig. 3, 5 & 6; Raghu et al., 2007). So far there is no report on inhibitory inputs on HS terminals in any fly species and the functional significance of the GABAergic Rdl-receptor expression in the HS-cell terminal remains to be analyzed. In VS-cells the axonal inhibition is more conclusive when considering the tuning of their receptive fields. VS-cells with lateral receptive fields become strongly excited by downward motion in the center of their receptive field and by upward motion in the frontal part of their receptive field (Chapter 7, Fig. S. 1; Krapp et al., 1998). These findings can be explained by a release of inhibition, if a hypothetical GABAergic inhibitory interneuron would receive input from frontal VS cells and connected on lateral VS-cells. Evidence for the existence of such an inhibitory interneuron has been obtained in current injections experiments performed in *Calliphora* (Haag and Borst, 2004). In these experiments positive injection of DC current in frontal VS cells caused a simultaneous hyperpolarization in lateral VS cells and vice versa. Such sign reversal and inhibition cannot be mediated via the described electrical coupling between VS cells (Haag and Borst, 2004). Thus, there is clear evidence for inhibitory chemical coupling between VS-cells via unknown other neurons. The Rdl receptors on the VS-cell axons discovered in this study could mediate this inhibition. Future work will allow to further untangle the circuitry and to derive a generic model of flow-field processing and visual course control in flies.

8.7 Chemical release sites of *Drosophila* VS- and HS-cells

The analysis of chemical release site of single neurons using immunolabeling and fluorescent imaging techniques is difficult and ambiguous due to the high amount of synapses in brain tissue and the optical resolution limit of light microscopy. To overcome this problem, Shamprasad Varija Raghu generated transgenic flies where GFP and the fluorescently tagged presynaptic protein n-Syb were expressed in single VS-cell clones (Chapter 3, Fig.1&2; Raghu et al., 2007). This experiment allowed localizing the presumed presynaptic release site of exclusively VS- and HS-cells while ignoring the expression in the rest of the brain. In these single cell clones the presynaptic marker n-Syb was found in the axonal termini but not in the dendrites, suggesting that the chemical output of VS- and HS-cell are only localized in the axonal termini. The neurotransmitters used by VS- and HS-cells are not known. Only one histochemical study suggests that HS-cells are glutamatergic (Sinakevitch and

Strausfeld, 2004). I performed guided patch clamp experiments in flies expressing GFP under the enhancer sequence of choline-acetyltransferase, which specifically highlight cholinergic neurons (Salvaterra P.M and Kitamoto, 2001). In these experiments GFP-positive VS-cells were recorded (data not shown). This is a strong indication that VS cells are acetylcholinergic. Much has been learned about the functional role of the electrical coupling in the VS-cell network, but the role of their chemical output remains unstudied. This finding opens a new exciting possibility to modulate the acetylcholinergic biochemistry to further uncover the VS-cell function in visually guided behavior.

8.8 Evidence of a cellular implementation of the Reichardt detector

Despite the precise specifications of the computational steps of motion vision, the neural mechanisms and circuitry presynaptic to the LPTCs have escaped so far from a detailed analysis. This is due to the small size of the constituting neurons and the high complexity of their neural architecture. We set out to elucidate the cellular implementation starting from the most outer neuropile, the lamina. Taking advantage of the two-component UAS/Gal4 system for targeted transgene expression (Brand and Perrimon, 1993), I manipulated different populations on lamina interneurons while simultaneously recording from untagged LPTC. By blocking the synaptic output using tetanus neurotoxin light chain (TNT; Sweeney et al., 1995), which cleaves synaptobrevin to suppress synaptic transmission, I could address the involvement of lamina monopolar cells in motion computation.

My first achievement was the improvement of the visualization of LPTCs somatas that allowed me to record from unlabeled LPTCs. This technical development enabled the use of the Gal4/UAS system to specifically disrupt specified presynaptic populations of interneurons leaving the LPTC properties unperturbed. Interestingly, this method helped me to reveal a temperature sensitivity of the TNT disruptor, which changes the effectiveness of the TNT disruptor dramatically (Chapter 7, Supp.Fig 2).

After having tested the functional parameters of TNT, I continued analyzing the involvement of different lamina monopolar cells in motion computation. My experimental results show that the simultaneous block of L1, L2 & L3 abolished motion sensitive responses, indicating that these cells give input to the motion detection circuitry

(Chapter 7, Fig2 & Supp. Fig 2). My results are in line with anatomical studies that proposed two pathways, the first using L1 and the second L2, to feed information into the motion detection circuitry (Bausenwein et al., 1992; Buchner et al., 1984). In accordance with this, a behavioral study observed that the block of L1 and L2 abolished optomotor responses in *Drosophila* (Rister et al., 2007). However, contradictory results have been published by a newer behavioral work, suggesting that L1 and L2 are not involved in motion vision (Zhu et al., 2009). This study came to the mentioned conclusion using TNT as a disruptor. In this respect, I found that TNT appears to function optimal only at temperatures above 29 °C. The suboptimal block of lamina interneurons is therefore probably the cause of the absence of any effect, since the experimental flies of this study were held at room temperature. In my experiments, flies in which the output of either L1 or L2 was blocked, the direction selective responses of all VS- and HS-cells tested were preserved for vertical and horizontal motion, respectively (Chapter 7, Fig2A). The only fundamental change was a reduction of the contrast sensitivity (Chapter 7, Fig2B). These results question the main findings presented by Rister et al. (Rister et al., 2007). This study suggests that at intermediate contrast L1 and L2 mediate motion vision in opposite directions: the L1 pathway mediates front-to-back and the L2 pathway back-to-front motion. In this work, the authors selectively expressed in either L1 or L2 cells the wild type histamine receptor ('ort'; Hardie, 1989) in a histamine-receptor null mutant. In this experimental conformation, any rescue seen in behavior after selective restoration would hint towards a sufficiency of the respective pathway. Since blocking the output of one neuronal subtype is basically the opposite of allowing it to receive input, we assumed that blocking either L1 or L2 with TNT is essentially similar to rescuing L2 or L1, respectively. This is a risky assumption in a network in which the connectivity between lamina neurons is extremely intermingled and where not much is known about the postsynaptic medullar interactions (Meinertzhagen and O'Neil, 1991; Takemura et al., 2008). Nevertheless, the information conveyed by the L1 or L2 synapses to the motion circuitry seems not to be in accordance with a unidirectional motion processing model.

In addition to the L1 and L2 pathways, the lamina cell L4 has also been speculated to be specialized in front-to-back motion processing (Braitenberg V. and Debbage, 1974). This is because L4 is the only lamina cell with an asymmetrical connectivity, receiving L2 input in one cartridge and impinging through two conspicuously backward

oriented collaterals to two L2 neurons in posterior lateral cartridges. A recent behavioral study (Zhu et al., 2009) found, using cell specific TNT expression, that flies in which L4 were blocked with the same *UAS-Gal4* line completely lose optomotor responses but retain wild type phototactic behavior. We found that in these flies the photoreceptor transmission was strongly disrupted. Therefore no conclusions can be drawn from our results and the mentioned behavioral study regarding the involvement of L4 in motion processing (Chapter 7, Fig. 4).

Finally, our data suggest a segregation of motion pathways that are involved in the detection of moving patterns with either increase (On) or decrease (Off) luminance (Chapter 7, Fig 3). In this respect, an electrophysiological study performed in the fly *Calliphora vicina* has shown that adjacent luminance steps of opposing polarity interact producing a motion sensitive response (Egelhaaf and Borst, 1992). This data is indicative for the absence of previously suggested separate Reichardt detectors specialized in On- and Off-motion detection (Franceschini et al., 1989), since a clear interaction of On- and Off-stimuli was measured. These results led to the hypothesis that the luminance polarity transmitted by each arm of the Reichardt detector is conserved and being further processed by a 'sign-correct' multiplication (Egelhaaf and Borst, 1992). If this interaction is accomplished by a synaptic interaction between two neurons, a postsynaptic signal should be enhanced when both presynaptic inputs either simultaneously increase (On) or decrease (Off). To the best of our knowledge, no corresponding synaptic mechanism has ever been described to accomplish this. However, if the brightness increments or decrements are represented in separate On- and Off-channels, each one carrying positive signals only, the synaptic mechanism underlying such an interaction is less complex, only requiring a supra linear input-output relationship. To fully mimic a sign-corrected multiplication, four subunits take care of all possible combinations between the On- and Off- input channels ('Four quadrant multiplier (Hassenstein and Reichardt, 1956)'). Our results are in line with such a four quadrant multiplication model, giving the first experimental indication for the input implementation to the motion detection circuitry. The future understanding of this implementation and the subsequent processing of the signals in the medulla will be key for the complete cellular description of motion processing in flies.

8.9 Concluding remarks

The studies presented here have their roots in the seminal work of Werner Reichardt and Bernhard Hassenstein performed half a century ago. Using the optomotor response of the beetle *Chlorophanus*, they developed a model which accounts for the optomotor response properties of many insects. In the last 50 years many attempts have been performed to understand the cellular implementation of this apparently “simple” network. However, the small size of the constituting interneurons and the true complexity of the underlying circuitry have hindered any functional understanding. The new genetic tools that allow physiological manipulations of specified populations of cells in *Drosophila* are therefore a promising approach to overcome some of the previously encountered difficulties. Behavioral experiments have already shown the strength of this methodology (Rister et al., 2007). Nevertheless, obtaining a precise description of the single computations of a neuronal network is extremely difficult with such approaches. This is because behavioral responses are the result of motion processing and a wide range of additional computations that give rise to the visually guided behavior. In contrast, the direct measurement of the LPTC responses primarily represents the output of the motion processing circuitry and therefore allows a more precise description of the presynaptic processing. Thus, the combination of electrophysiological methods with genetic manipulation of neuronal function in *Drosophila*, as presented in this work, is an encouraging method that promises new insights in the cellular processing within circuitries of the fly visual system.

9 Reference List

- Albright,T.D., Desimone,R., and Gross,C.G. (1984). Columnar Organization of Directionally Selective Cells in Visual Area Mt of the Macaque. *Journal of Neurophysiology* 51, 16-31.
- Barlow,H.B., Hill,R.M., and Levick,W.R. (1964). Retinal Ganglion Cells Responding Selectively to Direction + Speed of Image Motion in Rabbit. *Journal of Physiology-London* 173, 377-&.
- Barlow,H.B. and Levick,W.R. (1965). Mechanism of Directionally Selective Units in Rabbits Retina. *Journal of Physiology-London* 178, 477-&.
- Bausenwein,B., Buchner,E., and Heisenberg,M. (1990). Identification of H1 visual interneuron in *Drosophila* by [3H] 2-deoxyglucose uptake during stationary flight. *Brain Research* 509, 134-136.
- Bausenwein,B., Dittrich,A.P.M., and Fischbach,K.F. (1992). The optic lobe of *Drosophila melanogaster*. II. Sorting of retinotopic pathways in the medulla. *Cell Tissue and Research* 267, 17-28.
- Blondeau,J. (1981). Electrically evoked course control in the fly *Calliphora erythrocephala*. *Journal of Experimental Biology* 92, 143-153.
- Borst,A. (2009). *Drosophila's View on Insect Vision*. *Current Biology* 19, R36-R47.
- Borst,A. and Egelhaaf,M. (1990). Direction selectivity of fly motion-sensitive neurons is computed in a two-stage process. *Proceedings of the National Academy of Science USA* 87, 9363-9367.
- Borst,A. and Egelhaaf,M. (1992). In vivo imaging of calcium accumulation in fly interneurons as elicited by visual motion stimulation. *Proceedings of the National Academy of Science USA* 89, 4139-4143.
- Borst,A., Egelhaaf,M., and Haag,J. (1995). Mechanisms of dendritic integration underlying gain control in fly motion-sensitive interneurons. *Journal of Computational Neuroscience* 2, 5-18.
- Borst,A. and Haag,J. (2002). Neural networks in the cockpit of the fly. *J.Comp Physiol A Neuroethol.Sens.Neural Behav.Physiol* 188, 419-437.
- Borst,A., Reisenman,C., and Haag,J. (2003). Adaptation of response transients in fly motion vision. II: Model studies. *Vision Research* 43, 1311-1324.
- Braitenberg V. and Debbage,P. (1974). Regular Net of Reciprocal Synapses in Visual System of Fly, *Musca-Domestica*. *Journal of Comparative Physiology* 90, 25-31.
- Brand,A.H. and Perrimon,N. (1993). Targeted Gene-Expression As A Means of Altering Cell Fates and Generating Dominant Phenotypes. *Development* 118, 401-415.
- Brotz,T.M. and Borst,A. (1996). Cholinergic and GABAergic receptors on fly tangential cells and their role in visual motion detection. *Journal of Neurophysiology* 76, 1786-1799.
- Buchner,E. (1976). Elementary movement detectors in an insect visual system. *Biological Cybernetics* 24, 85-101.
- Buchner,E. (1984). Behavioural analysis of spatial vision in insects. In *Photoreception and vision in invertebrates*, M. A. Ali, ed. (New York, London: Plenum Press), pp. 561-621.
- Buchner,E., Buchner,S., and Bülthoff,I. (1984). Deoxyglucose mapping of nervous activity induced in *Drosophila* brain by visual movement. *Journal of Comparative Physiology A* 155, 471-483.

- Burns, M.E. and Arshavsky, V.Y. (2005). Beyond counting photons: Trials and trends in vertebrate visual transduction. *Neuron* 48, 387-401.
- Buschbeck, E.K. and Strausfeld, N.J. (1996). Visual motion - detection circuits in flies : small - field retinotopic elements responding to motion are evolutionarily conserved across taxa. *Journal of Neuroscience* 16, 4563-4578.
- Buschbeck, E.K. and Strausfeld, N.J. (1997). The relevance of neural architecture to visual performance: phylogenetic conservation and variation in dipteran visual systems. *J Comp Neurol* 383, 282-304.
- Chalfie, M., Tu, Y., Euskirchen, G., Ward, W.W., and Prasher, D.C. (1994). Green Fluorescent Protein As A Marker for Gene-Expression. *Science* 263, 802-805.
- Collett, T.S. (1980). Some operating rules for the optomotor system of a hoverfly during voluntary flight. *Journal of Comparative Physiology* 138, 271-282.
- Cuntz, H., Haag, J., and Borst, A. (2003). Neural image processing by dendritic networks. *Proc.Natl.Acad.Sci.U.S.A* 100, 11082-11085.
- Cuntz, H., Haag, J., Forstner, F., Segev, I., and Borst, A. (2007). Robust coding of flow-field parameters by axo-axonal gap junctions between fly visual interneurons. *Proc.Natl.Acad.Sci.U.S.A* 104, 10229-10233.
- Dickinson, M.H. (1999). Haltere-mediated equilibrium reflexes of the fruit fly, *Drosophila melanogaster*. *Philosophical Transactions of the Royal Society of London Series B-Biological Sciences* 354, 903-916.
- Douglass, J.K. and Strausfeld, N.J. (1995). Visual motion detection circuits in flies: peripheral motion computation by identified small-field retinotopic neurons. *Journal of Neuroscience* 15, 5596-5611.
- Douglass, J.K. and Strausfeld, N.J. (1996). Visual motion - detection circuits in flies : parallel direction - and non-direction-sensitive pathways between the medulla and lobula plate. *Journal of Neuroscience* 16, 4551-4562.
- Dubner, R. and Zeki, S.M. (1971). Response Properties and Receptive Fields of Cells in An Anatomically Defined Region of Superior Temporal Sulcus in Monkey. *Brain Research* 35, 528-&.
- Duistermars, B.J., Chow, D.M., Condro, M., and Frye, M.A. (2007). The spatial, temporal and contrast properties of expansion and rotation flight optomotor responses in *Drosophila*. *Journal of Experimental Biology* 219, 3218-3227.
- Egelhaaf, M. (1985). Figur-Grund Diskrimination durch Relativbewegung bei der Fliege: neuronale Grundlagen. Figure-ground discriminatin by relative motion in the visual system of the fly: Towards the underlying neuronal circuitry. *Verh.Dtsch.Zool.Ges.* 78, 226.
- Egelhaaf, M. and Borst, A. (1992). Are there separate ON and OFF channels in fly motion vision? *Visual Neuroscience* 8, 151-164.
- Egelhaaf, M., Borst, A., and Pilz, B. (1990). The role of GABA in detecting visual motion. *Brain Research* 509, 156-160.
- Egelhaaf, M., Borst, A., and Reichardt, W. (1989). The non-linear mechanism of direction selectivity in the fly motion detection system. *Naturwissenschaften* 76, 32-35.
- Egelhaaf, M., Borst, A., and Reichardt, W. (1989). Computational structure of a biological motion detection-detection system as revealed by local detector analysis in the fly's nervous system. *Journal of the Optical Society of America A* 6, 1070-1087.
- Elyada, Y.M., Haag, J., and Borst, A. (2009). Different receptive fields in axons and dendrites underlie robust coding in motion-sensitive neurons. *Nature Neuroscience* 12, 327-332.
- Euler, T., Detwiler, P.B., and Denk, W. (2002). Directionally selective calcium signals in dendrites of starburst amacrine cells. *Nature* 418, 845-852.

- Farrow,K., Borst,A., and Haag,J. (2005). Sharing receptive fields with your neighbors: tuning the vertical system cells to wide field motion. *J Neurosci.* 25, 3985-3993.
- Farrow,K., Haag,J., and Borst,A. (2006). Nonlinear, binocular interactions underlying flow field selectivity of a motion-sensitive neuron. *Nat.Neurosci.* 9, 1312-1320.
- Fayyazuddin,A., Zaheer,M.A., Hiesinger,P.R., and Bellen,H.J. (2006). The nicotinic acetylcholine receptor D alpha 7 is required for an escape behavior in *Drosophila*. *Plos Biology* 4, 420-431.
- Fermi,G. and Reichardt,W. (1963). Optomotorische Reaktionen der Fliege *Musca domestica*. Abhängigkeit der Reaktion von der Wellenlänge, der Geschwindigkeit, dem Kontrast und der mittleren Leuchtdichte bewegter periodischer Muster. *Kybernetik* 2, 15-28.
- Fischbach,K.F. and Dittrich,A.P.M. (1989). The optic lobe of *Drosophila melanogaster*. I. A Golgi analysis of wild-type structure. *Cell Tissue and Research* 258, 441-475.
- Franceschini,N., Kirschfeld,K., and Minke,B. (1981). Fluorescence of Photoreceptor Cells Observed In vivo. *Science* 213, 1264-1267.
- Franceschini,N., Riehle,A., and Le Nestour,A. (1989). Directionally selective motion detection by insect neurons. In *Facets of vision*, D. G. Stavenga and R. C. Hardie, eds. (Berlin,Heidelberg: Springer-Verlag), pp. 360-390.
- Fried,S.I. and Masland,R.H. (2007). Image processing: How the retina detects the direction of image motion. *Current Biology* 17, R63-R66.
- Fried,S.I., Munch,T.A., and Werblin,F.S. (2002). Mechanisms and circuitry underlying directional selectivity in the retina. *Nature* 420, 411-414.
- Fry,S.N., Rohrseitz,N., Straw,A.D., and Dickinson,M.H. (2009). Visual control of flight speed in *Drosophila melanogaster*. *Journal of Experimental Biology* 212, 1120-1130.
- Gao,S., Takemura,S.Y., Ting,C.Y., Huang,S., Lu,Z., Luan H., Rister,J., Thum,A.S., Yang,M., Hong,S.-T., Wang,J.W., Odenwald,W.F., White,B.H., Meinertzhagen,I.A., and Lee,C.-H. (2008). The neural substrate of spectral preference in *Drosophila*. *neuron* 60, 328-342.
- Gilbert,C. (1991). Membrane conductance changes associated with the response of motion sensitive insect visual neurons. *Zeitschrift fuer Naturforschung* 45c, 1222-1224.
- Götz,K.G. (1972). Visual control of orientation patterns. Processing of cues from the moving environment in the *Drosophila* navigation system. In *Information processing in the visual systems of arthropods*, R. Wehner, ed. (Berlin, Heidelberg, New York: Springer-Verlag), pp. 255-263.
- Götz,K.G. (1964). Optomotorische Untersuchungen des visuellen Systems einiger Augenmutanten der Fruchtfliege *Drosophila*. *Kybernetik* 2, 77-92.
- Götz,K.G. and Wenking,H. (1973). Visual control of locomotion in the walking fruitfly *Drosophila*. *Journal of Comparative Physiology* 85, 235-266.
- Haag,J. and Borst,A. (1996). Amplification of high-frequency synaptic inputs by active dendritic membrane processes. *Nature* 379, 639-641.
- Haag,J. and Borst,A. (2001). Recurrent network interactions underlying flow-field selectivity of visual interneurons. *Journal of Neuroscience* 21, 5685-5692.
- Haag,J. and Borst,A. (2002). Dendro-dendritic interactions between motion-sensitive large-field neurons in the fly. *Journal of Neuroscience* 22, 3227-3233.
- Haag,J. and Borst,A. (2004). Neural mechanism underlying complex receptive field properties of motion-sensitive interneurons. *Nat.Neurosci.* 7, 628-634.

- Haag,J. and Borst,A. (2005). Dye-coupling visualizes networks of large-field motion-sensitive neurons in the fly. *J.Comp Physiol A Neuroethol.Sens.Neural Behav.Physiol* 191, 445-454.
- Haag,J., Denk,W., and Borst,A. (2004). Fly motion vision is based on Reichardt detectors regardless of the signal-to-noise ratio. *Proc.Natl.Acad.Sci.U.S.A* 101, 16333-16338.
- Haag,J., Wertz,A., and Borst,A. (2007). Integration of lobula plate output signals by DNOVS1, an identified premotor descending neuron. *J Neurosci.* 27, 1992-2000.
- Hamada,F.N., Rosenzweig,M., Kang,K., Pulver,S.R., Ghezzi,A., Jegla,T.J., and Garrity,P.A. (2008). An internal thermal sensor controlling temperature preference in *Drosophila*. *Nature* 454, 217-U55.
- Hardie,R.C. (1984). Functional organization of the fly retina. In *Progress in Sensory Physiology* 5, H. Autrum, D. Ottoson, E. R. Perl, R. F. Schmidt, H. Shimazu, and W. D. Willis, eds. (Berlin, Heidelberg, New York, Tokyo: Springer-Verlag), pp. 1-79.
- Hardie,R.C. (1989). A histamine-activated chloride channel involved in neurotransmission at a photoreceptor synapse. *Nature* 339, 704-706.
- Hardie,R.C. and Raghu,P. (2001). Visual transduction in *Drosophila*. *Nature* 413, 186-193.
- Harris,W.A., Stark,W.S., and Walker,J.A. (1976). Genetic Dissection of Photoreceptor System in Compound Eye of *Drosophila-Melanogaster*. *Journal of Physiology-London* 256, 415-&.
- Hassenstein,B. (1991). Erzählte Erfahrungen I-Der Biologe-Bernhard Hassenstein. In *Freiburger Universitätsblätter*, Rombach Verlag), pp. 85-112.
- Hassenstein,B. and Reichardt,W. (1952). Systemtheoretische Analyse einer Verhaltensweise (der Wechsel-Folgen-Reaktion des Rüsselkäfers *Chlorophanus viridis*). *Verh.Dtsch.Zool.Ges.* 7, 95-102.
- Hassenstein,B. and Reichardt,W. (1956). Systemtheoretische Analyse der Zeit-, Reihenfolgen- und Vorzeichenbewertung bei der Bewegungspertzeption des Rüsselkäfers *Chlorophanus*. *Zeitschrift fuer Naturforschung* 11b, 513-524.
- Hausen,K. (1976). Functional characterization and anatomical identification of motion sensitive neurons in the lobula plate of the blowfly *Calliphora erythrocephala*. *Zeitschrift fuer Naturforschung* 31c, 629-633.
- Hausen,K. (1977). Struktur, Funktion und Konnektivität bewegungsempfindlicher Interneurone im dritten optischen Neuropil der Schmeißfliege *Calliphora erythrocephala*. Doctoral thesis,Tuebingen.
- Hausen,K. (1982a). Motion sensitive interneurons in the optomotor system of the fly. I. The Horizontal Cells: Structure and signals. *Biological Cybernetics* 45, 143-156.
- Hausen,K. (1982b). Motion sensitive interneurons in the optomotor system of the fly. II. The Horizontal Cells: Receptive field organization and response characteristics. *Biological Cybernetics* 46, 67-79.
- Hausselt,S.E., Euler,T., Detwiler,P.B., and Denk,W. (2007). A dendrite-autonomous mechanism for direction selectivity in retinal starburst amacrine cells. *Plos Biology* 5, 1474-1493.
- Heim,N. and Griesbeck,O. (2004). Genetically encoded indicators of cellular calcium dynamics based on troponin C and green fluorescent protein. *Journal of Biological Chemistry* 279, 14280-14286.
- Heisenberg,M. and Buchner,E. (1977). The role of retinula cell types in visual behavior of *Drosophila melanogaster*. *Journal of Comparative Physiology* 117, 127-162.
- Heisenberg,M., Wonneberger,R., and Wolf,R. (1978). Optomotor-blind (H31) -a *Drosophila* mutant of the lobula plate giant neurons. *Journal of Comparative Physiology* 124, 287-296.
- Horstmann,W., Egelhaaf,M., and Warzecha,A.K. (2000). Synaptic interaction increase optic flow specificity. *European Journal of Neuroscience* 12, 2157-2165.

- Hubel,D.H. (1959). Single Unit Activity in Striate Cortex of Unrestrained Cats. *Journal of Physiology-London* 147, 226-&.
- Hubel,D.H. and Wiesel,T.N. (1959). Receptive Fields of Single Neurones in the Cats Striate Cortex. *Journal of Physiology-London* 148, 574-591.
- Huberman,A.D., Wei,W., Elstrott,J., Stafford,B.K., Feller,M.B., and Barres,B.A. (2009). Genetic Identification of an On-Off Direction-Selective Retinal Ganglion Cell Subtype Reveals a Layer-Specific Subcortical Map of Posterior Motion. *Neuron* 62, 327-334.
- Jaervilehto,M. and Zettler,F. (1971). Localized intracellular potentials from pre- and postsynaptic components in the external plexiform layer of an insect retina. *Zeitschrift fuer vergleichende Physiologie* 75, 422-440.
- Jösch,M., Plett,J., Borst,A., and Reiff,D.F. (2008). Response properties of motion-sensitive visual interneurons in the lobula plate of *Drosophila melanogaster*. *Curr.Biol.* 18, 368-374.
- Katsov,A.Y. and Clandinin,T.R. (2008). Motion processing streams in *Drosophila* are behaviorally specialized. *Neuron* 59, 322-335.
- Kim,I.J., Zhang,Y.F., Yamagata,M., Meister,M., and Sanes,J.R. (2008). Molecular identification of a retinal cell type that responds to upward motion. *Nature* 452, 478-U11.
- Kirchner,W.H. and Srinivasan,M.V. (1989). Freely flying honeybees use image motion to estimate object distance. *Naturwissenschaften* 76, 281-282.
- Kirschfeld,K. (1967). Die Projektion der optischen Umwelt auf das Raster der Rhabdomere im Komplexauge von *MUSCA*. *Experimental Brain Research* 3, 248-270.
- Krapp,H.G., Hengstenberg,B., and Hengstenberg,R. (1998). Dendritic structure and receptive-field organization of optic flow processing interneurons in the fly. *Journal of Neurophysiology* 79, 1902-1917.
- Krapp,H.G. and Hengstenberg,R. (1996). Estimation of self - motion by optic flow processing in single visual interneurons. *Nature* 384, 463-466.
- Land,M.F. (1997). Visual acuity in insects. *Annual Review of Entomology* 42, 147-177.
- Land,M.F. and Collett,T.S. (1974). Chasing behavior of houseflies (*Fannia canicularis*). *Journal of Comparative Physiology* 89, 331-357.
- Laughlin,S.B., Howard,J., and Blakeslee,B. (1987). Synaptic limitations to contrast coding in the retina of the blowfly *Calliphora*. *Proc.R.Soc.Lond.B* 231, 437-467.
- Lee,T. and Luo,L. (1999). Mosaic analysis with a repressible neurotechnique cell marker for studies of gene function in neuronal morphogenesis. *neuron* 22, 451-461.
- Leech,C.A. and Sattelle,D.B. (1993). Acetylcholine receptor/channel molecules of insects. *EXS* 63, 81-97.
- Lettvin,J.Y., Maturana,H.R., Mcculloch,W.S., and Pitts,W.H. (1959). What the Frogs Eye Tells the Frogs Brain. *Proceedings of the Institute of Radio Engineers* 47, 1940-1951.
- Lima,S.Q. and Miesenbock,G. (2005). Remote control of behavior through genetically targeted photostimulation of neurons. *Cell* 121, 141-152.
- Luan,H.J., Peabody,N.C., Vinson,C.R., and White,B.H. (2006). Refined spatial manipulation of neuronal function by combinatorial restriction of transgene expression. *Neuron* 52, 425-436.
- Luo,L., Callaway,E.M., and Svoboda,K. (2008). Genetic dissection of neural circuits. *Neuron* 57, 634-660.

- Matruana HR and Frenk S. (1963). Directional movement and horizontal edge detectors in the pigeon retina. *Science*.
- Meinertzhagen, I. (2008). The Organization of Invertebrate Brains: Cells, Synapses, and circuits. *Journal of Morphology* 269, 1461.
- Meinertzhagen, I.A. and O'Neil, S.D. (1991). Synaptic organization of columnar elements in the lamina of the wild type in *Drosophila melanogaster*. *J. Comp Neurol.* 305, 232-263.
- Miesenbock, G., de Angelis, D.A., and Rothman, J.E. Visualizing secretion and synaptic transmission with pH/sensitive green fluorescent proteins. 1998.
Ref Type: Generic
- Miyawaki, A., Llopis, J., Heim, R., McCaffery, J.M., Adams, J.A., Ikura, M., and Tsien, R.Y. (1997). Fluorescent indicators for Ca²⁺ based on green fluorescent proteins and calmodulin. *Nature* 388, 882-887.
- Nakai, J., Ohkura, M., and Imoto, K. (2001). A high signal-to-noise Ca(2+) probe composed of a single green fluorescent protein. *Nat. Biotechnol.* 19, 137-141.
- Ng, M., Roorda, R.D., Lima, S.Q., Zemelman, B.V., Morcillo, P., and Miesenbock, G. (2002). Transmission of olfactory information between three populations of neurons in the antennal lobe of the fly. *neuron* 36, 463-474.
- Peabody, N.C., Pohl, J.B., Diao, F., Vreede, A.P., Sandstrom, D.J., Wang, H., Zelensky, P.K., and White, B.H. (2009). Characterization of the Decision Network for Wing Expansion in *Drosophila* Using Targeted Expression of the TRPM8 Channel. *Journal of Neuroscience* 29, 3343-3353.
- Pfeiffer, B.D., Jenett, A., Hammond, A.S., Ngo, T.T.B., Misra, S., Murphy, C., Scully, A., Carlson, J.W., Wan, K.H., Laverly, T.R., Mungall, C., Svirskas, R., Kadonaga, J.T., Doe, C.Q., Eisen, M.B., Celniker, S.E., and Rubin, G.M. (2008). Tools for neuroanatomy and neurogenetics in *Drosophila*. *Proceedings of the National Academy of Sciences of the United States of America* 105, 9715-9720.
- Raghu, S.V., Jösch, M., Borst, A., and Reiff, D.F. (2007). Synaptic organization of lobula plate tangential cells in *Drosophila*: gamma-aminobutyric acid receptors and chemical release sites. *Journal of Comparative Neurology* 502, 598-610.
- Raghu, S.V., Jösch, M., Sigrist, S.J., Borst, A., and Reiff, D.F. (2009). Synaptic Organization of Lobula Plate Tangential Cells in *Drosophila*: D7 Cholinergic Receptors. *Journal of Neurogenetics* 23, 200-209.
- Rajashekhar, K.P. and Shamprasad, V.R. (2004). Golgi analysis of tangential neurons in the lobula plate of *Drosophila melanogaster*. *Journal of Biosciences* 29, 93-104.
- Ramón y Cajal. *Recuerdos de mi vida*. 1923. Madrid: Pueyo. / English trans.(1966) *Recollections of my life*. MIT Press. Ref Type: Serial (Book, Monograph)
- Reichardt, W. (1957). Autokorrelations-Auswertung als Funktionsprinzip des Zentralnervensystems; (bei der optischen Bewegungswahrnehmung eines Insektes). *Zeitschrift fuer Naturforschung* 12b, 448-457.
- Reiff, D.F., Ihring, A., Guerrero, G., Isacoff, E.Y., Jösch, M., Nakai, J., and Borst, A. (2005). In vivo performance of genetically encoded indicators of neural activity in flies. *Journal of Neuroscience* 25, 4766-4778.
- Reiff, D.F., Thiel, P.R., and Schuster, C.M. (2002). Differential regulation of active zone density during long-term strengthening of *Drosophila* neuromuscular junctions. *Journal of Neuroscience* 22, 9399-9409.
- Riehle, A. and Franceschini, N. (1984). Motion detection in flies: parametric control over ON-OFF pathways. *Experimental Brain Research* 54, 390-394.
- Reisenman, C., Haag, J., and Borst, A. (2003). Adaptation of response transients in fly motion vision. I: Experiments. *Vision Research* 43, 1293-1309.

- Rister,J., Pauls,D., Schnell,B., Ting,C.Y., Lee,C.H., Sinakevitch,I., Morante,J., Strausfeld,N.J., Ito,K., and Heisenberg,M. (2007). Dissection of the peripheral motion channel in the visual system of *Drosophila melanogaster*. *Neuron* 56, 155-170.
- Rister J, Heisenberg M: (2006). Distinct functions of neuronal synaptobrevin in developing and mature fly photoreceptors. *Journal of Neurobiology*;66:1271-1284.
- Rossel,S. (1983). Binocular Stereopsis in An Insect. *Nature* 302, 821-822.
- Salvaterra P.M and Kitamoto,T. (2001). *Drosophila* cholinergic neurons and processes visualized with Gal4/UAS-GFP. *Gene Exp Patt* 1, 73-82.
- Schroll,C., Riemensperger,T., Bucher,D., Ehmer,J., Voller,T., Erbguth,K., Gerber,B., Hendel,T., Nagel,G., Buchner,E., and Fiala,A. (2006). Light-induced activation of distinct modulatory neurons triggers appetitive or aversive learning in *Drosophila* larvae
1. *Curr.Biol.* 16, 1741-1747.
- Schuling,F.H., Masterbroek,H.A.K., Bult,R., and Lenting,B.P.M. (1989). Properties of elementary movement detectors in the fly *Calliphora erythrocephala*. *Journal of Comparative Physiology A* 165, 179-192.
- Schuppe,H. and Hengstenberg,R. (1993). Optical properties of the ocelli of *Calliphora erythrocephala* and their role in the dorsal light response. *Journal of Comparative Physiology A* 173, 143-149.
- Scott,E.K., Raabe,T., and Luo,L.Q. (2002). Structure of the vertical and horizontal system neurons of the lobula plate in *Drosophila*. *Journal of Comparative Neurology* 454, 470-481.
- Seki,A., Miyachi,S., Hayashi,S., Kikukawa,T., Kubo,M., Demura,M., Ganapathy,V., and Kamo,N. (2007). Heterologous expression of Pharaonis halorhodopsin in *Xenopus laevis* oocytes and electrophysiological characterization of its light-driven C- pump activity. *Biophysical Journal* 92, 2559-2569.
- Sherman,A. and Dickinson,M.H. (2002). A comparison of visual and haltere-mediated equilibrium reflexes in the fruit fly *Drosophila melanogaster*. *The Journal of Experimental Biology* 206, 295-302.
- Siegert S, Scherf BG, Del Punta K, Didkovsky N, Heintz N, and Roska B (2009). Genetic address book for retinal cell types. *Nat.Neurosci. Epub ahead of print.*
- Sinakevitch,I. and Strausfeld,N.J. (2004). Chemical neuroanatomy of the fly's movement detection pathway. *Journal of Comparative Neurology* 468, 6-23.
- Single,S. and Borst,A. (1998). Dendritic integration and its role in computing image velocity. *Science* 281, 1848-1850.
- Sommer,S. and Wehner,R. (2005). Vector navigation in desert ants, *Cataglyphis fortis*: celestial compass cues are essential for the proper use of distance information. *Naturwissenschaften* 92, 468-471.
- Srinivasan,M.V. (1977). A visually-evoked roll response in the housefly. *Journal of Comparative Physiology* 119, 1-14.
- Srinivasan,M.V., Zhang,S., Altwein,M., and Tautz,J. (2000). Honeybee navigation: Nature and calibration of the "Odometer". *Science* 287, 851-853.
- Stange,G. (1981). The Ocellar Component of Flight Equilibrium Control in Dragonflies. *Journal of Comparative Physiology* 141, 335-347.
- Stange,G., Stowe,S., Chahl,J.S., and Massaro,A. (2002). Anisotropic imaging in the dragonfly median ocellus: a matched filter for horizon detection. *Journal of Comparative Physiology A-Neuroethology Sensory Neural and Behavioral Physiology* 188, 455-467.
- Strausfeld,N.J. (1976). *Atlas of an insect brain.* (Berlin, Heidelberg: Springer).
- Strausfeld,N.J. (1984). Functional neuroanatomy of the blowfly's visual system. In *Photoreception and vision in invertebrates*, M. A. Ali, ed. Plenum Publishing Corporation), pp. 483-522.

- Strausfeld,N.J. and Lee,J.K. (1991). Neuronal basis for parallel visual processing in the fly. *Visual Neuroscience* 7, 13-33.
- Sweeney,S.T., Broadie,K., Keane,J., Niemann,H., and Okane,C.J. (1995). Targeted Expression of Tetanus Toxin Light-Chain in *Drosophila* Specifically Eliminates Synaptic Transmission and Causes Behavioral Defects. *Neuron* 14, 341-351.
- Szobota,S., Gorostiza,P., Del Bene,F., Wyart,C., Fortin,D.L., Kolstad,K.D., Tulyathan,O., Volgraf,M., Numano,R., Aaron,H.L., Scott,E.K., Kramer,R.H., Flannery,J., Baier,H., Trauner,D., and Isacoff,E.Y. (2007). Remote control of neuronal activity with a light-gated glutamate receptor. *Neuron* 54, 535-545.
- Takemura,S.Y., Lu,Z.Y., and Meinertzhagen,J.A. (2008). Synaptic circuits of the *Drosophila* optic lobe: The input terminals to the medulla. *Journal of Comparative Neurology* 509, 493-513.
- Tomizawa,M. and Casida,J.E. (2001). Structure and diversity of insect nicotinic acetylcholine receptors. *Pest Management Science* 57, 914-922.
- Vanderbliek,A.M. and Meyerowitz,E.M. (1991). Dynamin-Like Protein Encoded by the *Drosophila*-Shibire Gene Associated with Vesicular Traffic. *Nature* 351, 411-414.
- Wagner,H. (1986). Flight performance and visual control of flight of the free-flying housefly (*Musca domestica*). II: Pursuit of targets. *Philosophical Transactions of the Royal Society of London B* 312, 553-579.
- Wassle,H. (2004). Parallel processing in the mammalian retina. *Nature Reviews Neuroscience* 5, 747-757.
- Wertz,A., Borst,A., and Haag,J. (2008). Nonlinear integration of binocular optic flow by DNOVS2, a descending neuron of the fly. *J Neurosci.* 28, 3131-3140.
- Wittlinger,M., Wehner,R., and Wolf,H. (2006). The ant odometer: Stepping on stilts and stumps. *Science* 312, 1965-1967.
- Yamaguchi,S., Wolf,R., Desplan,C., and Heisenberg,M. (2008). Motion vision is independent of color in *Drosophila*. *Proc.Natl.Acad.Sci.U.S.A* 105, 4910-4915.
- Yeandle,S. and Spiegler,J.B. (1973). Light-Evoked and Spontaneous Discrete Waves in Ventral Nerve Photoreceptor of *Limulus*. *Journal of General Physiology* 61, 552-571.
- Zemelman,B.V., Lee,G.A., Ng,M., and Miesenbock,G. (2002). Selective photostimulation of genetically ChARGed neurons. *Neuron* 33, 15-22.
- Zemelman,B.V., Nesnas,N., Lee,G.A., and Miesenbock,G. (2003). Photochemical gating of heterologous ion channels: Remote control over genetically designated populations of neurons. *Proceedings of the National Academy of Sciences of the United States of America* 100, 1352-1357.
- Zhang,F., Wang,L.P., Brauner,M., Liewald,J.F., Kay,K., Watzke,N., Wood,P.G., Bamberg,E., Nagel,G., Gottschalk,A., and Deisseroth,K. (2007). Multimodal fast optical interrogation of neural circuitry. *Nature* 446, 633-639.
- Zhu,Y., Nern,A., Zipursky,S.L., and Frye,M.A. (2009). Peripheral Visual Circuits Functionally Segregate Motion and Phototaxis Behaviors in the Fly. *Current Biology* 19, 613-619.

Acknowledgements

I want to thank all the people that contributed to the presented studies, most specially to my two direct advisers: Dierk F. Reiff and Alexander Borst. Their continuous support encouraged me to try as many ideas as I felt attracted to and their excellent guidance conducted me professionally during the last 5 years. I am also grateful to Shamprasad Varija Raghu, Bettina Schnell, Thomas Hendel, Väinö Haikala and Jing Shi, members of the “little fly” project, that constantly contributed with ideas and encouragement. Thanks to Yong Choe, Benedikt Berninger and Günther Zeck, for their advices during my thesis committee meetings. To Johannes Plett, the main brain behind the stimulus device, for discussions, music and quietness when needed. Moreover, I am thankful to the not yet mentioned present and former members of the expanded “big fly” group: Bulle (Jürgen Haag), Karl Farrow, Hermann Cuntz, Yishai Elyada, Adrian Wertz, Franz Weber, Huber Eichner, Friedrich Förster, Christoph Kapfer & Deusededit Spavieri for all the inputs and discussions. I want to specially thank the great technical support that I received from Wolfgang Essbauer, Christian Theile, Werner Heilmann, Andi Kucher and Herr Wintersberger. Without their continuous support, this project would not have been possible at the present extend. In addition, I have to thank the whole Department Borst and the Griesbeck Group for the friendly hand given during all this time. Moreover, I am much obliged to the Max Planck Society that supported me financially and scientifically during my PhD in our Martinsrieder institute. Finally, I want to thank three people outside science, my parents and my wife, for their unconditional help, patience and affection.

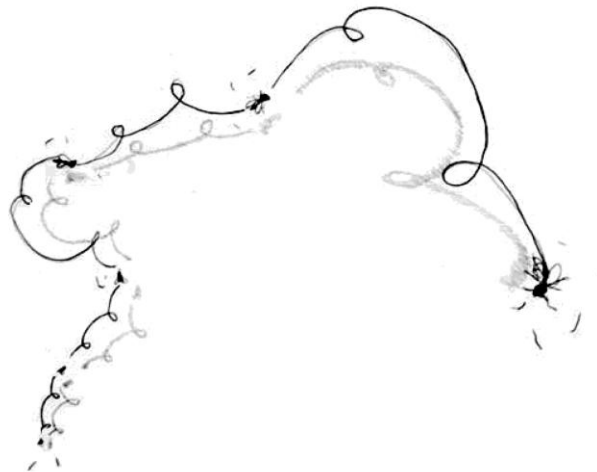


Illustration by Jorge Gonzalez Lohse

Curriculum vitae

Jösch Krotki, Maximilian Albert

Dipl. Biochem.

Contact details

Am Klopferspitz 18
Max Planck Institute of Neurobiology
Department for System and Computational Neurobiology
82152 Martinsried
Germany

E-mail: joesch@neuro.mpg.de

Education

- Sep 2005 – to date **PhD Thesis:** “Lobula Plate Tangential Cells in *Drosophila melanogaster*; Response properties, Synaptic Organisation & Input Channels”.
Max Planck Institute (MPI) of Neurobiology, Department of Systems and Computational Neuroscience.
Advisers: Prof. Alexander Borst and Dr. Dierk Reiff
- Sep 04 – Apr 05 **Diploma Thesis:** “Development of genetic tools for the genetic dissection of the motion detection pathway in *Drosophila*”.
MPI of Neurobiology, Department of Systems and Computational Neuroscience.
Advisers: Prof. Alexander Borst and Dr. Dierk Reiff
- Oct 1999 – Apr 2005 **Biochemistry Degree**
Eberhard Karls Universität, Tübingen and LMU, Munich.
- Mar – Sep 1999 **Physics and Astronomy studies**
Pontificia Universidad Católica de Chile.
- 1998 **Abitur**
Deutsche Schule / German School, Santiago de Chile.
Overall best student award class 1998.

Work experience

- 2007 Founder and head organizer of the first life-science PhD Symposium in Munich “>interact 2007”; www.interact-munich.org.
- 2006 Representative of the PhD Students of the MPI of Neurobiology.
- Aug. 2005 Scientific assistant in a glaciology research project of the CECS Institute (Chile) in Campos de Hielo Sur, Patagonia, Chile.
- Apr 2003 – Mar 2004 Lab rotation in six different Laboratories of the MPI of Biochemistry, MPI of Neurobiology and the Adolf-Butenandt-Institute, Munich.
- Mar 2002 Internship in the laboratories for Biogeochemistry at the Alfred Wegner Institut, Bremerhaven.

2001 - 2003 Scientific assistant in the Department of Physical Chemistry of the University Tübingen, working with polarized and time resolved fluorescence spectroscopy and UV/Vis spectroscopy.

Teaching experience

2005-2007 Assistant in the practical course of animal physiology at the LMU, Munich.

Courses

Aug 2007 Advance course in Computational Neuroscience, Arcachon, France. Gatsby and Bernstein Neuroscience Course.

Publications

1. Reiff DF, Ihring A, Guerrero G, Isacoff EY, Jösch M, Nakai J, Borst A.
In vivo performance of genetically encoded indicators of neural activity in flies. J. Neurosci. 2005 May 11; 25(19):4766-78.
2. Raghu SV, Jösch M, Borst A, Reiff DF.
Synaptic organization of lobula plate tangential cells in Drosophila: gamma-aminobutyric acid receptors and chemical release sites. J. Comp. Neurol. 2007 Jun 1; 502(4):598-610.
3. Jösch M, Plett J, Borst A, Reiff DF.
Response properties of motion-sensitive visual interneurons in the lobula plate of Drosophila melanogaster. Curr. Biol. 2008 Mar 11; 18(5):368-74.
4. Raghu SV, Jösch M, Siegrist S, Borst A, Reiff DF.
Synaptic Organization of Lobula Plate Tangential Cells in Drosophila: Dalpha7 Cholinergic Receptors. J. of Neurogenetics 2009; 23:200-209.
5. Schnell B, Jösch M, Förstner F, Raghu SV, Ito K, Borst A & Reiff DF.
Processing of horizontal optic flow in three visual interneurons of the Drosophila brain. *Submitted*.

Personal information

Language skills

German native level
Spanish native level
English advanced level
Portuguese conversational level

Personal interest

Wood carving
Sports: climbing and mountaineering, Tae kwon do.

Personal information

Nationalities: Chilean, German and Austrian.
Place of birth: Viña del Mar, Chile
Date of birth: 08. September 1980

Married to Joana Filipa Leitão Pinheiro Almeida Enes